Impact of fuels and exhaust aftertreatment systems on the unregulated emissions from mopeds, light and heavy-duty vehicles

Ph. D. Thesis Report

Author: Michaël Clairotte

Supervisor: Covadonga Astorga-Llorens

2014

Report EUR 25583 EN

European Commission
Joint Research Centre
Institute for Energy and Transport

Contact information
Covadonga Astorga-Llorens – Sustainable Transport Unit
Address: Joint Research Centre, Via Enrico Fermi 2749, TP 441, 21027 Ispra (VA), Italy
E-mail: covadonga.astorga-llorens@ec.europa.eu
Tel.: +39 0332 78 6110
Fax: +39 0332 78 5236

http://iet.jrc.ec.europa.eu/
http://ec.europa.eu/dgs/jrc/index.cfm
This publication is a Reference Report by the Joint Research Centre of the European Commission.

JRC 76177

EUR 25583 EN

ISBN 978-92-79-27305-6
ISSN 1018-5593
doi: 10.2790/67104

Luxembourg: Publications Office of the European Union, 2014

Printed in Italy

Abstract

Transport sector plays a key role in climate change and air pollution. Among the anthropogenic sectors, on-road transport is recognized as the first contributor to global warming, mainly due to its emission of carbon dioxide, ozone precursors and carbonaceous aerosols. In addition, on-road transport contributes to the deterioration of air quality by releasing nitrogen oxides, hydrocarbons, carbonyls, ammonia, and aerosols. However, the current European legislation of vehicles emissions focusses on a limited number of pollutants, namely hydrocarbons, carbon monoxide, nitrogen oxides, and particulate matter.

The aim of this work was to improve the knowledge about the emission factors of gas phase and particle-associated emissions from vehicle exhaust. The impacts of aftertreatment devices and fuel quality on regulated and unregulated species were studied. Several sampling campaigns with different types of vehicles were conducted in the vehicle emission laboratory (VELA) at the European Commission Joint Research Centre (EC-JRC) Ispra, Italy. The vehicles chosen were representative of some categories circulating in Europe (heavy duty vehicles, light duty vehicles, two-stroke mopeds), and either standard fuel or some alternative fuels (ethanol and liquefied petroleum gas) were used. The gas phase was monitored by a Fourier transform infrared spectrometer (carbonyls, nitrogen-containing species, small hydrocarbons), and a resonance-enhanced multiphoton ionization time-of-flight mass spectrometer (mono and polycyclic aromatic hydrocarbons). The particulate phase was analyzed by a high-resolution time-of-flight aerosol mass spectrometer (organic aerosol, chloride, nitrate), and a multiangle absorption photometer (black carbon).

The mopeds were found to have the higher emission factors of primary organic aerosol and polycyclic aromatic hydrocarbons. While efficient to reduce the regulated emissions, the after-treatment used to comply with the moped Euro 2 emission standard might be responsible of large emission of unregulated organic aerosols. Most of the emission linked to the gasoline light duty vehicles were released before the light-off of the catalyst. Whereas alternative fuels studied helped to reduce ozone precursor emissions, the pollutants associated to the cold start of the vehicle reduced this beneficial effect. Finally, the heavy duty diesel vehicles featured the highest nitrogen oxides and black carbon emissions. Despite efficient retrofit and after-treatment systems (for particles and nitrogen oxides), these vehicles could release significant amount of ammonia. These results provided valuable insights for the drafting of legislation related to the achievement of sustainable transport in Europe.

Keywords: Atmospheric pollution; on-road transport; unregulated emissions; alternative fuels; exhaust aftertreatment systems; mopeds.

Résumé

Le secteur du transport joue un rôle majeur dans le changement climatique et la pollution atmosphérique. Parmi les secteurs d'origine anthropique, le transport routier est considéré comme le premier contributeur au réchauffement climatique, due notamment aux émissions de CO_2, de précurseurs d'ozone, et d'aérosols carbonés (carbone noir). De plus, les émissions liées au transport routier telles que les oxydes d'azote, les hydrocarbures gazeux, les carbonyles volatiles, l'ammoniac et les aérosols, contribuent à la dégradation de la qualité de l'air. Cependant, l'actuelle réglementation Européenne relative aux émissions automobiles ne s'applique que sur un nombre restreint de polluants, à savoir les hydrocarbures gazeux, les oxydes d'azote, le monoxyde de carbone et les particules.

Le but de cette étude était d'approfondir l'état des connaissances en termes de facteurs d'émissions associés au transport, pour les polluants en phases gazeuse et solide. Un intérêt particulier a été apporté sur l'influence des systèmes de post-traitement des gaz d'échappement, et de la qualité du carburant, sur les émissions d'espèces réglementées et non-réglementées. Des campagnes de mesure ont été menées sur différentes catégories de véhicules dans le laboratoire d'étude des émissions (VELA) du centre commun de recherche de la commission Européenne (JRC-EC) à Ispra, en Italie. La flotte de véhicules choisie comprenait des camions (moyens et poids lourds), des voitures et des deux-roues formant un ensemble représentatif des véhicules circulant en Europe. En plus des carburants classiques, essence et diesel, les véhicules ont été alimentés avec des carburants alternatifs tels que le bioéthanol, et le gaz de pétrole liquéfié. Les émissions en phase gazeuse ont été mesurées par spectroscopie infra-rouge à transformé de Fourier (FT-IR ; pour les composés azotés, les carbonyles volatiles et les petits hydrocarbures), par spectrométrie de masse à temps de vol après ionisation multi-photonique résonnante (REMPI-ToF-MS ; pour les hydrocarbures aromatiques mono et polycycliques), par spectrométrie de masse haute résolution à temps de vol dédié à l'analyse des aérosols atmosphériques (HR-TOF-AMS ; pour les aérosols organiques), et par photométrie d'absorption multi-angle (MAAP ; pour le carbone élémentaire).

Parmi les véhicules étudiés, les scooters ont été les plus gros émetteurs d'aérosols organiques primaires et d'hydrocarbures mono et polycycliques. De plus, le système de post-traitement des gaz d'échappement étudié pour le scooter le plus récent (conforme à la réglementation Euro 2) pourrait être responsable d'émissions importantes d'aérosols organiques. Concernant les voitures, et en particulier celles équipées de moteurs à allumage par étincelle, la plupart de leurs émissions intervenaient en début de cycle, avant que la température d'amorçage du pot catalytique soit atteinte. Ces émissions liées au démarrage à froid du véhicule pouvaient masquer les effets bénéfiques des carburants alternatifs en terme d'émissions de précurseurs d'ozone. Finalement, les camions étaient les plus gros émetteurs de suie (carbone élémentaire) et d'oxydes d'azote. Bien que plusieurs systèmes de retrofit se soient montrés particulièrement efficaces pour réduire les émissions des polluants réglementés (particules et oxydes d'azote) de ces véhicules, certains d'entre eux produisaient des quantités significatives de NH_3. Ce projet a permis de collecter des informations précieuses pour l'élaboration de la législation relative au développement d'un transport durable en Europe.

Keywords : Pollution atmosphérique ; transport routier ; émissions non-réglementées ; systèmes de traitement des gaz d'échappement ; carburants alternatifs ; scooters.

To Christina and Gabriel

Acknowledgements

During this project, many people were involved, directly or indirectly, in improving the quality of this scientific work. I would like to highlight their investments by these few lines, and in advance, my apologies if I have forgotten anyone.

"Galanterie oblige", I would like to sincerely thank Cova for giving me the opportunity to achieve a doctorate in such a stimulating environment, and for her excellent project support, at all the levels, scientific and human.

I would like to acknowledge Alois Krasembrink and Giorgio Martini for hosting me in the Sustainable Transport Unit and Clean and efficient vehicles action respectively.

This project would not have been possible without the strong investment of my scientific supervisor from the University of Montpellier, Eric Tournié and Aurore Vicet. I really appreciated their help and insightful comments, all the more valuable that I was far from the University.

I really want to thank the referee members for taking part of this project assessment, and in particular, the reviewers Michel André and Jean-Luc Jaffrezo for their time invested in assessing my work and for their thoughtful advices and feedbacks on my manuscript which have helped in improving this current version.

This work is based on a significant fraction of experimental study and measurement campaigns. I am indebted to the whole VELA staff for their strong support, both technical and moral. Whatever the time to drive in a cold facility (-7°C), the intensity of the Major Lake summer storms when a cylinder has to be changed outside, the kind of specific handmade exotic pipe connection to design at the very last moment, they were here ! I really appreciated the mutual comfort when our national soccer teams were kicked out from the first round of world cup. So I would like to thank the INTER-national team: Urbano Manfredi, Rinaldo Colombo, Mirco Sculati, Gaston Lanappe, Franz Muehlberger, Mauro Cardario, Philippe Le-Lijour as well as Massimo Carriero, Stefano Alessandrini, Fausto Forni, Dominique Lesueur and François Montigny.

Over these 3 years, I shared my working space with two human and talented scientists: Thomas Adam and Alessandro Zardini. I really appreciated your advices and help in reviewing my scientific production. I also acknowledge my former colleagues from the Sustainable Transport Unit, Germano, Alexio, Vicente, Marteen, Monica, Giorgios, Thanasis, Makis, Christos, Hulusi, as well as Laura, Pierre, Alessandro and Adolfo.

Then, I spent great time in Villigen, hosting by PSI group, and following interesting and promising measurement campaign on mopeds emissions. I want to thank the former colleagues from the Swiss group, in particular André Prévôt, Maarten Heringa, Roberto Chirico and Stephen Platt.

The last step of a PhD comes through the writing phase, I appreciated the support from the INRA, and the UMR Eco&Sols in particular, by giving me the opportunity to conclude the manuscript redaction phase, and for the precious advices provided over the preparation of the Phd defense.

Living far from our country is a very enriching period; I wish whoever has to live this experience to encounter such wonderful persons like the ones I met. I really want to thank my closest “Italian" friends, Biagio, Mary, Davide, Natalya, Luca, Josette, Stefania, Aris, Carla, Matteo, Olivier, Bao, Mariana, Mehmet, Claudia, Fernanda, Marco, Fausto, Vassilis (la squadra del pallavolo), Komlan, Damien (for the unforgettable Italian lessons), and Mayeul (for showing me the light in R tunnel).

I would like to thank my family, for having accepted to see me less during these three years, and for their moral and ... logistical support along this experience.

Of course, one must give honour to whom honour is due, this project would not have been possible at all without having my wonderful wife beside me, for her strong support, also scientific, and for her contribution to our most beautiful and meaningful achievement of these three years: Gabriel.

Contents

List of Figures

List of Tables

Chapter 1

Introduction

Air pollution is responsible of climate change and constitute a threat to health (1). Greenhouse gases are responsible of the global warming, and the statement from the Intergovernmental Panel on Climate Change (IPCC) which associates emissions from human activity to climate change is now widely accepted. Episodes where deteriorated air quality was pointed out were numerous in the last few years. Not all them are recent, as demonstrated by the brown cloud which occurred in December 1952 in London. During a particular cold week in winter, the coal burning peaked and caused the formation of lethal smog. Sulfur dioxide and particles concentration in ambient air reached several thousand μg m^{-3} and was responsible of up to 16 000 deaths (2). And nowadays, this kind of episode is not exceptional. Lately, in December 2011, Beijing airport had to cancel flights due to thick smog caused by the combination of coal-fired power plant (located at the periphery of the town) associated with emission from on-road transport. In Beijing where, in average, 2000 new cars are registered each month, the particle concentration in atmosphere became a major concern. The main responsible of air quality deterioration are fine particles, with aerodynamic diameter below 2.5 μm (so-called $PM_{2.5}$). In 2012, the International Agency for Research on Cancer (IARC) has classified particles emitted from diesel engine combustion as carcinogenic (3). This emphasizes the key role played by transport in the air quality. The first section of this introduction will focus on the most climatically active species present in the atmosphere and the contribution from the transport sector on their emissions. Then, the health impact of traffic-related pollution is discussed in the second section. The regulation on emissions from transport in Europe is described in the third section. Finally, the current developments in the field of fuel quality, engine technology and aftertreatment devices that can affect the emission quality are approached in the fourth section. The introduction ends with the presentation of the main objectives of the study.

1.1 Climate change

The dry atmosphere is composed essentially by Nitrogen (N_2) at 0.78 mol mol^{-1} and oxygen (O_2) at 0.21 mol mol^{-1}. The third gas in concentration is Argon (Ar) with a volume fraction of 9300 ppmv (0.0093 mol mol^{-1}). Except water, other species which compose atmosphere are considered as trace species. Among them, carbon dioxide (CO_2) has a concentration of 394 ppmv (July 2012 data collected by the Mauna Loa Observatory in Hawaii), methane (CH_4) 1.8 ppmv, and nitrous oxide (N_2O) 0.3 ppmv (4). These three molecules, owing to their dipole moment, have the capability to absorb solar and terrestrial infrared radiation. Consequently, these species contribute to global warming and are considered as greenhouse gases (GHGs).

1.1.1 Global warming and radiative forcing

The earth receives energy from the sun by the way of solar radiation. In the atmosphere, a share of these radiations is directly absorbed by clouds and earth's surfaces, whereas another share is reflected back into space. Then, a share of these radiation reflected are absorbed by the clouds and the atmosphere before reaching space. The albedo defines the fraction of the incident radiation that is scattered backward. In average, earth's albedo is around 0.3, which means that 30% of the radiation received by earth is reflected. The concentration of greenhouse gases in atmosphere has an impact on the quantity of radiation absorbed. The Radiative Forcing (RF) is a term defined by the IPCC in order to assess, in the surface-troposphere system, the real impact of factors which contributes either to warming or cooling the earth's climate system (5). It measures the influence of these factors on the balance of incoming and outgoing energy in the earth-atmosphere system (6). According the IPCC, the RF of the principal climatically active species influenced by the human activity since industrial era are displayed in Fig. 1.1.

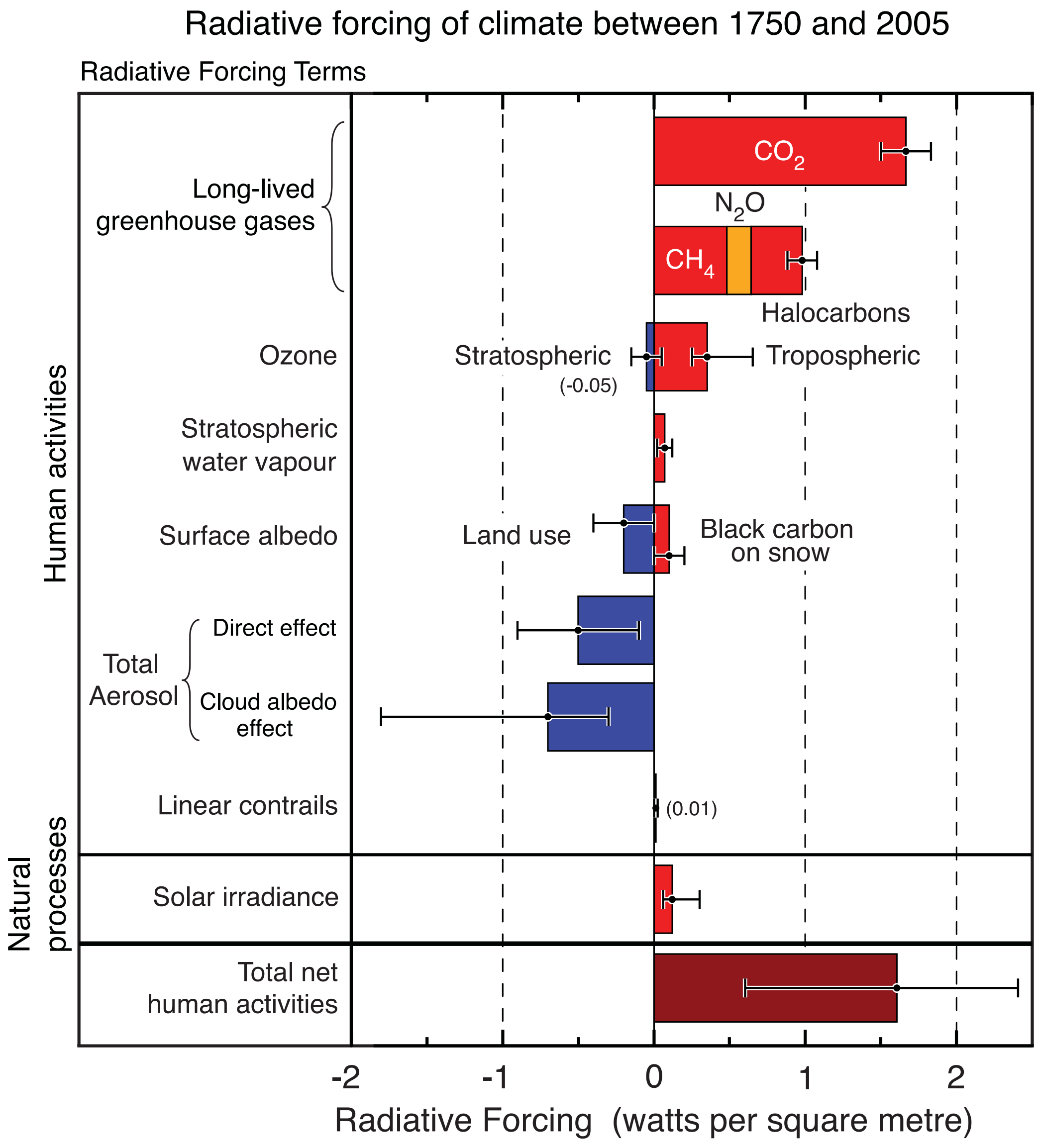

Figure 1.1: Principal components of the radiative forcing (RF) of climate change, associated with human activities or natural processes. - The values represent the RF of each component in 2005, considering the industrial era (1750) as background value (6).

Six families of compounds have a great RF. They are sorted between Long-Lived Greenhouses Gases (LLGHGs) including carbon dioxide (CO_2), methane (CH_4), nitrous oxides (N_2O) and halocarbons, and the short-lived species (SLS) including ozone (O_3) and aerosols (6).

Carbon dioxide (CO_2). CO_2 is the most abundant and also the most rapidly increasing LLGHGs. Its volume concentration increased by about 100 ppmv in 250 years, and ultimately, almost 20 ppmv increasing in 10 years between 1995 and 2005 (6). Once in the atmosphere, CO_2 is involved in several removal processes with different rates of uptake, thus, its residence time is defined in a range between 5 to 200 years (5). CO_2 comes mainly from the combustion of fossil fuel (coal, oil), for various purpose such as transportation, building heating, electricity transformation. The second source of CO_2 emission comes from the land use change (6). Forest clearing followed by cultivation, or conversion of grassland soils to pastures for grazing, are associated with a decrease of the carbon stock sequestrated in the soil and a release of this carbon to the atmosphere. This transfer of carbon, predominantly under the form of CO_2, occurs during the first years following the land use change, is estimated about 30% of the soil carbon (7).

Methane (CH_4). With an atmospheric residence time of 10 years, CH_4 is considered as a LLGHG (8). Its global warming potential is equivalent to 23 eq g CO_2 at 100 years time horizon (5) and its RF is the second largest after CO_2 (6). The main sources of CH_4 are anthropogenic, namely agriculture (livestock and rice production in particular), fossil fuel production, and anaerobic fermentation in landfills. However, biogenic sources, in particular wetlands, contribute as well in global CH_4 emissions (9). Methane is released during incomplete combustion of fuel in transportation, together with unburned hydrocarbons (10).

Nitrous oxide (N_2O). With an atmospheric residence time of more than 110 years, N_2O is considered as a LLGHG (6). According the IPCC, its global warming potential relative to CO_2 is equivalent to 296 eq g at 100 years time horizon (5). N_2O concentration has risen steadily and reached a concentration level of 319 ppb in 2005. N_2O comes mainly from agricultural process and is enhanced by nitrogen fertilizers (6). Though anthropogenic contribution from transport is low, it remains significant. In addition, this contribution is predicted to move towards 6-32% of the total N_2O flux growth rate as a consequence of the increase of global vehicle fleet (11).

Halocarbons (CFCs, HCFCs, and HFCs). Halocarbons term includes the bromo, chloro, and fluorocarbons which both contribute positively to the RF. These industrial chemicals are powerful greenhouse gases responsible of O_3 depletion, and therefore, they are regulated since 1987 by the Montreal Protocol. Whereas chlorofluorocarbons (CFCs), hydrochlorofluorocarbons (HCFCs), and chlorocarbons RF began to decline in 2003, hydrofluorocarbons (HFCs), perfluorocarbons (SF6) concentration increased significantly (6). The atmospheric residence time of these compounds vary from few to ten years, and some of them can reach more than 1000 years (5), so they can be considered as LLGHGs.

Ozone (O_3). Like CO_2, CH_4, and N_2O, the molecule of O_3 has the capability to absorb solar radiation. However, O_3 is involved in several photochemistry reactions and is continually produced and destroyed. Lifetime of O_3 is relatively short (few days in the troposphere), so it may be classified as a SLS. The consideration of O_3 RF in a strict sense required to distinguish stratospheric and tropospheric O_3. In the first case, the stratospheric ozone depletion (the “ozone hole") observed in 1985 by Farman et al (12) caused a cooling effect of the stratosphere. The different pathway responsible of stratospheric O_3 destruction involved hydrogen oxides (OH_x) nitrogen oxides (NO_x), chloride oxides (ClO_x), and bromide oxides (BrO_x) catalysis (4, 13, 14). ClO_x degradation at an altitude near 20 km induces ClO dimer catalytic cycle which is among the principal catalytic cycle destroying O_3 (13). The main source of ClO_x is anthropogenic and comes from halocarbons described previously.

In the second case, tropospheric O_3 is continually formed from precursors such as NO_x, CO, and Volatile Organic Compounds (VOCs) released by human activity (Fig. 1.2) (14, 15, 16). The photochemical reaction of VOCs and CO initiated by OH_x and catalyzed by NO_x results in O_3 production. The main driver of this production is NO_x concentration ($[NO_x]$) since its level is associated also to OH_x formation. Figure 1.3 summarizes the impact of fluctuation of $[NO_x]$ and [VOC] on O_3 formation (4). In this figure, ozone isopleths are used to estimate the impact of VOC and NO_x concentration fluctuation on the O_3 formation for a city where the ratio $[VOC]/[NO_x]$ is known (here the ratio of 8 is typical of North-American condition). Isopleths line display the constant 1-hour peak ozone. Two cases are distinguished, namely when $[NO_x]$ is low (NO_x limited regime) and when the $[NO_x]$ is high (VOC limited regime). The reduction of $[NO_x]$ in

NO_x limited regime is associated with lower O_3 formation (case B) whereas the same NO_x reduction in VOC limited regime can result in higher ozone production (case A).

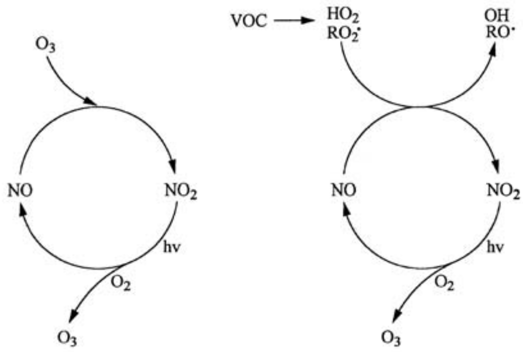

Figure 1.2: Basic reactions involving O_3 in the troposphere. - Reactions in presence of only NO_x results in no net formation of O_3 (left). Reactions in presence of NO_x and VOCs results in formation of O_3 (16).

Consequently, the variation of O_3 concentration in both stratospheric and tropospheric levels over industrial era resulted in opposite RF but the net effect of O_3 remains positive as described in Fig. 1.1

Aerosols. Fine aerosols are liquid and solid particles suspended in the air. Two categories of aerosols are distinguished: the aerosols directly produced from biogenic and anthropogenic sources - the primary aerosols, and aerosols formed in the atmosphere by chemical reaction, and condensation of semi-volatile gas-phase species - the secondary aerosols. Their reactions are very complex and dependent on the aerosol composition. The atmospheric lifetime of aerosols is highly variable, from hours to weeks, so these pollutants are classified as SLS (5). On one hand, organic carbon (OC), sulfate, and nitrate particles have the capability to scatter solar radiation back to space, therefore, these species contribute to increase the earth's albedo which results in a cooling effect (6, 18). The origin of these aerosols may be biogenic (dust, sea salt), biomass burning and fuel combustion (5). On other hand, black carbon (BC), also called soot, contributes to decrease the earth's albedo. Indeed, BC absorbs directly the energy from the incoming sunlight with the consequence to warm the atmosphere (6, 19). BC comes from the burning biomass, and a third of BC comes from fossil fuel burning, in transport (20). In addition to these direct effects, aerosols can also affect indirectly the climate.

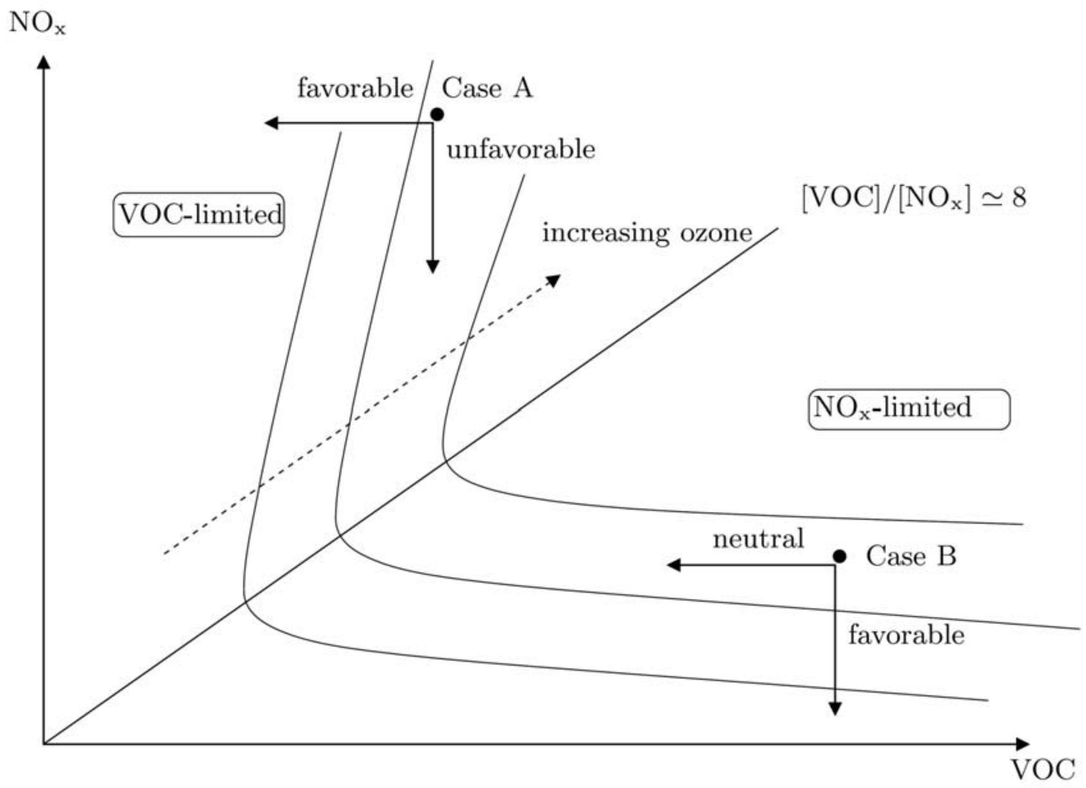

Figure 1.3: Chemical regimes which drive the tropospheric O$_3$ formation. - Diagram based on so-called empirical kinetic modeling approach (EKMA) from Dodge (17) adapted by Sportisse (4).

Hygroscopic aerosols modify cloud properties, acting as cloud condensation nuclei, and producing an increase of droplet number concentration and a decrease of droplet sizes. The result of this first indirect effect of aerosols is an enhancement of the cloud albedo (21). The second indirect effect is the consequence of smaller droplet sizes which inhibit precipitation formation and lengthen cloud lifetime (22). The overall effect of these two indirect effects is an increase of earths' albedo, and thus, a cooling effect. In addition, BC aerosol contained in the droplet absorbs solar radiation that can lead to the evaporation of clouds and therefore a reduction of clouds albedo. This effect is called semi-direct effect (23). Finally, BC can travel and its deposition on top of snow and ice causes premature melting and consequently a decrease of earth's albedo. However, the global impact of aerosols on climate change, combining direct, indirect, and semi-direct effects, results in a net cooling effect. It has been estimated that global aerosol effect since industrial era may have compensated 50% of the global warming caused by LLGHGs (6, 19).

1.1.2 Anthropogenic emissions from on-road transport sector

In the EU-15, the GHG emissions from transport increased by 17% between 1990 and 2009. The shares of CO_2, CH_4 and N_2O emissions from transport in the total GHG emissions of EU-15 account for 22%, 0.03% and 0.19% respectively (24). Figure 1.4 describes the the GHG emissions in transport by source category. CO_2 from on-road transportation represents the main share of the transport GHG emissions.

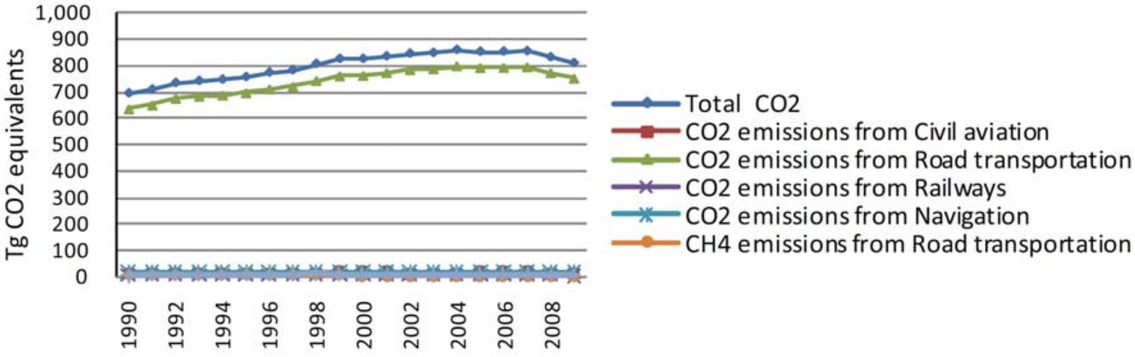

Figure 1.4: GHG emissions from transport in EU-15. - Source EEA (24).

Transport sector contributes to climate change (16% of integrated net forcing over 100 years from all current anthropogenic emission), specially road transport (25). The variation of pollutant concentrations relative to an unperturbed initial state can be related to several sources. Figure 1.5 displays the contribution of the previously described LLGHGs and SLS emitted by anthropogenic sector, and the ranking in terms of net sum of total RF, considering a constant year 2000 emissions. According to the figure, on-road transportation should be in 2020 the highest responsible of positive RF. Half of the positive RF is due to the SLS, and the rest from the LLGHGs (CO_2) (18).

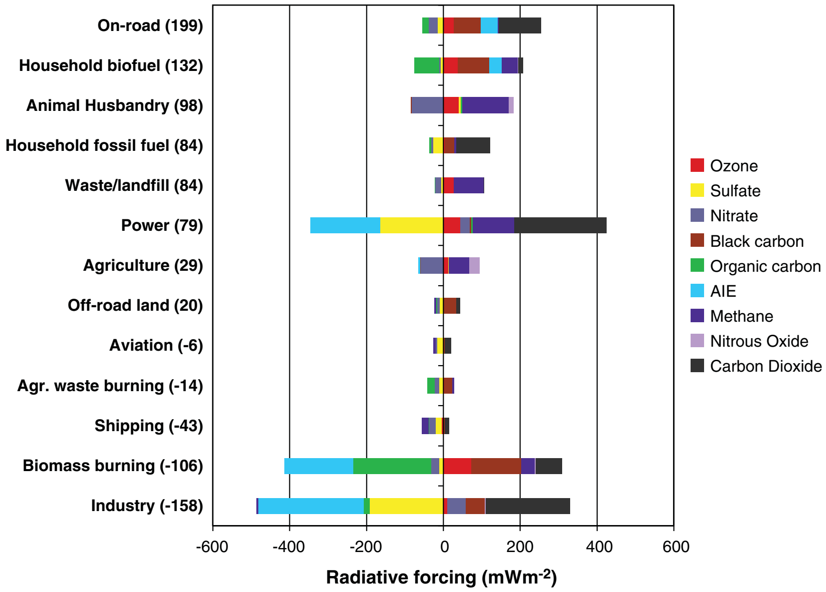

Figure 1.5: Net radiative forcing due to continuous year 2000 emissions by anthropogenic sectors at 2020. - Contribution from each species is displayed. The net sum of the radiative forcing of these species is indicated beside each sector (18).

A recent study related to RF from transport demonstrated that O_3 is the second dominating warming agent after CO_2 (25). Therefore, the study of O_3 precursors originate from fuel combustion (NO_x, CO and VOCs) is of major interest. Reducing on-road transport emission is a priority target in order to achieve a rapid abatement of anthropogenic radiative forcing (18). In addition, such action is in balance with recent studies which highlighted particular harmful properties of the traffic-related particles on human health (26, 27, 28, 29).

1.2 Health and environmental effect of traffic-induced pollution

A complete fuel combustion process produces CO_2 and H_2O. However, several by-products come along with these two main molecules. The first by-products result from the incomplete fuel oxidation which gives CO, hydrocarbons, and particulate matter. The second by-products are due to the oxidation of non-combustibles species available in the combustion chamber such as nitrogen gas N_2 present in the air, or sulfur present in the fuel and lubricant oil. The former is oxidized in NO_x, while the latter is oxidised in SO_x (30). Even released in extremely low quantities in comparison with CO_2 and H_2O, these species present risks to the environment, and in particular to human health.

Nitrogen oxides (NO_x). NO_x is a harmful compound, produced mainly in the atmosphere from anthropogenic sources, principally from combustion process of fossil fuel. The term NO_x stands for the sum of nitric oxide (NO) and nitrogen dioxide (NO_2). Nitrogen oxides are irritant for the respiratory tracts, in particular NO_2. NO_x is also a precursor of ground-level O_3 and it is also involved in the formation mechanism of acid rain. Traffic-induced emissions account for 65% of the total emission of NO_x in the troposphere (5). In the United States, 32% of the NO_x come from on-road vehicle and 30% from off-road vehicle (i.e. aircrafts and ships) (31). Diesel engines operate in leaner condition in comparison with gasoline engine, which means that Air/Fuel ratio (A/F) during diesel combustion is generally greater. This lean combustion stoichiometry has an impact on diesel engine emission, with an exhaust containing generally extremely low level of carbon monoxide and hydrocarbon, but more NO_x than gasoline exhaust.

Carbon monoxide (CO). CO is a pollutant of major concern from an environmental point of view because of its contribution to ground-level O_3 formation (together with NO_x and VOCs) which is a constituent of photochemical smog. CO is also highly toxic to humans since its direct action is to block oxygen uptake. Incomplete combustion of fossil fuel in road transport is one of the predominant sources of CO emissions (32).

Sulfur dioxide (SO_2). SO_2 is an eyes, throat and nose irritant. The effect of this pollutant is particularly focused on respiratory tracts, and is pronounced for persons with asthma. SO_2 emission is also associated to acid rain, and in combination with soot, is responsible of smog episodes in industrial areas. Released in the atmosphere, SO_2

can be further oxidised to SO_4 and sulfuric acid, forming aerosols in association with other pollutants or solid particles. Sulfur dioxide comes from the oxidation of sulfur contained in the fuel. Therefore, the EU legislation relating to the fuel quality has evolved the past several years to address this type of threat. For diesel fuel, Directive 93/12/EEC set sulfur content in fuel at 0.2 % by weight as from 1994 and 0.05 % as from 1996, then Directive 98/70/EC set 50 ppm by weight as from 2000, and finally Directive 2009/30/EC set 10 ppm as from 2011 (33, 34, 35). These Directives succeeded in decreasing progressively the concentration of SO_2 in the air. Scientists involved in the project Aphekom (Improving Knowledge and Communication for Decision Making on Air Pollution and Health in Europe) estimated that regulatory acts prevented 2200 premature deaths in 20 European countries, which valued 192 million euro (29).

Hydrocarbons (HC). Deriving from the incomplete combustion of fuel, lubricating oil, and pyrosynthetic reactions, the hydrocarbon group presents a large variety of compounds, including alkanes, alkenes, aromatics, and oxygenated organic compounds. Usually referred as VOCs, these species have the common characteristic to be in the gas phase at atmospheric condition, either because directly emitted in this state, or because the atmospheric dilution causes the evaporation of semivolatile organic compounds (SVOCs) from the combustion related primary organic aerosols (POA) (36, 37). Biogenic VOCs can dominate by a factor of 10 over the anthropogenic VOCs at worldwide scale but, in urban areas anthropogenic VOCs may be predominant (38).

Direct effect of VOCs on human health is specific for each singular species. Oxygenated compounds, such as formaldehyde and acetaldehyde are classified as human carcinogen and probably carcinogenic respectively by the U.S. Department of Health and Human Services (HHS) (39). Their emission can be originate from the lubricant oil or the oxygenated fuel used in the engine (40). Indeed, in Brazilian cities where implementation of high content ethanol fuel was operated, atmospheric level of formaldehyde and acetaldehyde has a close relationship with the vehicular fleet composition (41, 42, 43). Gas-phase polycyclic aromatic hydrocarbons (PAHs) can account for 20% of the total VOCs in urban area (44). PAHs are known to cause genetic damage and cancer (45, 46). Their harmful nature can be estimated with the toxicity equivalency factor approach where each individual PAH toxicity is appraised relatively to benzo[a]pyrene toxicity. The sum of the PAH toxicity calculated by this way gives the B[a]P toxicity equivalent (47). Beside their direct effect, VOCs undergo multiple physical and chemical reactions in the atmosphere, which can lead higher molecular weight SVOCs to evaporate from particle phase to gas phase, and condensate back to particle phase, thus increasing the secondary organic aerosols (SOA) production (14, 16, 36, 37). In addition, gas-phase reactions of VOCs, alkenes in particular, lead toward more oxygenated organic compounds and O_3 formation (14, 16).

Tropospheric ozone (O_3). O_3 is a powerful oxidant, and a major constituent of photochemical smog. Unlike the other pollutants described in this section, O_3 is not directly emitted by the transport sector, and its main precursors are CO, VOCs, under catalyst effect of NO_x (14, 16). Tropospheric O_3 is a global air pollution problem, with harmful impact on human health and natural ecosystems (48). Short term acute exposure to O_3 is associated with effects on lung function, respiratory symptoms, airway inflammation, allergic reactions and daily mortality, whereas long-term exposure can shorten life expectancy (48). In EU, an estimation from the European Environment Agency (EEA) states that annually, 21 400 premature deaths are related to O_3 (49). Considering the impact on vegetation, O_3 affects nutritional quality of major crop species and reduces their yields (50). This latter effect reduces terrestrial carbon pool in vegetation, and therefore, increase the RF of O_3 (48). Ground level O_3 in the troposphere has a concentration range between 20 and 60 ppb. In Urban area, this concentration can overpass 100 ppb (14), and even peak at more than 200 ppb during hot sunny summer days (48). The current U.S. National Ambient Air Quality Standard for O_3 is an 8-h average of 80 ppb. The Directive 2008/50/EC on ambient air quality and cleaner air for Europe sets daily 8-h average of 120 μg m^3 not to be exceeded on more than 25 days per calendar year averaged over three years (51). However, this threshold was overpassed in 17 EU Member States during summer 2010 (52). In EU, the recommendations are to monitor not only O_3 in ambient air, but also the precursors like NO_x and 30 hydrocarbons listed in the Directive 2002/3/EC (53). As described in the section 1.1.1, ground-level O_3 chemistry is difficult to predict by only reducing O_3 precursors. Indeed, in polluted regions where NO_x concentration are high, like in urban areas, efforts in NO_x concentration reduction can lead to an increase of urban O_3 concentration (VOCs limited regime).

Ammonia (NH_3). Ammonia is the third most abundant nitrogen containing compounds in the atmosphere (14). The total anthropogenic emission of ammonia amounted for 43 million of tons per year, which are 36% of the total budget including natural sources. Emission from agriculture is by far the most important of the anthropogenic sources (31, 54). Ammonia has adverse effect on vegetation close to its source (within a range of circa 5 km) (55). In addition, NH_3 reacts quickly in the atmosphere with HNO_3 and H_2SO_4 to form ammonium nitrate (NH_4NO_3) and ammonium sulphate (NH_4SO_4), which contributes to fine particles and visibility problem in a larger scale (up to 2500 km) (56, 57). Figure 1.6 illustrates the main sectors which contribute to the global NH_3 emission in United States (US) in 2005, according the National Emission Inventory (NEI) done by the US Environmental Protection Agency (EPA) (31). Although contribution from road transport sector represents 7% of the total US emission, a recent study pointed out that motor vehicle contribution can reach about 14% in South Coast Air Basin, and more than 70% in urban areas during winter (58). Ammonia related to traffic comes mainly from the Three-Way Catalyst (TWC) of the light-duty passenger cars. It is considered as a secondary pollutant since NH_3 is not a direct product of the fuel combustion, but is formed in the aftertreatment system during the DeNOx process (59). The formation mechanism of NH_3 involves NO and H_2. NO is generated by the oxidation of N_2 during combustion. H_2 is mainly produced in the catalyst during the water gas shift reaction of CO (60, 61). Accordingly, NH_3 formation in the catalyst is enhanced at rich conditions (low A/F ratios) where higher CO concentrations can produce more H_2 (62, 63, 64). The increase of the TWC equipped vehicle, together with the increase of the total vehicle explain the change of the NH_3 estimation by sector (65). However, it is expected that NH_3 emission factor decreases with increased of emission standard stringency (including NH_3 precursors like NO_x and CO) (66).

Particulate matter (PM). PM has a strong impact not only on climate change, but also on human health (27, 28). Despite the fact that primary biogenic sources (sea salts and dust) are the main contributor in net aerosol mass emissions (5), anthropogenic emission of PM from transport can represent up to 50 % in urban area (67, 68). The PM chemical composition is highly variable, with a mixture of organic and inorganic species, soot and water (4). Traffic-induced airborne particles are a complex mixture of solid and liquid material. The harmful effects of PM are due to both their physical and chemical properties. While most of the particles mass are contained in aerodynamic diameter range of 50 nm to 1000 nm (called accumulation range), the highest fraction of particles has a diameter below 100 nm (69). These latter particles are sorted in a class range between 10 and 100 nm, called transient nuclei range, and below 10 nm, called nucleation

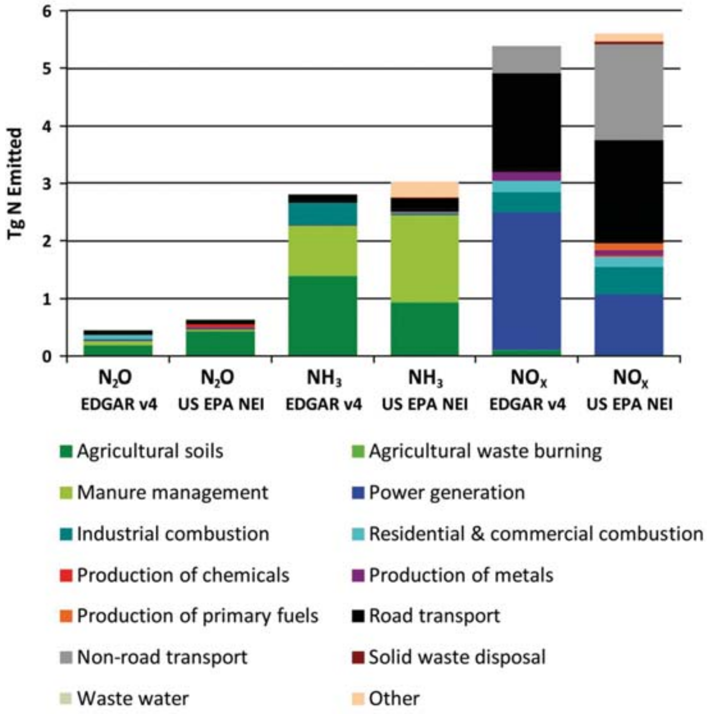

Figure 1.6: National Emission Inventory (NEI) of N_2O, NH_3, and NO_x in US for the year 2005. - The NEI carried out by the US EPA are compared with the Emissions Database for Global Atmospheric Research (EDGAR) developed jointly by the European Commission Joint Research Centre (EC-JRC) and the Netherlands Environmental Assessment Agency (31).

mode (70). Even if particulates could be formed by toxicologically inert material, the size distribution had to be taken into account since an increase number of adverse health effect has been demonstrated with decreasing particles size. The smaller is the particle, the more deeply it could penetrate in the respiratory ways and therefore in the lung air cells (69). The composition of the solid phase of these particles (soot, metal ashes), together with the compounds contained in the liquid phase (low volatility hydrocarbons, polycyclic hydrocarbons, and sulfuric acid) make them particularly hazardous to breath. The changes in size distribution and composition made their toxicity difficult to assess, however, several studies associated airborne particles concentration with respiratory and cardiovascular diseases (27, 71, 72). The particle deposition on the respiratory tracks can cause airways inflammation. This immune response consists in leukocytes and endothelial adhesion molecules production. These molecules induce temporary a blood hypercoagulability responsible of cardiovascular events (28).

The World Health Organization (WHO) has set an air quality guideline with limit value of 20 μg m^3 for PM$_{2.5}$ as annual average, however, this limit is not always respected. Scientists involved in the project Aphekom correlated the overpassing of this limit and the decrease of life expectancy. Between 2008 and 2011, in 25 European countries composed of 39 million inhabitants, the PM$_{2.5}$ exceeding limits led toward 19 000 deaths, 70% of which by cardiovascular diseases (29). The US EPA published in 2002 a health assessment document related to the effect of traffic-induced particles from diesel exhaust. Short-term and long-term exposures were reported. EPA stated that the short-term exposures were associated with irritation and inflammatory symptoms of the respiratory tracts, whereas the long-term exposures were likely to cause lung cancer hazards to humans (45). Diesel combustion process is heterogeneous; the air-fuel mixing occurs directly in the combustion chamber, enhancing diffusion-type burning instead of combustion of a well-mixed air-fuel mixture, as it occurs with gasoline combustion (73). Consequently, diesel particulate matter (DPM), along with NO$_x$, are the main drawbacks which lead the focus of car manufacturers to invest in control technology. Estimation of traffic-related contribution in airborne particles is difficult because non-combustion PM must be considered as well. Resuspended road dust, tires, and brake wear from vehicles became progressively noticeable along with the tightening of emission standard (67). In addition, measurement of composition and size distribution of particles is dependent upon the conditions of dilution and humidity, making comparison between studies difficult (74).

1.3 European legislation on vehicles emissions

The first emission legislation was initiated in US by the California Air Resources Board (CARB) in 1967, and was extended by the EPA to the global US territory in 1970. The same initiative was introduced by the EU in 1970 with the Directive 70/220/EEC (75). The pollutants addressed by these provincial and national regulations were NO_x, CO, HC, and PM mass. These environmental regulations became tighter overtime, with the significant reduction of the standards. The reduction of EU emission standards was implemented when vehicle or refinery technologies were available, in collaboration with the different stakeholders, like the oil companies' European association for environment, health and safety in refining and distribution (CONCAWE), the European Council for Automotive Research and Development (EUCAR), under the control of the European Commission (EC). Table 1.1 describes the evolution of EU emission standards for type approval of gasoline and diesel light-duty vehicles, diesel heavy-duty vehicles, and motorcycles.

In addition to Directives associated with regulation of direct emission from combustion engine, other regulatory acts at EU level contribute to the modification of the fuel quality, and therefore, have an impact on vehicle direct emissions. Firstly, the Renewable Energy Directive (RED) 2009/28/EC designed as a part of the so-called "EU Energy Package" aimed to promote the use of renewable energy, such as biofuels, in the transport sector (77). The mandatory target set by RED is 10% share of energy from renewable sources in transport in Community energy consumption by 2020. Secondly, the Fuel Quality Directive (FQD) 2009/30/EC defined requirements for petrol and diesel fuel in order to reduce fuels' life cycle GHG emissions (35). The target set by the FQD is 6% reduction of life cycle GHG emissions from fuel or energy supplied in 2020 in comparison with the 2010 fossil fuel baseline. A complete assessment of the GHG emitted in the global fuel life cycle should be mentioned, however fuel consumed by air transport are not covered by FQD (while RED include this fraction). Finally, an agreement was signed in 1998 between the European automobile manufacturers association and the EU in order to set a regulation of CO_2 emissions from light-duty vehicles

Standard	Implementation	THC	NMHC	NO_x	CO	$HC+NO_x$	PM
Spark Ignition (Gasoline) Light-Duty Vehicle [g/km]							
Euro 1	07/1992	-	-	-	2.72	0.97	-
Euro 2	01/1996	-	-	-	2.2	0.5	-
Euro 3	01/2000	0.2	-	0.15	2.3	-	-
Euro 4	01/2005	0.1	-	0.08	1	-	-
Euro 5	01/2009	0.1	0.068	0.06	1	-	0.005
Euro 6	09/2014	0.1	0.068	0.06	1	-	0.0045
Compression Ignition (Diesel) Light-Duty Vehicle [g/km]							
Euro 1	07/1992	-	-	-	2.72	0.97	0.14
Euro 2	01/1996	-	-	-	1.0	0.7	0.08
Euro 3	01/2000	-	-	0.5	0.64	0.56	0.05
Euro 4	01/2005	-	-	0.25	0.5	0.3	0.025
Euro 5	01/2009	-	-	0.18	0.5	0.23	0.005
Euro 6	09/2014	-	-	0.08	0.5	0.17	0.0045
Compression Ignition (Diesel) Heavy-Duty Vehicle [g/kWh]							
Euro I $\leq$ 85 kW	1992	1.1	-	8	4.5	-	0.612
Euro I $>$ 85 kW	1992	1.1	-	8	4.5	-	0.36
Euro II	10/1995	1.1	-	7	4	-	0.25
Euro III	10/2000	0.66	-	5	2.1	-	0.16/0.21 *
Euro III - EEV	10/2000	0.25	-	2	1.5	-	0.02
Euro IV	10/2005	0.46	-	3.5	1.5	-	0.02
Euro IV - EEV	10/2005	0.25	-	2.0	1.5	-	0.02
Euro V	01/2008	0.46	-	2.0	1.5	-	0.02
Euro V - EEV	01/2008	0.25	-	2.0	1.5	-	0.02
Euro VI $^{\circ}$	01/2014	0.13	-	0.4	1.5	-	0.01
Spark Ignition (Gasoline) Motorcycles and Mopeds [g/km]							
Euro 1 moped	06/1999	-	-	-	6	3	-
Euro 2 moped	06/2002	-	-	-	1	1.2	-
Euro 1 2-S M $^{\Delta}$	06/1999	4	-	0.1	8	-	-
Euro 1 4-S M $^{\triangle}$	06/1999	3	-	0.3	13	-	-
Euro 2 <150 cm^3	01/2004	1.2	-	0.3	5.5	-	-
Euro 2 $\geq$150 cm^3	01/2004	1	-	0.3	5.5	-	-
Euro 3 <150 cm^3	01/2006	0.8	-	0.15	2	-	-
Euro 3 $\geq$150 cm^3	01/2006	0.3	-	0.15	2	-	-

NMHC stands for Non-Methane Hydrocarbons. * for engine having swept volume < 0.75 dm^3 per cylinder and a rated power speed > 3000 min^{-1}. $^{\circ}$ for Euro VI emission standard, NH_3 and particle number are introduced, with limits of 10 ppm and 8.0 x 10^{11} respectively according regulation 582/2011 (76). $^{\Delta}$ stands for 2-stroke motorcycle. $^{\triangle}$ stands for 4-stroke motorcycle.

Table 1.1: European emission standards for light-duty, heavy-duty vehicles, and motorcycles. For light-duty vehicles, the test cycles are the urban plus extra urban driving cycles for Euro 1 and 2, and the New European Driving Cycles (NEDC) from Euro 3 onwards. For the heavy-duty vehicles, the test cycles are the ECE 49 for Euro I, ECE R49-02 for Euro II, the European Steady-State/European Load Response (ESL/ELR) from Euro III onwards. For mopeds and motorcycle, the test cycles are the ECE-47 and ECE-40 respectively.

(LDVs). Regulation 443/2009 set a limit of 130 g CO_2/km for a fleet of vehicle in 2015 and 95 g in 2020 (78). This regulation should promote the efficiency of internal combustion engine, which should move toward the more efficient diesel engines, and thus, toward more diesel specific pollutants. The Figure 1.7 describes the actual tendency over the world in terms of vehicle CO_2 emissions with the target enacted and proposed.

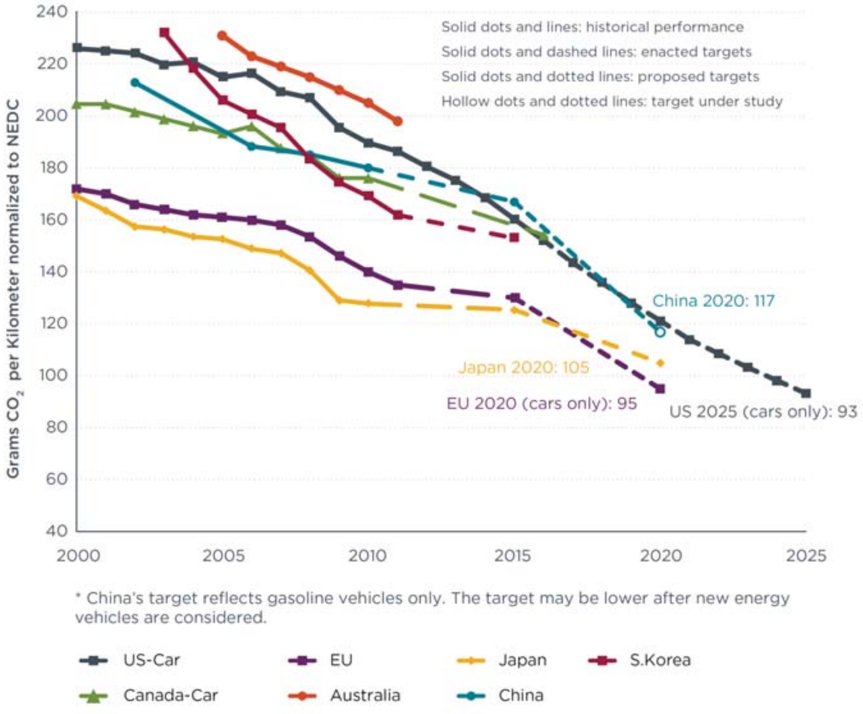

Figure 1.7: Vehicle CO_2 regulation by region. - Vehicle CO_2 regulation by region in terms of g km^{-1} over a New European Driving Cycle (79).

Regulation EC 725/2011 on “eco-innovation" related to the regulation 443/2009 defines procedures for the approval and certification of innovative technologies for reducing CO_2 emissions (80). This regulation allows cars manufacturers to grant a benefit up to 7 g/km in the calculation of the regulation 443/2009, by implementing either at a scale of one model, or at the scale of its complete fleet, an innovative technology. To be eligible, these technologies must be innovative (less than 3% market penetration in 2009), necessary for the base functions of the vehicle (comfort devices are excluded), verifiable with a minimum CO_2 saving threshold of 1 g km^{-1}, and not switchable by the driver (except in the case of the lights). As examples, several eco-innovation, improving vehicle lighting efficiency by moving toward LED technology, implementing solar roof on the vehicle to generate and store electricity in an on-board battery, or the engine encapsulation to maintain the engine compartment in warm condition longer, and by this way, reducing the cold start effect of the vehicle.

Modifications are expected in fuel quality, in line with these Directives, with an increase of biofuel contents in conventional fuel, or the development and implementation of alternative energy sources (LPG-CNG, electricity). To comply with the ambitious target set by the Regulation 443/2009, the diesel/gasoline ratio in EU is expected to increase as described in the Fig. 1.8 from the EEA.

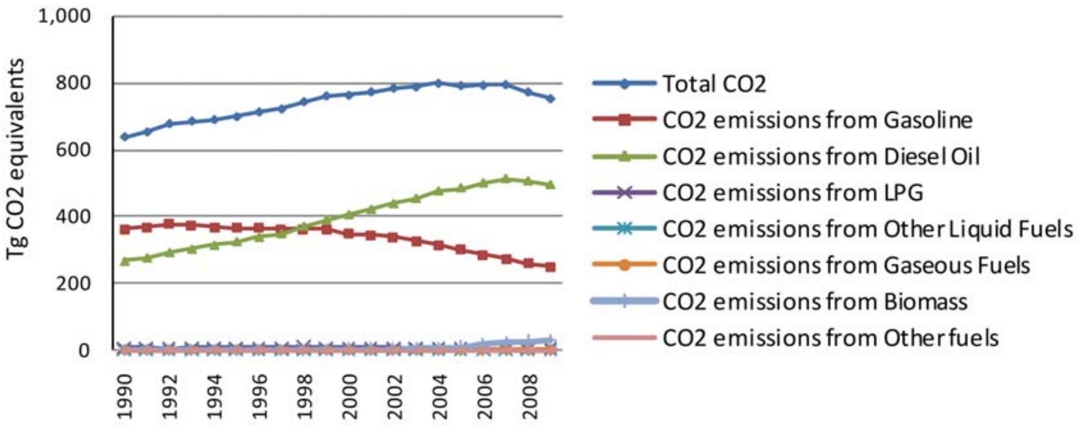

Figure 1.8: Share of CO_2 emission by fuel type from on-road transport in EU-15. - Whereas gasoline combustion CO_2 emission was dominating the road transport sector, diesel combustion overpassed gasoline level in 1998. The share of biomass combustion became substantially noticeable since 2005(24).

Life cycle analyses of alternative fuels such as biofuel indicates beneficial effect in terms of global warming, with lower emissions of regulated pollutant and CO_2. However, biofuel can have a side effect of increasing direct emissions of highly toxic unregulated pollutants. Such a circumstance has been noticed in Brazil where the implementation of ethanol in the fuel was associated with an increase of carcinogenic acetaldehyde and formaldehyde levels in ambient air (41, 42, 43). On the other hand, regulations applied to improve air quality can also have negative effect on the climate. SO_2 is known to induce asthma, bronchitis and heart failure. Therefore, sulfur content was regulated in fuel through Directives 93/12/EEC and 99/32/EC. The result was found to be very positive and beneficial to human health. However, emission of SO_x from transport sector has substantial cooling effect on climate (25). Figure 1.9 describes the global radiative forcing of transport subsectors by substances for 2000 relatively to preindustrial times. In some cases, regulation pushes policy makers to face a real dilemma.

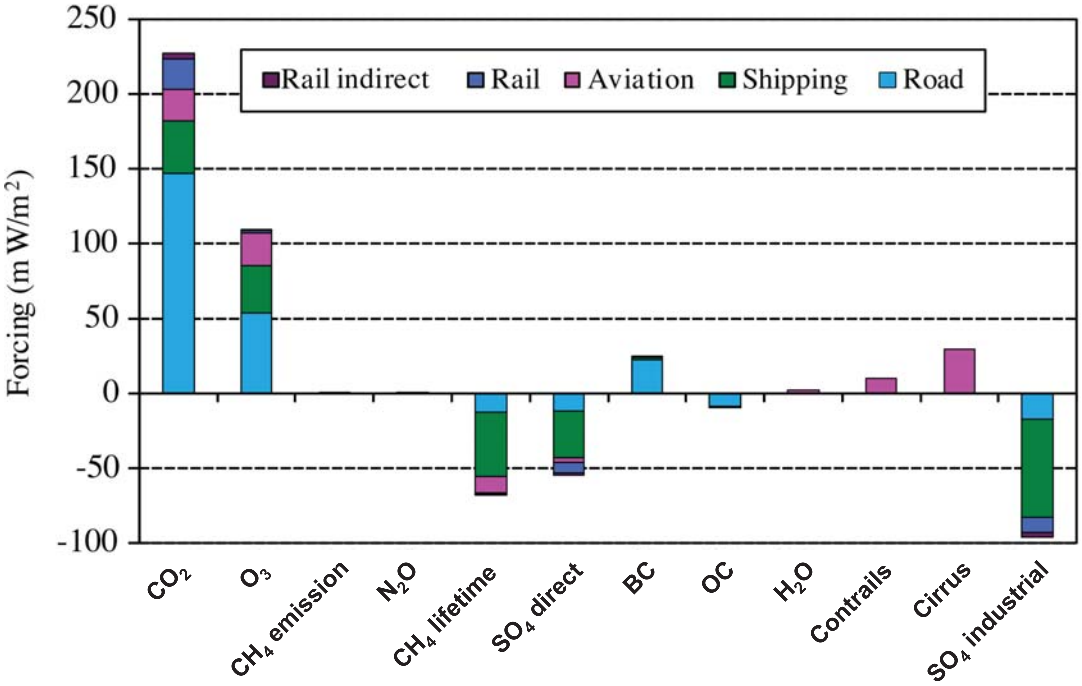

Figure 1.9: Global radiative forcing of transport subsectors by substances for 2000 relatively to preindustrial times. - Global radiative forcing of transport subsectors by substances for 2000 relatively to preindustrial times (25).

Regulations are not always a straight forward solution for the abatement of the pollution since compounds can react together in the atmosphere. The influence of tightening emission of one pollutant can have an impact on the atmospheric chemistry and lead toward the unexpected increased of other harmful pollutants, like tropospheric O_3 formation described in section 1.1.1. The great challenge to deal with when designing future regulations is not only linked to the risk or threats associated with regulated pollutants emissions such as CO_2, NO_x, or PM, but also to the unregulated pollutants.

New fuels, engine technologies or aftertreatment systems developed to comply with the latest regulation can be the source of unexpected environmentally harmful pollutants. Consequently, market penetration of new technologies must come along with a thorough control of the potential side effects, considering the state of knowledge in terms of environmental impact of pollutants. For this purpose, a particle number emission standards was introduced for light-duty and heavy-duty vehicles (Euro 6 and Euro VI respectively), or a NH_3 emission intensity limit (10 ppm) for heavy-duty vehicles (76, 81). The identification of these new pollutants, together with the more appropriate measurement methodology, is the task of the additional pollutants subgroup, included in a working party (WP29) in the institutional framework of the United Nations Economic Commission for Europe (UNECE). The WP29 aims to harmonize the light-duty regulation on a global scale. Considering the technical evolutions undergone by the on-road transport sector, the new gaseous pollutants planned to be included in the next emission regulation are three oxygenated hydrocarbons (formaldehyde, acetaldehyde, and ethanol), and three nitrogen species (NO_2, N_2O, and NH_3). While the first group of oxygenated species are closely linked to the growing share of oxygenated biofuel used in transport, ethanol in particular (see section 1.2), the second group is rather linked to the modern aftertreatment devices, and their tendency to generate catalytically induced harmful N-species. Consequently, the current developments in the field of biofuels, engine technology, and aftertreatement are addressed in the following section.

1.4 Current developments and possible alternatives to reduce emissions from on-road transport sector

1.4.1 Biofuel

The energy-chain efficiency of typical petrol engines is about 25% (82). Whereas energy contained in fuel is used to i/ speeding up the vehicle, ii/ compensate air resistance, and iii/ compensate rolling resistance; almost 75% of this energy is lost as heat. Improvement of the material used in the cars, lighter and stronger can lead toward substantial improvement of the efficiency. However, the energy-chain in Electric Vehicles (EV) engines are on average 3.5 times more efficient compare to internal combustion engines (82), so they could be an option to reduce the environmental impact of transportation. Indeed, EV use alternative energy paths which can secure mobility by making transport less dependent from crude oil (83). Peak oil estimation is a controversial issue as it required an exhaustive census of oil fields, however, a recent study from Murray and King (2012) pointed that oil production volume has reached a limit since 2005. As described in Fig. 1.10, this study based on elasticity between the demand and price, demonstrates an elasticity of crude oil production until 2004-2005 whereas from this date, production hardly follow the price of the barrel in spite of its increase (84).

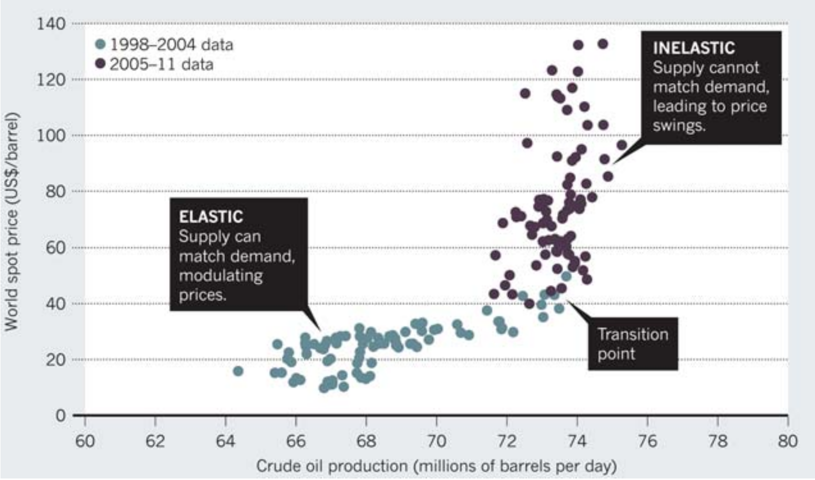

Figure 1.10: Worldwide crude oil production as a function of the oil price from 1998 to 2011. - The change of oil economics has been reached in 2005, date from which oil price increased without an direct increase of oil production (84).

However, the total cost of ownership is greatly influenced by the purchase cost of vehicles, which will be significantly higher until 2030 for EV if compared to internal combustion engines (85). For this reason, most optimistic scenarios forecasted to assess EV market penetration, expect a maximum of 25% by 2030 (see (86) and references therein). Consequently, an additional sustainable fuel has to be implemented in the near future to reduce GHG emissions from transport in accordance with RED and FQD guidelines. The four main sustainable sources pointed out nowadays are biofuels, hydrogen, natural gas, and synthesis gas, however, biofuels used in high proportion in fuel can be the most environment friendly energy source (87). Biofuels are referred to gas, liquid, and solid fuels predominantly produced from biomass. The biofuel market is actually the most mature in comparison with other options, making biofuel a promising candidate to fulfil the ambitious 10% share of energy from renewable sources set by the RED. In EU, the contribution of biomass burning in the total GHGs emission from transport sector became noticeable in 2005, as described in Fig. 1.8 (24).

Depending on the feedstock used for their production, several generations of liquid biofuels can be distinguished. First generation liquid biofuels technology used to convert corn, palm oil, and soy into fuel. However, this generation of biofuels raised a lot of controversy since its production competed with food supply. Considering the life-cycle analysis, first generation of biofuels could release as much GHGs as it saved, depending on the feedstock used, fertilization could lead toward important emission of N_2O (a LLGHG which is a by-product of N-fertilization), and therefore, enhancing the greenhouse warming (88). Second generation liquid biofuel uses non-food plants (perennial crops, fast growing trees, waste streams with large cellulose content), lowering their cost due to the lower competition with food production. Switchgrass is an example of potential biomass to use for the second generation of biofuel. It grows on land unsuitable for food crops. It is perennial (no need to re-plant it) and require very low quantity of fertilizer (thus low energy petroleum based chemical). For both generations, the production process consists in collecting the sugars from biomass and converting them into alcohol by fermentation process. Then, the right alcohol grade required is collected by distillation. The biodiesel is produced by transesterification of vegetable oil and animal fat with short chain alcohols (methanol or ethanol) forming fatty acid methyl/ethyl esters (89).

However, the second generation biofuels raised the problem of direct and indirect effect of land use change. The IPCC considers that land use change contributes to release carbon in the atmosphere, for instance when biofuel is produced from a new cropland (i.e. conversion of forest into agricultural land). This latter case is classified as direct land use change. Indirect land use change is caused by the crops grown to make biofuel instead of food on existing arable land, which generate the displacement of crops used to make food on new cropland (90). Therefore, even though non-food crop are used to produce biofuel, it could induce GHG emissions. For this reason, third generation of liquid biofuel were developed, produced from microbe and microalgae (87). The advantage of algae is the possibility to be grown in arid environments with brackish water, saltwater or polluted water. Figure 1.11 describes the different generation of biofuels, and their principal process of production.

The environmental benefit of biofuel in terms of GHG emissions are controversial, mainly because of the way to include land use change related to biofuel production (91). However, in terms of direct tailpipe emission, biofuels like ethanol are generally associated with significant reduction of CO and HC (including PAHs) (92, 93). Regarding biodiesel, most of the studies report significant reduction of PM, CO and HC (including

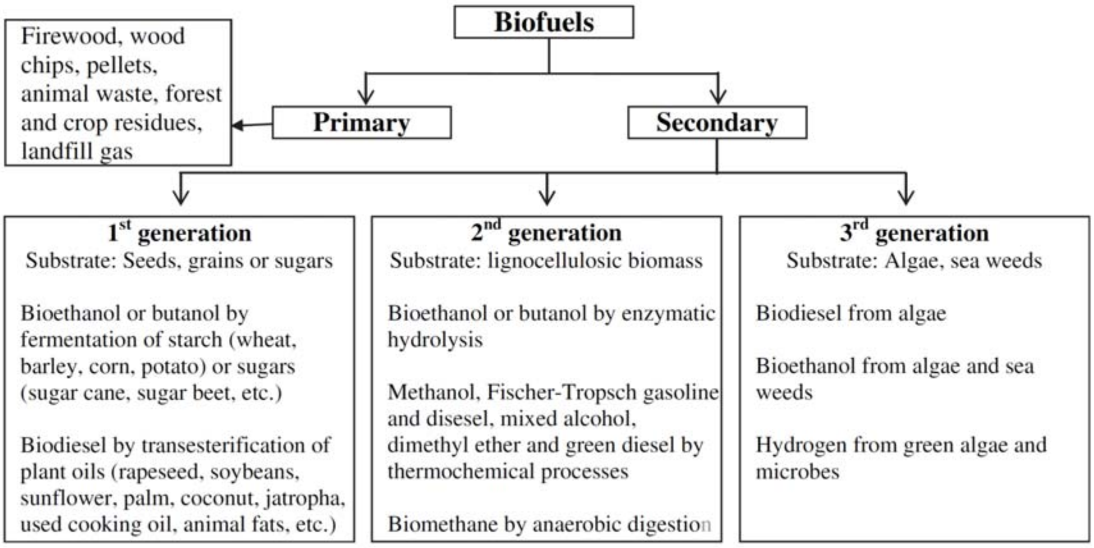

Figure 1.11: Different category of biofuels. - From (87).

PAHs), mainly because of the higher oxygen content and a more complete combustion (94, 95, 96, 97, 98). On the other hand, studies demonstrated that ethanol used in high concentration in gasoline can emits more harmful oxygenated compounds such as acetaldehyde and formaldehyde (99, 100, 101, 102). Some studies associate biodiesel fuel to high NO_x emissions (see (94) and references therein).

The key advantage of biofuels is the use of renewable sources for their production, such as natural bioresources, which are geographically more evenly shared over the world. Consequently, biofuels provide energy independence and security (87). The World Commission on Environment and Development (WCED) defined "sustainable development" as that which "meets the needs of the present without compromising the ability of future generations to meet their own needs" (103). According the WCED, the sustainable development requires a long term vision, where air pollution (that affects one generation) has lower ranking than global warming (that affect millennia), the latter has lower ranking than the loss of biodiversity (that is irreversible). Although biofuels can have some harmful effects on human health through their air quality impacts, the actual challenge is to minimize these effects by adapting engine technology and aftertreatement system to this alternative fuels.

1.4.2 Vehicle emissions control

Encouraged by the succession of emission standards, development and implementation of new technology was operated since 1970 to tackle the by-products of fuel combustion. The tasks to face were the reduction of NO_x to molecular nitrogen N_2, together with the oxidation of CO and unburned HC to CO_2 and H_2O. The strategies available to carry out pollutant emissions reduction were located at three different levels, starting from the tank (quality of the fuel), the engine (combustion process), and the tailpipe (aftertreatment devices).

1.4.2.1 Fuel quality

Improvement of fuel quality operated over the last decades through impurity reduction, or new fuel additives, lead toward great benefit for air quality. It was the case of SO_2 emission reduction which followed the regulatory acts on sulfur content in fuel described in section 1.2. Another example, the reduction of lead content in a fuel imposed by Directive 85/210/EEC resulted in an equivalent reduction of lead concentration in the air, consequently, lead was banished from gasoline fuel starting from 2000 onwards (104).

1.4.2.2 Engine technologies

Optimization of fuel combustion was a main target for car manufacturer which promote, in essence, efficient vehicles whose engines extract the maximum energy from the fuel. EGR stands for the exhaust gas recirculation. This system consists in returning a portion of engine's exhaust before the intake valve (in case of spark ignition engine), or to the pre-combustion chamber (for compression ignition engine). The reinjected gas absorbs a fraction of the calories produced by the combustion, and provides less oxygen to the mixture. Consequently, the air fuel mixture becomes poorer in oxygen, which cause a lower combustion temperature and thus decreases NO_x formation. The other side is the incomplete combustion which could occur if the EGR rate is not well adjusted, with the consequence of soot formation. The EGR technology is widely used to take care of NO_x abatement, while taking account of the PM-NO_x tradeoff (105). Consequently, EGR adjustment is operated in association with the injection strategy. Figure 1.12 illustrates the basic principle of EGR implementation in a diesel engine. The zones of NO_x and soot formation are expressed in terms of fuel:air ratio (flame equivalence ratio) and flame temperature. An early injection of the fuel improves the mixture with gas and prevents PM formation (106). Fuel injection technology is also a lever to improve the fuel efficiency and to reduce emissions. While diesel engines are equipped with a direct injection system into the combustion chamber, this technology was implemented only recently in modern gasoline engines, with the so-called Gasoline Direct Injection technology (GDI). Unlike conventional multi-point fuel injection where gasoline is injected in the intake track, in GDI pressurized gasoline is directly injected into the cylinders. Consequently, the engine can operate in stratified charge with air fuel mixture richer in oxygen, which reduces pumping losses and greatly improves engine efficiency. Turbocharging is popularly implemented in direct injection engines in order to pressurize air before injection. These injection technologies were exploited by the automobile industry to implement a downsize strategy. Downsizing consists in making smaller engine without losing power, and consequently resulting in more efficient vehicles.

1.4.2.3 Aftertreatment devices

Third, development of efficient aftertreatment devices were greatly promoted by the regulation standards. Spark ignition vehicles used Three-Way Catalysts (TWC) since the seventies (60). Following the so-called two-way catalyst which aimed to complete the oxidation of CO and HC to CO_2 and H_2O, the TWC had the capability to operate at the same time the reduction of NO_x to N_2. The basic principle of oxidation of unburned HC (equation 1.1) and CO (equations 1.2 and 1.3), together with the reduction of NO (equations 1.4, 1.6, and 1.8) and NO_2 (equations 1.5, 1.7, and 1.9) are provided below:

$$C_xH_y + \left(x + \frac{y}{4}\right) O_2 \rightleftharpoons xCO_2 + \frac{y}{2}H_2O, \tag{1.1}$$

$$CO + \frac{1}{2}O_2 \rightleftharpoons CO_2, \tag{1.2}$$

$$CO + H_2O \rightleftharpoons CO_2 + H_2, \tag{1.3}$$

$$NO + CO \rightleftharpoons \frac{1}{2}N_2 + CO_2, \tag{1.4}$$

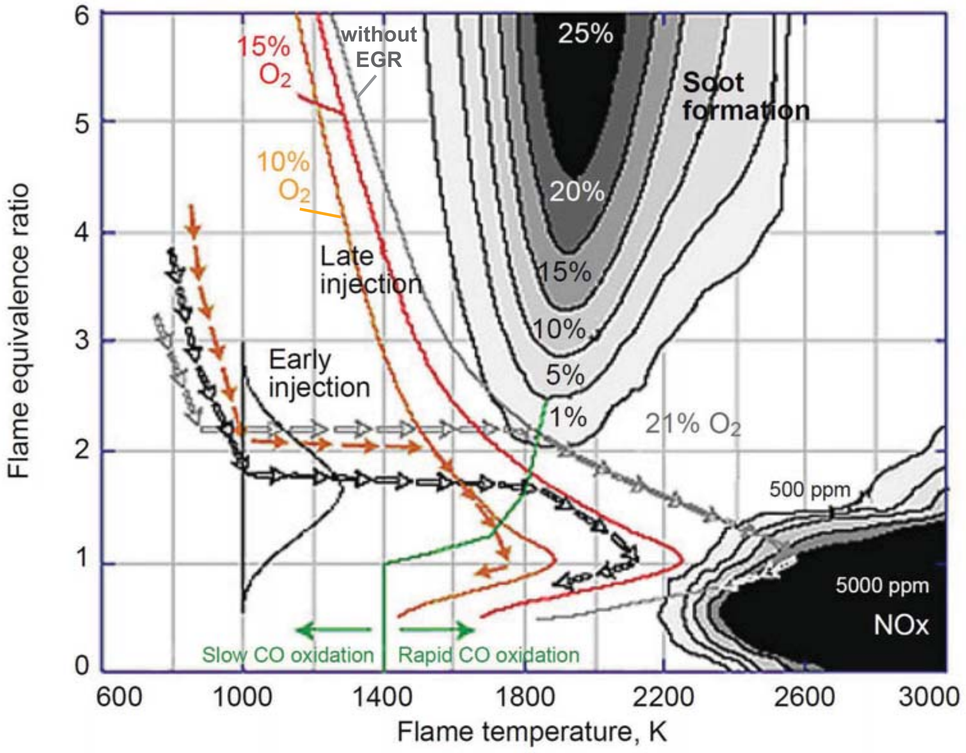

Figure 1.12: Principles of EGR used for diesel combustion and regimes of soot and NO_x formation expressed in terms of flame equivalence ratio (fuel:air ratio) and flame temperature. - EGR acts as a heat sink, and displace some of the oxygen induced with the fresh air charge. The grey curve indicates the engine operating condition without EGR. In case of early injection of exhaust gas, temperature of the flame becomes significantly lower, and O_2 available drop to 10% (orange curve), whereas in case of late injection, temperature of the flame become slightly higher (but still below the without EGR condition), and more O_2 is available (red curve). In both condition, EGR allows avoiding NO_x and soot formation zone, but engine injection strategy must take into account sufficient CO oxidation (green curve) (106).

$$NO_2 + 2CO \rightleftharpoons \frac{1}{2}N_2 + 2CO_2, \tag{1.5}$$

$$NO + H_2 \rightleftharpoons \frac{1}{2}N_2 + H_2O, \tag{1.6}$$

$$NO_2 + 2H_2 \rightleftharpoons \frac{1}{2}N_2 + 2H_2O, \tag{1.7}$$

$$\left(2x + \frac{y}{2}\right) NO + C_xH_y \rightleftharpoons \left(x + \frac{y}{4}\right) N_2 + xCO_2 + \frac{y}{2}H_2O, \tag{1.8}$$

$$\left(x + \frac{y}{4}\right) NO_2 + C_xH_y \rightleftharpoons \left(\frac{x}{2} + \frac{y}{8}\right) N_2 + xCO_2 + \frac{y}{2}H_2O. \tag{1.9}$$

The catalyst promotes these reactions at lower temperatures than required. However, above reactions require a minimum temperature to be carried out at the catalyst surface. Consequently, when the vehicle starts, the catalyst needs time to be effective, time during which the catalyst is heated up by the exhaust gas. The temperature where the catalytic reactions initiate is called the catalyst light-off temperature. This light-off is slightly different for each pollutant, and generally CO oxidation occurrs first (at lower temperatures) followed by HC and NO$_x$ reactions (107). In order to be fully operational for concomitant oxidation and reduction of the pollutants, the engine A/F ratio must be stoichiometric (A/F weight ratio around 14.6) as described in Figure 1.13. Higher A/F ratio causes lean combustion, whereas the contrary causes rich combustion. Usually, very close loop A/F ratio is necessary for the TWC to be efficient, however, the operating A/F window is narrow and a fluctuation out of the stoichiometric ratio comes along with emission peaks. NO$_x$ emission peaks usually appeared during sharp acceleration events when late compensation of lean combustion occurred.

Nowadays, the preferred TWC catalyst support is a ceramic monolith with honeycomb structure, coated by a mixture of magnesium oxide, silicon dioxide, and aluminium oxide. The catalyst material carried by the washcoat are usually precious metals, in particular platinum, palladium, and rhodium (107).

Lean NO$_x$ Trap (LNT) is another common technique used to reduce the NO$_x$ emission. The principle of this technique can be described in two steps. First, the NO$_x$ emitted during the lean driving conditions is adsorbed and stored in the catalyst washcoat. Then, the NO$_x$ is released and catalytically converted to nitrogen during the rich driving conditions. The catalyst washcoat is made of three main components, namely

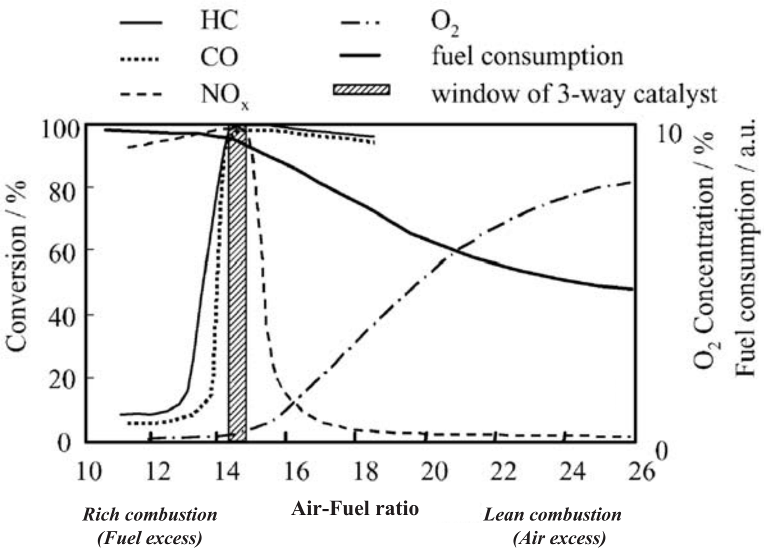

Figure 1.13: TWC performance and fuel consumption of a gasoline engine as a function of the A/F ratio. - TWC functions fully around a A/F ratio of 14.6. Higher A/F ratio (lean combustion) affect the NO_x reduction while lower ratio (rich combustion) affects the CO and HC oxidation (108).

an oxidant catalyst (like platinum), an adsorbent (like barium oxide), and a reduction catalyst (like rhodium). With this technique, the application of the TWC was extended to lean-combustion engines such as gasoline direct injection (GDI) and diesel engines (73).

The combustion stoichiometry in compression ignition engine is generally fuel-leaner in comparison with spark ignition engine. The direct emissions of CO, HC and NO_x from diesel engines are significantly lower than from gasoline engines (73, 109). However, the improvement of the TWC efficiency for gasoline engines made diesel engines' exhaust gas emissions more substantial, with larger unburned fuel, lubricant oil emissions and dry soot (107). Therefore, the first catalyst used to decrease diesel emissions was a Diesel Oxidation Catalyst (DOC) which has the same effect as the TWC on the HC and CO (equations 1.1 and 1.2), but with the addition to allow the oxidation of the soluble organic fraction (unburned fuel and lubricant oil) of the particulate matter. Therefore, DOC effect on the PM emissions results in a reduction of PM mass emission by a level of circa 20 up to 50% (110). With the same support as described for the TWC, the preferred oxidation catalyst material used is platinum.

Diesel Particle Filters (DPFs) have the capability to limit diesel exhaust PM emission by storing them. Since collected particles can cause, over time, an excessive exhaust gas pressure drop, filter regeneration is performed periodically. This operation is executed either continuously with passive filters, or periodically with active filters. In the first case, the regeneration is operated thermally by oxidation of PM to gaseous compounds (mainly CO_2) thanks to the temperature and the oxidizing species from the exhaust gas (O_2 and NO_x). This operation which occurs continuously during regular operation of the vehicle, is facilitated by the presence of some form of catalyst incorporated onto the filter or in the fuel as additives. These catalysts allow lower soot oxidation temperature. Therefore, these passive filters are grouped into two categories, the porous or fibrous substrates coated with catalysts (typically noble metals); and the uncoated substrates, which accumulate fuel-borne catalysts (typically transition metal oxides) (111). In the second case, the filter temperature is increased to a point where soots start oxidizing. An active strategy (i.e. fuel burner or electric heater) is operated at the filter level in order to regenerate it periodically, according to the vehicle's control system (73). These active filters are usually uncoated. Most of the filters, active and passive, are made of ceramic wall-flow monolith designed to force diesel aerosols through the porous walls. Whereas passive filters are generally promoted for heavy-duty application because of their simplicity and low cost, light-duty exhaust gas hardly reaches the sufficient temperature to ensure soot oxidation, even in presence of catalyst. Consequently, light-duty system usually adopts a combination of passive an active approach, usually through a specific engine management (73).

Finally, a combination of DOC (upstream) followed by a DPF (downstream) system was developed in order to allow DPF regeneration at temperature below 300°C. The principle discovered in 1989 by Cooper and Roth is based on the properties of diesel PM to be oxidized at lower temperature in presence of NO_2 in comparison with O_2 (112). This two-stage catalytic and passive filter was marketed under the designation of continuously regenerating trap. During the first stage, in addition with the oxidation of the HC and CO contained in the raw exhaust gas (equations 1.1, 1.2, and 1.3), the DOC operates as well the conversion of NO to NO_2. Then, the second stage achieved by the DPF consists in collecting the PM on the filters, and burning them with the NO_2 to give CO_2, H_2O and NO (73, 112). Although such system can be a source of secondary pollutants, such as specific nitrated PAHs which are the result of nitrification reactions between exhaust NO_x and PAHs contained in diesel soot (111), it was widely used for heavy-duty to meet Euro IV emission standard (113).

However, to comply with the latest emission standard Euro V, Selective Catalytic Reduction (SCR) using urea is one of the most widespread technique developed to achieve the 80-90% of NO_x reduction (114, 115). Given the trend toward more fuel efficiency and less CO_2 emissions, lean-burn condition were promoted in engines. However, previously described aftertreatment techniques are inefficient to reduce the thermally produced NO_x particularly present in this condition (107). Together with the EGR, SCR allow reducing NO_x in the tailpipe emission from diesel vehicles, however, the strategies of this two systems are different. Whereas the EGR aimed to reduce the NO_x formation during combustion, the SCR takes action after the combustion, to reduce the NO_x previously produced. The principle is to provide the aftertreatment device with a molecule to reduce NO_x to elemental nitrogen. This molecule is NH_3, which is produced from the decomposition of urea released in the catalyst surface under specific condition. Equations 1.10 and 1.11 describe the chemical decomposition of urea whereas equation 1.12 and 1.13 describe the chemical reaction between NH_3 and NO_x:

$$CO(NH_2)_2 \rightleftharpoons NH_3 + HNCO, \tag{1.10}$$

$$HNCO + H_2O \rightleftharpoons NH_3 + CO_2, \tag{1.11}$$

$$4NH_3 + 4NO + O_2 \rightleftharpoons 4N_2 + 6H_2O, \tag{1.12}$$

$$4NH_3 + 2NO + 2NO_2 \rightleftharpoons 4N_2 + 6H_2O. \tag{1.13}$$

In comparison with the EGR, the combustion can be optimized and the fuel economy is enhanced. However, a first drawback of urea-SCR is the necessity to have an additional tank, which adds weight to the vehicle. The urea strategy proposed by US car manufacturer is to keep on board a sufficient amount of urea to allow refilling at the same time of oil change, which can account for 28 L (considering 2% consumption rate relative to fuel and 18 000 km range) (106). In addition, the system requires the exhaust temperature to reach a sufficient temperature before releasing urea. This constraint makes urea-SCR unsuitable for start and stop driving behaviour such as garbage or delivery trucks. Whereas high range temperature performance of SCR was lately improved thanks to catalysts based on new zeolite, low range temperature performance are actually investigated via more accurate NO_2/NO_x control (106). Finally, the last drawback is linked to the secondary pollutant emissions due to the SCR. The less accurate control system of first generation urea-SCR were the source of NH_3 slip (from incomplete decomposition of urea) at low temperature operation, as well as isocyanic acid (116). However, slip catalyst were developed to remove these pollutants (117, 118).

In the case of motorcycle and scooters, the aftertreatment system depends on the size of the vehicle. For motorbike with engine displacement bigger than 600 cm^3, all elements of advanced emission control package are generally included, with TWC device. The modulation of O_2 in the exhaust by an open loop is progressively replaced by more sophisticated close loop control (119). For smaller motorbike and scooter, the application of an oxidant catalyst, in addition with a secondary air injection allows the engine to run with rich mixture combustion (low A/F) necessary to have a good drivability, with the aftertreatment required to limit HC and CO emissions. However, catalytic devices used for this category of vehicle are relatively less efficient than those used for light-duty vehicles, mainly because of their shorter size and their longer period before light-off (119).

The increasingly stringent regulations together with the fuel economy incentive pushed oil companies to provide cleaner fuel, and car manufacturers to optimize the engine combustion process, and to develop complex aftertreatment devices (106). As a result, a great improvement was achieved in terms of pollutant emission. However, new technology involves new environmental risks, even if small. The assessment of these risks is mandatory before spreading the technology in the market. Unregulated pollutants such as N_2O, NH_3, or nitrated PAHs for instance are known to be catalytically induced (10, 60, 61, 111). With the decrease of emission standards, these unregulated pollutants will start to contribute significantly to the threat that aftertreatment devices were designed to correct.

1.5 Aims of the project

In this project, the focus was on a few particular issues related to unregulated emissions from on-road transport. This mission was carried out within the Sustainable Transport

Unit (STU) of the Institute for Energy and Transport (IET) at the European Commission Joint Research Centre (EC-JRC), Ispra, Italy. This unit aimed to contribute to the European Commission's policy goals of achieving sustainable transport in Europe. The technical and scientific support provided by the STU is in part based on the Vehicle and Engine Emission Laboratories (VELAs). The experimental part of this project was conducted within these highly sophisticated facilities, with the involvement of *Composants à nanostructures pour Moyen Infra-Rouge* (nanoMIR) group of the *Institut d'Électronique du Sud* (IES), Montpellier, France. Invested in the development of specific measurement techniques based on Tunable Diode Laser Absorption Spectrometry (TDLAS), nanoMIR research group focuses on the implementation of TDLAS on the quantification of pollutants contained in exhaust gas such as CO, NH_3 and CH_4. Thanks to the combined scientific support from the STU and nanoMIR, this PhD thesis approaches the impact of alternative fuels and aftertreatment systems on the unregulated emissions from various categories of vehicles. The project is structured around four specific objectives addressed in four chapters. Each of these chapters is presented in the form of submitted or peer-reviewed scientific papers.

- Chapter 3 aims at giving an overview of the contribution from different category of vehicles in terms of regulated and unregulated gaseous and particulate emissions. A fleet of vehicles including mopeds, light-duty, and heavy-duty vehicles is investigated with emphasis on the relative pollutants contribution. Biofuels effect on emission is also studied together with several specific driving cycles. This part leads to appraise the actual situation with a detailed quantification of direct pollution related to on-road transport. The results of the chapter set solid basis to the overall project, by guiding the specific cases to explore more in detail along the following chapters.

- Chapter 4 is centred around a particularly polluting category of vehicles, the 50 cm^3 engine displacement two-stroke moped. The first regulation of moped emissions 97/24/EC came into force in 1999, followed by one amendment in 2002, however, 10 years later, the next amendment is still in preparation. A special interest was expressed on the aftertreatment devices, rather rudimentary in comparison with light-duty vehicles, and its effect on pollutant emissions. Original data treatment and statistics, based on multivariate analysis, are carried out on online emission data in order to investigate the correlations between gaseous and solid emission patterns.

- Chapter 5 is dedicated to the impact of alternative fuel on modern light-duty vehicle gaseous emissions, with two studies on high ethanol fuel content and liquefied petroleum gas (LPG). The objectives of these studies are to assess the level of unregulated gaseous emissions in comparison with standard gasoline fuel, with emphasis on the cold start events (before the light-off of the catalyst). Indeed, for some specific pollutants, these cold start emissions can account for more than 90% of the total emission of the vehicle during a journey.

- Finally, chapter 6 of this project deals with the emissions from buses and trucks, based on the recently established test facility for heavy-duty vehicles located at the IET of the EC-JRC, Ispra, Italy. The very first application of this facility is illustrated with a heavy-duty vehicle Euro III, representative of the trucks used in EU. Specific unregulated gaseous emissions such as PAHs were investigated for the first time online, with a chassis dynamometer dedicated to complete heavy-duty vehicles.

Before getting into these issues, the common experimental section is approached in chapter 2. In this section, the extensive set of instruments dedicated to the unregulated emission assessment is described. Among them, Fourier Transform Infrared Spectrometry (FTIR) dedicated to vehicle exhaust analysis was deployed to qualify and quantify specific gaseous pollutants like nitrogen species (NO, NO_2, N_2O, and NH_3). Then, Gas Chromatography (GC) and High Performance Liquid Chromatography (HPLC) were carried out to assess O_3 precursors and carbonyls. The technical performances of these methods were particularly appraised since some of them are part of the candidate methods selected by additional pollutants subgroup involved in the World Forum for Harmonization of Vehicle Regulations (WP29) of the United Nations Economic Commission for Europe (UNECE).

The document ends with general conclusions and perspectives related to the different subjects studied.

Chapter 2

Materials & methods

The experimental part of this project has been carried out in the vehicle emission laboratories (VELAs) at the European Commission - Joint Research Centre (EC-JRC) at Ispra (Italy). These laboratories aim to evaluate the impact of vehicles on environment under simulated road driving conditions, in order to contribute to the European Commission's policy goals of achieving sustainable transport in Europe. An extensive set of analytical instruments and sensors are connected to the laboratory in order to monitor the dynamic data together with the emissions of the vehicle. Due to the complexity of the gaseous mixture at the exhaust, these instruments and sensors are various, consequently, in the scope of this section, only a selection of the most relevant techniques are described in the detail. The principle of the other specific instruments employed for the project (i.e. high-resolution time-of-flight aerosol mass spectrometer, multiangle absorption photometer, fast mobility particle sizerĚ) can be found in the experimental section of the different subsequent chapters. The first part describes the VELA, including on-road simulation principle, driving cycles, and regulated emission monitoring. In the second part, an instrumentation dedicated to the gaseous pollutants characterization - online Fourier Transform Infrared Spectrometer (FTIR) - is approached. The third and the fourth parts, describe the methodologies followed to monitor the carbonyls and VOCs, based on offline techniques.

2.1 The vehicle emission laboratories (VELAs)

The qualitative and quantitative characterization of the regulated and unregulated pollutant emitted by on-road transport is of major interest in order to assess the impact on air quality and climate change. The contribution of on-road transport sector in the total anthropogenic emissions can be estimated by monitoring directly the primary emissions during field experiments, using on-vehicle portable exhaust emission system (called PEMS), or during laboratory experiments. The latter allows better accuracy and repeatability but it is costly and requires highly sophisticated and complex intrumentations. Laboratory experiments are generally used for regulatory purpose, like engine or vehicle certification. The testing methods are standardized and can be applied to engines on a test-bench, or for complete vehicles on a chassis dynamometer. In the scope of this study, vehicle emission characterizations have been done in different VELA facilities, designed to study from power 2-wheelers to light-duty, to heavy-duty vehicles (Fig. 2.1).

Figure 2.1: VELA facilities - The Vehicle Emission Laboratories, JRC - Italy

2.1.1 Simulation of vehicle loading using a chassis dynamometer

The car physics can be simulated in a laboratory thanks to a chassis dynamometer. When a car is driven at a constant speed, the motor delivers a tractive force to the road via the wheels. In order to move, this force must compensate two main constrains namely the air resistance (the dragging force, predominant at high speeds), and the rolling resistance (the rolling force, predominant at low speeds). This latter constrain is the sum of the friction of the road against the wheels rubber, the wheels against the axles, etc... The sum of these constraints is the velocity dependent friction force:

$$F_{friction} = A + Bv + Cv^2, \tag{2.1}$$

where A can be referred to the tire losses (in N), B to the bearing losses (in N s m^{-1}) and C to the friction losses that increase with the square of the speed, mainly the aerodynamic drag (in N s^2 m^{-2}). When the vehicle increases his velocity, an additional acceleration dependent force is applied to the system:

$$F_{inertia} = M \times dv/dt, \tag{2.2}$$

where M characterizes the inertial mass of the vehicle (in kg) and dv/dt the acceleration of the vehicle (in m s^{-2}). Finally, the height modification of the vehicle while driving changes the energy of the system. A grade dependent force can be added to the system:

$$F_{gravitational} = W \times Sin\left(ArcTan\frac{G\%}{100}\right), \tag{2.3}$$

where W stands for the weight of the vehicle and $G_{\%}$ for the slope of the road grade. The road load equation computed with sum of these 3 equations allows calculating the total resistance force received by the vehicle on real condition (see Fig. 2.2A):

$$F_{resistance} = A + Bv + Cv^2 + (M \times dv/dt) + \left(W \times Sin\left(ArcTan\frac{G\%}{100}\right)\right). \tag{2.4}$$

A chassis dynamometer aims to simulate, in a laboratory, forces applied on vehicle while driving on real condition. The first step consisted in calibrating the resistance of the chassis, according to the characteristics of the vehicle. This resistance depended on the airflow body of the vehicle and the friction on the chassis dynamometer. Vehicles have additional frictional losses on the chassis dynamometer, consequently this amount of losses must be estimated to be removed from the final simulation as described in Fig.

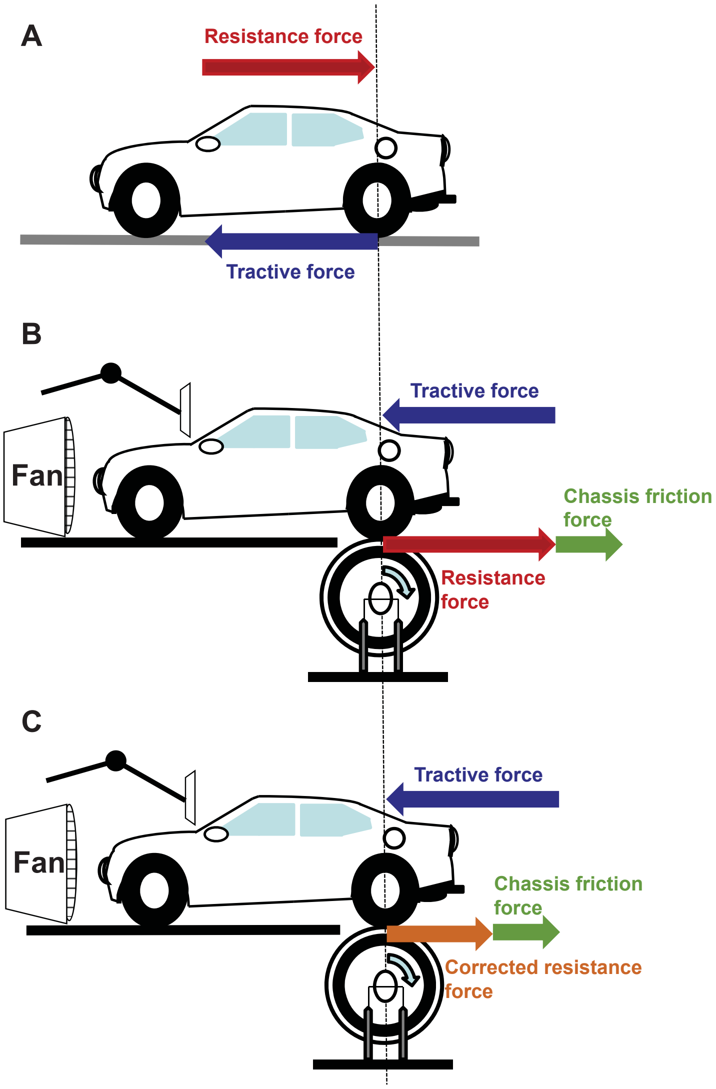

Figure 2.2: Chassis dynamometer basic principle - A - Summary of the forces involved in a car driven at constant speed, in real condition. B - Summary of the forces involved in a car driven at constant speed, in a chassis dynamometer study without roller friction correction, and C - with roller friction correction estimated by a coast down test.

2.2B. A pre-test, called coast-down test, was carried out at different constant speeds in order to set a simplified quadratic equation of the resistance force and to estimate A, B and C, taken into accounts the chassis losses:

$$F_{corr.resistance} = F_0 + F_1 v + F_2 v^2, \tag{2.5}$$

where F_0, F_1 and F_2 are the corrected coefficient computed with a quadratic regression technique. Finally, this equation was used to set precisely the chassis dynamometer load in order to reflect the on-road resistance force (see Fig. 2.2C).

2.1.2 Driving cycles

The driving cycles are employed in chassis dynamometer studies as support to achieve reproducible tests. They contain all the information regarding the speed and gear selection as a function of time. The driver must follows the cycle as close as possible, based on a "driver's aid" system diplayed on a screen located in front of the vehicle. A wide range of parameters can be studied during chassis dynamometer experiments such as regulated and regulated emissions, fuel consumption and so forth. Numerous driving cycles have been developed for these purposes. However, a majority of tests are carried out on a limited number of driving cycle, notably the ones defined by the legislation. These regulatory driving cycles were initially created for type approval emission test required for all new vehicle models. Not all of them simulate realistic driving behavior but the emission data generated by these cycles are reproducible and comparable since many references in the scientific literature relate to them. These driving cycles are gathered in a report which specified their main characteristics like average speed, average acceleration, number of stop (120). The main driving cycles used in this project are based on the EU legislation. The ECE-47 is the European regulatory test cycle for mopeds (121). The Common ARTEMIS driving cycle (CADC) has been developed to simulate typical driving behavior of light-duty vehicles in Europe (122). The European transient cycle (ETC) is the regulatory test cycle for heavy-duty diesel vehicles (123). Finally, the new European driving cycle (NEDC) is the regulatory test cycle for light- and medium-duty vehicles (75). These cycles are displayed in Fig. 2.3.

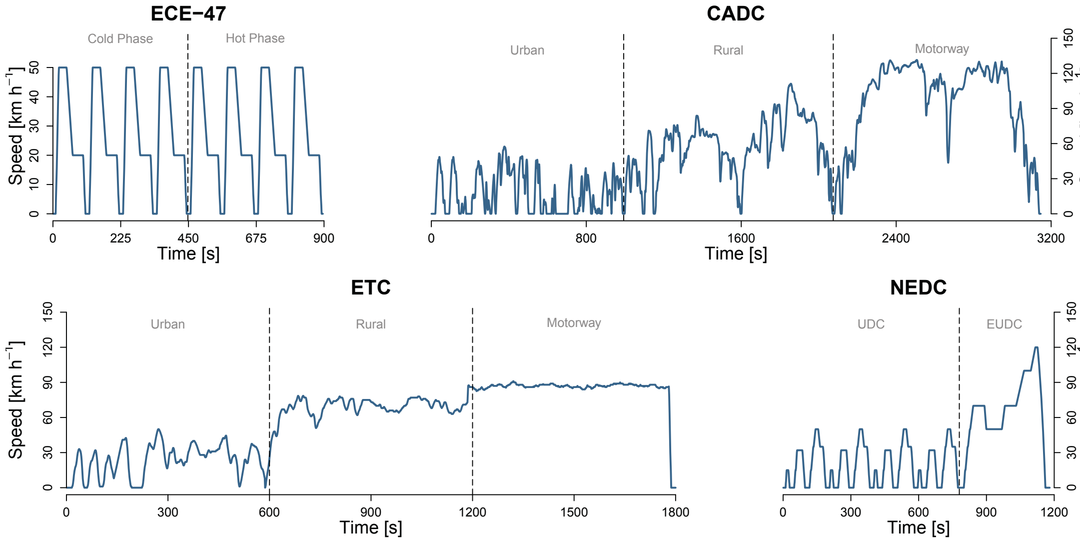

Figure 2.3: Main driving cycles studied - European regulatory test cycle for mopeds (ECE-47), Common ARTEMIS driving cycle (CADC), European transient cycle for heavy-duty vehicles (ETC), and the new European driving cycle (NEDC) for light- and medium-duty vehicles.

2.1.3 Regulated emission measurements

As described in the introduction, the following pollutants are actually regulated for vehicle emission: CO, NO_x, non-methane hydrocarbons (NMHC), CH_4 and particulate matter. These emissions were measured using standard methodologies defined by the related legislation. These pollutants were not analyzed freshly at the tailpipe of the vehicle, but after dilution of the raw exhaust. With this dilution step, water condensation in the sampling line was avoided. Moreover, this process simulated dilution process occurring in the atmosphere. In addition, this system allowed pollutant emissions factors quantification to be carried out independently of the real raw exhaust flow. Indeed, this last point was the core interest from a technical point of view. The high variability of the composition, the density, and the temperature of the raw exhaust gas make its flow rate tricky to estimate. Consequently, a dilution tunnel is conventionally implemented, in the laboratory setup. Then, calculation of the pollutant was based on the Constant Volume Sampler (CVS) approach. The whole raw exhaust gas was constantly drawn out from the tailpipe to the dilution tunnel, where filtered dilution air was mixed in order to decrease the temperature, and to reach a constant total flow rate. This total flow rate was maintained using critical flow venturis and pressure sensors. Figure 2.4 shows a schematic diagram of the dilution tunnel and its integration in the global experimental setup in the case of VELA 2. For regulatory purpose, a collection step from the CVS, either in a bag (gaseous pollutant), or on a filter (particulate pollutant), was carried out.

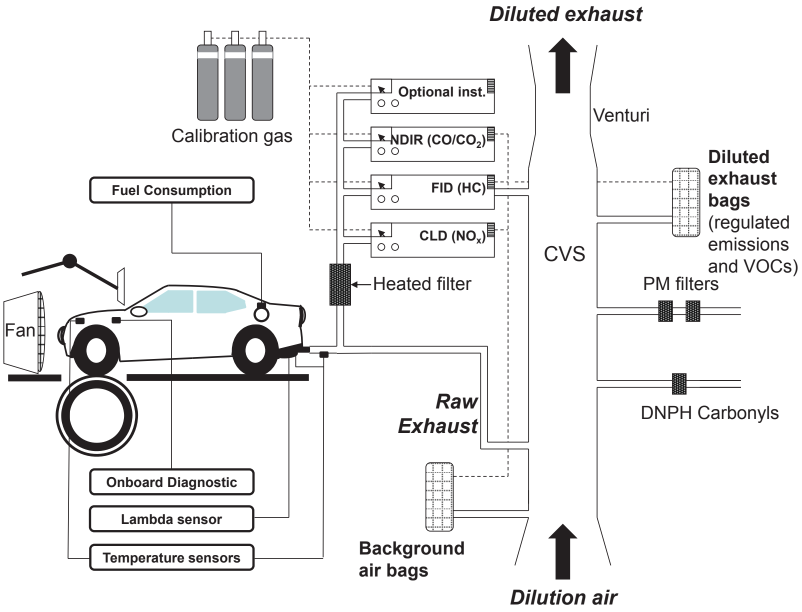

Figure 2.4: VELA schematic diagram of the experimental setup - The dilution tunnel connected at the tailpipe aimed to dilute the raw exhaust with fresh filtered air. The regulated emission were measured in the collecting bags with a non-dispersive infrared (CO/CO$_2$), a chemiluminiscence (NO$_x$) and a heated flame ionization (total hydrocarbons) detectors. Additional instruments (“Optional inst.") were connected for specific research purposes either at the tailpipe or at the dilution tunnel.

In case of gaseous pollutants, collection with a constant sampling flow rate from the dilution tunnel into a bag allowed obtaining a representative collected gas of the total gas which passed through the dilution tunnel during the sampling period. The amount of pollutant collected in the bag only differed from the total amount of pollutant which passed through the tunnel by a factor. This factor is the ratio of the total diluted exhaust volume (which passed through the dilution tunnel during the cycle), by the gas volume collected in the bag. Both volumes are calculated by integrating constant flow rates over the sampling period (CVS and bag flow rates respectively), so this ratio was easy to estimate. Then, a series of analyzers were connected to the exhaust bags. Once the sampling period was finished, the collected gas was drawn towards the corresponding analyzers. In accordance with Directive 70/220/EEC and its following amendments (75), the regulated emissions from all vehicles were measured with the following analyzers: non-dispersive infrared (NDIR for CO/CO_2), a chemiluminiscence (CLD for NO_x) and a heated (191°C) flame ionization detector (FID for THC) (Horiba, Kyoto, Japan for VELA 2, and AVL, Graz, Austria for VELAs 1 and 7). Once the volume concentration of regulated pollutants measured, the calculation of the emission factor was done with the following equation:

$$EF_X = \left(\frac{V_{mix} + V_{bag}}{V_{bag}} \right) \times [X] \times V_{bag} \times \frac{1}{D_{cycle}}, \tag{2.6}$$

where EF_X stands for the emission factor of the pollutant X (in g km^{-1}). The volume of diluted gas that passed through the dilution tunnel, expressed at standard conditions for temperature and pressure (T: 273.15 K and P: 100 kPa), is V_{mix} (in m^3). In the same way, the volume of gas collected in the bag is V_{bag} (in m^3). The volume concentration of X measured in the bag is *[X]* (in g m^3), and the driven distance corresponding to the sampling period is D_{cycle} (in km).

For the solid emissions, glass-fiber filters (47 mm-Pallflex, PALL, New-York, US) were connected to the dilution tunnel to collect the particles emitted during the driving cycle. After particle collection, and according to the legislated method for diesel vehicles (124), the filters were weighted after a minimum stabilization period of one hour at 22°C and 50% humidity. Total particulate mass was calculated with the following equation:

$$EF_{PM} = \left(\frac{V_{mix} + V_{filter}}{V_{filter}} \right) \times M_{PM} \times \frac{1}{D_{cycle}}, \tag{2.7}$$

where EF_{PM} stands for the particulate matter mass emission (in g km^{-1}). The volume of diluted gas that passed through the dilution tunnel, expressed at standard conditions for temperature and pressure (T: 273.15 K and P: 100 kPa), is V_{mix} (in m^3). In the same way, the volume of gas which passed through the filter is V_{filter} (in m^3). The mass of the particles collected on the filter is M_{PM} (in g), and the driven distance corresponding to the sampling period is D_{cycle} (in km).

According the regulation 692/2008, there is a difference between the THC regulated methodology between gasoline and diesel vehicles (81). Since diesel vehicle exhaust gas contain heavy hydrocarbons, the bags measurement is inadequate (HC could condensate on the bags surface). Consequently, for regulatory purpose, HC emission from diesel vehicles is monitored online with the FID connected by a heated sampling line and filter (191°C) to the dilution tunnel.

The analyzers used for gaseous regulated emission measurement had the capability to be connected directly at the tailpipe of the vehicle. These sensors can monitor online the dynamic volume concentration of the pollutants over the cycle driven, with 1 Hz temporal frequency. This measurement methodology was not indicated in the scope of the legislation; however, the outputs were mostly informative and were often used in the framework of this project. Indeed, these comprehensives data were correlated with other dynamic parameters such as velocity of the vehicle, temperature of the catalyst, and instantaneous fuel consumption. The integration of the recorded signals provided valuable quality control information when compared with the emission factors resulting from the bags. The estimation of emission factors using online volume concentration was calculated as follows:

$$EF_X = \frac{\int_{t_1}^{t_2} \frac{[X]_{v,t}}{10^6} \times F_{exhaust,t} \times MW_X \times \frac{P}{RT} dt}{D_{cycle}}, \tag{2.8}$$

where EF_X is the emission factor of the compound X (in g km^{-1}), estimated within a period interval from t_1 and t_2. $[X]_{v,t}$ and $F_{exhaust,t}$ are the instantaneous volume concentration of X (in ppm) and exhaust flow rate (in m^3 s^{-1}) respectively. MW_X stands for the molecular weight of the compound X (in g mol^{-1}). The measurement is carried out at a pressure P (in Pa), and a temperature T (in K). R is the gas constant (8.314 J K^{-1} mol^{-1}). The driven distance corresponding to the sampling period is D_{cycle} (in km). So at standard conditions for temperature and pressure (T: 273.15 K and P: 100 kPa), the equation becomes:

$$EF_X = \frac{\int_{t_1}^{t_2} \frac{[X]_{v,t}}{10^6} \times F_{exhaust,t} \times MW_X \times 4.403.10^4 dt}{D_{cycle}}. \tag{2.9}$$

Table 2.1 displays an overview of the main characteristics of the different laboratories at the JRC.

Laboratory	Vehicle	Chassis dynamometer	Constant Volume Sampler (in m^3 min^{-1})	Temperature of the cell
VELA 1	Motorbikes Passenger cars	Diameter: 1.22 m Inertia range: 150-3500 kg Max speed: 200 km h^{-1}	[1.5 ; 11.25]	[-7 ; 20]°C
VELA 2	Passenger cars 4 Wheels cars Light/medium commercial vehicles	Diameter: 1.22 m Inertia range: 454-4500 kg Max speed: 200 km h^{-1}	[3 ; 30]	[-10 ; 35]°C
VELA 7	Heavy duty vehicles Buses	Diameter: 1.82 m Inertia range: 800-30000 kg Max speed: 200 km h^{-1}	[10 ; 150]	[-30 ; 50]°C

Table 2.1: Main characteristics of the vehicle emission laboratories at JRC Ispra.

2.2 Fourier transform infrared spectrometer dedicated to automotive gaseous emission monitoring

Besides the official methods used to monitor the regulated pollutant, Fourier Transform Infrared (FTIR) analyzer is an instrument which allows monitoring several gaseous pollutants, and among them, the additional pollutants defined by the WP29 (see section 1.3). These species absorb infrared radiation between 400 cm^{-1} to 4000 cm^{-1}. Within this range of wavelength, called Mid Infrared (MIR) domain, molecules with dipole moments can absorb electromagnetic radiations and changes their rotational and vibrational movements. The first commercial version of analyzer dedicated to vehicle emission monitoring was developed by Volkswagen (Germany) and Nicolet (USA) in 1990 (125). This System for Emission Sampling and Measurement (called SESAM) was able to monitor up to 25 different automotive exhaust gas compounds.

2.2.1 Basic principle

The analyzer consists of an IR source, an interferometer, a sampling cell, and the detector.

The IR source was made of silicon carbide (globar). The thermal radiation of this black body, heated at circa 1000°C, was used as source for MIR spectroscopy.

A Michelson interferometer was used to generate a continuous IR spectrum. The device consisted of two mirrors and a beam splitter as described in Fig. 2.5A. The beam was split 50/50 by a half silvered mirror; half of the signal was reflected by a fixed mirror whereas half was reflected by a movable mirror. The recombination of the two beams created an interferogram where intensity of light I depended on the optical retardation, so on the position δ of the movable mirror. The signal intensity for a specific position of the movable mirror *I(δ)* is expressed as a function of the wavenumber σ as followed:

$$I(\delta) = \int_{-\infty}^{+\infty} 0.5I(\sigma) \times cos(2\pi\delta\sigma)d\sigma. \tag{2.10}$$

Then, the interferogram *I(δ)* was proportional to the Fourier cosine transform of *I(σ)*, and the IR spectra *I(σ)* was computed by the inverse Fourier transform. *I(δ)* is expressed as a function of the wavenumber σ as followed:

$$I(\sigma) = cste \int_{-\infty}^{+\infty} I(\delta) \times cos(2\pi\delta\sigma)d\delta. \tag{2.11}$$

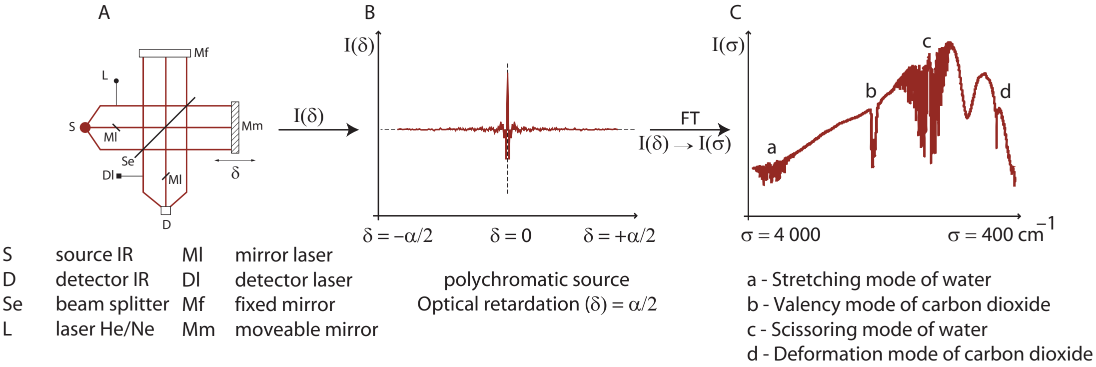

Figure 2.5: Fourier transform spectroscopy basic principle - A: Michelson interferometer optical setup; B: Interferogram measured when M_m is moving within a range of -α and +α. δ=0 is the zero path difference or zero retardation; C: IR spectrum example of CO_2 and H_2O calculated after Fourier transform

Figure 2.5 describes the different steps of data acquisition. A laser He/Ne was included in the system. The highly coherent light (at 632.8 nm) emitted by the laser allowed adjusting the number of sampling points necessary to obtain a correct resolution of the interferogram. Finally, different apodization functions were used as filter function to remove secondary maxima from the interferogram. The spectral resolution in cm^{-1} depended on the maximum retardation α in cm. For instance, a spectral resolution of 0.5 cm^{-1} was reached with a mirror displacement of 2 cm, which required a robust optical setup. Consequently, to maintaining a good spectral resolution (below 1 cm^{-1}) with the high acquisition frequency (required to monitor sharp concentration fluctuation in vehicle exhaust, i.e. above 1 Hz), is the specificity of FTIR spectrometer dedicated to automotive emission.

The gas cell was located after the interferometer. A hermetic tube composed of 2 mirrors and 2 IR transparent windows generally made of potassium bromide KBr (transmission limit: 400 - 43000 cm^{-1}) was used to host the flow of sampled gas. A multi reflection of the signal allowed increasing the optical path length in the sample, and consequently, increasing the absorbance of the sample (Beer-Lambert law).

Finally, the detector consisted in a liquid nitrogen cooled Mercury Cadmium Telluride (HgCdTe) semiconductor. The fast response and the sensitivity of these quantic detectors made them appropriate to the measurement of particularly transient exhaust gas composition.

2.2.2 Specificity of FTIR spectrometer dedicated to automotive emission

The FTIR spectrometer allows to measuring the concentration of up to 20 exhaust compounds by a multivariate calibration based on a factory developed model. Figure 2.6 displays the absorption in the MIR range of several nitrogen species usually emitted in vehicle exhaust. As described by this figure, the areas where individual species absorb the IR often overlap. For instance, the absorbance of water, displayed with inversed scale in the upper part of the graphic, can cover the specific absorption wavelength of NO_2. Consequently, the calibration model has been developed following different steps. Firstly, a PCA has been carried out to extract the informative region of the spectra for every individual species. Then this informative region where compared in order to isolate the specific wavelength area where none other species absorbs. These specific wavelengths were finally used to compute a multiple least-squares regression (MLR) model which aimed to predict the volume concentration of the compound. For each wavelength selected, the model assumed a linear relationship between concentration and absorption. For each compounds, standard gas cylinders of several concentration levels were used to calibrate the model. The latter can be expressed as an equation as follows:

$$[Y]_{pred} = A + B_1\lambda_1 + B_2\lambda_2 + B_3\lambda_3 + \cdots B_n\lambda_n + \epsilon, \tag{2.12}$$

where $[Y]_{pred}$ stands for the predicted volume concentration of the compound Y (in ppm), computed using the n specific wavelengths λ_n where Y has an absorption (namely the independent variables), and their weights in the regression model B_n. The offset of the model is A, and the residuals are expressed by ϵ. It must be borne in mind that according the Beer-Lambert law, and the ideal gas law (in force for the exhaust gas), the previously described model is valid for a defined optical path length, temperature and pressure.

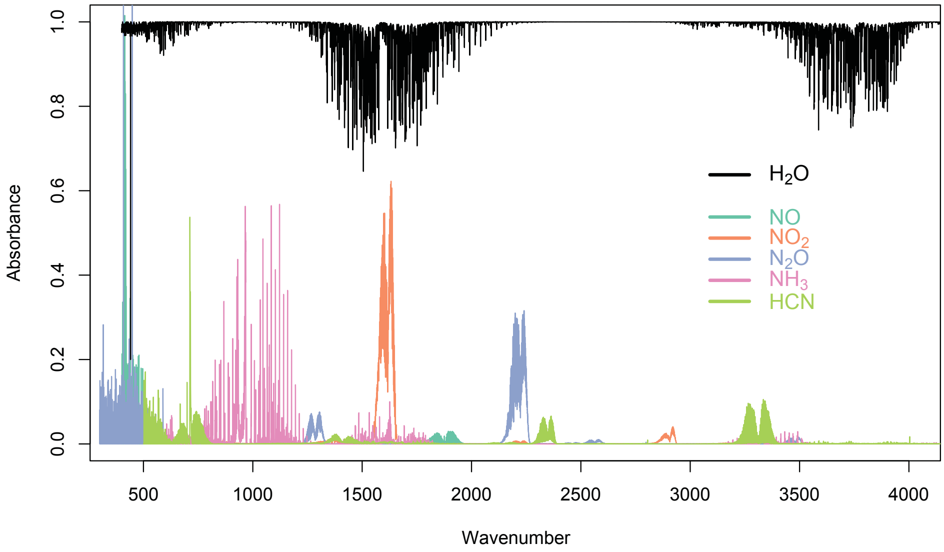

Figure 2.6: FTIR spectra of a selection of nitrogen species emitted by a vehicle - Measurement operated at 191°C and 1 Atm. NO: 49 ppm, NO_2:136 ppm, N_2O: 93 ppm, NH_3:186 ppm, HCN: 80 ppm, H_2O: 2000 ppm in reversed axis. Reference MGRefsMaster (2006) (126)

Implementation of the FTIR spectrometer for exhaust gas measurement required the acquisition of an averaged background spectrum from N_2 or pure air. This daily background spectrum was systematically subtracted to the new spectra registered by the instrument. The calibration of the instrument was based on a factory developed multivariate model. CO, CO_2 and NO_x measurements from the previously described analyzers were used to check the HR-FTIR calibration model. The quantification limit for each compound was estimated with the values obtained from the measurement of the background air, by summing 3 times the standard deviation of the measured value to the averaged value (see Tab. 2.2).

Compounds	**LoQ [ppm]**	**Compounds**	**LoQ [ppm]**
Nitric oxide (NO)	0.5	Carbon dioxide (CO_2)*	0.1
Nitrogen dioxide (NO_2)	0.2	Water (H_2O)*	1.6
Nitrous oxide (N_2O)	0.4	Carbon monoxide (CO)	0.7
Ammonia (NH_3)	0.4	Methane (CH_4)	2.4
Hydrogen cyanide (HCN)	0.3	Acetylene (C_2H_2)	0.6
Ethene (C_2H_4)	0.6	Ethane (C_2H_6)	0.2
Propylene (C_3H_6)	1.5	1.3-Butadiene (C_4H_6)	2.3
Isobutylene (C_4H_8)	1.2	Toluene (C_7H_8)	5.2
Methanol (CH_3OH)	0.8	Sulfur dioxide (SO_2)	1.5
Formaldehyde (CH_2O)	0.5	Acetaldehyde (CH_3CHO)	1.6

Table 2.2: Non-exhaustive list of compounds monitored by HR-FTIR dedicated to automotive emission with their limits of quantification (from MKS Multigas analyzer 2030 instrument). LoQ stands for limit of quantification. * Volume concentration unit in %.

FTIR spectrometers dedicated to real time analysis of automotive emission must have a high acquisition frequency in order to register fast changes of volume concentration resulting from sharp accelerations. These instruments can generally reach an acquisition frequency of up to 5 Hz. The output signal can be used either to monitor the fluctuation of pollutant emission along the speed profile, or to express the emission factor of pollutants. The latter case needs to integrate the mass concentration signal over the time. This operation requires knowing precisely the mass concentration, which is estimated according the ideal gas law as followed:

$$M_{X,t} = \frac{[X]_{v,t}}{10^6} \times F_{exhaust,t} \times MW_X \times \frac{P}{RT}, \tag{2.13}$$

where $M_{X,t}$ is the mass emission of the compound X (in g s^{-1}), $[X]_{v,t}$ is the volume concentration of X (in ppm), and $F_{exhaust,t}$ is the exhaust flow rate (in m^3 s^{-1}). MW_X stands for the molecular weight of the compound X (in g mol^{-1}). The measurement is carried out at a pressure P (in Pa), and a temperature T (in K). R is the gas constant (8.314 J K^{-1} mol^{-1}). So at standard conditions for temperature and pressure (T: 273.15 K and P: 100 kPa), the equation becomes:

$$M_{X,t} = \frac{[X]_{v,t}}{10^6} \times F_{exhaust,t} \times MW_X \times 4.403.10^4. \tag{2.14}$$

The volume concentration and the exhaust flow rate are instantaneous measurement. Consequently, in order to estimate accurately the mass emission, 2 pre-processing operations had to be achieved. First of all, the two signals were precisely synchronized.

This operation was harder than it seems since these two parameters were measured, or estimated, at different points of the experimental setup. The volume concentration was measured at the tailpipe, through a heated line of 2-3 meters (residence time in the heated line < 1s), whereas the exhaust flow rate was estimated generally at the CVS. Consequently, the synchronization of the signal was a mandatory step to warrant a correct estimation of the mass concentration. In the second place, the correct exhaust flow estimation was in itself a technical challenge that justified the implementation of CVS (see previous paragraph). The fluctuation of gas composition together with the temperature was the main difficulty to monitor accurately the flow. This parameter was often estimated either by difference between the total CVS flow and the dilution air flow, or using the CO_2 volume concentration ratio between the tailpipe and the CVS. The schematic flowchart displayed in Fig. 2.7 highlight the main steps followed to achieve this operation.

In the scope of this project, two instruments were used. On the one hand, raw exhausts from heavy duty vehicles and buses were analyzed with an FTIR instrument connected to the VELA 7 (Nicolet Antaris IGS Analyzer - Thermo Electron Scientific Instruments LLC, Madison, WI, USA). This spectrometer had a 1 Hz acquisition frequency, and multipath gas cell of 2 m. On the other hand, raw exhausts from light and medium duty vehicle as well as 2 wheelers were analyzed with a portable FTIR instrument in the VELA 1 and 2 (Multigas analyzer 2030 - MKS, Wilmington, MA, USA). This instrument was a prototype designed to operate in standalone, potentially in on-board condition (in a truck, a ship Ě). This spectrometer reached 5 Hz acquisition frequency with a multipath gas cell of 5.11 m. Both instruments were made up with a Michelson interferometer (spectral resolution: 0.5 cm^{-1}, spectral range: 600-3500 cm^{-1}) and a liquid nitrogen cooled mercury cadmium telluride detector (MCT). The raw exhaust was sampled directly from the tailpipe of the vehicles with a heated PTFE (politetrafluoroetilene) line and a pumping system (flow: ca. 10 L min^{-1}, T: 191°C) in order to avoid the absorption of hydrophilic compounds (i.e. NH_3, NO_2, carbonyls, or ethanol) in condensed water. The residence time of the undiluted exhaust gas in the heated line before the FTIR measurement cell was less than 2 seconds. The measurement temperature was set to 191°C, with a working pressure of 860 hPa (±10) and 1013 hPa (±20) for the Nicolet Antaris IGS analyzer and the Multigas analyzer 2030 respectively.

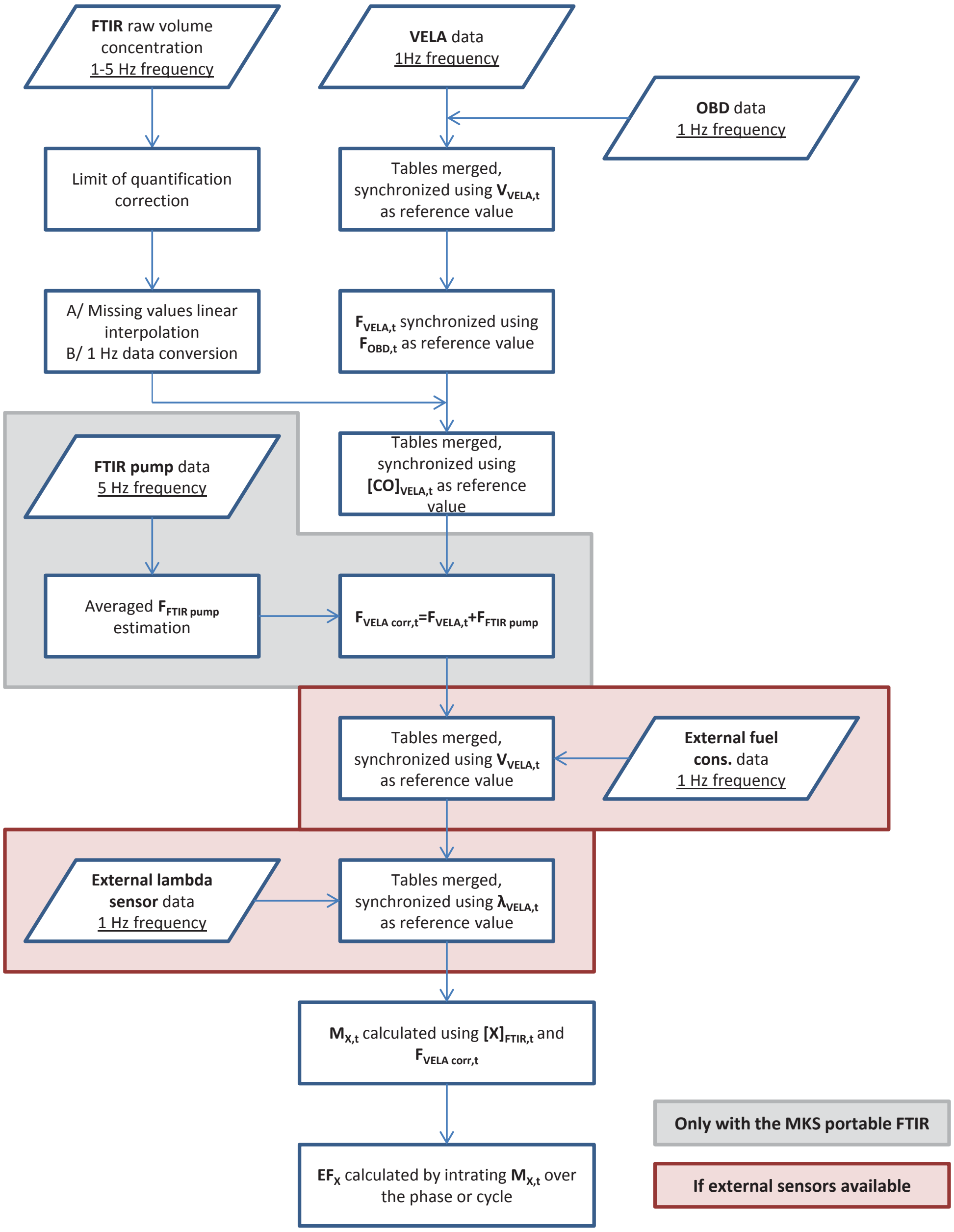

Figure 2.7: Flowchart of mass emission calculation from FTIR volume concentration data - OBD stands for on-board diagnostics, which is the vehicle's self-diagnostic which contains informations such as velocity, air fuel ratio, engine temperature. The OBD information is usually available in modern vehicles

2.3 High performance liquid chromatography for carbonyls analysis

Aldehydes and ketones are part of the VOCs from the exhaust gas. Formaldehyde (an aldehyde) emissions from on-road vehicles are regulated under the CARB standards since 1987 (127, 128), and actually, several US states have adopted this regulation. Carbonyls are also regulated in Brazil since 1997. According to the CARB, the first step of the measurement procedure consisted in collecting the aldehydes and ketones emitted in the gas phase of the vehicle exhaust. A 2,4-dinitrophenylhydrazine (DNPH) derivatization was operated on the carbonyl functional group of the molecule, either by impingers containing acidified DNPH solution, or by DNPH-coated cartridges (Sep-Pak DNPH - Waters, Milford, MA, USA) (129). The cartridge method was selected in the scope of this study and air sample was drawn from the CVS through the cartridge with a flow of 1 L min^{-1}. The second step of the measurement consisted in eluting the DNPH-derivatives compounds from the catridges using 2.5 mL of acetonitrile (CH_3CN) in a 5 mL volume flask. Then, deionized H_2O was added to adjust the flask. Finally, the last step consisted in measuring these samples by High-Performance Liquid Chromatography (HPLC), with an ultraviolet/visible detection (1100 Series - Agilent, Santa Clara, CA, USA). During this step, the compounds were injected in a column chromatography, where the compounds were retained by the C_{18} coated silica gel stationary phase. Then, elution of the retained compounds was carried out with a gradient elution, on which the most polar and small compounds eluted first, following by progressively the most hydrophilic compounds. The output of the column was connected to a detector which analyzed the absorbance of DNPH derivatives compounds while passing. The retention time of the peak detected informed about the quality of the compounds while the area of the peak informed about the quantity of the compounds.

Method improvement - The method chosen for this analysis was based on the guidelines from the CARB. The test procedure specifies 13 carbonyls to be monitored, namely formaldehyde, acetaldehyde, acrolein, acetone, propionaldehyde, crotonaldehyde, methacrolein, butyraldehyde, 2-butanone, benzaldehyde, valeraldehyde, p-tolualdehyde, and hexaldehyde. The in use HPLC method employed at the laboratory had the limitation of not separating properly two pairs of these carbonyls: acrolein (CH_2CHO) / acetone (CH_3COCH_3), and butyraldehyde ($CH_3CH_3CH_3CHO$)

/ 2-butanone ($CH_3CH_2COCH_3$). The method has been improved in order to increase the resolution for the separation of these 2 pairs. The resolution can be expressed with the Purnell formula as follows:

$$R_s = \frac{1}{4}\sqrt{N}\left(\frac{k^{'}}{1+k^{'}}\right)\left(\frac{\alpha - 1}{\alpha}\right), \tag{2.15}$$

where R_s is the resolution between the two peaks (the higher is the resolution, the better is the separation), N is the plate number of the second peak, α is the separation factor between the two peaks to be separated, and $k^{'}$ is the retention factor of the second peak. In order to improve the resolution, without changing the composition of the stationary and mobile phases (equal $k^{'}$, α and working temperature), the solution was to increase the number of plate, either by increasing the length of the column, or by decreasing the specific length of a theoretical plate. In order to maintain a short analysis duration and to avoid longitudinal diffusion of the peak (peak width), the optimisation focussed on the length of theorical plate. Consequently, the number of plate was enhanced by decreasing the particle size of the stationary phase to 5 μm. The improved HPLC method used a “New Allure AK” column (200 x 4.6 mm, 5 μm particle size, 60 pore size - Restek Corporation, USA) with a temperature of 30°C. The detector diode array was set at 365 nm. The injection volume was 50 μL, and the mobile phase flow rate was 1.5 mL min^{-1}. The resulting chromatogram, displaying the correct separation of the 2 pairs of compounds, is shown in Fig. 2.8.

Method validation - For each modification applied to an analytical method, a validation is required. To do so, an experimental design was followed, which consisted in injecting 3 sets of standard, including 9 levels of concentration each, at 3 different days. This methodology of validation allows assessing the repeatability, reproducibility, limit of detection, limit of quantification, and range of the method. The validation has been done for each of the 13 carbonyls. A F-test (99% confidence level) was carried out to validate the regression model and the concentration range. The regression model applied was validated as linear for a range up to 1 mg L^{-1} (2 mg L^{-1} for formaldehyde). Table 2.3 summarizes the main output of the validation process. The quantification limits of the method for each carbonyl, expressed as emission factor, and calculated considering a NEDC, are also indicated.

These results can be illustrated with the accuracy profile approach defined by Feinberg (130), where the trueness (bias) and the intermediate precision are displayed for

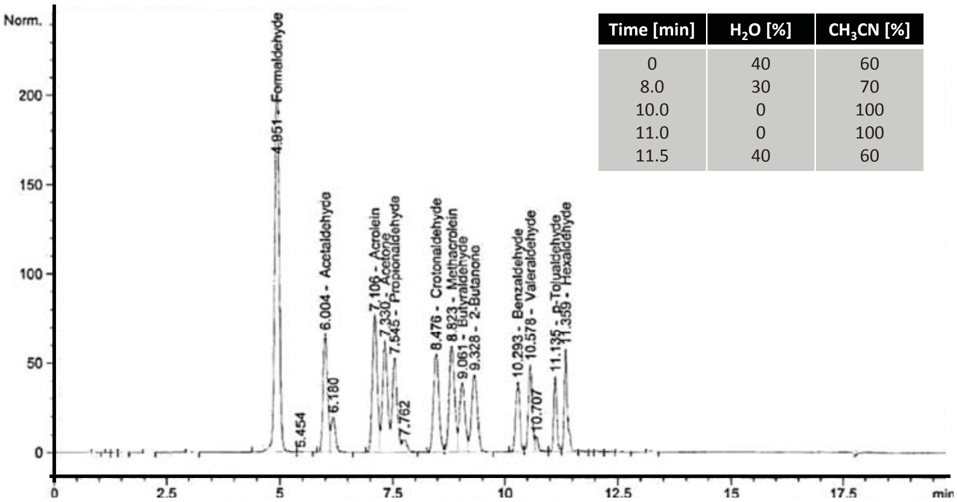

Time [min]	H_2O [%]	CH_3CN [%]
0	40	60
8.0	30	70
10.0	0	100
11.0	0	100
11.5	40	60

Figure 2.8: Chromatogram of DNPH derivatized carbonyls standard solution - Calibration chromatogram, all compounds at 0 6 mg.L^{-1} in their non-derivatized form except formaldehyde (1.2mg L^{-1}). The gradient elution method is displayed at the top right of the chromatogram.

	Linear Model			**Detection Limit**	**Quantification Limit**		
Compounds	**Slope**	**Intercept**	**R^2**	**μg L^{-1}**	**μg L^{-1}**	**μg/cartridge**	**μg km^{-1*}**
Formaldehyde	1150	16	0.9996	29	63	0.32	164
Acetaldehyde	721	4	0.9996	13	30	0.15	78
Acrolein	897	6	0.9997	13	30	0.15	79
Acetone	746	4	0.9997	13	28	0.14	73
Propionaldehyde	658	3	0.9997	12	28	0.14	74
Crotonaldehyde	724	3	0.9997	11	27	0.13	70
Methacrolein	785	4	0.9997	12	28	0.14	73
Butyraldehyde	520	3	0.9997	12	26	0.13	69
2-Butanone	644	3	0.9997	11	26	0.13	68
Benzaldehyde	494	4	0.9997	15	30	0.15	77
Valeraldehyde	448	3	0.9997	13	28	0.14	74
p-Tolualdehyde	434	3	0.9996	14	33	0.17	87
Hexaldehyde	436	2	0.9996	14	33	0.16	85

Table 2.3: Summary of the calibration linear models for the 13 carbonyls. * Quantification limit of carbonyls emission factors calculated considering a NEDC (11 km and 20 min) with a CVS flow rate of 8.6 m^3 min^{-1} and a cartridge sampling flow of 1.5 L min^{-1}.

every single level of the calibration range. This graphical mode is provided for the case of acetaldehyde in Fig. 2.9.

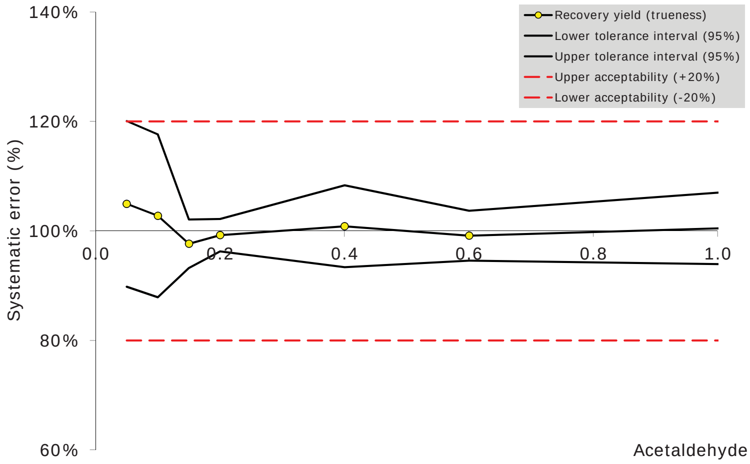

Figure 2.9: Accuracy profile for Acetaldehyde analyzed after DNPH derivatization by HPLC - Accuracy is illustrated as a continuous line with the average recovered concentration for each level as a circle. The concentration levels are displayed on the X-axis. The limits of the tolerance interval are represented by two symmetrical continuous thin lines. The acceptability limits (-20%, +20%) are illustrated as red dashed lines. All results are expressed as % of the target value. Whereas tolerance interval is included into the acceptability limits in the range (0.05-1 mg l^{-1}), the method can be declared as valid over this domain (130).

The emission factor of carbonyls emitted by a vehicle can be expressed as follows:

$$EF_{RO} = \left(\frac{Area_{RO} - B_{RO}}{A_{RO}}\right) \times V_{flask} \times \left(\frac{V_{CVS}}{V_{pump} D_{cycle}}\right), \tag{2.16}$$

where EF_{RO} is the emission factor of the carbonyl RO over the cycle (in mg km^{-1}). $Area_{RO}$ is the area of the peak corresponding to the carbonyl RO in the chromatogram. A_{RO} and B_{RO} are the slope and the intercept respectively of the linear model for the carbonyl RO (cf. Table 2.3). V_{flask} is the volume of the volumetric flask used (in L). V_{CVS} and V_{pump} are the total volume which passed through the CVS and the cartridge sampling pump respectively (in m^3), expressed at standard conditions for temperature and pressure (T: 273.15 K and P: 100 kPa). D_{cycle} is the total distance driven by the vehicle (in km) over the sampling period. A blank was systematically measured over the cycle by sampling diluted air. However, carbonyls concentrations measured by HPLC in the blanks were always found below the detection limit of the instrument.

2.4 Dual column gas chromatography with flame ionisation detectors for volatile organic compounds analysis

In addition to the determination of the HC emitted by the on-road vehicle, a more comprehensive analysis can be carried out to assess the speciation of the VOCs. This analysis is of importance since VOCs contribute differently to ground-level ozone formation, or to health damage. The technique followed to quantify these VOCs is well described elsewhere (131), consequently, here only a short description will be provided. The VOCs were collected from the CVS in opaque polyvinyl fluoride (PVF) bags (ca. 10 litres). These sample bags were subsequently analyzed within 30 min by a dual-column gas chromatography with dual flame ionization detectors (6890, Agilent, Santa Clara, USA). Prior injection into this instrument, a thermal desorption unit (UNITY) and an auxiliary sampling device (Air Server - Markes International, Pontyclun, UK) were used to collect samples from PVF bags. This process consisted in an enrichment step of the sampled gas by thermal treatment at -15°C, followed by a thermodesorption/injection step into the gas chromatograph at 130°C. The gas contained in the PVF bag was sampled at 40 mL min^{-1} during a period of 2 to 10 min (depending on the volume concentration of VOCs in the bag). The total flow of the CVS together with the level of HC emission of the vehicle were the main parameters which influenced this sampling time. For instance, 2 min sampling were set in a case of a 2-stroke scooter Euro 1 with a CVS flow rate of 4.4 $\text{m}^3\ \text{min}^{-1}$, whereas 10 min sampling were set in a case of a heavy-duty vehicle Euro V with a CVS flow rate of 120 $\text{m}^3\ \text{min}^{-1}$. VOCs separation was operated with 2 capillary columns: a nonpolar wall coated open tubular column (WCOT - DB-1, Agilent, Waldbronn, Germany), dedicated to the separation of the aromatic hydrocarbons (based on their boiling points), and a porous layer open tubular column (PLOT - Al_2O_3/KCl, Agilent, Waldbronn, Germany), dedicated to the separation of the lighter aliphatic hydrocarbons. Figure 2.10 displays the chromatograms obtained for the exhaust of a light-duty Euro 3 gasoline vehicle over a NEDC (result from a previous study with the same instrument as the one used for this project (131)).

A selection of 22 VOCs (from C_2 to C_9) listed as ozone precursors in the European air quality Directive 2002/3/EC (53) were monitored (see table 2.4). The calibration of the instrument has been operated with a multi-standard gas cylinder (National Physical Laboratory, Middlesex-UK).

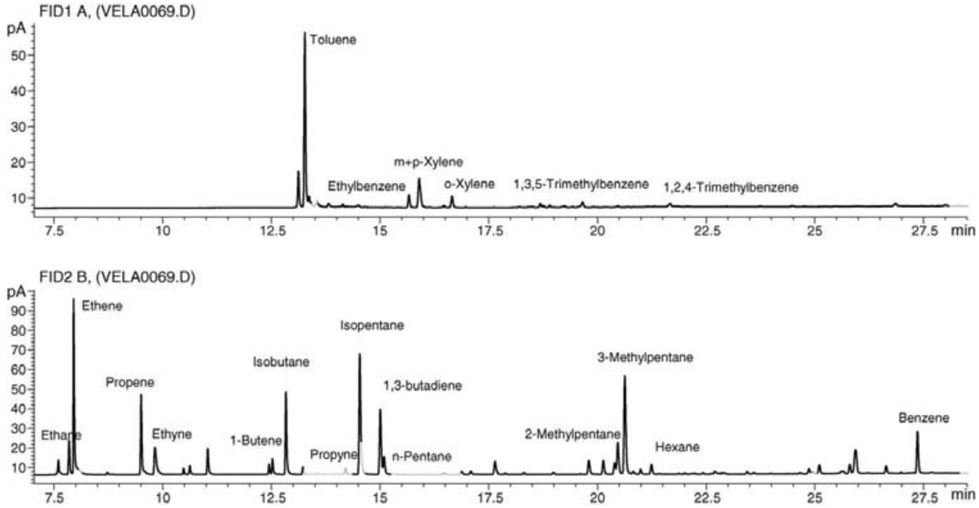

Figure 2.10: Chromatogram of VOC separation from the exhaust of a light-duty Euro 3 gasoline vehicle over a NEDC - The vehicle was equipped with a three-way catalyst (from Latella et al (131)). The upper and the lower chromatograms were obtained with the WCOT and the PLOT columns respectively.

Compounds	MIR [g O_3/g VOC]	Compounds	MIR
Acetylene	1.24	Ethylene	9.07
Ethane	0.31	Formaldehyde	8.96
Propene	11.57	Propane	0.56
1-Butene	10.22	1.3-Butadiene	13.47
cis-2-Butene	13.22	trans-2-Butene	13.88
n-Butane	1.32	i-Butane	1.34
Isoprene	10.68	1-Pentene	7.73
2-Pentene	10.23	n-Pentane	1.53
i-Pentane	1.67	Benzene	0.81
n-Hexane	1.43	i-Hexane*	1.66
Toluene	3.97	n-Heptane	1.26
Ethyl benzene	2.79	m+p-Xylene**	7.43
o-Xylene	7.48	n-Octane	1.09
i-Octane***	1.18	1,2,4-Trimeth. benzene	7.18
1,2,3-Trimeth. benzene	11.25	1,3,5-Trimeth. benzene	11.22
Total non-methane hydrocarbons	-		

Table 2.4: VOCs known as ozone precursor substances recommended for measurement according to Directive 2002/3/EC relating to ozone in ambient air (53). The corresponding maximum increment reacticity (MIR) values were defined by Carter (132).* averaged MIR of the isomers 2-methylpentane, 3-methylpentane, and 2,3-dimethylbutane. ** averaged MIR of the m-Xylene and p-Xylene. *** MIR of the 2-methylheptane.

The emission factor of VOCs emitted by a vehicle can be expressed as follows:

$$EF_X = \frac{[X]}{10^9} \times \frac{t_{calibration}}{t_{sample}} \times V_{CVS} \times MW_X \times \frac{1}{D_{cycle}} \times \frac{P}{RT}, \tag{2.17}$$

where EF_X is the emission factor of the compound X over the cycle (in g km^{-1}). *[X]* is the volume concentration of X (in ppb), $t_{calibration}$ and t_{sample} are the enrichment time of the calibration gas and the sample gas respectively (homogeneous unit), before the injection in the gas chromatograph. V_{CVS} is the total volume which passed through the CVS (in m^3), expressed at standard conditions for temperature and pressure (T: 273.15 K and P: 100 kPa). MW_X stands for the molecular weight of the compound X (in g mol^{-1}). D_{cycle} is the total distance driven by the vehicle (in km) over the sampling period. The measurement is carried out at a pressure P (in Pa), and a temperature T (in K). R is the gas constant (8.314 J K^{-1} mol^{-1}). So at standard conditions for temperature and pressure (T: 273.15 K and P: 100 kPa), the equation becomes:

$$EF_X = \frac{[X]}{10^9} \times \frac{t_{calibration}}{t_{sample}} \times V_{CVS} \times MW_X \times \frac{1}{D_{cycle}} \times 44.03. \tag{2.18}$$

Ozone formation potential calculation - The maximum increment reactivity approach (MIR) developed by Carter (132) was used to assess the potential of VOCs to contribute to ozone formation. This approach has been used for regulatory purpose in California. In this concept, the potential of 180 different VOCs to form O_3 was quantified thanks to a chemically detailed box model. In this scenario, the MIR of a VOC i was determined when VOC/NO$_x$ atmospheric composition leads a small increase of individual VOC (E$_i$) to a maximum of peak ozone concentration ([O$_3$]$_p$). In other terms, MIR is calculated over all VOC/NO$_x$ when this ratio leads [O$_3$] to the maximum sensitivity to VOC:

$$MIR_i = max\left\{\frac{d[O_3]_p}{[E]_i}\right\}. \tag{2.19}$$

Then, ozone formation potential (OFP) for each of the VOCs (including carbonyls) was calculated using the MIR values, as described in the following equation:

$$OFP = \sum \left(MIR_i \times [E]_i\right). \tag{2.20}$$

Chapter 3

Overview of on-road transport emissions

Emissions of organic aerosol mass, black carbon, particle number, and regulated and unregulated gases from mopeds and light and heavy-duty vehicles with different fuels

R. Chirico[a,b], M. Clairotte[c,h], T.W. Adam[c], B. Giechaskiel[c,f], M.F. Heringa[a], M. Elsasser[d,e], G. Martini[c], U. Manfredi[c] T. Streibel[e], M. Sklorz[e], R. Zimmermann[d,e], P.F. DeCarlo[a,g], C. Astorga[c], U. Baltensperger[a], A.S.H. Prevot[a]

Atmospheric Chemistry and Physics - Submitted

[a] Laboratory of Atmospheric Chemistry, Paul Scherrer Institute, 5232 Villigen PSI, Switzerland

[b] Italian National Agency for New Technologies, Energy and Sustainable Economic Development (ENEA), UTAPRAD-DIM, Via E. Fermi 45 - 00044 Frascati (RM), Italy

[c] European Commission Joint Research Centre Ispra, Institute for Energy, Sustainable Transport Unit, 21027 Ispra, Italy

[d] Institute of Ecological Chemistry, Cooperation Group complex molecular systems/Joint Mass Spectrometry Centre, Helmholtz Zentrum München, 85764 Neuherberg, Germany

[e] Chair of Analytical Chemistry / Joint Mass Spectrometry Centre, Institute of Chemistry, University of Rostock, 18051 Rostock, Germany

[f] AVL List GmbH, Hans-List-Platz 1, Graz, Austria

[g] now at Department of Civil, Architectural and Environmental Engineering, Drexel University, Philadelphia, USA

[h] now at INRA, UMR Eco&Sols, 34060 Montpellier, France

Abstract

A sampling campaign with seven different types of vehicles was conducted in 2009 at the vehicle test facilities of the Joint Research Centre (JRC) in Ispra (Italy). The vehicles chosen were representative of some categories circulating in Europe and were fueled either with standard gasoline or diesel and some with blends of rapeseed methyl ester biodiesel. The aim of this work was to improve the knowledge about the emission factors of gas phase and particle-associated regulated and unregulated species from vehicle exhaust. Unregulated species such as black carbon (BC), primary organic aerosol (OA) content of particulate matter, particle number (PN), monocyclic and polycyclic aromatic hydrocarbons (PAHs) and a selection of unregulated gaseous compounds, including nitrous acid (N_2O), ammonia (NH_3), hydrogen cyanide (HCN), formaldehyde (HCHO), acetaldehyde (CH_3CHO), sulfur dioxide (SO_2), and methane (CH_4), were measured in real time with a suite of instruments including a high-resolution aerosol time-of-flight mass spectrometer, a resonance enhanced multi-photon ionization time-of-flight mass spectrometer, and a high resolution Fourier transform infrared spectrometer. Diesel vehicles, without particle filters, featured the highest values for particle number, followed by gasoline vehicles and mopeds. The particles from diesel and gasoline vehicles were mostly made of BC with a low fraction of OA, while the particles from the mopeds were mainly composed of OA. Mopeds were characterized by surprisingly high emissions factors for OA, which were orders of magnitude higher than for the other vehicles. The heavy-duty diesel vehicle (HDDV) featured the highest nitrogen oxides (NO_x) emissions, while the mopeds had the highest emissions for total hydrocarbons and aromatic compounds due to the unburned and partially burned gasoline and lubricant oil mixture. Generally, vehicles fuelled with biodiesel blends showed lower emission factors of OA and total aromatics that those from the standard fuels. The mopeds were the main emitters of aromatic compounds, followed by the gasoline vehicle, the diesel vehicles and the HDDV.

Keywords: vehicle; regulated emission; organic aerosol; black carbon; aromatic compound; polyaromatic hydrocarbon; PAH; biodiesel; Aerodyne Aerosol Mass Spectrometer.

3.1 Introduction

Vehicles are still a significant source of air pollution in Europe even though the introduction of new technologies has led to substantial reductions (67). Gasoline vehicles emit mostly carbon monoxide (CO), hydrocarbons (HC) and nitrogen oxides (NO_x=NO+NO_2), while diesel vehicles without aftertreatment devices emit relatively small amounts of CO and HC but large amounts of NOx and particulate matter (PM) (67). In southern Europe and in some Asian countries, the urban traffic scenario of many cities is characterized by the presence of a high density of two-wheel motor vehicles, which are important sources of PM and HC (133, 134).

NO_x, volatile and semi-volatile organic compounds (VOCs and SVOCs) and CO are precursors for photooxidants, such as ozone and peroxyacetyl nitrate, and secondary aerosol formation in ambient air (15, 36, 38). Aerosols can have a direct radiative forcing (scattering and absorption of solar and infrared radiation) and an indirect radiative forcing (alteration of cloud properties and precipitation patterns) (135).

In urban environments, there is evidence that adverse non-carcinogenic and carcinogenic effects might be associated with exposure to diesel particulate matter (DPM) (27, 45). The organic aerosol (OA) can be an important constituent of PM and it can contain toxic or carcinogenic chemicals including polycyclic aromatic hydrocarbons (PAHs) (136, 137). Different studies have tried to correlate the toxicity of DPM with its chemical constituents like organic and elemental carbon (71, 138).

Aromatic hydrocarbons and in particular PAHs are a very important class of organic compounds from the health perspective, which are emitted from virtually all combustion sources and they are often used as tracers for motor vehicle exhaust (133, 137, 139). Aromatic hydrocarbons are present in unburned petroleum and lubricating oil and they are often produced during combustion processes. Various conditions affect the aromatic hydrocarbon composition in the exhaust, such as fuel composition, fuel to air ratio, engine combustion temperature, or fuel injection timing (140, 141).

Concerning diesel and gasoline vehicles, European regulations have continuously introduced more stringent limits for different exhaust pollutants (CO, NO_x, PM, etc). Moreover the European Commission has added a particle number limit to its Euro 5/6 emission standards for light-duty diesel vehicles (Co-decision Regulation EC 715/2007 and Comitology Regulation EC 692/2008) (81). For two-wheel motor vehicles, the

European Directive 97/24/EC (Euro 2) introduced a substantial reduction of CO and a lower limit for the sum of HC and NOx (121). A new regulation is expected in the coming years (Euro 3 and Euro 4).

Fuel improvements, especially sulfur content reduction, was one way to reduce vehicle emissions (142). To reduce fossil fuel dependence and emissions, and to respect the more stringent regulations, in particular for PM, other fuels like bio-fuels (i.e. biodiesel) have been introduced. Biodiesel are fatty acid methyl or ethyl esters made from vegetable oils or animal fats that can be used in diesel engines. Various studies have shown that the use of biodiesel reduces the emissions of HC, CO and PM and the improvements are mainly due to the higher oxygen content of the fuels compared to diesel fuel (94, 97, 143, 144).

The introduction of newer technologies and the use of aftertreatment devices, to comply with newer regulations, have effectively reduced the emissions from motor vehicles. Three-way catalytic converters (TWC) reduce emissions of CO, HC, and NO_x by more than 90%, while for diesel vehicles the use of abatement devices is needed to get lower emissions of NO_x and PM (67, 110, 113). Catalytic converters were also adapted at the tailpipe of two-wheel motor vehicles to comply with the Euro 2 emission standard. Nevertheless, mopeds remain a considerable source of pollutants (134, 145, 146).

In order to develop inventories for gaseous or particulate motor vehicle emissions, emission factor values (EF) are needed (i.e. the amount of a pollutant emitted per kilometer or per unit of fuel burned). Current methods for deriving emission factors range from measurement of single vehicles, to vehicle fleets using dynamometers, roadways or tunnels or estimates based on remote sensing of fuel consumption (147).

A lot of studies have been conducted in order to provide insight into the origin of the vehicle emissions and to establish effective vehicle emission control strategies. For instance, Yanowitz et al. (1999) (148) measured the regulated emissions from heavy-duty diesel vehicles, Shah et al. (2004) (149) measured mass and organic matter, Thompson et al. (2004) (142, 150) measured particle number, and Lev-On et al. (2002) (151) unregulated pollutants like PAHs. Regulated and unregulated emissions from passenger car have been characterized by many researchers e.g. (152, 153, 154, 155, 156, 157). Some studies have also compared different vehicle categories for regulated pollutants and particle number emissions e.g. (158). Recently size resolved and chemically resolved characterization of the non-refractory part of the emitted particulates was measured from in-use vehicles (159). However, according to our knowledge, there are no studies that measured simultaneously regulated and unregulated pollutants for different types of vehicles.

The aim of this work was to improve the knowledge about the emission factors of a comprehensive set of gas phase and particle-associated regulated and unregulated species for different classes of vehicles. A sampling campaign with seven different types of vehicles was conducted in 2009 at the vehicle test facilities of the Joint Research Centre (JRC) in Ispra (Italy). The vehicles chosen were representative of vehicle categories circulating in Europe, comprising a Euro III heavy-duty diesel vehicle, a Euro 3 diesel passenger car, Euro 4 diesel passenger cars, a Euro 4 gasoline car, a Euro 3 diesel van, and Euro 1 and Euro 2 mopeds. All vehicles were tested using the European legislative driving cycles, steady state cycles and speed ramp sequences. Vehicles were fueled either with standard gasoline or diesel, and eventually some of them were also run with blends of rapeseed methyl ester biodiesel. Results on regulated emissions will be presented together with results from unregulated emissions.

In particular, the black carbon and the primary organic aerosol content of particulate matter were investigated with a multi-angle absorption photometer (MAAP) and an Aerodyne high resolution time of flight aerosol mass spectrometer (HR-ToF-AMS), respectively. Particulate mass (PM) was measured according to the legislation methods and particle number with a condensation particle counter (CPC). Monocyclic and polycyclic aromatic hydrocarbons were measured by a resonance enhanced multi-photon ionization instrument coupled with a time of flight mass spectrometer (REMPI-ToF-MS). Nitrogen species (NO, NO_2, N_2O, NH_3 and HCN), oxygenated small compounds (formaldehyde, acetaldehyde), sulfur dioxide and methane were monitored by a high resolution Fourier transform infrared spectrometer (HR-FTIR). The data may serve as reference for emission ratios of various compounds for different type of vehicle emission that are often used for the interpretation of ambient data and are difficult to find in the literature.

3.2 Materials and methods

3.2.1 Vehicles and Fuels

The following vehicles were tested: a Euro III heavy-duty diesel vehicle (HDDV(EIII)), a Euro 3 diesel light-duty passenger car (Diesel-P(E3)), a Euro 3 diesel light-duty van (Diesel-V(E3)), a Euro 4 diesel light-duty passenger car (Diesel-P(E4)), a Euro 4 gasoline light-duty passenger car (Gasoline-P(E4)), a Euro 1 moped (Moped(E1)) and a Euro 2 moped (Moped(E2)). The technical characteristics of the vehicles are summarized in Tab. 3.1. The HDDV(EIII) was not equipped with any aftertreatment device, while the diesel and gasoline vehicles were equipped with a diesel oxidation catalyst (DOC) and a three-way-catalyst (TWC), respectively. The Moped(E1) has an oxidation catalyst, while the Moped(E2) featured a secondary air injection system (SAS) and an oxidation catalyst.

The experiments were conducted with commercial diesel and gasoline fuels. The sulfur content in the diesel fuels was either less than 50 ppm or less than 10 ppm (Tables 3.1 and 3.5). Some experiments were performed with 10% and 30% rapeseed methyl ester (RME) biodiesel fulfilling the EN14214 biodiesel standard added to the commercial diesel fuel. Two-stroke mopeds with 50 cm^3 displacement engines were tested with conventional gasoline-lubricant (2%) mixture. The gasoline fuel complied with the certified reference fuel CEC RF-02-99 oxy 0.8-1.2 according to Directive 97/24/EC and 98/70/EC (34, 121). Mineral oil was used for the Moped(E1), while semi-synthetic oil was used for Moped(E2). The effect of the alternative fuel (30% biodiesel blend) on the emission factors of the all investigated compounds are summarized in Tables 3.6 and 3.7.

Vehycle type	**Heavy-duty truck**	**Light-duty Vehicle**	**Passenger transport**	**Light-duty Vehicle**	**Light-duty Vehicle**	**Motorcycle**	**Motorcycle**
Vehicle code (for Figures)	HDDV(EIII) (HDDV(EIII))	Diesel-P(E3) (D-P(E3))	Diesel-V(E3) (D-V(E3))	Diesel-P(E4) (D-P(E4))	Gasoline-P(E4) (G-P(E4))	Moped(E1) (M(E1))	Moped(E2) (M(E2))
Data production	15/03/2002	12/02/2002	19/10/2006	25/09/2006	10/06/2008	26/10/2007	22/04/2004
km start program	140000	48923	15132	68141	29707	7716	5574
Vehicle mass [kg]	8000	1305	1975	1105	1182	90	110
Combustion type	Compression ignition	Compression ignition	Compression ignition	Compression ignition	Spark ignition	2-stroke	2-stroke
Engine supply	T-DI	T-DI	DI common rail	DI common rail	Gasoline	Carburetor gasoline+oil	Electronic DI gasoline+oil
Engine capacity [cm^{-3}]	5880	1995	2179	1248	1596	50	50
Max power @ rpm	176 kW @ 3500 rpm	74 kW @ 3250 rpm	74 kW @ 4000 rpm	55 kW @ 3000 rpm	85 kW @ 4500 rpm	2.8 kW @ 4875 rpm	2.8 kW
Aftertreatment	None	DOC	DOC	DOC	TWC	Oxi-cat	Oxi-cat+SAS
EU emission standard	1999/96/CE Euro III	Swiss emission standard [FTP75] Euro 3 equivalent	2001/1/CE Euro 3	2003/76/CE B Euro 4	2003/76/CE B Euro 4	97/24/CE Euro 1	97/27/5/CE Euro 2
Fuels used (sulfur)	D 10 ppm	D 10 or 50 ppm	D 10 or 10+30% Bio	D 10 or 10+10% Bio	G	G+2% lube	G+2% lube

Table 3.1: Technical characteristics of the vehicles and fuels tested with each vehicle (T-DI=Turbo Direct Injection; DI=Direct Injection; DOC=Diesel Oxidation Catalyst; TWC= Three Way Catalyst; SAS=Secondary Air injection System, D=Diesel fuel, G=Gasoline fuel; Bio=Biodiesel).

3.2.2 Sampling system

The tests were performed on the Vehicle Emission Laboratory (VELA) chassis dynamometers of the Institute for Environment and Sustainability (IES) of the EC-JRC Ispra, Italy. Three different laboratories were used: two for the passenger cars, one for the two-wheel motor vehicles and a new test facility for the HDDV(EIII) (160, 161). A typical schematic diagram of the experimental systems is shown in Fig. 3.1.

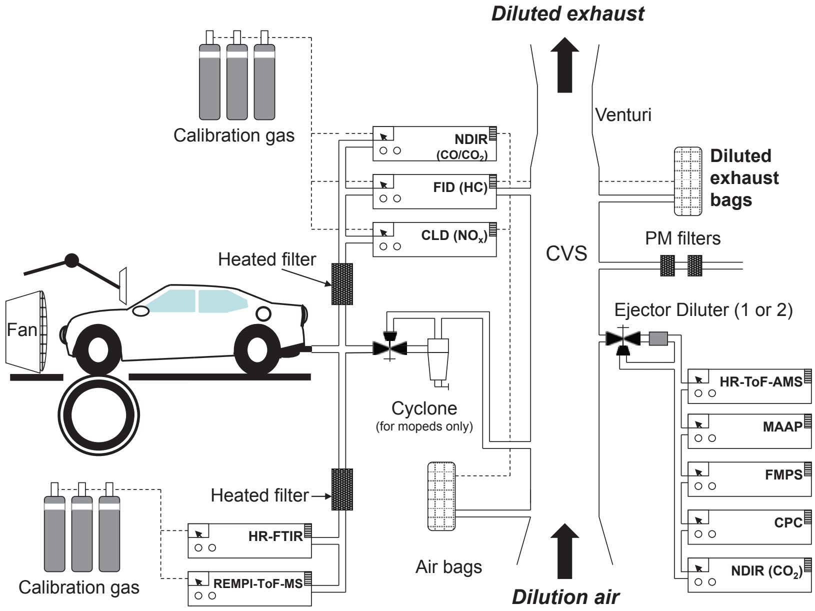

Figure 3.1: General schematic diagram of the experimental setup. - Diagram adapted from (162)).

A full flow dilution tunnel with constant volume sampler (CVS) was used to dilute the exhaust according to the European legislation for passenger cars and mopeds. Most instruments were connected to the dilution tunnel directly or with one or two ejector diluters (Dekati Ltd, Tampere, Finland) in series depending on the emissions levels. The flow of the dilution air in the dilution tunnel and the number of diluters used for each experiment are reported in Tab. 3.5 in the Supplementary Material, together with other information about every single test (type of cycle, engine temperature, type of fuel). The dilution ratio provided by each diluter was ≈1:12. For the experiments with two-wheel motor vehicles, a cyclone (50% cut-point diameter of 20 μm) was added between the tailpipe and the dilution tunnel in order to protect the instruments connected to the

CVS from oil droplets. The REMPI-ToF-MS and the HR-FTIR were directly connected to the tailpipes of the vehicles (see instrumentation below).

3.2.3 Instrumentation

3.2.3.1 High resolution time of flight aerosol mass spectrometer (HR-ToF-AMS)

An Aerodyne high resolution time of flight aerosol mass spectrometer (HR-ToF-AMS) was used during this campaign for real-time measurements of the submicron non refractory aerosol components such as organic aerosol (OA), sulfate (SO_4), and nitrates. A detailed description of the instrument is given in DeCarlo et al. (2006) (163), while the basic principles are reported in Chirico et al. (2010) (164). Table 3.2 summarizes the instruments used and the compounds they measured.

The flow calibration, the servo position check, the lens alignment and the size calibration were performed at the beginning of the campaign, while the ionization efficiency (IE) calibration was performed at the beginning and once every week. The baseline, the m/z and single ion calibrations were performed every day. The averaging time was 5 seconds in V mode (3 seconds in MS mode and 2 seconds in PToF mode).

Data analysis was performed in Igor Pro 6.03A (Wavemetrics, Lake Oswego, OR) using the AMS Analysis Toolkit Squirrel v.1.44. The AMS fragmentation table (165) was modified to account for the contribution of the gas phase species to m/z 44, 29 and 16-20. For organic signals at m/z 28 and 18 the fragmentation table suggested by Aiken et al. (2008) (166) was used. Gas phase corrections were made by HEPA filtered air sampled at the end of each test with the vehicle engines at idle mode. The temporal fluctuation of the diluted CO_2 concentration was measured during each run and taken into account to estimate the temporal contribution of the organic aerosol at m/z 44. A particle collection efficiency of unity was assumed to estimate the aerosol mass concentration.

3.2.3.2 Carbon dioxide analyzer

Carbon dioxide (CO_2) was measured with a differential, non-dispersive, infrared (NDIR) gas analyzer (LI-7000, LI-COR Biosciences). A two-point calibration in the range 0-560

Gas phase		Particulate phase
HR-FTIR	**REMPI-ToF-MS**	**HR-ToF-AMS**
NO	Benzene	Organic aerosol
NO_2	Toluene	Sulfate
N_2O	C_2-Benzene	**MAAP**
NH_3	C_3-Benzene	Black carbon
HCN	Napthalene	**CPC**
HCHO	Methyl-Naphthalene	Particle number
CH_3CHO	C_2-Naphthalene	**FILTERS**
SO_2	C_3-Naphthalene	Total PM
CH_4	Phenanthrene	
NDIR	Methyl-Phenanthrene	
CO	C_2-Phenanthrene	
CO_2	C_3-Phenanthrene	
FID	Pyrene	
THC		
CLD		
NO_x		

Table 3.2: List of the investigated compounds.

ppm was performed with 560 ppm CO_2 gas bottle standard and CO_2-free air bottle before the campaign. The instrument was run with 1-second time resolution.

3.2.3.3 Multi-angle absorption photometer (MAAP)

Black carbon (BC) concentrations in PM_1 were measured with a MAAP (Model 5012, Thermo) equipped with a PM_1 size cut. The BC content of the aerosols was quantified by measuring the optical absorption of light at 630 nm by particles collected on a glass fiber filter, correcting for the scattering effects of the filter and particles (167). A mass specific absorption cross section of 6.6 m^2 g^{-1} at 630 nm was used to convert the absorption measurement into a BC mass concentration. The instrument was run with 1-second time resolution.

3.2.3.4 Condensation particle counter (CPC)

A condensation particle counter (CPC, model 3022A, TSI) was used to measure the particle number concentration. Particles are guided through a chamber where the particles are enlarged by condensation of supersaturated butanol vapor into droplets of about 10 μm and are optically detected. The instrument has 50% detection for 7-nm particles and 90% detection for 15-nm particles. The maximum concentration that can be measured by the instrument is 9.99 10^6 particles cm^{-3}. The instrument was run with 5-second time resolution.

3.2.3.5 Resonance enhanced multi-photon ionization time-of-flight mass spectrometer (REMPI-ToF-MS)

Monocyclic aromatics and PAHs were measured by a REMPI (resonance enhanced multi-photon ionization) instrument coupled with a ToF mass spectrometer. This technique is a sensitive on-line method for the detection of gaseous aromatic compounds. A heated sampling system with PM filter (200°C, 4 L min^{-1}) was orthogonally connected to the tailpipe of the vehicles. The transfer line consisted of a deactivated silica capillary (length 1.5 m; inner diameter i.d. $=$ 0.32 mm; T $=$ 220°C) by which a constant volume of exhaust was continuously drawn into the instrument (flow rate 8 mL min^{-1}; residence time $<$1 s). This enabled to analyze undiluted and non-aged exhaust.

The principle of REMPI-TOF-MS was already described in detail (168) therefore, only a brief description is given here: Fundamental Nd:YAG laser pulses (1064 nm) are used for non-linear generation of UV light (266 nm). The UV pulses are directed into the ionization chamber straight underneath the inlet needle of the transfer line. Soft photoionization of the aromatics in the exhaust is induced by a sequential two-photon absorption process via an electronic transition state. The generated molecular ions are extracted into the flight tube of the reflectron ToF-MS . Mass spectra are recorded via a transient recorder PC card (Acquires, Switzerland) and data processing is done with a custom-made LabView (National Instruments, USA) program.

Calibration is carried out by applying external gas standards (benzene, toluene, xylene) (169). Where no calibration gases are available, compounds were semi-quantified by taking into account the ratios of the photoionization cross-section of the target compound and a calibrated species. The photoionization cross-section is a property that accounts for the compound's probability of being ionized under certain conditions and is constant for a fixed UV wavelength and photon density (170). As a consequence, the ratio of two photoionization cross-sections is also constant. These ratios were determined beforehand under lab-conditions for a large number of compounds. In principle, 20 complete mass spectra per second can be recorded since a 20 Hz laser was used. In this work, on-line data was averaged to a time-resolution of 1 Hz.

3.2.3.6 High resolution Fourier transform infrared spectrometer (HR-FTIR)

Small chain HC (saturated and unsaturated with less than 4 carbons), nitrogen species (NO, NO_2, N_2O, NH_3 and HCN), sulfur dioxide (SO_2) as well as other oxygenated small compounds (formaldehyde, acetaldehyde, methanol) were monitored with a high resolution Fourier transform infrared spectrometer (HR-FTIR - MKS Multigas analyzer 2030, Wilmington, MA). The sampling point was placed directly at the tailpipe to minimize any compound wall-losses. Therefore, the HR-FTIR was connected to the same sampling system as the REMPI-ToF-MS.

3.2.3.7 Regulated compound analyzers

Gas phase regulated compounds were measured in accordance with legislative methods for vehicle emissions using a non-dispersive infrared spectrometer (NDIR, CO and CO_2), a chemiluminescence detector (CLD, NO_x) and a heated flame ionization detector (HC, Hartmann & Braun in VELA1, HORIBA in VELA2 and AVL AMA 4000 advanced in VELA7).

3.2.4 Test protocols

Different driving cycles were conducted in accordance with the type of vehicles tested. Figure 3.2 shows the test cycles used during this work and the information about some parameters of the legislative cycles is reported in Tab. 3.3 (120). All tests were performed in accordance with the related legislative regulation and following amendments (171).

The tests with the HDDV(EIII) were carried out following the FIGE Cycle, the New European Driving Cycle (NEDC) and a steady state cycle. The FIGE cycle, from which the European Transient Cycle (ETC) has been derived, is based on road-type-specific driving patterns of HD and comprises three parts: the first part simulates the driving in urban areas, the second part on rural roads and the last one on motorways. The NEDC is used for emission type approval from passenger vehicles, but in this study it was also used to test the HDDV(EIII) and therefore, the maximum speed was limited to 90 km h^{-1}. During the speed ramps with the HDDV(EIII) the speed increased from idle to 40, 60 and 90 km h^{-1} and each speed was held constant for 5 minutes.

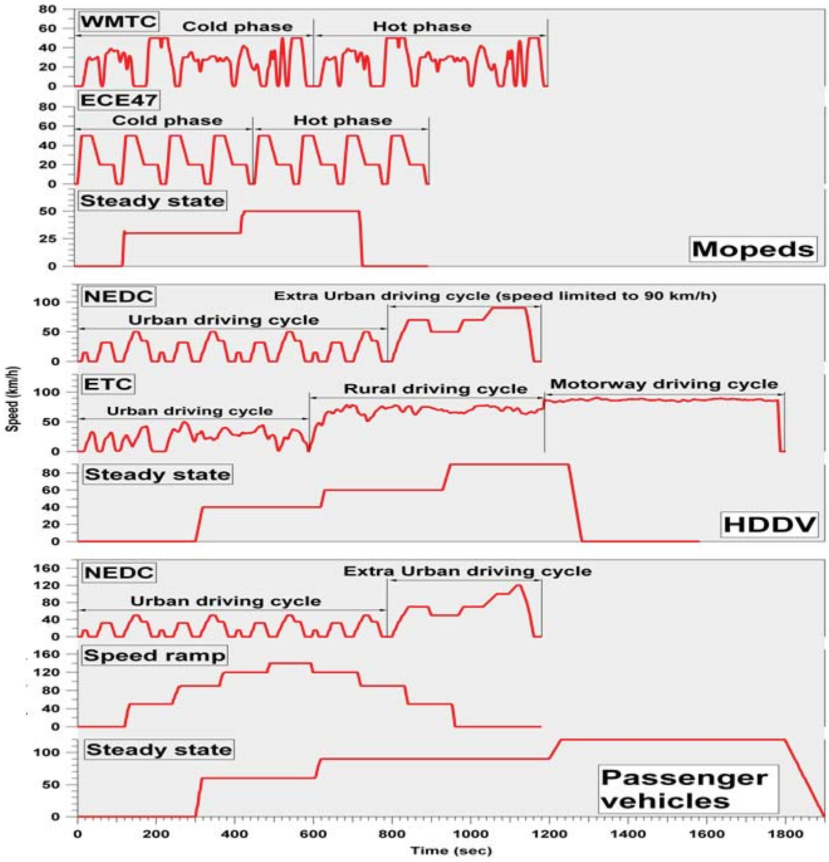

Figure 3.2: - Speed profiles of regulated (NEDC, ETC, WMTC, ECE-47) and unregulated (speed ramp, steady state) test cycles.

Cycle	NEDC	UDC	EUDC	ETC	ETC Urban	ETC Rural	ETC Motorway	WMTC*	ECE-47
Total distance [m]	110117	4060	6955	29494	3874	11557	14063	7874	6720
Total time [s]	1180	780	400	1800	600	600	600	1200	896
Driving time [s]	939	540	365	1800	600	600	600	1050	784
Drive time spent accelerating [s]	278	212	119	522	245	218	59	414	88
% of the time accelerating	23.6	27.2	29.8	29.0	40.8	36.3	9.8	34.5	9.8
Average speed [km h^{-1}]	33.6	19.0	62,6	59.0	23.3	69.3	84.4	23.6	27
Maximum speed [km h^{-1}]	120	50	120	90.8	50	78.5	90.8	50	50
Accelerations per km	2.8	12.1	0.6	2.2	22.2	9.4	9.3	11.7	1.2
Average positive acceleration [m s^{-2}]	0.3	0.3	0.5	0.2	0.3	0.2	0.0	0.4	1.2

Table 3.3: Typical parameters of the regulated cycles.*Custom WMTC with the first part repeated twice and reduced speed.

The tests with passenger vehicles were performed following the NEDC, steady state speed tests and speed ramps. Steady state tests and speed ramps were performed to characterize the vehicle emissions at different speeds. During the speed ramp tests, the speed was gradually increased from idle to 50, 90, 120 and 140 km h^{-1}, then the same step-wise sequence was repeated backwards. Each steady-speed step lasted 2 min (acceleration or deceleration included). With the steady state tests, the speed increased from idle to 60, 90 and 120 km h^{-1} and the first two speeds were held constant for 2.5 minutes, and the last two for 5 minutes.

The tests with the mopeds were performed using the European legislative driving cycle for 2-stroke 50cc displacement engines (ECE-47), a "short version" of the worldwide motorcycle test cycle (WMTC) and a steady state test. The aim of the WMTC is to harmonize the test protocols for motorcycles to establish a more realistic driving cycle. It consists of three different phases and in this study only the first part (phase 1) was taken into account, because phase 2 and phase 3 simulate extra-urban driving conditions for motorbikes and are not suitable for mopeds. The speed in phase 1 was limited to 50 km h^{-1} in order to align the test conditions with ECE-47 and the mopeds' engine performances. In the WMTC a cold phase to warm up the engine is not considered, thus the WMTC was repeated twice in succession to compare the results with those from the ECE-47 test. The first WMTC was considered as the "cold phase", while the second WMTC was considered as the "hot phase". The cold and hot phases in the ECE-47 and in the WMTC were both investigated. In the WMTC there are more load changes than in the ECE-47 test and the speed is less constant. The duration of the modified WMTC is 1200 seconds, while the duration of ECE-47 test is 896 seconds. The steady state test had a first part with no load, then the speed was gradually increased to 30 km h^{-1} and to 50 km h^{-1} and at the end the no-load condition was repeated. Each speed was held constant for 5 minutes.

3.2.5 Calculations

The data acquired by the various instruments were first corrected for the delay in time due to the different sampling points and flows. Signals from the instruments connected to the CVS (OA, BC and particle concentrations) were synchronized using the CO_2 concentration measured at both tailpipe and CVS (see Fig. 3.1) according to the subsequent methodology. The first step consisted in calculating the CO_2 concentration in the CVS based on the CO_2 concentration measured with the NDIR detector at the tailpipe:

$$[CO_2]_{CVS,t} = \frac{([CO_2]_{TP,t} \times F_{exh,t}) + ([CO_2]_{Back,t} \times F_{dilution,t})}{F_{CVS}}. \tag{3.1}$$

The instantaneous concentration of CO_2 at the tailpipe, in the dilution tunnel, and in the dilution air are $[CO_2]_{TP,t}$, $[CO_2]_{CVS,t}$ and $[CO_2]_{Back,t}$ respectively (homogeneous units). The background CO_2 concentrations in the dilution air were obtained by multiplying the measured concentrations after dilution with the dilution ratios calculated from CO_2 measurements at the tailpipe and after the dilution steps. For the calculation of the dilution ratios, background CO_2 was measured before the beginning of each experiment during 5 min in order to compute an averaged constant value for the whole test. The instantaneous flow rates of the exhaust, the dilution tunnel, and the dilution air are $F_{TP,t}$, $F_{CVS,t}$ and $F_{Back,t}$ respectively. The flow rates were estimated in the standard conditions for temperature and pressure (T: 273.15 K and P: 100 kPa).

The second step consisted in synchronizing the signals computed with equation 3.1, with the CO_2 concentration monitored with the NDIR analyzer connected after the ejector diluters (if used). The precise synchronization was done using the highest correlation coefficient of the linear regression between both signals. The phase delay estimated in this way was applied to the signals of the other instruments connected at the CVS (OA, BC and particle concentrations). The slope of the linear regression was considered as the dilution factor DF (applied by the ejector diluters) between the CVS and the instruments. Once synchronized, the last step was the integration of the instrument signals over the cycle in order to estimate the emission factors:

$$EF_x = \frac{\overline{[x]} \times DF \times \overline{F_{CVS}} \times t}{D}. \tag{3.2}$$

The emission factor of the compound x is EF_x in mg km^{-1}. $\overline{[x]}$ stands for the averaged concentration of the compound x in mg m^3 monitored by the instrument during the cycle or the sub-cycle. DF is the dilution ratio estimated previously. The flow rate of the dilution tunnel is $\overline{F_{CVS}}$ in m^3 min^{-1}, and the duration of the cycle or sub-cycle is t in min. D is the distance driven in km. The emission factor expressed in mg m^{-3} of exhaust can result from the equation 3.2 by changing the distance in denominator by the exhaust flow rate integrated over the cycle duration. Tables 3.8, 3.9, 3.10, and 3.11 report the emissions factors for OA, BC and particles number. Data presented in this paper are not corrected for wall losses because they were negligible (<5% for 20 nm particles and negligible for 100 nm particles).

Only the average values are reported in the tables either when the relative standard deviation (RSD%) was below 15% (for tests with three repetitions) or when the relative percent difference (RPD%) was below 15% (for tests with two repetitions). Otherwise, values from each tests are reported together with the average values. In the figures are reported only the average values.

3.3 Results

The results will be presented separately for the gaseous compounds and the particles.

3.3.1 Particle emissions

Black carbon (BC from MAAP), organic aerosol mass (OA from AMS), and particle number (PN from CPC) were measured from the CVS. Figure 3.3 shows the results for different speeds (PN, OA and BC), Fig. 3.4 shows the results for regulated test cycles (total mass, OA+BC), while Figures 3.8, 3.9, and 3.10 show the results for all cycles (PN, OA, BC, OA/BC). Tables 3.8, 3.9, 3.10, and 3.11 (OA, BC, PN, OA/BC) summarize the results for all cycles.

3.3.1.1 Organic aerosol mass emission

The organic aerosol mass emissions ranged between 5-40 mg km_{-1} for the HDDV(EIII), 0.12-18 mg km_{-1} for the diesel vehicles, <0.02 mg km_{-1} for the gasoline and 30-470 mg km_{-1} for the mopeds (Figures 3.8, 3.9, 3.10, and Tables 3.8, 3.9, 3.10, 3.11). For the speed ramps and steady state tests the EF(OA) was in the range 5.4-22 mg km^{-1} for the HDDV(EIII), 0.12-18 mg km^{-1} for the diesel vehicles, 85-405 mg km^{-1} for the mopeds and 9 10^{-4}-0.012 mg km^{-1} for the gasoline vehicle. For the regulated test cycles (ETC, NEDC and ECE-47) the EF(OA) was 13-33 mg km^{-1} for the HDDV(EIII), 0.8-10 mg km^{-1} for the diesel vehicles, 50-420 mg km^{-1} for the mopeds (hot phases only) and 2 10^{-3}-9 10^{-3} mg km^{-1} for the gasoline vehicle. It should be noted that OA emission

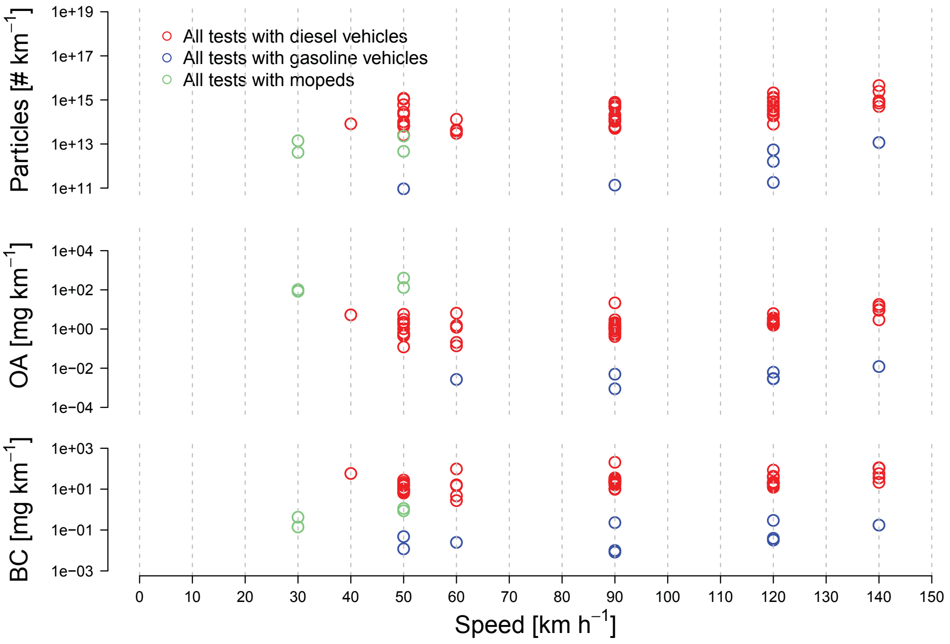

Figure 3.3: - Overview emission factors of particles, organic aerosol and black carbon from all types of vehicles at different speeds.

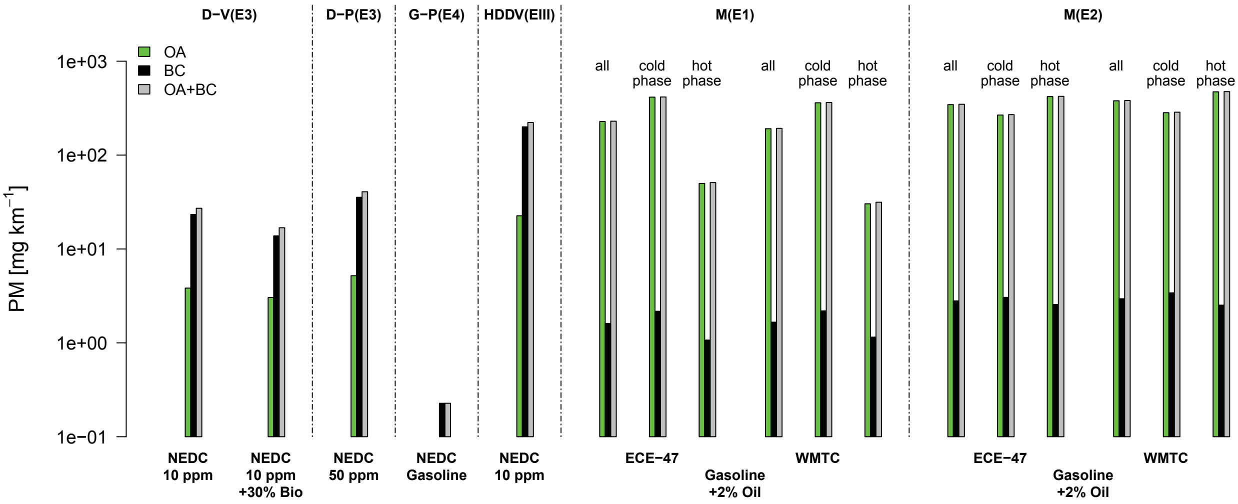

Figure 3.4: - Emission factors of OA, BC and OA+BC mass from regulated test cycles.

factors do not only depend on the combustion concept, engine load and temperature, fuel and lubricant but also on many other parameters, like cold start, speed, accelerations, pre-history and dilution (172, 173, 174, 175).

Extremely high emissions were observed for the two mopeds, which use a mixture of gasoline fuel and lubricant oil. The huge OA emissions may be explained by unburned or incompletely combusted oil from the high scavenging losses of this type of vehicles. Moped(E1), with an oxidative catalyst, showed higher emission of OA during the cold phases of both the ECE-47 and the WMTC cycles, while Moped(E2), equipped with an oxidative catalyst and a secondary air system showed the highest emission factors for OA (EF(OA)) during the hot phases of both ECE-47 and WMTC. The different behavior of the emissions can be attributed mainly to the combustion strategy of the two mopeds (Moped(E1) was equipped with a carburetor while Moped(E2) had a direct injection technology) and to the different exhaust temperature due to the secondary air injection system (162). The different exhaust gas temperatures, light-off temperatures of the catalysts (temperature at which the conversion of an exhaust gas component reaches 50%) and efficiencies affected also the results. Similar conclusions were also drawn by other authors (e.g. (145, 176)).

In comparison with the mopeds, the HDDV and the diesel vehicles had one order of magnitude lower OA emissions. It clearly demonstrates the efficiency of four stroke engines and the effect of the oxidation catalysts. Gasoline vehicles had 3 orders of magnitude lower emissions than the diesel vehicles. This has to do with the low concentration of particles (note that the OA refers to organic material on particles). The OA from the Euro 4 vehicle was 66% (NEDC) and 43±49% (speed ramp, average value ±1 standard deviation) lower than from the Euro 3 vehicle (both with 10 ppm sulfur in the fuel). This result may be vehicle specific (engine calibration and oxidation catalyst) and cannot necessarily be extended to other vehicles.

With 10% biodiesel blend (Diesel-P(E4)) and with 30% biodiesel blend (Diesel-V(E3)) a reduction in the OA emissions was observed: reduction by 22% and 21% during the NEDC cycle for Diesel-P(E4) and the Diesel-V(E3), respectively, and by 35±12% for the speed ramp with Diesel-V(E3). The reduction of the sulfur fuel content from 50 to 10 ppm did not affect the OA emissions, as expected.

In general, the highest emission factors were obtained at higher speeds for the diesel and gasoline vehicles (90 km h^{-1} for the HDDV(EIII) and at 140 km h^{-1} for the diesel light-duty vehicles), while for the legislative driving cycles the highest EF(OA) among the four-wheel vehicles were observed during the urban part of the cycles (UDC for the NEDC cycle and urban for the ETC cycle) characterized by low speeds. High OA emissions at low speeds can be explained by the lower conversion of the catalyst due to the lower exhaust gas temperatures. This is especially true for the cold start cycles and for the first seconds of the cycle where the catalyst hasn't reached its light-off temperature. The effect is more profound at accelerations where the combustion is incomplete. At high speeds desorption and/or pyrolysis of organic material deposited in the vehicle tailpipe and aftertreatment device or the transfer hose to the CVS could explain the high OA emissions (177). The tailpipe and the aftertreatment devices have been found to store substantial amounts of particles which are emitted at accelerations or high speeds (178).

For the HDDV(EIII) (no aftertreatment device) the first acceleration in the UDC part of the NEDC and in the urban part of the ETC yielded a peak in the OA concentration that was 440 and 320 times higher than the average concentration for the remaining UDC and Urban part of the cycles, respectively. 70% (NEDC) and 17% (ETC) of total organic emissions during the whole cycles were produced with this first acceleration. In the last part of the ETC cycle (Motorway) both the higher average speed (84.4 km h^{-1}) and the lower dilution ratio can be the reasons for the higher OA emission compared to the second part of the cycle (Rural, 69.3 km h^{-1}) as both phases have a similar number of accelerations per km.

There are two possible reasons for the high OA at high speeds: Either due to desorption from the vehicle and sampling system pipes or due to lower dilution ratios in the dilution tunnel. Concerning the first explanation, high OA can be found at high speeds is desorption and/or pyrolysis of organic material deposited in the vehicle tailpipe and aftertreatment device or the transfer hose to the CVS (177).

Concerning the second explanation, it has been shown that the OA mass measurement can be affected by the dilution of the exhaust. For example, $PM_{2.5}$ mass emitted by a diesel power generator with no aftertreatment devices can decrease by 50% when the dilution ratio is increased from 20:1 to 350:1 (173). This mass reduction has been associated with semi-volatile organic compounds (SVOCs) that shift to the gas phase with increasing dilution to maintain thermodynamic equilibrium (173). In the case of the HDDV(EIII), during the high speed part of the cycles the dilution ratios in the dilution tunnel were lower than those associated to the low speed parts. For instance, the dilution ratio in the last part of the FIGE cycle (motorway) was 103 compared to the second part of the cycle (rural) where it was 158 (for the UDC and the EUDC parts of the NEDC the dilution ratios were 330 and 166, respectively). Moreover, for the steady state test with the HDDV(EIII) the average dilution ratio for the 40 and 60 km h^{-1} speeds were 210, while for the 90 km h^{-1} the dilution ratio was 98.

To evaluate the effect of the dilution on the OA concentration, two speed ramp tests with Diesel-V(E3) were performed with different dilution ratios using either only one or two ejector diluters. With one ejector diluter after the CVS, the range of the final dilution ratios was 34-115, while with two ejector diluters the range was 473-1600, which included also atmospherically relevant dilution ratios (>1000). Constant engine conditions were observed within the two different speed ramps. A 14-fold difference in the dilution ratio between the two tests with the same vehicle did not affect the OA concentration measurements at the tailpipe probably because either the 14-fold difference in the dilution ratios was not enough to have an influence on the volatility of the SVOCs or more time was needed to reach thermodynamic equilibrium. For all speeds the ratio of the OA concentrations from the two experiments was ≈1 with the exception of the 140 km h^{-1} speed where the ratio was ≈2 but with higher OA concentration for higher dilution, in contrast to the expectation. Two speed ramp tests with the Moped(E2) were also performed with different dilution ratios (≈250±50 when one diluter was used, 4000±500 with two) and also in this case the OA concentrations at the tailpipe were not affected by differences in the final dilution and the ratio was ≈1 for both speeds. These results are in agreement with other researchers who found that for residence times in the order of 1 second, the primary dilution (in the CVS in our case) is the most important in the adsorption/condensation/nucleation of the volatile precursors (e.g. (179, 180)).

3.3.1.2 Black carbon mass emission

With the speed ramps and steady state tests the EF(BC) was in the range 59-208 mg km^{-1} for the HDDV(EIII), 2.8-113 mg km^{-1} for the diesel vehicles, 0.14-1.15 mg km^{-1} for the mopeds and 0.01-0.30 mg km^{-1} for the gasoline vehicle (Figures 3.3, 3.4, 3.8, 3.9, 3.10, and Tables 3.8, 3.9, 3.10, 3.11). For the regulated test cycles (ETC, NEDC, and hot ECE-47 for Heavy-duty vehicle, light-duty vehicle, and mopeds, respectively) the

EF(BC) was 168 mg km^{-1} for the HDDV(EIII), 14-36 mg km^{-1} for the diesel vehicles, 0.23 mg km^{-1} for the gasoline vehicle, and 1.1-2.6 mg km^{-1} for the mopeds. Thus, the HDDV(EIII) was the main emitter of BC during the tests with both legislative and unregulated driving cycles.

One striking finding is that for diesel vehicles at 140 km h^{-1}, a speed higher than the maximum during the cycles, the BC emissions are often extremely high due to the very low air to fuel ratio and incomplete combustion. Similarly, for the HDDV(EIII) the emissions at 90 km h^{-1} (its maximum speed) were the highest. In general, the emissions at steady state were lower than during the cycles indicating that a high contribution to BC originates from the acceleration of the vehicles.

For both mopeds the BC emissions were higher (62±41%) during the cold phases of the cycles (ECE-47 and WMTC).

With 10% biodiesel (Euro 4 vehicle) the EF(BC) was reduced by 20% and with 30% biodiesel (Euro 3 vehicle) the EF(BC) was reduced by 41% (NEDC), 26±15% (speed ramp) and 45±6% (steady state) lower. Similar reductions have been found by other researchers (143).

3.3.1.3 OA to BC ratios

The OA/BC ratios of the diesel vehicles during the steady state and speed ramp tests were below 0.2 with only a few exceptions, always remaining below 1. These ratios are well within the range of values found in the literature, typically determined from filter measurements (152, 181). The OA/BC ratios from diesel vehicles were always higher in the UDC part of the NEDC cycle, and in the urban part of the ETC cycle. Values up to ≈0.25 were obtained in the UDC part, while ratios below 0.1 were found in the EUDC part. The lower ratios for the second part of the cycles are due to the higher decrease of the OA compared to the BC. For all experiments with the diesel vehicles and the HDDV, the OA emissions in the EUDC part of the cycle was on average 69±15% lower than the UDC part, while for the BC emissions the reduction was only 8±23%. As explained previously the cold start results in high OA emissions which significantly decrease as the catalyst reaches its light off temperature (114). OA/BC values below 0.2 were also found for the gasoline vehicle. For the gasoline vehicle the OA/BC ratios were equivalent in both part of the NEDC cycle. This is in accordance with other researchers who found similar fractions of OA and BC for gasoline vehicles (e.g. (182, 183)).

For the mopeds the OA/BC values were between 27 and 725 (idle not included, Fig. 3.5 and Tab. 3.11). For the ECE-47 and WMTC tests the OA/BC values measured from the mopeds were 115-142. For the Moped(E1) the cold phases of the ECE-47 and WMTC cycles had the highest OA/BC ratios, while for the Moped(E2) the highest values were found during the hot phases. These ratios are within the range found by other researchers as well and confirm that the emitted aerosol contains a large amount of volatile and semi-volatile material.

3.3.1.4 Particle number emissions

The particle number emissions of the HDDV(EIII) and diesel light-duty vehicles (LDV) were in the order of 10^{14} km^{-1}. The emissions of the gasoline vehicles were in the order of 10^{12} km^{-1}, while those of the mopeds were in the order of 10^{13} km^{-1} (Figures 3.3, 3.8, 3.9, 3.10, and Tables 3.8, 3.9, 3.10, 3.11).

Typical size distributions from vehicle emissions are bimodal with a usually volatile nucleation mode (diameter <30 nm) and an accumulation mode (median diameter between 50 and 100 nm) (69). The nucleation mode, similarly to OA, is sensitive to many parameters like engine, fuel, operation mode, sampling conditions, etc., while the accumulation mode generally depends mainly on the engine operating mode. Particle number emissions in this study were determined with a CPC connected to the CVS. Total (volatile and non-volatile) particles >7 nm were measured and reported.

For the HDDV(EIII) the increase of the emissions with increasing speed was correlated with the increase of the accumulation mode, since no nucleation mode appeared with this vehicle. The PN emissions behavior was thus similar to the BC behavior (see Tab. 3.8). Diesel vehicles in addition showed high PN emissions at the beginning of the cycle and during the accelerations. A cold start is generally associated with a nucleation mode due to the low hydrocarbons oxidation efficiency of the catalyst. The accelerations also result in nucleation mode particles due to the low available surface for condensation of the volatile species. A speed dependence of EF(PN) was already found in other studies (e.g. (184, 185)) for both HDV and LDV. More details about these topics can be found in Giechaskiel et al. (160, 186).

At 50 and 90 km h^{-1} speeds during the speed ramp test the particle emissions were higher when the speed sequence was repeated backwards from 140 km h^{-1} to idle than for the sequence from idle to 140 km h^{-1} for diesel vehicles while the opposite was observed for gasoline cars. The emissions of the diesel cars are connected with the exhaust temperature which enhances the oxidation of SO_2 to SO_3 in the DOC and the subsequent conversion to sulfuric acid (H_2SO_4) during dilution and sampling. The sulfuric acid acts as condensation nuclei, enhancing number concentrations (160, 187, 188, 189, 190, 191).

At speeds lower than 140 km h^{-1}, more than 95% of the total mass (sum of the non-refractory species measured by the HR-ToF-AMS and BC) from diesel passenger vehicles was made only of BC and OA, while at 140 km h^{-1} (including the acceleration from 120 km h^{-1} to 140 km h^{-1}) a sharp increase in particle-associated sulfate was measured (in these cases, sulfate represented up to 70% of the total PM). A tail in the sulfate concentration was then present when the speed was decreased until idle (186). The addition of either 10% or 30% biodiesel most of the times lowered the particle number emissions for diesel vehicles even if for some single speeds the particle number was higher (50 and 90 km h^{-1} speeds with 30% biodiesel). In general, many authors have reported an increase in particle number emission in the nucleation mode when biodiesel blends were used but the very low sulfur content of biodiesel fuels can also be an explanation for the decrease in nanoparticle concentrations ((94) and references therein).

For the Moped(E2) with the SAS and oxidation catalyst, the particle emission factors were 3.4-5.0 times higher than for the Moped(E1) with oxidation catalyst only (steady state and hot phases of ECE-47 and WMTC cycles). Both but especially Moped(E1) had higher emissions during the cold phases of the ECE-47 and WMTC cycles in agreement with other studies (e.g. (176)).

It should be mentioned that some particle number measurements were conducted according to the new UNECE Regulation 83 for light-duty vehicles (i.e. only the non-volatile particle concentration was measured, using hot dilution and an evaporation tube at 300°C) (81). The results showed that the non-volatile particle number concentration was similar to the total concentration (i.e., no nucleation mode particles existed) at low speeds. However, at high speeds, due to the formation of a nucleation mode, the non-volatile particles were <10% of the total concentration. More details can be found in Giechaskiel et al. (2010) (186).

3.3.2 Trace gas emissions

3.3.2.1 Regulated gaseous compound and CO_2 emissions

The HC emissions from the gasoline vehicle were above the limit of 0.1 g km^{-1} (+15%) defined by regulations for Euro 4 vehicles, and also the sum of HC plus NO_x from the Diesel-P(E3) and the Diesel-P(E4) were above the limit of 0.56 g km^{-1} (+36%) and 0.3 g km^{-1} (+70%) defined for the Euro 3 and the Euro 4 diesel vehicles, respectively (Fig. 3.5 and Tab. 3.12). The gasoline vehicle complied with the Euro 4 regulation for NO_x, while only the Diesel-V(E3) with reference diesel fuel and 30% biodiesel blended complied with the Euro 3 emission standard for NO_x. The NO_x emissions from the Diesel-P(E3) and Diesel-P(E4) were above the limits (0.5 g km^{-1} for Euro 3 and 0.25 g km^{-1} for Euro 4). The NO_x emissions of gasoline and diesel passenger vehicles were 6-10 times lower than the emissions from the HDDV(EIII) over the entire NEDC cycle. The NO_x emission was reduced by a factor of 1.7 from Diesel-P(E3) to Diesel-P(E4). With biodiesel the NO_x emission increased only by 5% compared to the standard diesel fuel.

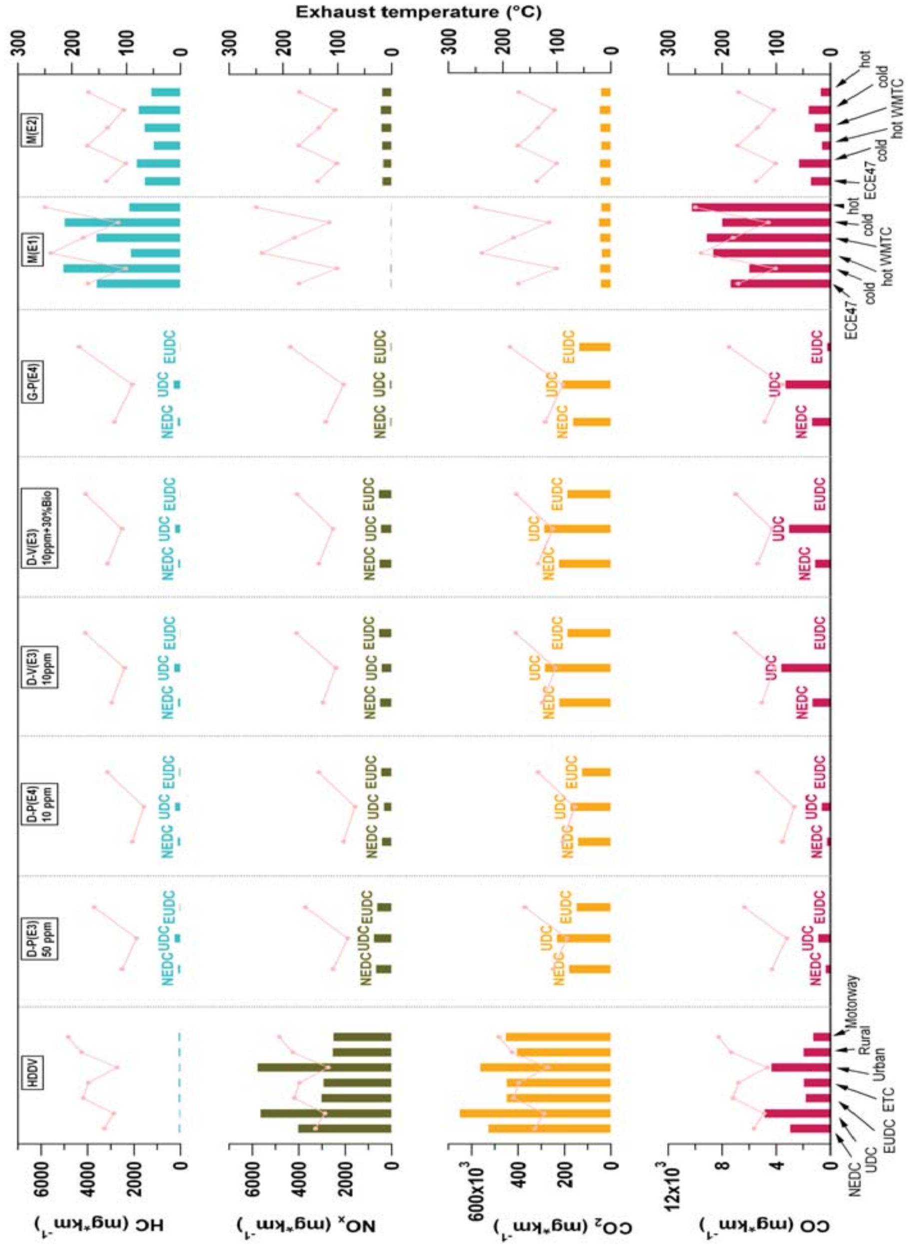

Figure 3.5: - Emission factors of regulated compounds and CO_2.

In accordance with the European legislation, only the hot phase of the ECE-47 was taken into account to define if the emissions of NO_x plus HC from the mopeds complied with the limits. The EF(NO_x+HC) for Moped(E1) were below the emission limit of 3 g km^{-1}, while for Moped(E2) the emission was 1.2-1.3 times higher than the limit (1.2 g km^{-1}). The EF(NO_x) of the Moped(E2) was 14 and 18 fold higher than of the Moped(E1) for the entire ECE-47 and WMTC cycles, respectively. The EF(NO_x) for the Moped(E2) from the cold (0.35 g km^{-1}) and hot (0.39 g km^{-1}) phase of the ECE-47 were higher than the values (<0.20 g km^{-1}) measured from other Euro 2 mopeds (134).

Among the various vehicles, the mopeds were those with the highest emissions of HC. Considering the cycles used for emission homologations of passenger vehicles and mopeds (NEDC, hot phase from ECE-47) and the NEDC also for the HDDV(EIII) (the NEDC was used for the HDDV(EIII) for comparison even though this is not used for the homologation of trucks), the EF(HC) for mopeds were 11-36 times higher than for the other vehicles. With 30% biodiesel the EF(HC) decreased by 15% compared to the same vehicle powered with standard diesel. The lowest emission of HC from the HDDV(EIII) could be explained by the higher engine temperature, which provided a more complete fuel combustion.

The emissions of CO were below the limits for the Diesel-P(E3) and Diesel-P(E4), and above for the Diesel-V(E3) (+108%) and Gasoline-P(E4) (+36%). Using biodiesel the EF(CO) decreased by 15% but the value was still above the limit. A decrease in CO emissions when biodiesel was added to the diesel has been considered a general trend, partially explained by the enhancement in the complete combustion due to the additional oxygen content in the fuel ((94) and references therein). The EF(CO) of the HDDV(EIII) from the NEDC and the ETC cycles were higher than the emissions from the other passenger vehicles but the Moped(E1) featured the highest EF(CO). Most of the CO emissions appeared during the start up of the engines when the low temperature of the engines did not allow for a more complete combustion and oxidation in the catalysts. Reductions in EF(CO) up to 99% were measured between the urban part and the extra-urban part of the NEDC cycle. Only for the Moped(E1) the EF(CO) increased from the cold phases to the hot phases of the ECE-47 and WMTC cycles. The EF(CO) for the Moped(E2) are in good agreement with the values measured from other Euro 2 mopeds (134). In general, the emissions of HC and CO were higher during the coldest phases of the cycles (UDC in the NEDC, cold phase in ECE-47, etc) and this behavior reflects the well-known occurrence of incomplete combustion while the engine and catalytic converter have not warmed up yet. The different results from the two mopeds, with higher emissions of HC and CO for Moped(E1) and higher emissions of NOx for Moped(E2), could be related to the older oxidative catalyst of the Moped(E1) and the SAS of the Moped(E2). The presence of SAS together with an efficient catalyst could contribute to the reduction of the HC and CO and to the increase of NO_x for Moped(E2).

The HDDV(EIII) showed the highest emissions of CO_2, followed by passenger vehicles and mopeds. The emission from the HDDV(EIII) was on average (total NEDC and ETC cycles) 2.7 times higher than the emissions from passenger vehicles and 11 times higher than the emissions from mopeds. The effect of biodiesel the EF(CO_2) over the entire NEDC cycle was not noticeable.

3.3.2.2 Unregulated trace gas emissions

The emissions of a selection of unregulated gaseous compounds, such as nitrogen-containing compounds (NO, NO_2, N_2O, NH_3, HCN), small oxygenated organic compounds (formaldehyde, acetaldehyde), SO_2 and methane for the various tests are shown in Fig. 3.6 and reported in Tab. 3.13. The nitrogen compounds had in general higher emission factors than the other compounds with the only exception of Moped(E1) where the CH_4 emission factor was highest. Within the nitrogen compounds, the NO emissions were the most important for all vehicles (up to 96% of the total nitrogen-containing compounds). The HDDV(EIII) had the highest EF(NO), being 5-233 higher than the emissions of the other vehicles. The contribution of NO to NO_x was 85% for the HDDV(EIII) (average value from ETC and NEDC), 59% for the Diesel-V(E3)-10ppm, 55% for the Diesel-V(E3)-30%Bio, more than 99% for the Gasoline-P(E4), and more than 98% for the mopeds. In Alvarez et al. (2008) (192), NO was 75% of the NO_x emitted from diesel vehicles without particle filter, while for Euro 4 gasoline vehicles the NO_x emissions almost entirely consisted of NO. The formation of NO_2 in diesel vehicles is due to the presence of an oxidation catalyst, and the relative contribution to NO_x increases at higher temperature when the light-off of the DOC is reached (114). NO_2 emissions are a greater concern than NO emissions because NO_2 is toxic and is a direct precursor for ozone formation. NO_2 concentrations remain high and still surpass the legal thresholds in various areas in Europe in spite of substantial NO_x reductions, due to the shift from NO to NO_2 emissions (67, 192, 193, 194). Gasoline-P(E4) with regular fuel and Moped(E1) had the highest emission factors of NH_3 (4.2-6.5 mg km^{-1}; 19-31% of the total nitrogen-containing compounds) while for the other vehicles the relative contribution was below 0.015%. The EF(NH_3) for the gasoline vehicle was 1.4 times higher than the EF(NH_3) from Moped(E1). The gasoline vehicle featured high EF(NH_3) because in the gasoline vehicles NH_3 is produced in the TWC under reducing conditions when the light-off temperature is reached. The formation mechanism involves NO and H_2. NO is generated by the oxidation of N_2 during combustion whereas H_2 is mainly produced in the catalyst during the water gas shift reaction of CO (60, 61). The emissions of NH_3 can also dominate over those of NO during the cold start in particular at low ambient temperature (102, 157). The lambda value showed a rich combustion in Moped(E1) and with these conditions NH_3 production was favored (62, 63).

The Moped(E1) and the HDDV(EIII) had the highest emissions of HCN (1.0-1.2 mg km^{-1}), comprising 5.2-6.5% of the total nitrogen-containing compounds for the Moped(E1) and only 0.04-0.06% for the HDDV(EIII). HCN is a toxic compound that is produced from NO_x by reduction reactions (195, 196). The Diesel-V(E3), with regular fuel and with biodiesel, had the highest emission factors of N_2O (13-53 mg km^{-1}; 4.2-5.6% of the total nitrogen compounds). For the other vehicles the values were lower than 2.5 mg km^{-1}.

The emission of the sum of formaldehyde and acetaldehyde was 4.28-159 mg km^{-1} for the Diesel-V(E3), 65 mg km^{-1} for the Moped(E2) (average between the two cycles), 50 mg km^{-1} for the HDDV(EIII) (average between the two cycles), 41 mg km^{-1} for the Moped(E1) (average between the two cycles), 38 mg km^{-1} for the Diesel-V(E3)-30%Bio, and 1.3 mg km^{-1} for the Gasoline-P(E4). The carbonyl emission rates of diesel vehicles were found to be higher than those of gasoline vehicles. In 2006, diesel/gasoline emission ratios of 7.9 and 6.3 for formaldehyde and acetaldehyde, respectively were measured in the Caldecott tunnel (U.S.A.) (197). Considering only the NEDC tests with the conventional diesel and gasoline fuels, the average diesel/gasoline emission ratios from this work were 35-136 and 26-90 for HCHO and CH_3COH, which confirms the importance of diesel vehicles in the emissions of carbonyl compounds. The HDDV(EIII) was the vehicle with the highest EF(SO_2) (63 mg km^{-1}), while the Moped(E1) featured the highest emission of CH_4 (71 mg km^{-1}).

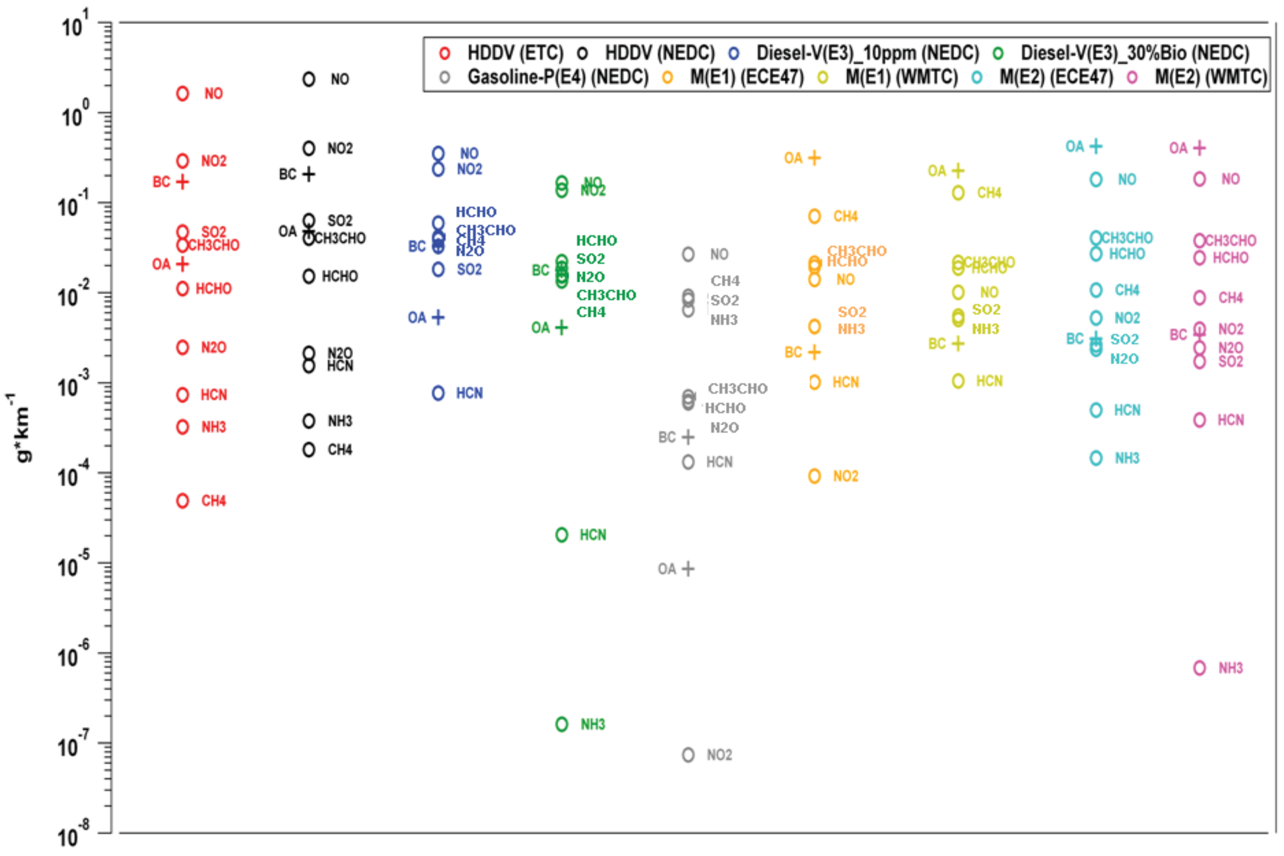

Figure 3.6: - Emission factors of gas phase unregulated compounds, OA and BC from regulated test cycles.

3.3.2.3 Monocyclic and polycyclic aromatic hydrocarbon emissions

The measurements of the gaseous monocyclic and polycyclic aromatic hydrocarbons comprised 13 substituted and non-substituted compounds (Fig. 3.7 and Tables 3.14, 3.15). The mopeds featured the highest emissions of aromatic compounds (99-211 mg km^{-1}), followed by the gasoline vehicle (47 mg km^{-1}) and the diesel vehicle with the HDDV(EIII) (5.3-10 mg km^{-1}).

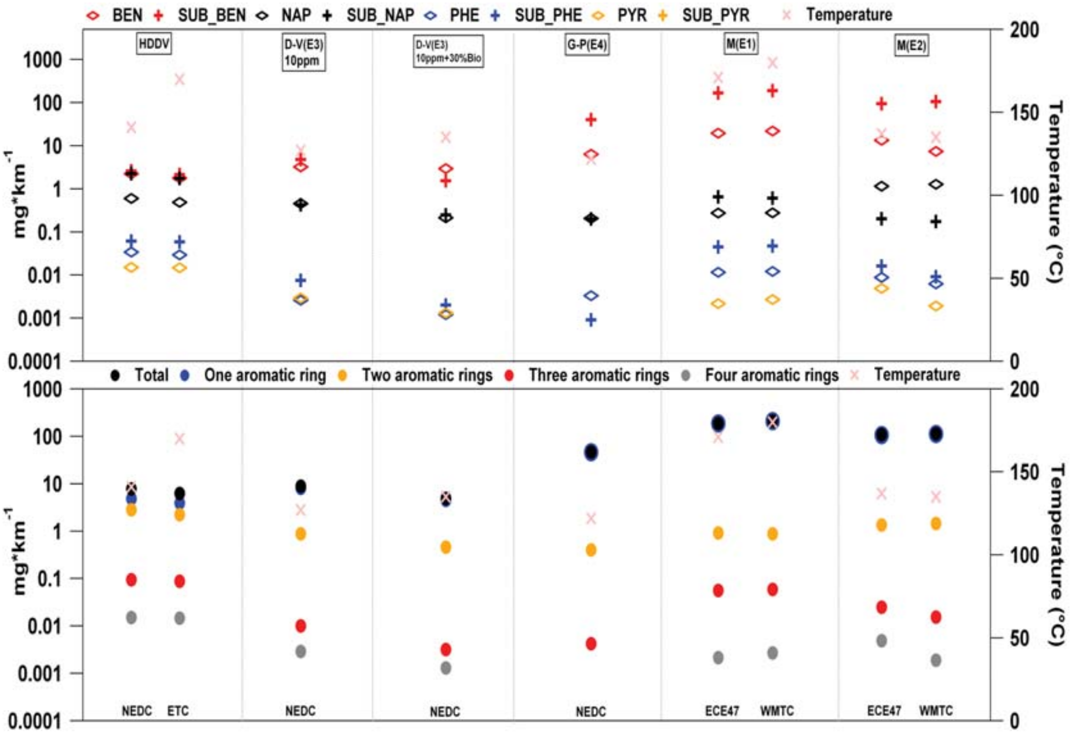

Figure 3.7: - Emission factors of aromatic compounds from regulated test cycles.

More than 99% of the total emissions of monocyclic and polycyclic aromatic hydrocarbons from the mopeds and the gasoline vehicle were made of benzene plus substituted benzenes, 87% for the Diesel-V(E3) and 56% from the HDDV(EIII). Around 7.1-13% and 29-43% of the total emissions were due to naphthalene and substituted naphthalene for the Diesel-V(E3) and the HDDV(EIII), respectively. The contribution of PAHs with 3 and 4 rings to the total emissions was less than 1.9% for all vehicles. The emissions of mono-aromatic compounds (MAHs) from the Gasoline-P(E4) was 8.3-12 and

5.0-6.9 times higher than the emissions from the HDDV(EIII) and Diesel-V(E3) vehicle, respectively, while the emissions of PAHs from the HDDV(EIII) and Diesel-V(E3) were 4.0-8.0 and 1.8-2.6 times higher than the gasoline vehicle. Previous chassis dynamometer tests with 13 gasoline and 17 diesel vehicles have shown that on average the emissions of MAHs from gasoline vehicles are 6 times higher than the emissions from diesel vehicles (154). The HDDV(EIII) had the highest emission of PAHs (1.6-3.2 mg km^{-1}, NEDC and ETC cycles), followed by the mopeds (0.93-1.5 mg km^{-1}, Moped(E1) and Moped(E2) for ECE-47 and WMTC cycles), and for the other vehicles the emission was below 1.0 mg km^{-1}.

The benzene/toluene ratio is sometimes used as photochemical clock for urban plumes traveling away from traffic sources because toluene is five times as reactive as benzene with OH radicals; therefore, a change in the ratio is observed during the aging of the plume (198, 199). The average benzene/toluene values measured for the primary emissions were 3.3-3.9 for the HDDV(EIII), 2.3-2.6 for Diesel-V(E3) vehicle (3.8 for Diesel-V(E3) with biodiesel), 0.45 for the gasoline vehicle and 0.24-0.90 for the mopeds. Thus, this ratio can not only vary with plume age but also with the vehicle types.

With biodiesel the total aromatic emissions from the Diesel-V(E3) decreased by 37-51%. The emissions of MAHs and PAHs decreased by 34-52% and 37-56%, respectively. Experiments conducted in a six-cylinder heavy-duty diesel engine fuelled with pure diesel and biodiesel blends (2%, B2; 5%, B5 and 20%, B20) have also shown a reduction in the emissions of MAHs (4.2%, B2; 8.2%, B5; 21.1%, B20) and of PAHs (2.7%, B2; 6.3%, B5; 17.2%, B20) (98). The main sources of aromatic compounds from vehicles are pyrosynthesis processes from small unstable molecules (free radicals) and unburned or partially burned aromatics from fuels (140). Emissions of aromatic compounds are directly correlated to the initial concentration in the fuel (140). Using biodiesel the emissions of aromatics were thus reduced because of the lower aromatic content in the biodiesel blend. Also the excess of air might have produced a more efficient combustion of aromatics (140).

The combustion temperature of the engines affects the amount of alkylated aromatics in exhaust (140). As the temperature increases, the alkyl-substituted-to-parent compound ratio decreases. The ratios of the emission factors of substituted aromatics over the emissions of the parent compounds are reported in Tab. 3.4. The two mopeds were the vehicles with the highest emissions of substituted-benzene.

Vehicles	Cycles	Sub-BEN/BEN	Sub-NAP/NAP	Sub-PHE/PHE
HDDV(EIII)	NEDC and ETC	1.1-1.4	3.4-3.9	1.6-2.1
Diesel-(E3) 10ppm	NEDC	0.84-2.3	0.75-1.1	1.3-3.5
Diesel-V(E3) 30%Bio	NEDC	0.52	1.2	1.7
Gasoline-P(E4)	NEDC	6.3	0.96	0.28
Moped(E1)	ECE-47 and WMTC	8.5-8.6	2.2-2.4	4.0
Moped(E2)	ECE-47 and WMTC	4.0-15	0.13-0.24	0.99-2.3

Table 3.4: Emission factors of substituted aromatics over the emission factors of the parent compounds (Sub=substituted; BEN=benzene; NAP= napthalene; PHE= phenanthrene).

3.4 Conclusion

The emission factors of gas phase and particle-associated regulated and unregulated species from seven different vehicles circulating in Europe were presented. The aim of this work was to improve the knowledge about the emission factors from the various vehicles tested with legislative European driving cycles, steady state cycles and speed ramp sequences using standard gasoline and diesel fuels but also rapeseed methyl ester biodiesel blend.

Diesel vehicles, without particle filters, featured the highest emissions of particle number, followed by mopeds and then gasoline vehicles. The particles from diesel vehicles were mainly made of BC with a low fraction of OA, while the particles from the mopeds were mainly OA. Mopeds were characterized by surprisingly high emissions factors for OA, which were orders of magnitude higher than for the other vehicles.

Higher emissions of particle number and OA were observed at higher speeds. However, cold start emissions and accelerations were the main contributors to the high emissions of particle number, BC and OA.

The heavy-duty diesel vehicle featured the highest NO_x emissions, while the gasoline vehicle had the highest emissions of NH_3 due to the reducing conditions in the three-way catalyst. The NO emissions were the most important for all vehicles within the nitrogen compounds analyzed.

The mopeds featured the highest emissions for HC and aromatic compounds due to the unburned and partially burned gasoline and lubricant oil mixture. Mopeds, and in general two-stroke engines, are important for urban transport in many cities in Europe and even more in Asian megacities congested by traffic. Thus, the findings of this paper confirm that powered two-wheelers are a potentially important source of enhanced pollution in urban areas (PM, PAHs) due to the delay in more stringent emission regulations.

The measurements of the gaseous monocyclic and polycyclic aromatic hydrocarbons from all vehicles were dominated by aromatic compounds with one and two rings. The gasoline vehicle had higher emissions of mono-aromatic compounds than diesel vehicles, while the diesel vehicles featured higher emission of polycyclic aromatic hydrocarbons than the gasoline vehicle.

With biodiesel the emission factors of OA, HC, BC and total aromatics were lower than those from the regular fuel, confirming biodiesel as a valid alternative fuel to reduce diesel engine exhaust emissions.

The results presented in this paper can be used to compare or check emissions and emission ratios in emission inventories for non-regulated compounds which are used in chemical transport models. Also ambient concentration ratios can be compared with the presented results. Since the number of tested vehicles and the number of repetition of each test for each vehicle were rather low, more measurements of unregulated compounds including vehicles of the latest generation are needed to provide a more reliable basis for emission estimates for current and future vehicle fleets in Europe.

- **Acknowledgments**

The VELA staff is acknowledged for their skillful technical assistance conducting the vehicle tests, in particular U. Manfredi as responsible for the VELA laboratory and G. Martini for the fruitful discussions. This work was supported by the Competence Center Energy and Mobility (CCEM) in the context of the project NEADS (Next Generation Exhaust Aftertreatment for Diesel Propulsion Systems).

3.5 Supplementary Materials

Vehicle	Date	Exp.	Cycle	Engine temperature	Fuel type	CVS dilution air	Ejector diluter
HDDV(EIII)	02.04.2009	2	NEDC	hot	10 ppm	80 m^3 min^{-1}	1
HDDV(EIII)		3	ETC	hot	10 ppm	80 m^3 min^{-1}	1
HDDV(EIII)	03.04.2009	1	NEDC	cold	10 ppm	80 m^3 min^{-1}	1
HDDV(EIII)		2	ETC	hot	10 ppm	80 m^3 min^{-1}	1
HDDV(EIII)		3	steady state	hot	10 ppm	80 m^3 min^{-1}	1
HDDV(EIII)	06.04.2009	1	ETC	cold	10 ppm	80 m^3 min^{-1}	1
HDDV(EIII)		2	NEDC	hot	10 ppm	80 m^3 min^{-1}	1
HDDV(EIII)		3	steady state	hot	10 ppm	80 m^3 min^{-1}	1
HDDV(EIII)	07.04.2009	1	steady state	cold	10 ppm	80 m^3 min^{-1}	1
Diesel-P(E3)	08.04.2009	3	steady state	hot	10 ppm	7.5 m^3 min^{-1}	2
Diesel-P(E3)		4	speed ramp	hot	10 ppm	11 m^3 min^{-1}	1
Diesel-P(E3)	09.04.2009	1	NEDC	cold	10 ppm	6 m^3 min^{-1}	2
Diesel-P(E3)	14.04.2009	1	NEDC	cold	50 ppm	6 m^3 min^{-1}	1
Diesel-P(E3)		2	steady state	hot	50 ppm	7.5 m^3 min^{-1}	2
Diesel-P(E3)		3	speed ramp	hot	50 ppm	11 m^3 min^{-1}	2
Diesel-P(E3)	15.04.2009	1	NEDC	cold	50 ppm	6 m^3 min^{-1}	2
Diesel-P(E4)	16.04.2009	1	NEDC	cold	10 ppm	6 m^3 min^{-1}	1
Diesel-P(E4)		3	speed ramp	hot	10 ppm	6 m^3 min^{-1}	2
Diesel-P(E4)	17.04.2009	1	NEDC	cold	10 ppm + 10%biodiesel	6 m^3 min^{-1}	2
Gasoline-P(E4)	20.04.2009	1	NEDC	cold	gasoline	6 m^3 min^{-1}	0
Gasoline-P(E4)		2	steady state	hot	gasoline	6 m^3 min^{-1}	0
Gasoline-P(E4)		3	NEDC	cold	gasoline	6 m^3 min^{-1}	0
Gasoline-P(E4)	21.04.2009	1	NEDC	cold	gasoline	6 m^3 min^{-1}	0
Gasoline-P(E4)		2	speed ramp	hot	gasoline	6 m^3 min^{-1}	0
Gasoline-P(E4)		3	speed ramp	hot	gasoline	12 m^3 min^{-1}	0
Diesel-V(E3)	27.04.2009	1	NEDC	cold	10 ppm	12 m^3 min^{-1}	2
Diesel-V(E3)		2	steady state	hot	10 ppm	12 m^3 min^{-1}	1
Diesel-V(E3)		3	steady state	hot	10 ppm	12 m^3 min^{-1}	1
Diesel-V(E3)		4	NEDC	cold	10 ppm	12 m^3 min^{-1}	1
Diesel-V(E3)		5	speed ramp	hot	10 ppm	15 m^3 min^{-1}	2
Diesel-V(E3)	28.04.2009	1	NEDC	cold	10 ppm	12 m^3 min^{-1}	2
Diesel-V(E3)		2	speed ramp	hot	10 ppm	15 m^3 min^{-1}	1
Diesel-V(E3)	29.04.2009	1	NEDC	cold	10 ppm + 30%biodiesel	12 m^3 min^{-1}	1
Diesel-V(E3)		2	steady state	hot	10 ppm + 30%biodiesel	12 m^3 min^{-1}	1
Diesel-V(E3)		3	speed ramp	hot	10 ppm + 30%biodiesel	15 m^3 min^{-1}	1
Diesel-V(E3)	30.04.2009	1	NEDC	cold	10 ppm + 30%biodiesel	12 m^3 min^{-1}	2
Moped(E1)	04.05.2009	1	ECE-47	cold	Unleaded fuel + 2%oil	4.5 m^3 min^{-1}	1
Moped(E1)		3	steady state	hot	Unleaded fuel + 2%oil	4.5 m^3 min^{-1}	1
Moped(E1)		4	WMTC	cold	Unleaded fuel + 2%oil	4.5 m^3 min^{-1}	1
Moped(E1)		5	ECE-47	hot	Unleaded fuel + 2%oil	4.5 m^3 min^{-1}	1
Moped(E2)	05.05.2009	1	ECE-47	cold	Unleaded fuel + 2%oil	4.5 m^3 min^{-1}	1
Moped(E2)		2	steady state	hot	Unleaded fuel + 2%oil	4.5 m^3 min^{-1}	2
Moped(E2)		3	steady state	hot	Unleaded fuel + 2%oil	4.5 m^3 min^{-1}	1
Moped(E2)		5	ECE-47	cold	Unleaded fuel + 2%oil	4.5 m^3 min^{-1}	1
Moped(E2)		6	WMTC	hot	Unleaded fuel + 2%oil	4.5 m^3 min^{-1}	1

Table 3.5: Descriptions of the tests.

Species	**Cycle**	**Diesel-V(E3)**		
		Regular fuel 30%	**Biodiesel**	**% change**
OA [mg km^{-1}]	NEDC	3.83	3.04	-21
	UDC	7.68	6.52	-15
	EUDC	1.59	1.00	-37
	60 km h^{-1}	0.21	0.14	-33
	90 km h^{-1}	0.80	0.42	-48
	120 km h^{-1}	6.20	1.90	-69
	50 km h^{-1}	1.80	1.05	-42
	90 km h^{-1}	0.99	0.54	-45
	120 km h^{-1}	2.35	1.62	-31
	140 km h^{-1}	18.2	9.82	-46
	120 km h^{-1}	2.18	1.67	-23
	90 km h^{-1}	1.12	0.61	-46
	50 km h^{-1}	0.56	0.47	-16
BC [mg km^{-1}]	NEDC	23.3	13.8	-41
	UDC	22.5	15.9	-29
	EUDC	23.8	12.6	-47
	60 km h^{-1}	4.75	2.78	-41
	90 km h^{-1}	20.8	9.95	-52
	120 km h^{-1}	21.2	12.5	-41
	50 km h^{-1}	17.7	9.41	-47
	90 km h^{-1}	23.6	16.4	-31
	120 km h^{-1}	19.5	14.2	-27
	140 km h^{-1}	113	108	-4
	120 km h^{-1}	20.0	16.0	-20
	90 km h^{-1}	18.6	10.8	-42
	50 km h^{-1}	8.15	7.06	-13
CO [mg km^{-1}]	NEDC	1333	1132	-15
	UDC	3608	3069	-15
	EUDC	8	nd	
CO_2 [g km^{-1}]	NEDC	222	224	1
	UDC	283	286	1
	EUDC	187	187	0
NO_x [mg km^{-1}]	NEDC	477	499	5
	UDC	407	436	7
	EUDC	519	537	3
HC [mg km^{-1}]	NEDC	107	91	-15
	UDC	269	228	-15
	EUDC	13	12	-8
PM [mg km^{-1}]	NEDC	62.5	44.9	-28
	UDC	42.9	47.8	11
	EUDC	74	40.1	-46
Particles [# km^{-1}]	NEDC	2.24.10^{14}	1.48.10^{14}	-34
	UDC	2.85.10^{14}	2.19.10^{14}	-23
	EUDC	1.89.10^{14}	1.06.10^{14}	-44
	60 km h^{-1}	4.44.10^{13}	3.06.10^{13}	-31
	90 km h^{-1}	2.01.10^{14}	1.06.10^{14}	-47
	120 km h^{-1}	3.59.10^{14}	1.92.10^{14}	-47
	50 km h^{-1}	1.03.10^{14}	7.97.10^{13}	-23
	90 km h^{-1}	1.52.10^{14}	1.18.10^{14}	-22
	120 km h^{-1}	3.17.10^{14}	2.22.10^{14}	-30
	140 km h^{-1}	9.26.10^{14}	7.26.10^{14}	-22
	120 km h^{-1}	1.20.10^{15}	8.38.10^{14}	-30
	90 km h^{-1}	2.14.10^{14}	6.70.10^{14}	213
	50 km h^{-1}	2.22.10^{14}	2.83.10^{14}	27

Table 3.6: Effect of Biodiesel on emission factors for different species. nd: non detectable

Species	**Cycle**	**Regular fuel**		**30% Biodiesel**	**% change**	
		1	**2**		**30%Bio vs 1**	**30%Bio vs 2**
NO [g km−1]	**NEDC**	$5.38.10^{-01}$	$1.68.10^{-01}$	$1.66.10^{-01}$	-69	-1,5
NO_2 [g km−1]		$3.47.10^{-01}$	$1.26.10^{-01}$	$1.37.10^{-01}$	-61	8,4
N_2O [g km−1]		$5.26.10^{-02}$	$1.28.10^{-02}$	$1.57.10^{-02}$	-70	23
NH_3 [g km−1]		nd	nd	$1.62.10^{-07}$		
HCN [g km−1]		$1.14.10^{-03}$	$3.96.10^{-04}$	$2.05.10^{-05}$	-98	-95
HCHO [g km−1]		$9.41.10^{-02}$	$2.45.10^{-02}$	$2.22.10^{-02}$	-76	-9,4
CH_3CHO [g km−1]		$6.45.10^{-02}$	$1.83.10^{-02}$	$1.54.10^{-02}$	-76	-15
SO_2 [g km−1]		$3.02.10^{-02}$	$6.28.10^{-03}$	$1.87.10^{-02}$	-38	198
CH_4 [g km−1]		$6.55.10^{-02}$	$1.32.10^{-02}$	$1.35.10^{-02}$	-79	2,2
Benzene [mg km−1]	**NEDC**	3.646	2.814	2.934	-20	4,3
Toluene [mg km−1]		1.408	1.197	0.765	-46	-36
C_2-Benzene [mg km−1]		1.143	1.082	0.551	-52	-49
C_3-Benzene [mg km−1]		0.520	4.178	0.213	-59	-95
Napthalene [mg km−1]		0.496	0.409	0.212	-57	-48
Methyl-Naphthalene [mg km−1]		0.393	0.220	0.165	-58	-25
C_2-Naphthalene [mg km−1]		0.114	0.063	0.060	-48	-5,4
C_3-Naphthalene [mg km−1]		0.036	0.023	0.022	-41	-6,2
Phenanthrene [mg km−1]		0.0014	0.0038	0.0012	-9	-67
Methyl-Phenanthrene [mg km−1]		0.0010	0.0053	0.0008	-19	-85
C_2-Phenanthrene [mg km−1]		0.0005	0.0053	0.0007	31	-87
C_3-Phenanthrene [mg km−1]		0.0002	0.0026	0.0005	159	-79
Pyrene [mg km−1)		0.0015	0.0043	0.0013	-11	-69

Table 3.7: Effect of Biodiesel on emission factors for different species.

Type of vehicle	Cycle	# of repetitions	Sub-cycle	Exhaust temperature		OA		BC		OM/BC	Particle number	
				AVG	STD	AVG		AVG			AVG	
				[°C]		[mg km^{-1}]	[mg m^3]	[mg km^{-1}]	[mg m^3]		[# km^{-1}]	[# m^3]
HDDV (EIII)	Steady state	3	All	134	54	19.7	3.75	159	30.5	0.12	3.15 10^{14}	6.04 10^{13}
			idle	50	5	-	0.943	-	6.05	0.21	-	1.86 10^{13}
			40 km h^{-1}	112	7	5.35	1.23	59.1	13.8	0.09	8.33 10^{13}	1.93 10^{13}
			60 km h^{-1}	153	3	6.53	1.84	98.3	27.9	0.07	1.34 10^{14}	3.80 10^{13}
			90 km h^{-1}	213	3	21.9	4.20	208	49.9	0.11	5.20 10^{14}	9.97 10^{13}
			idle	136	14	-	0.303	-	2.77	0.11	-	3.87 10^{12}
	NEDC	3*	NEDC	141	36	22.6	3.84	200	33.6	0.11	2.37 10^{14}	4.07 10^{13}
			UDC	123	25	39.2	5.03	266	33.7	0.15	2.03 10^{14}	2.66 10^{13}
			EUDC	180	22	12.2	2.59	158	33.7	0.08	2.58 10^{14}	5.46 10^{13}
	ETC	3*	ETC	170	42	21.3	4.29	168	33.9	0.13	2.90 10^{14}	5.73 10^{13}
			Urban	117	25	33.0	4.91	194	28.9	0.17	1.70 10^{14}	2.49 10^{13}
			Rural	183	12	13.3	4.55	151	51.6	0.09	2.04 10^{14}	6.81 10^{13}
			Motorway	207	9	19.5	3.73	164	31.3	0.12	4.00 10^{14}	7.51 10^{13}
Diesel P(E3) 10 ppm	Steady state	1	All	N.A.								
			idle	37	9	-	2.01	-	9.58	0.21	-	4.61 10^{13}
			60 km h^{-1}	111	19	1.24	1.56	15.1	19.0	0.08	3.95 10^{13}	4.97 10^{13}
			90 km h^{-1}	210	23	1.62	1.74	29.2	31.5	0.06	6.33 10^{13}	6.82 10^{13}
			120 km h^{-1}	N.A.								
	NEDC	1	NEDC	111	49	5.31	3.32	31.1	19.5	0.17	7.37 10^{13}	4.62 10^{13}
			UDC	87	27	9.88	4.08	35.3	14.6	0.28	1.06 10^{14}	4.36 10^{13}
			EUDC	162	44	2.62	2.35	28.7	25.8	0.09	5.50 10^{13}	4.94 10^{13}
	Speed ramp	1	All	225	108	6.36	2.57	62.1	25.1	0.10	5.86 10^{14}	2.37 10^{14}
			idle	32	3	-	0.245	-	2.84	0.09	-	6.11 10^{12}
			50 km h^{-1}	74	17	3.20	1.00	28.1	8.75	0.11	6.67 10^{13}	2.07 10^{13}
			90 km h^{-1}	164	21	2.14	1.17	32.7	17.9	0.07	1.40 10^{14}	7.64 10^{13}
			120 km h^{-1}	277	17	3.31	2.55	41.7	32.1	0.08	4.82 10^{14}	3.71 10^{14}
			140 km h^{-1}	372	15	9.19	5.57	57.9	35.1	0.16	5.10 10^{14}	3.09 10^{14}
			120 km h^{-1}	348	17	3.69	2.32	86.4	54.3	0.04	5.92 10^{14}	3.72 10^{14}
			90 km h^{-1}	301	10	2.99	2.02	22.5	15.1	0.13	7.91 10^{14}	5.34 10^{14}
			50 km h^{-1}	272	12	2.25	0.81	21.7	7.79	0.10	1.11 10^{15}	3.99 10^{14}
			idle	218	17	-	0.37	-	2.19	0.17	-	1.02 10^{14}

Table 3.8: OA, BC and particle emissions and exhaust temperature from heavy-duty vehicle (HDDV-(EIII)) and light-duty diesel vehicle (Diesel-P(E3)). *=only 2 tests for particle number; N.A.=not available; N.D.=below limit of detection.

Type of vehicle	Cycle	# of repetitions	Sub-cycle	Exhaust temperature		OA		BC		OM/BC	Particle number	
				AVG	STD	AVG		AVG			AVG	
				[°C]		[mg km^{-1}]	[mg m^3]	[mg km^{-1}]	[mg m^3]		[# km^{-1}]	[# m^3]
Diesel P(E3) 50 ppm	Steady state	1	All	N.A.								
			idle	33	8	-	1.89	-	14.2	0.13	-	$3.94\ 10^{13}$
			60 km h^{-1}	103	24	1.54	1.98	16.5	21.2	0.09	$3.99\ 10^{13}$	$5.14\ 10^{13}$
			90 km h^{-1}	205	21	1.37	1.51	26.3	28.9	0.05	$5.89\ 10^{13}$	$6.49\ 10^{13}$
			120 km h^{-1}	N.A.								
	NEDC	1	NEDC	111	49	5.19	3.27	35.5	22.4	0.15	$8.20\ 10^{13}$	$5.17\ 10^{13}$
			UDC	86	27	9.53	3.94	41.5	17.2	0.23	$1.19\ 10^{14}$	$4.93\ 10^{13}$
			EUDC	161	44	2.65	2.41	31.9	29.1	0.08	$6.01\ 10^{13}$	$5.47\ 10^{13}$
	Speed ramp	1	All	212	107	3.95	1.65	26.7	11.18	0.15	$1.58\ 10^{15}$	$6.63.\ 10^{14}$
			idle	25	3	-	0.632	-	1.97	0.32	-	$8.49\ 10^{12}$
			50 km h^{-1}	64	16	5.72	1.81	9.34	2.95	0.61	$6.55\ 10^{13}$	$2.07\ 10^{13}$
			90 km h^{-1}	152	22	1.83	1.02	21.4	11.91	0.09	$5.42\ 10^{13}$	$3.02\ 10^{13}$
			120 km h^{-1}	264	14	1.83	1.42	19.6	15.21	0.09	$2.37\ 10^{14}$	$1.85\ 10^{14}$
			140 km h^{-1}	350	18	2.99	1.77	21.7	12.89	0.14	$4.54\ 10^{15}$	$2.70\ 10^{15}$
			120 km h^{-1}	338	12	1.60	1.24	22.2	17.27	0.07	$2.11\ 10^{15}$	$1.64\ 10^{15}$
			90 km h^{-1}	297	11	1.40	0.94	24.5	16.37	0.06	$5.29\ 10^{14}$	$3.53\ 10^{14}$
			50 km h^{-1}	257	12	0.63	0.23	14.8	5.29	0.04	$6.13\ 10^{14}$	$2.20\ 10^{14}$
			idle	187	18	-	0.31	-	1.59	0.20	-	$7.76\ 10^{13}$
Diesel P(E4) 10 ppm	NEDC	1	NEDC	89	43	1.79	1.49	19.1	15.9	0.09	$8.30\ 10^{13}$	$6.92\ 10^{13}$
			UDC	67	20	2.32	1.29	17.8	9.91	0.13	$6.06\ 10^{13}$	$3.39\ 10^{13}$
			EUDC	135	40	1.48	1.73	19.8	23.1	0.07	$9.59\ 10^{13}$	$1.12\ 10^{14}$
	Speed ramp	1	All	190	100	4.50	4.23	38.7	36.4	0.12	$1.02\ 10^{15}$	$9.64\ 10^{14}$
			idle	26	2	-	0.531	-	9.01	0.06	-	$1.58\ 10^{13}$
			50 km h^{-1}	54	10	0.123	0.133	6.50	7.03	0.02	$2.57\ 10^{13}$	$2.78\ 10^{13}$
			90 km h^{-1}	126	16	1.16	1.62	35.9	49.8	0.03	$5.18\ 10^{13}$	$7.18\ 10^{13}$
			120 km h^{-1}	234	14	1.77	1.66	42.8	40.2	0.04	$8.05\ 10^{13}$	$7.55\ 10^{13}$
			140 km h^{-1}	338	11	14.1	11.3	36.3	29.0	0.39	$2.47\ 10^{15}$	$1.98\ 10^{15}$
			120 km h^{-1}	319	14	2.74	2.65	38.0	36.8	0.07	$1.33\ 10^{15}$	$1.29\ 10^{15}$
			90 km h^{-1}	269	13	1.09	1.66	27.6	41.9	0.04	$4.43\ 10^{14}$	$6.73\ 10^{14}$
			50 km h^{-1}	225	11	0.453	0.516	10.5	11.9	0.04	$1.20\ 10^{15}$	$1.36\ 10^{15}$
			idle	165	17	-	0.308	-	8.83	0.03	-	$9.54\ 10^{14}$
10 ppm + 10% Bio	NEDC	1	NEDC	87	41	1.40	1.17	15.2	12.6	0.09	$4.83\ 10^{13}$	$3.65\ 10^{13}$
			UDC	66	20	2.42	1.35	13.0	7.24	0.19	$5.66\ 10^{13}$	$3.15\ 10^{13}$
			EUDC	131	38	0.81	0.95	16.3	19.1	0.05	$3.62\ 10^{13}$	$4.24\ 10^{13}$

Table 3.9: Effect of Biodiesel on emission factors for different species from light-duty diesel vehicles (Diesel-P(E3) and Diesel-P(E4)).
*=only 2 tests for particle number; N.A.=not available; N.D.=below limit of detection.

Type of vehicle	Cycle	# of repetitions	Sub-cycle	Exhaust temperature		OA		BC		OM/BC	Particle number	
				AVG	STD	AVG		AVG			AVG	
				[°C]		[mg km^{-1}]	[mg m^3]	[mg km^{-1}]	[mg m^3]		[# km^{-1}]	[# m^3]
Diesel V(E3) 10ppm	Steady state	2	All	187	77	3.49	1.26	20.6	7.54	0.17	2.74 10^{14}	1.00 10^{14}
			idle	49	4	-	0.03	-	0.32	0.07	-	1.29 10^{12}
			60 km h^{-1}	131	23	0.21	0.12	4.75	2.59	0.05	4.44 10^{13}	2.39 10^{13}
			90 km h^{-1}	209	7	0.80	0.59	20.8	15.4	0.04	2.01 10^{14}	1.48 10^{14}
			120 km h^{-1}	266	1	6.20	2.34	21.2	8.00	0.29	3.59 10^{14}	1.36 10^{14}
	NEDC	2	NEDC	127	47	3.83	1.52	23.3	9.21	0.16	2.24 10^{14}	8.89 10^{13}
			UDC	103	29	7.68	1.96	22.5	5.73	0.34	2.85 10^{14}	7.30 10^{13}
			EUDC	176	37	1.59	0.92	23.8	13.8	0.07	1.89 10^{14}	1.10 10^{14}
	Speed ramp	2	All	204	87	5.22	2.13	42.5	17.3	0.12	5.80 10^{14}	2.37 10^{14}
			idle	51	5	-	0.34	-	6.58	0.05	-	1.73 10^{13}
			50 km h^{-1}	114	15	1.80	0.70	17.7	6.85	0.11	1.03 10^{14}	3.99 10^{13}
			90 km h^{-1}	188	5	0.99	0.61	23.6	14.6	0.04	1.52 10^{14}	9.36 10^{13}
			120 km h^{-1}	260	2	2.35	0.84	19.5	6.93	0.12	3.17 10^{14}	1.13 10^{14}
			140 km h^{-1}	363	13	18.2	7.16	113	43.7	0.16	9.26 10^{14}	3.62 10^{14}
			120 km h^{-1}	308	22	2.18	0.84	20.0	7.67	0.11	1.20 10^{15}	4.64 10^{14}
			90 km h^{-1}	240	8	1.12	0.87	18.6	14.4	0.06	2.14 10^{14}	1.65 10^{14}
			50 km h^{-1}	209	9	0.56	0.27	8.15	3.87	0.07	2.22 10^{14}	1.05 10^{14}
			idle	159	9	-	0.72	-	4.15	0.18	-	1.79 10^{13}
Diesel V(E3) 10ppm + 30% Bio	Steady state	1	All	186	75	1.27	0.48	11.2	4.22	0.11	1.62 10^{14}	6.11 10^{13}
			idle	51	3	-	0.03	-	0.24	0.14	-	1.23 10^{12}
			60 km h^{-1}	137	15	0.14	0.10	2.78	2.00	0.05	3.06 10^{13}	2.20 10^{13}
			90 km h^{-1}	206	8	0.42	0.30	9.95	7.27	0.04	1.06 10^{14}	7.74 10^{13}
			120 km h^{-1}	264	2	1.90	0.71	12.5	4.71	0.15	1.92 10^{14}	7.24 10^{13}
	NEDC	2	NEDC	135	40	3.04	1.20	13.8	5.45	0.22	1.48 10^{14}	5.82 10^{13}
			UDC	108	31	6.52	1.67	15.9	4.07	0.41	2.19 10^{14}	5.60 10^{13}
			EUDC	175	33	1.00	0.58	12.6	7.26	0.08	1.06 10^{14}	6.10 10^{13}
	Speed ramp	1	All	203	90	2.93	1.20	34.1	14.0	0.09	5.11 10^{14}	2.09 10^{14}
			idle	48	4	-	0.33	-	3.92	0.08	-	1.95 10^{13}
			50 km h^{-1}	112	18	1.05	0.43	9.41	3.80	0.11	7.97 10^{13}	3.22 10^{13}
			90 km h^{-1}	185	7	0.54	0.34	16.4	10.3	0.03	1.18 10^{14}	7.38 10^{13}
			120 km h^{-1}	260	3	1.62	0.58	14.2	5.08	0.11	2.22 10^{14}	7.94 10^{13}
			140 km h^{-1}	365	18	9.82	3.64	108	40.0	0.09	7.26 10^{14}	2.70 10^{14}
			120 km h^{-1}	308	20	1.67	0.62	16.0	5.98	0.10	8.38 10^{14}	3.14 10^{14}
			90 km h^{-1}	240	9	0.61	0.48	10.8	8.45	0.06	6.70 10^{14}	5.25 10^{14}
			50 km h^{-1}	205	5	0.47	0.22	7.06	3.33	0.07	2.83 10^{14}	1.34 10^{14}
			idle	159	9	-	0.40	-	2.48	0.16	-	2.81 10^{13}

Table 3.10: Effect of Biodiesel on emission factors for different species from light-duty van (Diesel-V(E3)). *=only 2 tests for particle number; N.A.=not available; N.D.=below limit of detection.

Type of vehicle	**Cycle**	**# of repetitions**	**Sub-cycle**	**Exhaust temperature**		**OA**		**BC**		**OM/BC**	**Particle number**	
				AVG	**STD**	**AVG**		**AVG**			**AVG**	
				[°C]		**[mg km^{-1}]**	**[mg m^3]**	**[mg km^{-1}]**	**[mg m^3]**		**[# km^{-1}]**	**[# m^3]**
Gasoline P(E4)	Steady state	1	All	233	120	0.0025	0.0034	0.0452	0.0540	0.064	$8.69\ 10^{11}$	$1.04\ 10^{12}$
			idle	37	5	-	0.0018	-	0.0409	0.057		$4.79\ 10^{10}$
			60 km h^{-1}	124	33	0.0027	0.0050	0.0251	0.0456	0.060	$1.60\ 10^{10}$	$2.91\ 10^{10}$
			90 km h^{-1}	243	7	0.0009	0.0016	0.0101	0.0186	0.063	$4.66\ 10^{9}$	$8.61\ 10^{9}$
			120 km h^{-1}	372	15	0.0029	0.0038	0.0399	0.0525	0.073	$1.63\ 10^{12}$	$2.15\ 10^{12}$
	NEDC	2	NEDC	122	58	0.0087	0.0115	0.227	0.300	0.039	$2.28\ 10^{12}$	$3.02\ 10^{12}$
			UDC	89	30	0.0198	0.0194	0.512	0.503	0.038	$5.41\ 10^{12}$	$5.32\ 10^{12}$
			EUDC	187	43	0.0022	0.0037	0.0596	0.0989	0.034	$4.52\ 10^{11}$	$7.50\ 10^{11}$
	Speed ramp	2	All	235	133	0.0134	0.0168	0.314	0.395	0.042	$3.78\ 10^{12}$	$4.79\ 10^{12}$
			idle	39	1	-	0.0328	-	1.28	0.022	-	$1.16\ 10^{12}$
			50 km h^{-1}	66	7	N.D.	N.D.	0.0484	0.0853	N.A.	$9.31\ 10^{10}$	$1.66\ 10^{11}$
			90 km h^{-1}	178	21	0.0050	0.0080	0.233	0.377	0.022	$1.37\ 10^{11}$	$2.15\ 10^{11}$
			120 km h^{-1}	332	18	0.0063	0.0076	0.299	0.359	0.023	$1.82\ 10^{11}$	$2.17\ 10^{11}$
			140 km h^{-1}	449	18	0.0123	0.0124	0.176	0.177	0.067	$1.18\ 10^{13}$	$1.19\ 10^{13}$
			120 km h^{-1}	415	14	0.0030	0.0038	0.0327	0.0417	0.086	$5.48\ 10^{12}$	$7.00\ 10^{12}$
			90 km h^{-1}	323	20	N.D.	N.D.	0.0084	0.0157	N.A.	$1.09\ 10^{10}$	$2.03\ 10^{10}$
			50 km h^{-1}	234	15	N.D.	N.D.	0.0121	0.0249	N.A.	$8.76\ 10^{9}$	$1.80\ 10^{10}$
			idle	163	10	-	N.D.	-	N.D.	N.A.	-	$8.50\ 10^{10}$
M(E1) un-leaded fuel + 2% oil	Steady state	1	All	146	94	122	463	0.760	2.87	161	$4.55\ 10^{12}$	$1.72\ 10^{13}$
			idle	29	1	-	-	-	0.244	0	-	N.A.
			30 km h^{-1}	71	20	104	434	0.143	0.599	725	$4.18\ 10^{12}$	$1.75\ 10^{13}$
			50 km h^{-1}	237	57	133	625	1.15	5.43	115	$4.67\ 10^{12}$	$2.19\ 10^{13}$
			idle	213	34	-	13	-	0.264	48	-	$9.54\ 10^{11}$
	ECE-47	2	ECE-47	171	80	228	950	1.61	6.66	142	$7.04\ 10^{12}$	$2.91\ 10^{13}$
			cold	101	54	414	1685	2.17	8.81	190	$9.70\ 10^{12}$	$3.94\ 10^{13}$
			hot	239	25	49.9	213	1.07	4.51	47	$4.51\ 10^{12}$	$1.90\ 10^{13}$
	WMTC	1	WMTC	180	84	191	716	1.66	6.20	115	$5.89\ 10^{12}$	$2.21\ 10^{13}$
			cold	115	66	361	1343	2.19	8.16	165	$7.35\ 10^{12}$	$2.74\ 10^{13}$
			hot	250	23	30.3	114	1.15	4.32	26.5	$4.51\ 10^{12}$	$1.70\ 10^{13}$
M(E2) un-leaded fuel + 2% oil	Steady state	2	All	128	67	293	609	0.96	1.99	281	$2.00\ 10^{13}$	$4.16\ 10^{13}$
			idle	28	1	-	7.41	-	4.52	-	-	$2.39\ 10^{12}$
			30 km h^{-1}	84	26	85.4	193	0.43	0.97	128	$1.42\ 10^{13}$	$3.21\ 10^{13}$
			50 km h^{-1}	192	26	405	1000	0.88	2.16	441	$2.33\ 10^{13}$	$5.74\ 10^{13}$
			idle	173	26	-	292	-	0.69	485	-	$3.98\ 10^{12}$
	ECE-47	2	ECE-47	137	47	345	753	2.80	6.18	124	$1.80\ 10^{13}$	$3.96\ 10^{13}$
			cold	101	43	267	568	3.05	6.61	85.7	$1.90\ 10^{13}$	$4.09\ 10^{13}$
			hot	172	10	420	936	2.56	5.75	169	$1.72\ 10^{13}$	$3.84\ 10^{13}$
	WMTC	1	WMTC	135	46	379	833	2.95	6.49	128	$1.79\ 10^{13}$	$3.93\ 10^{13}$
			cold	105	46	283	622	3.41	7.49	83.0	$1.71\ 10^{13}$	$3.76\ 10^{13}$
			hot	170	9	472	1036	2.52	5.53	188	$1.86\ 10^{13}$	$4.08\ 10^{13}$

Table 3.11: Effect of Biodiesel on emission factors for different species from light-duty gasoline vehicle (Gasoline-P(E4)) and mopeds (M(E1) and M(E2)). *=only 2 tests for particle number; N.A.=not available; N.D.=below limit of detection.

Type of vehicle	**Cycle**	**# of repetitions**	**Sub-cycle**	**Exhaust temperature**		**CO**	**CO$_2$**	**NO$_x$**	**HC**
				AVG	**STD**	**AVG**	**AVG**	**AVG**	**AVG**
				[° C]		**[mg km^{-1}]**	**[g km^{-1}]**	**[mg km^{-1}]**	**[mg km^{-1}]**
HDDV (EIII)	NEDC	3	NEDC	141	36	2979	528	4024	59
			UDC	123	25	4871	652	5636	39
			EUDC	180	22	1796	450	3016	72
	ETC	3	ETC	170	42	1930	450	2925	69
			Urban	117	25	4345	564	5772	54
			Rural	183	12	1958	404	2513	74
			Motorway	207	9	1277	454	2488	70
Diesel P(E3) 50 ppm	NEDC	1	NEDC	108	51	325	179	657	106
			UDC	81	31	896	233	749	250
			EUDC	159	44	14	149	608	28
Diesel P(E4) 10 ppm	NEDC	1	NEDC	89	43	234	142	392	119
			UDC	67	20	622	173	332	234
			EUDC	135	40	8	125	427	52
Diesel V(E3) 10 ppm	NEDC	2	NEDC	127	47	1333	222	477	107
			UDC	103	29	3608	283	407	269
			EUDC	176	37	8	187	519	13
Diesel V(E3) 10ppm + 30% Bio	NEDC	2	NEDC	135	40	1132	224	499	91
			UDC	108	31	3069	286	436	228
			EUDC	175	33	N.D.	187	537	12
Gasoline P(E4)	NEDC	3	NEDC	122	58	1363	164	51	115
			UDC	89	30	3329	209	72	292
			EUDC	187	43	210	137	38	11
M(E1) unleaded fuel + 2% oil	ECE-47	2	ECE-47	171	80	7335	44	28	3580
			cold	101	54	5985	47	37	5037
			hot	239	25	8674	40	19	2134
	WMTC	1	WMTC	180	84	9118	47	23	3594
			cold	115	66	7992	52	32	4981
			hot	250	23	10243	42	14	2207
M(E2) unleaded fuel + 2% oil	ECE-47	2	ECE-47	137	47	1452	45	372	1510
			cold	101	43	2312	48	353	1873
			hot	172	10	601	42	391	1151
	WMTC	1	WMTC	135	46	1157	46	416	1525
			cold	105	46	1620	49	449	1789
			hot	170	9	690	42	382	1258

Table 3.12: Emissions of regulated compounds and CO$_2$.

	HDDV (EIII)												P(E4)
	NEDC						ETC						NEDC
	1	2	3	AVG	STDV	RSD	1	2	3	AVG	STDV	RSD	AVG
Unit	g km^{-1}	g km^{-1}	g km^{-1}	g km^{-1}	g km^{-1}	%	g km^{-1}	g km^{-1}	g km^{-1}	g km^{-1}	g km^{-1}	%	g km^{-1}
NO	2.38	2.57	2.11	2.35	$1.88\ 10^{-1}$	8.0	1.52	1.62	1.75	1.63	$9.42\ 10^{-2}$	5.8	$2.68\ 10^{-2}$
NO_2	$4.00\ 10^{-1}$	$4.57\ 10^{-1}$	$3.49\ 10^{-1}$	$4.02\ 10^{-1}$	$4.39\ 10^{-2}$	10.9	$2.79\ 10^{-1}$	$2.88\ 10^{-1}$	$3.07\ 10^{-1}$	$2.91\ 10^{-1}$	$1.17\ 10^{-2}$	4.0	$1.48\ 10^{-7}$
N_2O	$2.22\ 10^{-3}$	$1.04\ 10^{-3}$	$3.11\ 10^{-3}$	$2.12\ 10^{-3}$	$8.48\ 10^{-4}$	39.9	$3.42\ 10^{-3}$	$1.47\ 10^{-3}$	$2.55\ 10^{-3}$	$2.48\ 10^{-3}$	$7.97\ 10^{-4}$	32.1	$6.00\ 10^{-4}$
NH_3	$4.84\ 10^{-4}$	$2.36\ 10^{-4}$	$4.15\ 10^{-4}$	$3.78\ 10^{-4}$	$1.05\ 10^{-4}$	27.7	$3.68\ 10^{-4}$	$2.54\ 10^{-4}$	$3.51\ 10^{-4}$	$3.24\ 10^{-4}$	$5.00\ 10^{-5}$	15.4	$6.48\ 10^{-3}$
HCN	$1.52\ 10^{-3}$	$1.46\ 10^{-3}$	$1.67\ 10^{-3}$	$1.55\ 10^{-3}$	$8.76\ 10^{-5}$	5.7	$4.86\ 10^{-4}$	$7.34\ 10^{-4}$	$9.86\ 10^{-4}$	$7.35\ 10^{-4}$	$2.04\ 10^{-4}$	27.8	$1.32\ 10^{-4}$
HCHO	$1.68\ 10^{-2}$	$1.68\ 10^{-2}$	$1.23\ 10^{-2}$	$1.53\ 10^{-2}$	$2.13\ 10^{-3}$	13.9	$1.06\ 10^{-2}$	$1.01\ 10^{-2}$	$1.26\ 10^{-2}$	$1.11\ 10^{-2}$	$1.09\ 10^{-3}$	9.8	$6.25\ 10^{-4}$
CH_3CHO	$4.07\ 10^{-2}$	$4.47\ 10^{-2}$	$3.60\ 10^{-2}$	$4.05\ 10^{-2}$	$3.58\ 10^{-3}$	8.9	$3.43\ 10^{-2}$	$3.19\ 10^{-2}$	$3.50\ 10^{-2}$	$3.37\ 10^{-2}$	$1.29\ 10^{-3}$	3.8	$6.99\ 10^{-4}$
SO_2	$7.86\ 10^{-2}$	$4.18\ 10^{-2}$	$6.93\ 10^{-2}$	$6.33\ 10^{-2}$	$1.56\ 10^{-2}$	24.7	$8.02\ 10^{-2}$	$1.05\ 10^{-2}$	$5.08\ 10^{-2}$	$.72\ 10^{-2}$	$2.85\ 10^{-2}$	60.5	$8.33\ 10^{-3}$
CH_4	$7.09\ 10^{-5}$	$4.55\ 10^{-4}$	$1.70\ 10^{-5}$	$1.81\ 10^{-4}$	$1.95\ 10^{-4}$	107.8	$7.50\ 10^{-6}$	$8.00\ 10^{-6}$	$1.31\ 10^{-4}$	$4.90\ 10^{-5}$	$5.83\ 10^{-5}$	119.0	$9.14\ 10^{-3}$

	M(E1) unleaded fuel + 2% oil				M(E2) unleaded fuel + 2% oil				Diesel V(E3)			Diesel V(E3) + Bio
	ECE-47			WMTC	ECE-47			WMTC	NEDC			NEDC
	1	2	AVG	1	1	2	AVG	1	1	2	AVG	1
Unit	g km^{-1}	g km^{-1}	g km^{-1}	g km^{-1}	g km^{-1}	g km^{-1}	g km^{-1}	g km^{-1}	g km^{-1}	g km^{-1}	g km^{-1}	g km^{-1}
NO	$1.59\ 10^{-2}$	$1.21\ 10^{-2}$	$1.40\ 10^{-2}$	$1.01\ 10^{-2}$	$1.81\ 10^{-1}$	$1.82\ 10^{-1}$	$1.82\ 10^{-1}$	$1.84\ 10^{-1}$	$5.38\ 10^{-1}$	$1.68\ 10^{-1}$	$3.53\ 10^{-1}$	$166\ 10^{-1}$
NO_2	$5.99\ 10^{-5}$	$1.24\ 10^{-4}$	$9.22\ 10^{-5}$	N.D.	$5.71\ 10^{-3}$	$4.82\ 10^{-3}$	$5.26\ 10^{-3}$	$3.96\ 10^{-3}$	$3.47\ 10^{-1}$	$1.26\ 10^{-1}$	$2.36\ 10^{-1}$	$1.37\ 10^{-1}$
N_2O	N.D.	N.D.	-	N.D.	$2.38\ 10^{-3}$	$2.37\ 10^{-3}$	$2.37\ 10^{-3}$	$2.45\ 10^{-3}$	$5.26\ 10^{-2}$	$1.28\ 10^{-2}$	$3.27\ 10^{-2}$	$1.57\ 10^{-2}$
NH_3	$4.76\ 10^{-3}$	$3.64\ 10^{-3}$	$4.20\ 10^{-3}$	$5.06\ 10^{-3}$	$2.89\ 10^{-4}$	$3.08\ 10^{-6}$	$1.46\ 10^{-4}$	$6.84\ 10^{-7}$	N.D.	N.D.	-	$1.62\ 10^{-7}$
HCN	$1.06\ 10^{-3}$	$9.72\ 10^{-4}$	$1.01\ 10^{-3}$	$1.05\ 10^{-3}$	$4.62\ 10^{-4}$	$5.33\ 10^{-4}$	$4.98\ 10^{-4}$	$3.88\ 10^{-4}$	$1.14\ 10^{-3}$	$3.96\ 10^{-4}$	$7.67\ 10^{-4}$	$2.05\ 10^{-5}$
HCHO	$2.08\ 10^{-2}$	$1.80\ 10^{-2}$	$1.94\ 10^{-2}$	$1.88\ 10^{-2}$	$2.74\ 10^{-2}$	$2.69\ 10^{-2}$	$2.71\ 10^{-2}$	$2.44\ 10^{-2}$	$9.41\ 10^{-2}$	$2.45\ 10^{-2}$	$5.93\ 10^{-2}$	$2.22\ 10^{-2}$
CH_3CHO	$2.33\ 10^{-2}$	$1.93\ 10^{-2}$	$2.13\ 10^{-2}$	$2.17\ 10^{-2}$	$4.01\ 10^{-2}$	$4.12\ 10^{-2}$	$4.07\ 10^{-2}$	$3.80\ 10^{-2}$	$6.45\ 10^{-2}$	$1.83\ 10^{-2}$	$4.14\ 10^{-2}$	$1.54\ 10^{-2}$
SO_2	$4.57\ 10^{-3}$	$3.88\ 10^{-3}$	$4.22\ 10^{-3}$	$5.54\ 10^{-3}$	$3.12\ 10^{-3}$	$2.17\ 10^{-3}$	$2.64\ 10^{-3}$	$1.73\ 10^{-3}$	$3.02\ 10^{-2}$	$6.28\ 10^{-3}$	$1.82\ 10^{-2}$	$17\ 10^{-2}$
CH_4	$7.80\ 10^{-2}$	$6.36\ 10^{-2}$	$7.08\ 10^{-2}$	$1.29\ 10^{-1}$	$1.16\ 10^{-2}$	$9.86\ 10^{-3}$	$1.07\ 10^{-2}$	$8.81\ 10^{-3}$	$6.55\ 10^{-2}$	$1.32\ 10^{-2}$	$3.94\ 10^{-2}$	$1.35\ 10^{-2}$

Table 3.13: Emission factors for species measured with FTIR. Diesel V(E3) + Bio refers to diesel van with 10 ppm sulphur and 30% biofuel, and P(E4) to gasoline light-duty vehicle, average of 2 tests.

	HDDV (EIII)									Gasoline P(E4)
	NEDC			ETC						NEDC
	1	2	AVG	1	2	3	AVG	STDV	RSD	1
Unit	mg km^{-1}	mg km^{-1}	mg km^{-1}	mg km^{-1}	mg km^{-1}	mg km^{-1}	mg km^{-1}	mg km^{-1}	%	mg km^{-1}
Benzene	2.5	1.9	2.2	1.7	1.6	2.0	1.8	0.16	9.1	6.3
Toluene	0.77	0.50	0.63	0.44	0.47	0.51	0.47	0.03	6.3	13.8
C_2-Benzene	1.5	0.88	1.2	0.99	1.1	0.86	0.99	0.11	11.4	20.7
C_3-Benzene	0.83	0.72	0.78	0.61	0.69	0.70	0.66	0.04	6.1	5.4
Napthalene	0.55	0.64	0.60	0.35	0.40	0.70	0.48	0.15	31.5	0.20
Methyl-Naphthalene	0.77	1.2	0.96	0.46	0.58	1.16	0.73	0.30	41.3	0.14
C_2-Naphthalene	0.77	0.79	0.78	0.44	0.59	0.82	0.62	0.15	25.0	0.052
C_3-Naphthalene	0.51	0.44	0.48	0.29	0.40	0.48	0.39	0.08	20.0	0.0093
Phenanthrene	0.045	0.023	0.034	0.025	0.032	0.031	0.029	0.003	11.4	0.0033
Methyl-Phenanthrene	0.045	0.021	0.033	0.025	0.035	0.028	0.029	0.004	13.5	0.0009
C_2-Phenanthrene	0.029	0.012	0.021	0.019	0.024	0.020	0.021	0.002	10.6	N.D.
C_3-Phenanthrene	0.010	0.004	0.007	0.0068	0.0085	0.0072	0.007	0.001	9.9	N.D.
Pyrene	0.021	0.009	0.015	0.013	0.017	0.014	0.014	0.002	12.2	N.D.

Table 3.14: Emission factors of monocyclic and polycyclic aromatic hydrocarbons from heavy-duty and gasoline light-duty vehicles.

	M(E1) fuel + 2% oil		M(E2) fuel + 2% oil				Diesel V(E3) 10ppm			Diesel V(E3) +30% Bio
	ECE-47	WMTC	ECE-47			WMTC	NEDC			NEDC
	AVG	1	1	2	AVG	1	1	2	AVG	1
Unit	mg km^{-1}	mg km^{-1}	mg km^{-1}	mg km^{-1}	mg km^{-1}	mg km^{-1}	mg km^{-1}	mg km^{-1}	mg km^{-1}	mg km^{-1}
Benzene	19.5	21.8	19.7	7.1	13.4	7.3	3.6	2.8	3.2	2.9
Toluene	50.1	53.8	21.8	29.8	25.8	28.5	1.4	1.2	1.3	0.76
C_2-Benzene	99.4	116.1	52.0	72.6	62.3	69.9	1.1	1.1	1.1	0.55
C_3-Benzene	16.9	18.0	4.4	6.3	5.3	6.1	0.52	4.2	2.3	0.21
Napthalene	0.27	0.27	0.98	1.3	1.1	1.3	0.50	0.41	0.45	0.21
Methyl-Naphthalene	0.35	0.33	0.13	0.12	0.13	0.12	0.39	0.22	0.31	0.17
C_2-Naphthalene	0.20	0.19	0.06	0.04	0.050	0.040	0.11	0.063	0.089	0.060
C_3-Naphthalene	0.093	0.085	0.040	0.010	0.025	0.013	0.036	0.023	0.030	0.022
Phenanthrene	0.011	0.012	0.012	0.0055	0.009	0.0062	0.0014	0.0038	0.003	0.0012
Methyl-Phenanthrene	0.021	0.021	0.010	0.0032	0.007	0.0044	0.0010	0.0053	0.003	0.0008
C_2-Phenanthrene	0.017	0.018	0.009	0.0022	0.006	0.0035	0.0005	0.0053	0.003	0.0007
C_3-Phenanthrene	0.0067	0.0078	0.0077	0.0001	0.004	0.0012	0.0002	0.0026	0.001	0.0005
Pyrene	0.0021	0.0027	0.0086	0.0012	0.005	0.0019	0.0015	0.0043	0.003	0.0013

Table 3.15: Emission factors of monocyclic and polycyclic aromatic hydrocarbons from mopeds and diesel van.

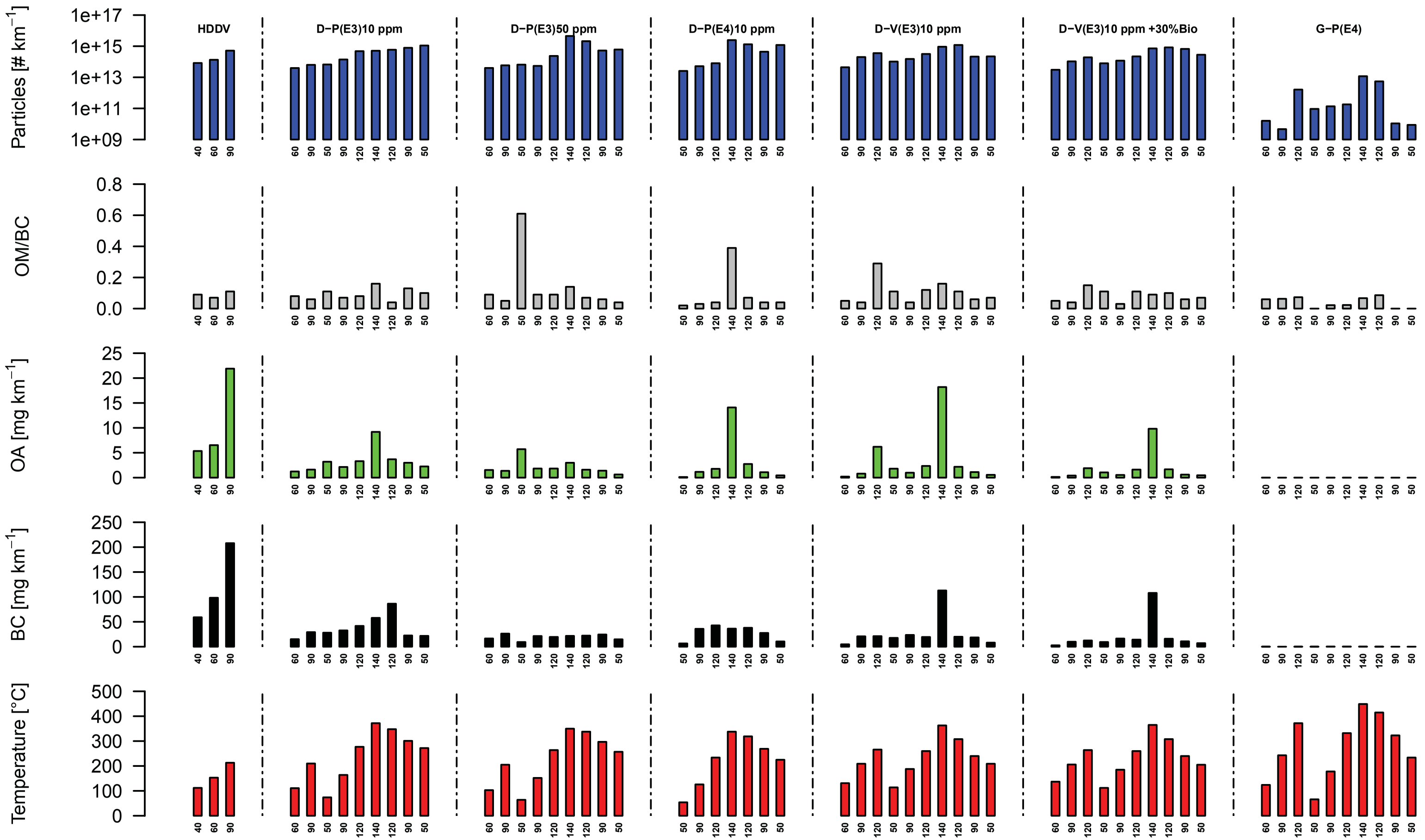

Figure 3.8: - Emission factors of particles, organic aerosol and black carbon from all types of vehicles except mopeds during the steady state and speed ramp cycles.

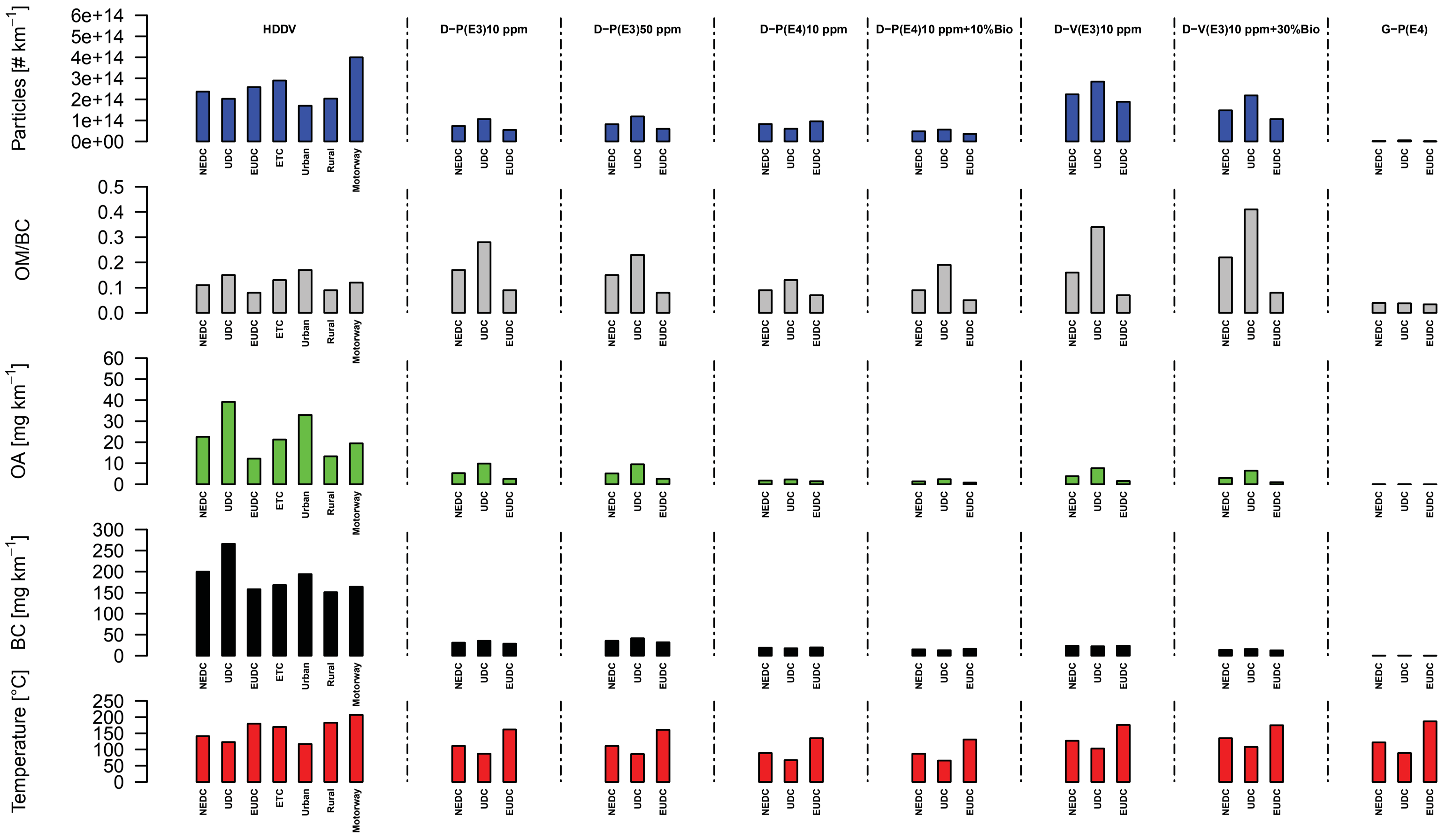

Figure 3.9: - Emission factors of particles, organic aerosol and black carbon from all types of vehicles except mopeds during the various regulatory cycles.

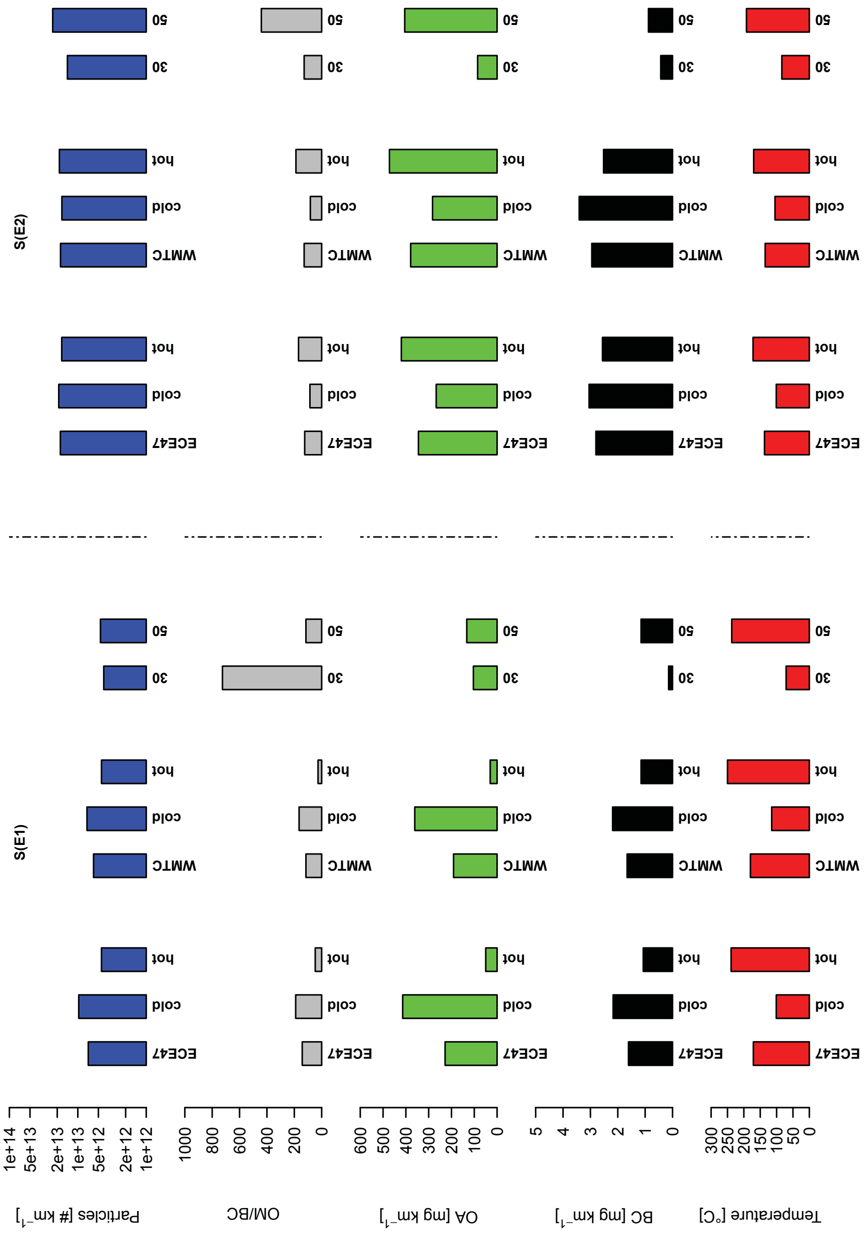

Figure 3.10: - Emission factors of particles, organic aerosol and black carbon from mopeds the various cycles.

Chapter 4

Moped exhaust emissions

Online characterization of regulated and unregulated gaseous and particulate exhaust emissions from two-stroke mopeds: A chemometric approach

M. Clairotte[a], T.W. Adam[a], R. Chirico[b,c], B. Giechaskiel[a,f], U. Manfredi[a], M. Elsasser[d,e], M. Sklorz[e], P.F. DeCarlo[h] , M.F. Heringa[b], R. Zimmermann[d,e], G. Martini[a], A. Krasenbrink[a], A. Vicet[g], E. Tournie[g], A.S.H. Prevot[b], C. Astorga[a]

Analytica Chimica Acta - 2012, volume: 717, pages: 28-38

[a] European Commission Joint Research Centre Ispra, Institute for Energy, Sustainable Transport Unit, 21027 Ispra, Italy

[b] Paul Scherrer Institut, Laboratory of Atmospheric Chemistry, CH-5232 Villigen, Switzerland

[c] Italian National Agency for New Technologies, Energy and Sustainable Economic Development (ENEA), UTAPRAD-DIM, Via E. Fermi 45, 00044 Frascati, Italy

[d] Institute of Ecological Chemistry, Cooperation Group Complex Molecular Systems/Joint Mass Spectrometry Centre, Helmholtz Zentrum München, 85764 Neuherberg, Germany

[e] Chair of Analytical Chemistry/Joint Mass Spectrometry Centre, Institute of Chemistry, University of Rostock, 18051 Rostock, Germany

[f] AVL List GmbH, Hans-List-Platz 1, 8020 Graz, Austria

[g] Institut dŠElectronique du Sud (IES), UMR CNRS 5214, Case 067, Université Montpellier 2, 34 095 Montpellier Cedex 05, France

[h] Drexel University, Department of Civil, Architectural and Environmental Engineering, Philadelphia, PA 19104, United States

Abstract

Two-stroke mopeds are a popular and convenient mean of transport in particular in the highly populated cities. These vehicles can emit potentially toxic gaseous and aerosol pollutants due to their engine technology. The legislative measurements of moped emissions are based on offline methods; however, the online characterization of gas and particulate phases offers great possibilities to understand aerosol formation mechanism and to adapt future emission standards. The purpose of this work was to study the emission behavior of two mopeds complying with different European emission standards (Euro 1 and Euro 2). A sophisticated set of online analyzers was applied to simultaneously monitor the gas phase and particulate phase of exhaust on a real time basis. The gaseous emission was analyzed with a high resolution Fourier transform infrared spectrometer (FTIR; nitrogen species) and a resonance-enhanced multiphoton ionization time-of-flight mass spectrometer (REMPI-ToF-MS; polycyclic aromatic hydrocarbons: PAH), whereas the particulate phase was chemically characterized by a high-resolution time-of-flight aerosol mass spectrometer (HR-ToF-AMS; organic, nitrate and chloride aerosol) and a multiangle absorption photometer (MAAP; black carbon). The physical characterization of the aerosol was carried out with a condensation particle counter (CPC; particle number concentration) and a fast mobility particle sizer (FMPS; size distribution in real time). In order to extract underlying correlation between gas and solid emissions, principal component analysis was applied to the comprehensive online dataset. Multivariate analysis highlighted the considerable effect of the exhaust temperature on the particles and heavy PAH emissions. The results showed that the after-treatment used to comply with the latest Euro 2 emission standard may be responsible for the production of more potentially harmful particles compared to the Euro 1 moped emissions.

Keywords: aerosol mass spectrometer; black carbon; 2-Stroke engine; online measurement; polycyclic aromatic hydrocarbons; multivariate analysis.

4.1 Introduction

Emissions from transport are principal contributors to atmospheric pollution and have an important effect on the climate. It is stated that the on-road transport sector will be the most important anthropogenic source of positive net radiative forcing in 2020 (18). Control of air pollutants from transport is highly challenging for the policy makers (200). Powered two wheelers (PTWs) are a popular and economic alternative to resolve traffic problems in congested cities. Across the 27 European Union countries, the PTWs in use were estimated around 33 million in 2006, including 12.9 million of mopeds (119). In Asia, motorcycles account for up to 75% of the whole vehicle fleet, and among these, 85% are powered by 2-stroke engines (201, 202). These vehicles are important contributors of air pollutants, especially the two-stroke motorcycles (145). 50 cm^3 PTW mopeds are high emitters of harmful compounds like particles and polycyclic aromatic hydrocarbons (PAH), and are often used in densely populated areas (203). Whereas European legislation became more stringent for passenger cars and heavy duty vehicles (Euro 6/Euro VI respectively), new steps of regulation for PTW will still take some time to come into force (204). Moreover, legislation for PTW is focused only on a few compounds, which are carbon monoxide (CO) and the sum of total hydrocarbon and nitrogen oxides ($HC + NO_x$). However, recently scientific studies have focused on the negative effects of unregulated compounds like PAH, particulate matter (PM), and carbonyls on health and air pollution (146, 205, 206, 207). Although these studies give valuable information, most of them are obtained with offline measurement systems following a collection procedure (i.e. bags, cartridges, etc.), which can cause losses and artifact formation. In addition, investigation of formation mechanisms of exhaust pollutants is difficult due to the lack of time-resolved emission data. However, a strong influence of the cold start of the engine and the catalyst has been reported (134).

The aim of this study is to simultaneously characterize the gas phase and the particulate phase of moped exhaust on a real-time basis. Therefore, an original set of sophisticated online measurement analyzers was applied. The driving cycles performed were the European standard driving cycle for PTW below 50 cm^3, ECE-47 (121) and the World-wide Motorcycle Test Cycle WMTC (208). Particle analysis was performed in terms of chemical composition (organic, nitrate, and chloride aerosol; black carbon) and physical characteristics (size distribution, particle number concentration). Concerning the gas phase, the regulated emissions of CO, NO_x and HC were monitored. In addition, a variety of unregulated gaseous compounds like PAH, carbonyls, small hydrocarbons and nitrogen species were analyzed. Two in-use mopeds were investigated, which were equipped with different engine technologies (carburetor, direct injection) and complied with two different European (EU) emission standard limits (Euro 1 and Euro 2). Some previous studies showed that direct injection (DI) mopeds tend to emit more particles when the engine warms up (134, 203). The online emission characterization carried out in this study might help to more deeply understand this behavior and the impact of newer technologies (used to comply with the Euro 2 standard) on the unregulated pollutants.

Conventional statistical approaches of data treatment in the field of vehicle emission are based on emission factors. Thus, only the total amount emitted during the different phases of the driving cycle are considered. On the other hand, the correlation of real-time emission data and online recorded physical variables (e.g. temperature, speed, consumption, combustion stoichiometry) might help to find relationships and understand the complex formation mechanisms of exhaust constituents. Therefore, besides conventional illustration of gas and solid emissions, an original exploratory analysis based on multivariate analysis was carried out in this study. Principal component analysis (PCA) was applied to the online data in order to classify the emission fluctuation during the driving cycles. For this approach, the pollutantsŠ online emission signals during the driving cycle were considered as fingerprints. Then, PCA was used to estimate signal similarities and to identify gas or particulate pollutants with identical emission patterns.

4.2 Experimental Section

4.2.1 Test facilities

This study was conducted in the Vehicle Emission Laboratory (VELA) at the Joint Research Centre (JRC) Ispra, Italy. A chassis dynamometer (Roller bench 48"; AVL Zoellner GmbH, Germany) using a full dilution tunnel with a constant volume sampler (CVS) with a critical flow venturi was used for vehicle testing. The analytical instruments were either connected to the tailpipe or to the dilution tunnel. A cyclone (cutoff size >20 μm) was added between the tailpipe and the dilution tunnel in order to protect analytical instruments at the CVS from droplets, whereas instruments at the tailpipe were preceded by a heated filter. As mentioned in the directive in force for 2-wheel motor vehicles (121), the CVS flow rate was adjusted at 4.42 m^3 min^{-1}, which was appropriate to maintain a suitable pressure at the vehicle tailpipe. The experimental system is illustrated in Fig. 4.1.

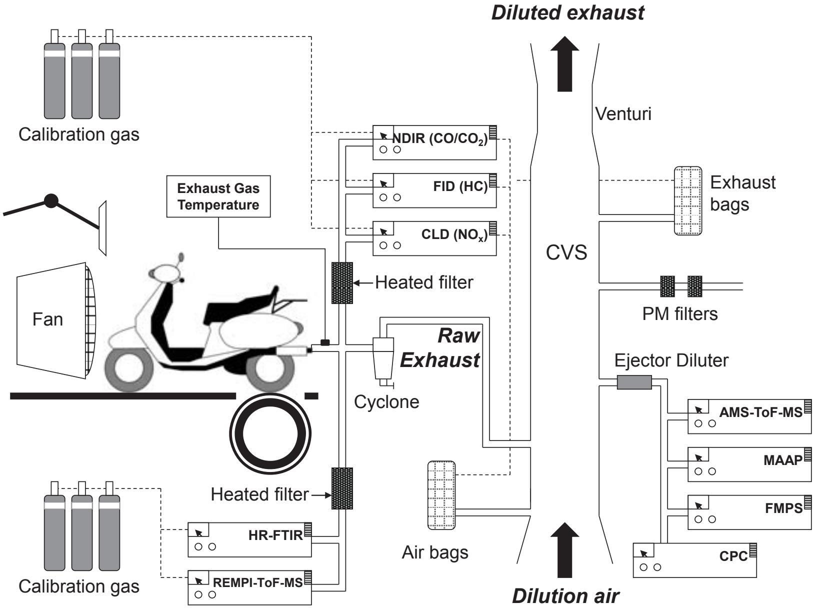

Figure 4.1: VELA1 description. - Schematic diagram of the experimental setup.

4.2.2 Test fleet and test cycle

The two mopeds used for this study were carefully selected in order to evaluate different behaviors of a Euro 1 and a Euro 2 during the test cycles. The Euro 1 moped was equipped with a 50 cm^3 carburetor engine with a catalyst (Euro1-Cb). The Euro 2 moped had a 50 cm^3 DI engine followed by an oxidant catalyst and a secondary air system (SAS) (Euro2-DI). The SAS system is an emission control strategy which provides supplemental fresh air before the catalyst in order to lead to a more complete combustion of the exhaust gases. Two-stroke engines need to be fed with a mixture of oil and gasoline in order to lubricate the combustion chamber during operation. Mineral oil was used for the Euro1-Cb and semi-synthetic oil for the Euro2-DI. The reference fuel (CEC RF-02-99 oxy 0.8-1.2) and oil characteristics are indicated in Table 4.2 and

4.3 in supplementary materials. Two driving cycles were carried out, the legislative ECE-47 driving cycle and a more realistic WMTC described in a previous study (134). The differences in terms of emission factors were found negligible in this latter study consequently, in the framework of this paper, discussion of the results focuses on the legislative ECE-47 driving cycle. However, unregulated emissions factors from the WMTC were indicated in the Table 4.4 in supplementary materials. The ECE-47 cycle consists of eight identical elementary modules performed with a cold engine at test start. For type approval under the European legislation, only the last four modules, called hot phase, are taken into consideration. Hence, the first four modules are only used to warm-up the engine prior to the official measurement and are called cold phase. Two test repetitions were achieved for each moped and the differences in terms of emission factors were founds lower than 5% for most the pollutants measured, so a 3^{rd} was not conducted. The exhaust temperature was monitored directly after the tailpipe (Fig. 4.1) with a thermocouple. The fuel consumption was estimated by means of a carbon balance formula, with the gasoline density and the online measurements of HC, CO and CO_2.

4.2.3 Analytical instrumentation

4.2.3.1 Gas phase measurements

The gas phase was sampled directly from the tailpipe with a heated line and a pumping system (flow: ca. 4 L min^{-1}, temperature: 191°C) in order to avoid any condensation and to be able to investigate both raw and undiluted exhaust. In fact, compounds like ammonia (NH_3) or nitrogen dioxide (NO_2) are well known for their ability to remain adsorbed on the sampling system surface, mostly in the presence of condensed water (209). Small hydrocarbons, nitrogen species (NO, NO_2, N_2O, NH_3 and HCN) and other oxygenated small compounds (formaldehyde, acetaldehyde) were monitored by a high resolution Fourier transform infrared spectrometer (HR-FTIR, MKS Multigas analyzer 2030, Wilmington, MA). The system (optical cell length: 5.11 m, spectral resolution: 0.5 cm^{-1}, spectral range: 600-3500 cm^{-1}, flow: 4.5 L min^{-1}, acquisition frequency: 1 Hz) allows the quantification of up to 20 exhaust compounds by a multivariate calibration based on a factory developed model.

Monocyclic and PAH were measured by resonance enhanced multi-photon ionization (REMPI) coupled to time of flight (ToF) mass spectrometry (Mass Spectrometry Centre, University of Rostock). This technique is known to be a soft and sensitive on-line method for the detection of gaseous aromatic compounds. The heated transfer line of the resonance-enhanced multiphoton ionization time-of-flight mass spectrometer (REMPI-ToF-MS) was attached orthogonally to the heated sampling line of the HR-FTIR described above. The former consisted of a deactivated silica capillary (length 1.5 m; inner diameter 0.32 mm; $T = 220°C$) by which a constant volume of exhaust was continuously drawn into the instrument (flow 8 mL min^{-1}; residence time <1 s). The principle of REMPI-ToF-MS is described in detail in the literature (168); therefore, only a brief description is given here. Fundamental Nd:YAG laser pulses (1064 nm) are used for non-linear generation of UV light (266 nm). The UV pulses are directed into the ionization chamber straight underneath the inlet needle of the transfer line. Soft photoionization of the aromatics in the exhaust is induced by a sequential two-photon absorption process via an electronic transition state. The generated molecular ions are extracted into the flight tube of the reflectron ToF-MS. Mass spectra are recorded via an ultrafast analog to digital converter card (Acqiris, Switzerland), whereby data processing is done by a LabView (National Instruments, USA) based custom-made software. Calibration is carried out by applying external gas standards (benzene, toluene, xylene). Compounds, where no calibration gases are available, were semiquantified by multiplying the measured signal by the ratio of the photoionization cross-section of the target compound and one of the calibrated species. These ratios were determined beforehand under lab-conditions for a large number of compounds (e.g. naphthalene, phenanthrene, pyrene, chrysene and their higher homologues) at the Mass Spectrometry Centre of the 196 University of Rostock. In principle, 20 complete mass spectra per second can be recorded. Here, mass spectra were averaged to a time resolution of 1 Hz. In the following, the sum of benzene, naphthalene, phenanthrene and their derivatives is referred to "benzene group", "naphthalene group" and "phenanthrene group", respectively.

Furthermore, regulated emissions were recorded according to the legislative methods (CO/CO_2: non-dispersive infrared spectrometer (NDIR), NO_x: chemiluminescence detector (CLD), THC: heated flame ionization detector (FID)) (Hartmann and Braun, Germany).

A selection of ozone precursors was sampled from the dilution tunnel, in order to evaluate the ozone formation potential (OFP) of each moped. This concept uses the emission factors of a selection of volatile organic hydrocarbons (from C_2 to C_9, including carbonyl compounds) listed in the EU directive in force for ambient air (53). The volatile hydrocarbons were collected in Tedlar bags and measured with a dual column GC-FID (131), whereas carbonyls were collected with 2,4-dinitrophenylhydrazine-silica cartridges and measured with a C_{18} HPLC-UV system as described in (210, 211). The OFP was estimated according to the maximum incremental reactivity concept proposed by Carter (132).

4.2.3.2 Particle phase measurements

Particles emitted were sampled from the full dilution tunnel (CVS) where the whole exhaust gas is diluted (flow: ca. 4.4 m^3 min^{-1}, temperature: ca. 22°C, average dilution: ca. 200 in idle and 20 in max speed), with an additional ejector diluter (Dekati Ltd., Tampere, Finland) to avoid saturation of the analytical systems (dilution factor circa 10). PM was determined in terms of physical and chemical characteristics. The particle number concentration was measured by a TSI 3022A condensation particle counter (CPC) (212). Particle size distribution along the cycles was measured with a TSI 3091 fast mobility particle sizer (FMPS). This system allows the detection of the particles size diameter within a range of 5.6-560 nm with 32 channels resolution and an acquisition frequency of 1 Hz (213). It enables the investigation of fast changes of the size distribution during transient speed and has been used during ambient field and emission laboratory studies (214, 215). In order to monitor aerosol black carbon (BC), a Thermo 5012 multi-angle absorption photometer (MAAP) was used (167). Thereby, aerosol is collected on a glass fiber filter tape and the light absorption through the filter is determined. Concerning the chemical composition of the non-refractory fraction of the aerosol, an aerodyne high-resolution time-of-flight aerosol mass spectrometer (HR-ToF-AMS) was applied to monitor organics as well as nitrate, sulfate and chloride species. A full description of this technique is available in the literature (163), hence, only a short description is given here. After the CVS and the ejector diluter, the diluted exhaust was sampled through an aerodynamic lens. Particles within the range from 30 nm to ca. 1 μm vacuum aerodynamic diameter (100% transmission between 70 and 500 nm, substantial transmission between 30-70 nm and 500-2500 nm) are focused in a particle beam which is guided to a 600°C tungsten element where a thermal vaporization occurs followed by electron ionization at 70 eV. During this process, only non-refractory species are vaporized. The ions are extracted into a time-of-flight spectrometer and are detected by a multichannel plate detector. The ToF was operated in V-mode (flight distance around 1.3 m) and data were averaged with a frequency of 0.2 Hz. Total particulate mass was determined by weighing, according to the legislated method for diesel vehicles (124). Thereby, a fraction of the diluted exhaust was drawn through two successive glass-fiber filters (47 mm-Pallflex, PALL, New York, USA). The filters were weighted after a minimum stabilization period of 1 h at 22°C and 50% humidity.

The gas and particulate volumetric emissions were measured at different temperatures (191°C and 22°C respectively). The mass emission was calculated by using a normalized flow rate corrected at 0°C and 1 atm.

4.2.4 Data processing and statistics

The experimental analytical setup consisted of several instruments with various acquisition frequencies and connected at different sampling points (Fig. 4.1). Since a major objective of this study was to find the connection between the gas and particle emissions, the first task was to synchronize all systems. Hence, instruments connected directly to the tailpipe (FTIR, REMPI-ToF-MS) were adjusted by means of the identical NO measurement of FTIR and CLD detector. An additional CO_2 gas analyzer (LI-7000, LI-COR Biosciences) was connected to the CVS to correct for time shifts of the instruments which sampled from the CVS (CPC, FMPS, HR-ToF-AMS and MAAP). A time-resolution of 1 Hz was used for the data set. Differing time-resolutions were either averaged (REMPI-ToF-MS) or computed by linear interpolation (CPC, AMS-ToF-MS and MAAP). Short time losses of data recording were also eliminated by linear interpolation. This interpolation was only applied when time gaps were shorter than 5 s and 10 s, for gas and solid measurements, respectively.

In order to highlight pollutants which followed similar emission behaviors during the cycle, a PCA was carried out on the dynamic signals. This exploratory analysis was preferred to a confirmatory factor analysis because no prior hypotheses were considered to explain the correlation between variable (here the pollutants). The basic objective of the PCA was to reduce the data set and find the best space to project the samples. This dimension reduction process created a limited number of eigenvector, called principal components (PCs), which explained most of the total variance of the data set. On the first hand, the projection of the variables according to the calculated PC enabled a graphical representation called correlation circle. This representation was useful to estimate the respective contribution of variables to the PC calculation. The variables correlated, thus with similar emission patterns during the cycle, were clustered together in the correlation circle. This approach allowed focusing on interpretation of the variation of the emissions, independently of absolute values since the data set was normalized. On the second hand, the projection of the samples (here the emission measurements every second) in this sub-space previously created allowed to display the score plot. The relative positions of samples reflected their similarities. Samples were discriminated according to explanatory factors that were graphically highlighted. In the context of this work, two factors were studied, namely the exhaust temperature and the fuel consumption. In the case of the exhaust temperature, for example, all the samples were sorted according to this factor every second. The data were split into three sub-classes, according to the exhaust temperature 3-quantiles, so that every sub-class contained the same number of emission points. Thus, the sub-class called “temp. 100%" regrouped all the measurement points belonging to the third higher temperature quantile. Therefore, all the instantaneous emission points measured when the exhaust temperature was almost maximum (occurring during the last part of the cycle, when the engine was warm) were gathered in this sub-class. The purpose was to find trajectories between the different sub-classes of point, which could suggest correlation between the variables (the pollutant) and the factors. Data pre-processing and statistical calculations were performed in the R-statistical environment (GNU project) with the “ade4" package (216).

4.3 Results and discussion

Table 4.1 summarizes the results for the gas and particulate phases.

4.3.1 Gas phase

4.3.1.1 Regulated emissions

Regulated and a selection of unregulated exhaust constituents of the two mopeds are presented in Table 4.1 for the ECE-47 cycle and in Table 4.4 in supplementary materials

				Euro 1 - Carburetor with OC		**Euro 2 - Direct Injection with OC and SAS**	
Compounds			**Analytical Techniques**	**Cold Phase**	**Hot Phase**	**Cold Phase**	**Hot Phase**
Gas Phase	**g km^{-1}**	CO*	NDIR	5.99 (0.36)	8.67 (0.21)	2.31 (0.26)	0.60 (0.06)
		CO Standards$^\circ$			6		1
		HC*	FID	5.04 (0.01)	2.13 (0.01)	1.87 (0.03)	1.15 (0.15)
		NO$_x$*	CLD	0.037 (0.005)	0.019 (0.003)	0.352 (0.005)	0.391 (0.008)
		HC+NO$_x$ Standards$^\circ$			3		1.2
	mg km^{-1}	CO$_2$ in g km^{-1*}	NDIR	47.1 (1.8)	40.2 (1.4)	48.3 (0.8)	42.2 (0.1)
		NO	HR-FTIR	18.3 (2.5)	9.8 (2.9)	161.9 (5.9)	200.9 (6.3)
		NO$_2$		0.36 (0.06)	nd	6.33 (0.61)	4.21 (0.64)
		N$_2$O		nd	nd	2.60 (0.19)	2.15 (0.18)
		NH$_3$		2.03 (0.59)	6.39 (0.98)	1.87 (0.03)	0.13 (0.17)
		HCN		0.94 (0.07)	1.10 (0.05)	0.62 (0.02)	0.38 (0.09)
		CH$_4$		53.8 (5.0)	87.8 (15.4)	13.6 (2.2)	7.9 (0.3)
		HCHO (formaldehyde)		22.5 (1.6)	16.3 (2.5)	27.4 (1.2)	26.9 (0.6)
		CH$_3$CHO (acetaldehyde)		24.2 (3.7)	18.4 (2.0)	42.6 (0.6)	38.8 (2.1)
		Benzene group	REMPI-	303 (18)	104 (2)	177 (23)	119 (17)
		Naphthalene group	ToF-	1.43 (0.02)	0.46 (0.03)	1.61 (0.12)	1.11 (0.11)
		Phenanthrene group	MS	0.083 (0.007)	0.030 (0.005)	0.017 (0.014)	0.032 (0.003)
Solid Phase		PM.Mass$^\triangle$	Balance	90 (2)	14 (2)	53 (5)	117 (8)
		PM.Organics (mass)	AMS-	189 (9)	24 (5)	139 (97)	223 (45)
		PM.Nitrate (mass)	ToF-	0.104 (0.005)	0.011 (0.001)	0.146 (0.090)	0.282 (0.087)
		PM.Chloride (mass)	MS	0.021 (0.001)	0.005 (0.001)	0.012 (0.008)	0.019 (0.007)
		PM.Black.Carbon (mass)	MAAP	0.91 (0.05)	0.47 (0.03)	1.60 (0.13)	1.37 (0.20)
		PM.Median Diameter en nm	FMPS	165.5	124.1	124.1	143.3
		PM.Volume in mm^3 km^{-1}		19.9 (0.5)	3.5 (0.7)	19.8 (9.7)	28.2 (1.0)
		PM.Number in # 10^{12} km^{-1}	CPC	3.78 (0.02)	1.82 (0.02)	9 (2)	8.8 (0.3)

Table 4.1: Regulated and unregulated emission factors from the 2 mopeds during the official ECE-47 cycle (mean of 2 tests, standard deviation in parenthesis). OC: oxidant catalyst, SAS: secondary air system, nd: non detectable (methods:* measurement after bags sampling,$^\circ$ according to 97/24/EC,$^\triangle$ according to 98/69/EC).

for the WMTC cycle. With respect to emission standard regulation (Table 4.1), the Euro1-Cb CO emissions (8.67 g km^{-1}) were beyond the respective legislative CO limit (6 g km^{-1}) whereas the Euro2-DI (1.54 g km^{-1}) was slightly above the HC + NO_x standard (1.2 g km^{-1}). The main benefit of the legislative norm Euro 2 was the substantial reduction of CO, and to a smaller extent, the sum of HC and NO_x. The values from the Euro1-Cb and the Euro2-DI showed an evident effort to reduce emissions. Probably this was mainly achieved by DI technology, the catalytic converter and the SAS system. Two-stroke mopeds usually run in rich condition in order to maintain a good drivability. Most likely, the DI contributed to the HC and CO reduction, since it allowed a leaner combustion stoichiometry (higher air/fuel ratio). However, this condition led to higher NO_x emission, but concerning European standard the increase of the sum considered for regulative purposes (HC + NO_x) is generally low. In addition, the SAS allowed to achieve a better combustion efficiency of the oxidant catalyst by adding additional oxygen resulting in lower amounts of HC and CO (217).

4.3.1.2 Non-aromatic unregulated emissions

Emission factors of selected unregulated gaseous exhaust components are shown in Table 4.1. In addition, a rough estimation of the direct global warming potential (GWP) of the two mopeds was carried out by the monitored long-lived greenhouse gases carbon dioxide (CO_2), methane (CH_4), and nitrous oxide (N_2O). The GWP calculation was performed based on the CO_2 equivalent of these compounds defined by the Intergovernmental Panel on Climate Change (135). In hundred years time horizon, 1 g of CH_4 and 1 g of N_2O have the equivalent GWP of 25 and 298 g of CO_2 respectively. During the whole ECE-47 cycle, the Euro2-DI moped released less CH_4 (11 mg km^{-1}) compared to the Euro1-Cb (71 mg km^{-1}), which can probably be explained by the presence of the SAS and the oxidant catalyst. But in return, the Euto 2 moped emitted a non-negligible amount of N_2O (2.4 mg km^{-1}) which is 10-fold more potent than CH_4. However, for both scooters, N_2O and CH_4 contributed less than 3% of the total CO_2 equivalent emitted during the whole cycle and no difference between Euro1-Cb and Euro2-DI was observed (45 ± 2 eq.g CO_2 km^{-1} and 46.2 ± 0.5 eq.g CO_2 km^{-1} respectively). For comparison, the average CO_2 emission from the latest light-duty vehicles in Europe, Japan and Korea is around 143 g CO_2 km^{-1} (218). In return, the calculated OFPs were 6.23 g O_3 km^{-1} and 2.40 g O_3 km^{-1} for the Euro1-Cb and the Euro2-DI respectively. These values are in accordance with a previous study which showed that 2-stroke OFP can be 10 times more important in comparison with catalyzed diesel and gasoline light duty vehicles (131). The Euro 2 moped presented a lower contribution to ozone precursor emission, which was most likely a consequence of its after-treatment system (oxidant catalyst + SAS). The emission factors of formaldehyde and acetaldehyde, the most abundant carbonyls in vehicle exhaust, are presented in Table 4.1. Formaldehyde is known to be a human carcinogen (39). The Euro2-DI emitted higher amounts of both carbonyls than the Euro1-Cb. This was the case for the cold phase as well as for the hot phase of the ECE-47.

The detailed online mass emissions of selected trace gases are depicted in Fig. 4.2. The FTIR real-time determination of NH_3, N_2O and CH_4 mass emissions in Fig. 4.2 A-C, are shown with the driving cycle ECE-47 in gray in the background. An increasing amount of NH_3 was emitted by the Euro1-Cb with short-time maxima of up to 145 μg s^{-1} during the hot phase, which was equivalent to a volumetric concentration of 40 ppm (Fig. 4.2A). This amount was notable if we consider that the upcoming European standard legislation for heavy duty engines (Euro VI) allows a maximum NH_3 emission of 10 ppm (219). NH_3 is a relevant aerosol precursor, which could be formed by reactions of CO and NO with hydrogen gas produced from a waterŰgas shift reaction in the catalyst (66). The emission factor of NH_3 from the Euro1-Cb was even higher than from gasoline light duty Euro 4 (with a three way catalyst) studied in parallel during this measurement campaign (220). The contribution of NH_3 reached more than 35% of the total nitrogen species (NO_x + HCN) measured in the hot phase (Table 4.1). The combustion stoichiometry for the two mopeds was estimated by means of the emissions of HC, CO, CO_2 and O_2. The results confirmed that the Euro2-DI moped was operating in leaner condition (higher air/fuel ratio), which greatly limits the formation of ammonia. A sharp peak of N_2O during each acceleration appeared only for this moped (Fig. 4.2B). CH_4 is illustrated in Fig. 4.2C and as for N_2O, increased emissions appeared mainly during the accelerations. However, the patterns were different for the two vehicles. Whereas CH_4 emission increased along the cycle for the Euro1-Cb, the opposite tendency was observed for the Euro2-DI. As mentioned earlier, this behavior might be explained by the catalyst progressively reaching its optimal working condition.

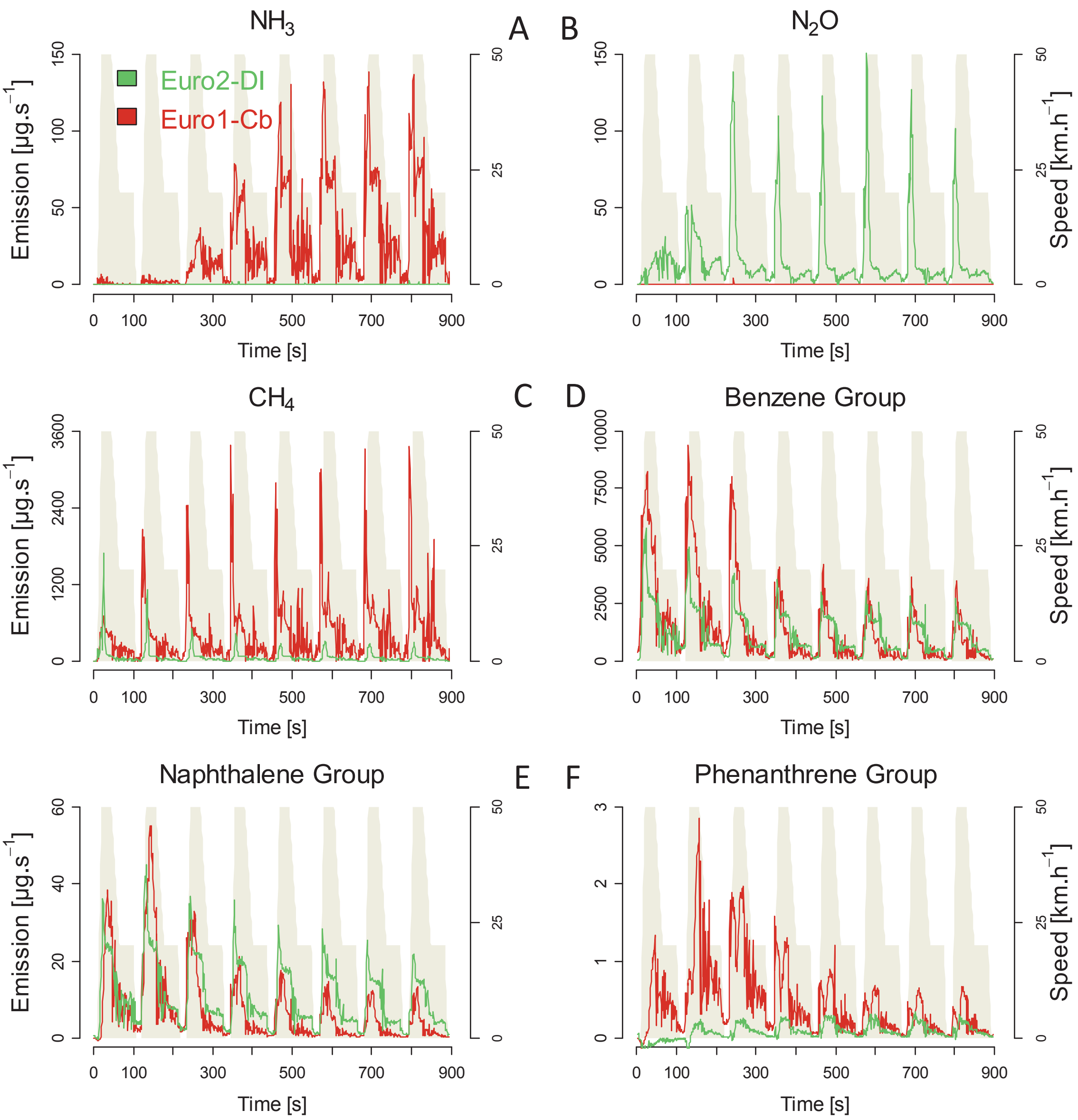

Figure 4.2: Unregulated emission factors. - Online mass emissions of a selection of unregulated gaseous compounds during the ECE-47 cycle.

4.3.1.3 Mono and polycyclic aromatic hydrocarbons

PAH compounds emitted by two-stroke were already investigated in some previous studies (134, 201, 203), however, all these results were based on offline methods. The REMPI-ToF-MS real-time determination of the benzene group (monocyclic aromatic hydrocarbons), the naphthalene group and the phenanthrene group (polycyclic aromatic hydrocarbons) for both mopeds are presented in the Fig. 4.2D to E. It is known that these species are present in the gas phase of moped exhaust (221). First of all, the highest emission occurred during acceleration and full load (50 km h^{-1}), i.e. when the fuel consumption was high. The benzene group reached the highest values of all investigated aromatics with a maximum emission rate during the cold phase of almost 10 mg s^{-1} for the Euro1-Cb and 6 mg s^{-1} for the Euro2-DI (Fig. 4.2D). The naphthalene group showed 100-fold and the phenanthrene group approximately 10 000-fold lower values than the benzene group, which is illustrated in Fig. 4.2E and F. Whereas the benzene compounds emission was maximum for the Euro1-Cb during the three first elementary modules (before 300 s), the two mopeds released an equivalent amount of monoaromatics compounds during the second part of the cycle. On the other hand, the Euro2-DI emitted more naphthalene (and derivatives) during the whole ECE-47 despite of the greatest emission of the Euro1-Cb during the second module (ca. 150 s, Fig. 4.2E). This was more evident at the second half of the cycle, which resulted in more than the double amount of naphthalenes released by the Euro2-DI moped during the hot phase (1.11 mg km^{-1}) compared to the Euro1-Cb (0.46 mg km^{-1}). Finally, the older moped featured higher signals of the phenanthrene group compared to the Euro2-DI (Fig. 4.2F). Different patterns for the emissions of these three groups could be observed. The emission of the benzene group decreased with the acceleration events along the ECE-47 cycle (in particular for Euro2-DI, and after the second module for Euro1-Cb). However, the emission of the PAH groups (naphthalene and phenanthrene groups) behaved differently with a maximum emission during the second module followed by a decrease in the six consecutive modules. This tendency was more pronounced for the phenanthrene group, and the Euro2-DI showed even only one single increase after the first module. For this moped, phenanthrene was not detectable during the first module. This could either suggest a later formation or adsorption/desorption on the catalyst surface or exhaust pipe.

In general, the maximum emissions of aromatics for both mopeds were constant during the later modules. This stabilization occurred earlier for the Euro2-DI moped, and the influence of the cold start effect was less pronounced. The combustion strategy, the after-treatment device and the lower exhaust gas temperature might be the reason for this. In addition, PAH distributions are presented for each module of the ECE-47 in Fig. 4.3. Despite the equivalent total emission of naphthalene compounds of both mopeds, the distributions of the naphthalene derivatives (methyl, dimethyl and so on) were different. Whereas Euro2-DI emitted mostly naphthalene, the Euro1-Cb featured a more complex composition. The different types of oil or the after-treatment system might explain this dissimilarity. However, the Euro1-Cb also showed larger diminution along the cycle (from 2 mg in the 2^{nd} module to 0.4 mg in the 8^{th} module) compared to the Euro2-DI (from 1.6 mg in the 2^{nd} module to 1 mg in the 8^{th} module).

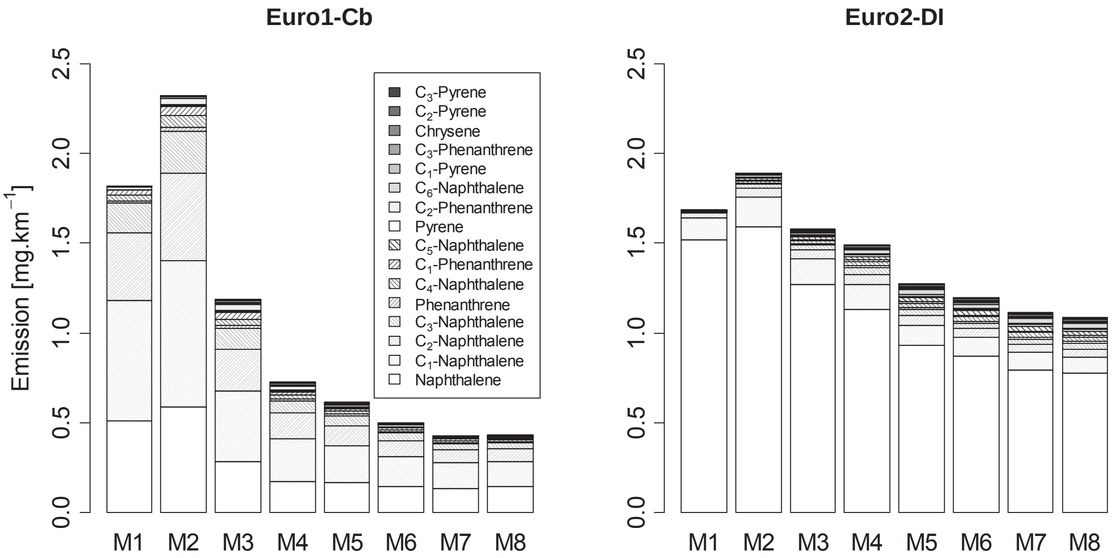

Figure 4.3: PAH speciation. - PAH distribution during the 8 modules (called from M1 to M8) of the ECE-47 cycle for the two mopeds.

4.3.2 Particulate phase

4.3.2.1 Chemical composition

Particle emission factors are presented in the lower part of Table 4.1. Euro2-DI emitted more PM during the hot phase. This behavior of the DI moped was already reported in different studies (134, 222) and will be discussed later. Based on the HR-ToF-MS and MAAP results, PM was mostly composed of organic aerosol, a mixture of lubricant and fuel droplets from scavenging losses of the two-stroke engines. The sulfate species were below the detection limit of the HR-ToF-MS. The BC represented only 0.5.2% of the particulate organic mass. Although the overall EC/OC ratio was almost identical for the two mopeds during the ECE-47 cycle, the ratio was higher in the cold phase for the Euro1-Cb whereas the more elevated ratio for the Euro2-DI was obtained during the hot phase mainly due to the OC reduced emissions at these phases. The comparison of total PM, obtained by weighing and by summing the contents of organic, nitrate and chloride aerosol with the BC (determined by HR-ToF-AMS and MAAP) shows a systematic lower yield with the legislative method (from 43% to 62%). According to the legislation, a period of 1 h must be respected between the collection and the weighing step (at 22°C and 50% of humidity), which may cause loss of most of the volatile compounds from the particles collected on the filter surface (124). However, in contrast to diesel vehicles, most of the emitted mass is non-refractory and thus lost in the evaporation tube. Figure 4.4A shows the organic aerosol emission for both mopeds. Whereas Euro1-Cb produced more organic particulate mass during the cold phase (with a peak of 8 mg s^{-1} during the second module), the Euro2-DI showed a completely opposite behavior, with the highest emission during the hot phase. This tendency was the same for the non-refractory nitrate and chloride aerosol (Fig. 4.4C and D). The exhaust temperature (upper part of Fig. 4.4A) showed a divergent trend starting at the third acceleration (around 300 s). Whereas the exhaust of Euro1-Cb was around 300°C at the end of the ECE-47, the Euro2-DI reached a plateau around 200°C. Most likely, the SAS of Euro2-DI causes the lower exhaust temperature, and consequently, at least some of the difference of the organic aerosol emission between the two mopeds.

Black carbon followed a similar trend as organic aerosol for the Euro1-Cb (Fig. 4.4B); however, the values were two orders of magnitude lower. In return, the BC did not follow the organic aerosol trend for the Euro2-DI. Whereas the organic particulate mass was negligible at the beginning of the cycle, the BC was constantly emitted in the same range during the eight accelerations of the official cycle. Finally, the organic aerosol emissions from the Euro2-DI were 10 times greater than from a heavy duty truck

Euro III (without after-treatment device) studied in parallel during this measurement campaign, however, the emissions of BC from this truck were 100 times higher (161).

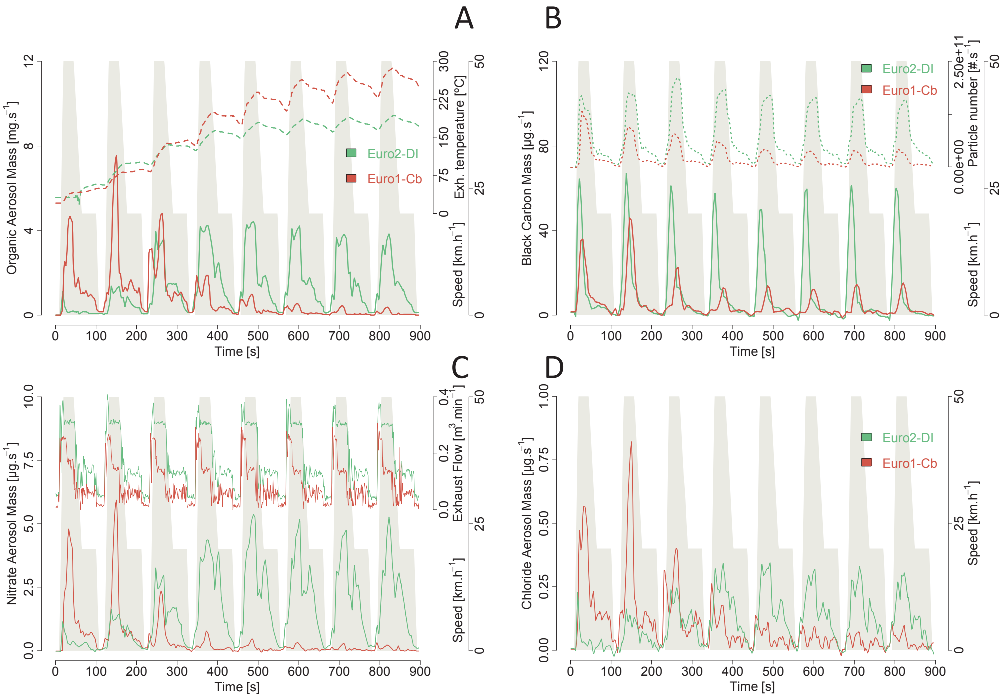

Figure 4.4: PM emission profiles. - Online mass emissions of organic aerosol with exhaust temperature (A), black carbon with particle number (B), non-refractory nitrate aerosol with exhaust flow rate (C) and non-refractory chloride (D) during the ECE-47 cycle for both mopeds.

4.3.2.2 Particle number and size distribution

The particle number for the two mopeds monitored by the CPC is presented in Fig. 4.4B (upper part). Both vehicles emitted similar particle numbers at the beginning of the cycle (1.5 x 10^{11} # s^{-1}), but as for BC, the emission of particle number decreased significantly during the following accelerations for Euro1-Cb. In contrast, the Euro2-DI scooter had similar particle number emissions during all accelerations. The mean diameter of the Euro1-Cb particles decreased as well during the cycle (Fig. 4.5). The higher temperature (above 150°C) in the exhaust system is probably responsible for this depletion leading to less condensable mass as indicated by lower organic mass emissions shown in Fig. 4.4A. The Euro2-DI moped presented a completely different behavior; the mean diameter started increasing during the first two modules and flattened out at approximately 110 nm. The particle number maxima remained constantly high (1.6 x 10^{11} # s^{-1}) in comparison with the Euro1-Cb (4.5 x 10^{10} # s^{-1}). Particle number and mean diameter fluctuation led to more PM for the Euro2-DI moped during the hot phase. It seems that the particle number follows the BC pattern while the mean diameter the organic matter (i.e. larger mean diameter with higher organic matter concentration). This leads us to the assumption that the particles consist of non-volatile soot cores covered by organic material. The Euro2-DI moped showed a noticeable bimodal size distribution with a nucleation peak (particle diameter <10 nm), which always appeared during the deceleration from 50 km h^{-1} to 20 km h^{-1}. This nucleation mode was also present during the two first modules for the Euro1-Cb moped, but attenuated in the following modules probably due to the higher temperature with less condensable organics. This effect occurred at every deceleration when the exhaust gas was under 200°C. During accelerations the organic matter was in the order of 2.5 g m^3, a quantity that is largely enough to form a separate volatile nucleation mode (in absence of sulfuric acid precursors). This is in agreement with Giechaskiel et al. (186). The nucleation mode would not be measured with the new European Union's PN measurement approach where the exhaust is measured after a hot dilution and an evaporation tube at 300-400°C for the removal of volatiles and semi-volatiles (186, 223, 224). Preliminary results showed that this approach reduces the OC accumulation mode particles but does not completely evaporate them (186). Concluding, the newer technology Euro2-DI did not reduce the PM and PN emissions, and in some cases they even exceeded the Euro1-Cb.

4.3.3 Multivariate approach: principal component analysis

PCA was carried out with the entire data set at 1 Hz time resolution for each moped. The gaseous emissions of all compounds listed in Table 4.1 were considered except NO_x. N_2O was not detectable in the Euro1-Cb gas exhaust, therefore, it was not considered for the PCA of this moped. For the same reason, NH_3 was excluded from the Euro2-DI PCA. Regarding the particulate phase, the variables listed in Table 4.1 were considered for the PCA except PM because it was determined by an offline measurement.

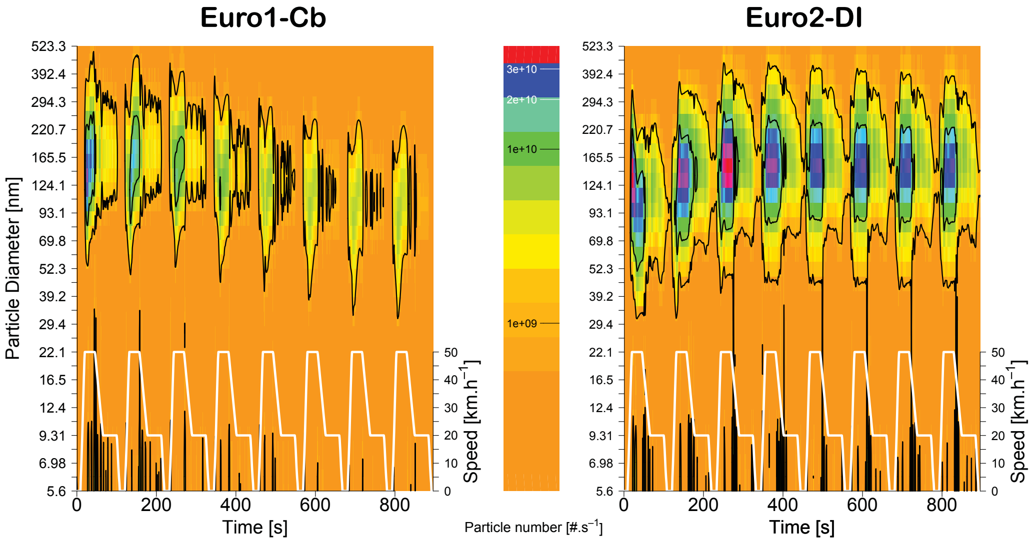

Figure 4.5: PM distribution. - Particle size distribution of Euro1-Cb and Euro2-DI mopeds during the ECE-47 cycle.

The results from Section 4.3.2.2 suggest to take the nucleation mode into consideration. Consequently, the number of particles with diameters below 10 nm (“PM Nucl. Number") was calculated and included as variable in the PCA. In addition, the mean diameter of the accumulation mode (diameter over 30 nm, “PM Acc. Diameter") was included as variable instead of the median diameter (“PM.Median Diameter").

Two PCs were sufficient to explain almost 80% of the total variance for each moped; as a consequence, only two-dimensional correlation circles are presented for every moped. In addition, two explanatory factors, namely the fuel consumption and exhaust temperature were projected in the correlation circle in order to emphasize underlying correlations. Figure 4.6A illustrates the PCA correlation circle for the Euro1-Cb. The two PCs explained 80% of the variance with a strong first PC (PC1, 58% of the variance). Compounds close to each other and to the correlation circle represent similar emission behavior. This is the case for a cluster in the lower right part constituted by CO_2, CO, HCN, HC, HCHO (formaldehyde), CH_3CHO (acetaldehyde), and to a lower extent, NO and CH_4. These compounds followed more or less the same emission pattern.

The projection of the samples discriminated with respect to the fuel consumption is shown in the score plot Fig. 4.6B. The 3-quantiles (namely “Fuel cons. 33%" to “Fuel cons. 100%") depicted a trajectory in the direction of the formed cluster. According to this representation, the cluster was linked to this explanatory factor and will be called fuel consumption cluster (FC cluster). The presence of CO_2 in the FC cluster is obvious since this species is a main product of the combustion process. In return, the presence of the carbonyl species (HCHO and CH_3CHO) in this FC cluster was interesting. A previous study has highlighted the influence of the air/fuel ratio on carbonyl emissions (225). In the present study, projection of this explanatory factor did not show a strong effect (data not shown) and the fuel consumption factor had a greater correlation with carbonyls. On the other hand, a solid emission cluster appeared on the upper right part of the correlation circle (Fig. 4.6A) regrouping the variables organic aerosol and BC mass, as well as particle volume and particle number. The mean diameter of the accumulation mode was not so close to this cluster and the number of particle belonging to the nucleation mode was poorly explained by the 2 PC selected. An intermediate behavior of the aromatic compounds with the localization between the FC cluster and this particle cluster could be observed. The heavier the PAH, the closer it appeared to the particle group. This can be explained by the fact that PAH are potential precursors of soot formation (226).

Figure 4.6C illustrates the influence of temperature in the Euro1-Cb PCA model. This illustration confirms the negative effect of temperature on the particle formation since particles were predominantly present at lower temperatures (3-quantile “temp 33%"), hence at cold engine conditions. The same was found for the PAHs, which confirmed the large decrease shown in Fig. 4.3 for the Euro1-Cb. This particle cluster confirmed the previous results discussed in Section 4.3.2.2 and species regrouping in this group were partly influenced by the cold start. The NO_2 variable was also close to the particle group, and as indicated in Table 4.1, this compound was only emitted during the cold phase of the cycle. NO_2 is toxic and is a direct precursor for ozone formation. It is considered with NH_3 as secondary pollutant of catalytic converter systems (generally three way catalyst). The emissions of these two species are generally anticorrelated, and highly dependent on the air/fuel ratio (157). In the correlation circle (Fig. 4.6A), the O_2 variable was near to NO_2 which could suggest a preferential formation during a high air/fuel ratio. In contrast, NH_3 emission showed not only a positive relation with the fuel consumption, but also with the temperature, which means that NH_3 was predominantly emitted during the high consumption events, when the exhaust temperature was rather elevated. To summarize the Euro1-Cb emission pattern, the vehicle studied showed a conventional behavior since it emitted most of the pollutants proportionally to its fuel consumption. In addition, this carburetor moped featured a negative correlation of the exhaust or engine temperature with the particle emissions (organic aerosols and BC). The mean diameter of the accumulation mode as well as particle volume and particle number were also influenced by the cold start, which suggested either a more efficient engine or the evaporation of oil and fuel droplets in the exhaust pipe during the cycle.

Figure 4.6D represents the correlation circle for the Euro2-DI. The two PCs explained 83% of the total variance. The PC1 (63% of the variance) was linked to the fuel consumption since the axis formed by the 3-quantiles depicted a trajectory almost parallel to the PC1 axis (Fig. 4.6E). Therefore, the FC cluster for the Euro2-DI was composed by CO_2, HCHO, CH_3CHO, NO_2, O_2 and NO. According to this representation, the NO_2 appeared during the high consumption events, probably as reaction product when the NO from the combustion chamber and the O_2 provided by the SAS were simultaneously released. The carbonyls were correlated with O_2 for the Euro2-DI FC cluster. This suggests a preferential formation of HCHO, CH_3CHO in lean condition (high air/fuel ratio), which is in agreement with Magnusson et al. (225). In comparison with the Euro1-Cb correlation circle, an almost identical particle cluster was positioned in the upper left part of the correlation circle (Fig. 4.6D). However, the total particle number (“PM Number") and especially the BC variables were not within this group.

The particle cluster still included the organic aerosol mass as well as the particle volume, but the projection of the temperature factor showed an opposite behavior compared to the Euro1-Cb (score plot Fig. 4.6C and F). An increase of the mean diameter of the particle accumulation mode occurred with the raise of the exhaust temperature, when the engine was warming up. Indeed, among the temperature 3-quantiles depicted, the main difference appeared between the first (<133°C) and the second (between 133 and 168°C) quartile (during the cold phase of the cycle). In addition, the BC was not highly correlated with the particle cluster, but with the naphthalene group and the HC variables. Emissions of these species remained constant or even decreased whereas the particle group emissions were enhanced during the cold phase. Finally, the N_2O and the particle number of the nucleation mode were not explained by this PCA model. However, these species were mainly associated with the transient speed events, hence during short periods. This information accounted for a

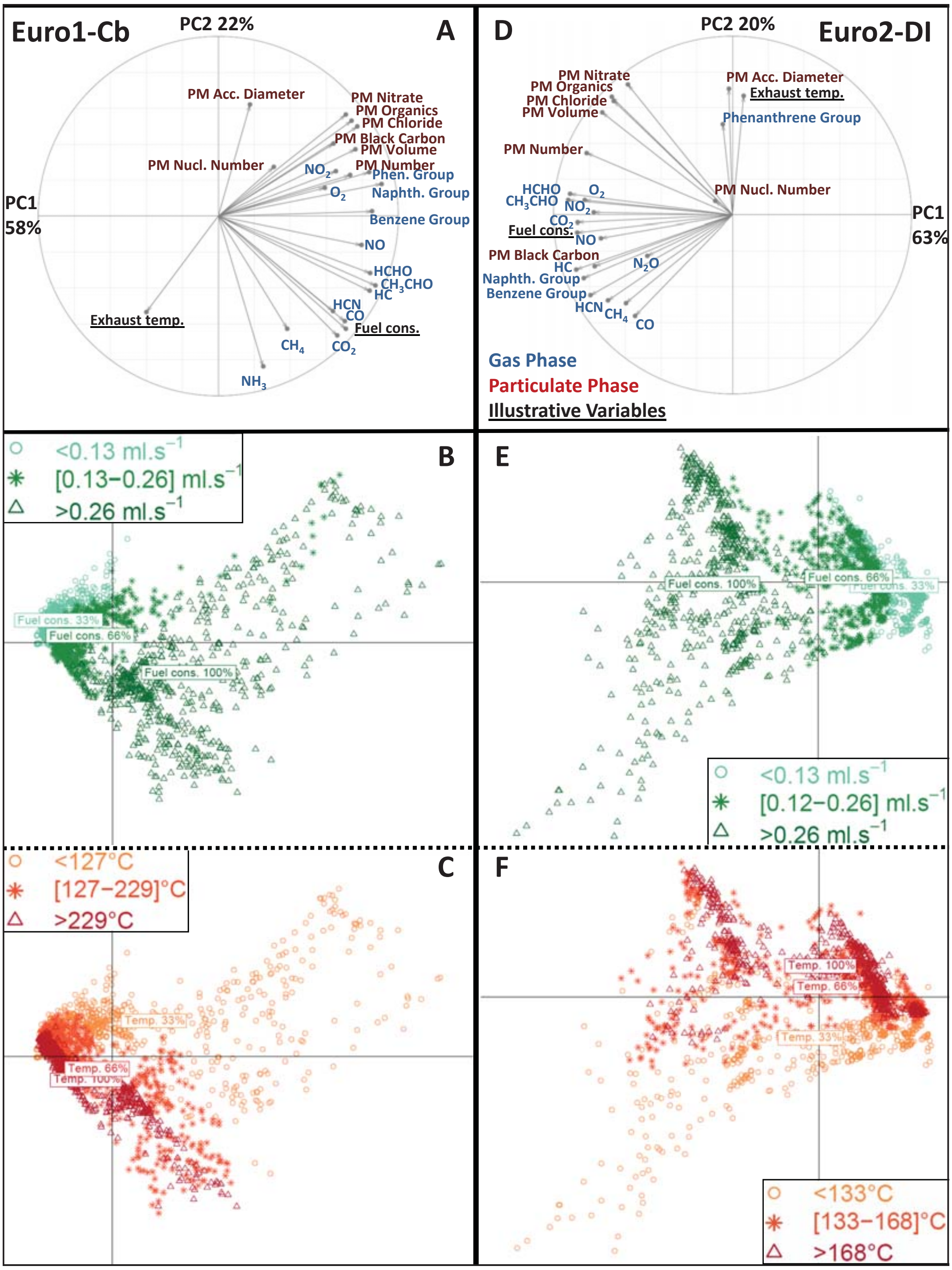

Figure 4.6: Chemometric approach on emission profiles. - PCA of solid and gas emission pattern during the ECE-47 cycle for the Euro1-Cb (left) and the Euro2-DI moped (right). Correlation circles (A and D) and score plots with fuel consumption (B and E) and exhaust temperature (C and F) projections.

minor part of the dataset total variance, and including an additional PC in the model might be able to explain these variables.

Finally, the major scattering of the points occurred, for both mopeds, when the consumption was maximum (third 3-quantile) as indicated in Fig. 4.6B and E with the triangle points. That particular case occurred specifically during the full sharp acceleration when the emissions were the highest in comparison with the following part of the driving cycle. These specific emissions represent the most part of the total variance to explain, which explains the important scattering of the fuel consumption third 3-quantile. In addition, considering the interaction with the exhaust temperature factor, it can be observed that the points which contributed greatly to the scattering of the fuel consumption third 3-quantile belonged to the exhaust temperature first 3-quantile, hence the lower exhaust temperature (circle points in Fig. 4.6C and F). It stresses the considerable impact of the cold start (i.e. when the engine and the after-treatment were cold) on the pollutant emissions, especially during the full acceleration of the vehicles.

4.4 Conclusion

For the first time a set of different online instruments was applied to simultaneously monitor the gas phase and the particulate phase of the exhaust of two-stroke scooters. In addition, a PCA was conducted to find the most influential parameters. This multivariate analysis allowed a deep characterization of the online emission patterns. The accumulation of signal during transient events was sufficient to notice possible correlations between emissions and physical factors. Thus, the influence of exhaust temperature on PAH and particle emissions was highlighted. Results suggest that the modern technology used to lower regulated compounds might have a negative effect on unregulated compounds like carbonyls and organic aerosol. The impact of these harmful pollutants in term of air quality and climate impact (secondary organic aerosol formation) should be studied. Finally, the presented study stresses the necessity to modify the list of regulated compounds in the upcoming legislation for PTWs.

- **Acknowledgments**

The VELA staff is acknowledged for their skilful technical assistance, in particular R. Colombo, M. Sculati, G. Lanappe, F. Muehlberger, and P. Le Lijour. The authors also thank S. Preys for his valuable comments on the multivariate data analysis, and V. Franco Garcia for his skilful help on the data processing.

4.5 Supplementary Materials

Properties	**CEC RF-02-99**
Density @ 15°C	0.7592 kg L^{-1}
Sulphur Content	<10 mg kg^{-1}
Octane Number RON	99.2
Octane Number MON	87.5
DVPE	59.8 kPa
Distillation Initial Boiling Point	35.5°C
Evaporated @ 100°C	51.6%vol
Evaporated @ 150°C	84.8% vol
Final Boiling Point	193.5°C
Aromatics	29.6% v/v
Olefins	4.2% v/v
Benzene	0.2% v/v
Oxygenates	4.9% v/v
Oxygen content	0.9% m/m

Table 4.2: Characteristics of the used reference fuel (CEC RF-02-99 oxy 0.8-1.2).

Properties	**Euro 1 - Carburetor mineral oil**	**Euro 2 - Direct Injection semi-synthetic oil**
Composition		
Severely solvent refined mineral oil (IP346 DMSO extract <3%)	Ca. 85% m/m	Ca. 65% m/m
Aliphatic hydrocarbon solvent (CAS 64742-47-8, Xn, R65,R66)	10-20% m/m	-
Naphtha hydro treated heavy (CAS 64742-48-9, Xn, R65, R66)	-	20-50% m/m
Physical state	Oily liquid	Oily liquid
Colour	Red	Brown
Appearance	Bright and clear	Bright and clear
Odour	Weak	Weak
pH	Neutral	Not known
Boiling range	Initial boiling point (oil base) >176°C	Not known
Melting Point	<-30°C	-45°C
Flash Point	>61°C (ASTM D 93, P-M)	97°C (ASTM D 93, P-M)
Autoflammability / ignition	210°C (oil base)	Not known
Upper explosion limit	7.0% vol. -air (oil base)	Not known
Lower explosion limit	0.6% vol. -air (oil base)	Not known
Vapour pressure, 20°C	Appr. 0.04 kPa (oil base)	Not known
Viscosity, kinematic, 40°C	52 mm^2 s^{-1}	44.3 mm^2 s^{-1}
Relative density, 15°C	0.88	0.86
Water solubility	Not soluble	Not soluble
Partition coefficient, log(n-octanol/water)	Not known	<3

Table 4.3: Physical and chemical properties of the lubricant oil used.

			Analytical Techniques	**Euro 1 - Carburetor with OC**		**Euro 2 - Direct Injection with OC and SAS**	
Compounds				**1^{st} Phase**	**2^{nd} Phase**	**1^{st} Phase**	**2^{nd} Phase**
Gas Phase	**$g\ km^{-1}$**	CO^*	NDIR	9.0 (1.0)	11.0 (1.0)	1.5 (0.1)	0.70 (0.01)
		HC^*	FID	5.0 (0.1)	2.3 (0.1)	1.85 (0.08)	1.25 (0.01)
		$NO_x{}^*$	CLD	0.0325 (0.0002)	0.015 (0.002)	0.42 (0.04)	0.37 (0.02)
		$CO_2{}^*$	NDIR	52.4 (0.4)	42.7 (0.8)	49.6 (0.5)	42.5 (0.2)
		NO	HR-FTIR	0.014	0.006	0.17 (0.01)	0.19 (0.01)
		NO_2		0.0001	nd	0.0058 (0.0001)	0.0020 (0.0004)
		N_2O		nd	nd	0.0029 (0.0001)	0.0020 (0.0001)
		NH_3		0.0029	0.0073	nd	nd
		HCN		0.0010	0.0011	0.0004 (0.0001)	0.0003 (0.0001)
		CH_4		0.10	0.16	0.0091 (0.0009)	0.0079 (0.0008)
		HCHO (formaldehyde)		0.022	0.015	0.025 (0.001)	0.024 (0.001)
		CH_3CHO (acetaldehyde)		0.025	0.022	0.0440 (0.001)	0.037 (0.001)
	$mg\ km^{-1}$	Benzene group	REMPI-	353	100	183	132
		Naphthalene group	ToF-	1.40	0.38	1.63	1.18
		Phenanthrene group	MS	0.088	0.029	0.014	0.016
Solid Phase		$PM.Mass^{\triangle}$	Balance	90 (2)	14 (2)	71 (1)	100 (3)
		PM.Organics (mass)	AMS-	169	14	150	226
		PM.Nitrate (mass)	ToF-	0.073	0.009	0.19	0.26
		PM.Chloride (mass)	MS	0.020	0.003	0.012	0.016
		PM.Black.Carbon (mass)	MAAP	0.99	0.53	1.70	1.23
		PM.Median Diameter en nm	FMPS	165.5	107.5	124.1	143.3
		PM.Volume in $mm^3\ km^{-1}$		18.1	2.7	17.8	23.4
		PM.Number in # $10^{12}\ km^{-1}$	CPC	3.20	1.81	8.2	7.9

Table 4.4: Regulated and unregulated emission factors from the 2 mopeds during the "WMTC -2 urban phases" cycle (standard deviation in parenthesis). SAS: Secondary Air System, nd: non detectable (methods:* measurement after bags sampling,$^{\triangle}$ according to 98/69/EC).

Chapter 5

Alternative fuels and powertrain technologies effects on exhaust emissions

5.1 Part A - Bioethanol fuel

Effects of low temperature on the cold start gaseous emissions from light-duty vehicles fuelled by ethanol-blended gasoline

M. Clairotte[a], T.W. Adam[a], A.A. Zardini[a], U. Manfredi[a], G. Martini[a], A. Krasenbrink[a], A. Vicet[b], E. Tournie[b], C. Astorga[a]

Applied Energy - 2013, volume: 102, pages: 44-54

[a] European Commission Joint Research Centre Ispra, Institute for Energy, Sustainable Transport Unit, 21027 Ispra, Italy
[b] Institut dŠElectronique du Sud (IES), UMR CNRS 5214, Case 067, Université Montpellier 2, 34 095 Montpellier Cedex 05, France

Abstract

According to Directives 2003/30/EC and 2009/28/EC of the European Parliament and the Council, Member States should promote the use of biofuel. Consequently, since 2011 all fuels on the market used for transport purpose must contain a fraction of 5.75% renewable energy sources. Ethanol in gasoline is a promising solution to reach this objective. In addition to decrease the dependence on fossil fuel, ethanol contributes to reducing air pollutant emissions during combustion (carbon monoxide and total hydrocarbons), and has a positive effect on greenhouse gas emissions. These considerations rely on numerous emission studies performed in standard conditions (20-30°C), however, very few emission data are available for cold ambient temperatures, as they prevail in winter times in e.g., Northern Europe.

This paper presents a chassis dynamometer study examining the effect of ethanol (E75-E85) versus gasoline (E5) at standard and low ambient temperatures (22°C and -7°C, respectively). Emissions of modern passenger cars complying with the latest European standards (Euro4 and Euro5a) were recorded over the New European Driving Cycle (NEDC) and the Common Artemis Driving Cycle (CADC). Unregulated compounds such as methane, ammonia, and small chain hydrocarbons were monitored by an online Fourier Transformed Infra-Red spectrometer. In addition, a number of ozone precursors (carbonyls and volatile organic hydrocarbons) were collected and analyzed offline by liquid and gas chromatography in order to evaluate the ozone formation potential (OFP) of the exhaust.

Results showed higher unregulated emissions at -7°C than at 22°C, regardless of the ethanol content in the fuel blend. More carbonyls were associated with oxygenated fuel, and acetaldehyde emissions were found particularly enhanced at -7°C with E75. In addition, elevated methane emission was measured at low ambient temperature when ethanol fuel was used. Moreover, the OFP of the exhaust gas at -7°C increased with the amount of ethanol in gasoline when the cold start excess emissions were included. However, regardless of the ambient temperature, the ammonia and toluene emissions associated to E75-E85 were lower than with E5.

Keywords: unregulated emissions; alcohol fuel; vehicle cold start; ozone formation potential; ethanol; ammonia.

5.1.1 Introduction

Nowadays, the transport sector contributes significantly to air pollution and climate change (227, 228) and on-road transportation is considered as a key issue for the next decade (18, 229). At the same time, the European Union (EU) attempts to promote the share of energy from renewable sources in transport with an objective of 10% by 2020 (77, 230), and to decrease fuel life cycle greenhouse gas (GHG) emissions (35). This tendency has also been followed in the United States since 2005 by the Environmental Protection Agency (EPA). In the last version of the Renewable Fuel Standard (RFS II), EPA has set a target of 36 billion gallons of renewable fuel to be blended with gasoline by 2022 (30). Ethanol in gasoline may be considered a promising alternative which reduces some regulated gaseous emissions such as carbon monoxide (CO) and total hydrocarbons (THC) (92, 231) as well as sulphur dioxide (SO_2) (232). It also contributes to decrease the emission of GHGs by increasing the plant-based carbon content in the fuel, and thus, by closing the carbon cycle. In addition, depending on the feedstock used, ethanol in gasoline can be recognized as sustainable (233). Therefore, the EU certified recently several programs e.g. the "Greenergy Brazilian Bioethanol verification programme", for the biofuel target under the renewable energy directive (77, 234). Despite the favorable effects on some primary regulated emissions and GHGs, ambient air measurements taken in several areas where high ethanol content in gasoline was implemented highlight the deterioration of air quality. The presence of significant amounts of health-related compounds such as potentially carcinogenic carbonyls and ozone precursors was found (41, 42, 43). Indeed, chassis-dynamometer studies on primary emissions demonstrated such side effects of ethanol-blended fuels a decade ago (99, 100, 235, 236). On the contrary, a recent study in Rio de Janeiro states that modern engine technology and aftertreatment together with a higher fuel quality lead toward an improvement of the air quality (237). However, all these investigations are based on measurements carried out at ambient temperature (about 20°C) and limited information is available on the emissions of vehicles running with ethanol blended fuel at lower temperature (238, 239). Only the type approval for light-duty (LD) vehicles fuelled with reformulated gasoline (RFG) is currently implemented in EU at low temperature (-7°C, the so-called type 6 test). This is not the case for fuel with ethanol content higher than 5% (81). However, such assessment is necessary for emission characterization and modelling before considering the widespread use of ethanol fuel in large scale. Therefore, this study aimed to investigate the impact of fuels with high ethanol content on the regulated and unregulated gases emitted by modern LD vehicles at low temperature. The ammonia (NH_3) was evaluated more in detail because of its impact on human health and vegetation (55). Moreover, it can form ammonium aerosols which have a direct and indirect effect on climate, and contribute to local visibility problems (57). The transport sector increasingly contributes to the total atmospheric NH_3 emission especially during winter when agricultural sources decrease (65). Thereby, the motor vehicle fraction can reach up to 73% in urban areas (58). Finally, the emissions of ozone precursors and the influence of the cold engine start were evaluated in more detail.

5.1.2 Experimental section

5.1.2.1 Chassis dynamometer experiments

This study was conducted at the European Commission Joint Research Centre (EC-JRC) Ispra, Italy, in the Vehicle Emission Laboratory (VELA). The facility includes a test cell with controlled temperature and relative humidity to mimic the typical conditions in Europe (temperature range: [-10 ; 35]°C; relative humidity: 50%). The tests were performed on chassis dynamometer (inertia range: [454-4500] kg), designed for two-wheel and four-wheel drive light-duty (LD) vehicles (two 1.22 m roller benchs - Maha GmbH, Germany). The emissions fed to a Constant Volume Sampler (CVS, Horiba, Japan) using a critical Venturi nozzle to regulate the flow (CVS flow range: [3; 30] $m^3\ min^{-1}$). A series of thermocouples monitored the temperature of the oil, cooling water, pre and post-catalyst exhaust, and ambient conditions.

Three LD gasoline vehicles (Car 1 to 3) and two LD flexi-fuel vehicles (Car 4 and 5) were tested. Car 1 to 4 complied with the Euro 4 emission standard; whereas Car 5, equipped with a modern direct injection engine, complied with the Euro 5a emission standard (81).

Two driving cycles have been applied, the official New European Driving Cycle (NEDC) which is used for type approval of LD vehicles in Europe, and the Common ARTEMIS Driving Cycles (called hereinafter CADC). The NEDC is a cold-start driving cycle (i.e., performed with a cold engine at the beginning of the cycle), which includes a first urban phase of 780 s (UDC) followed by an extra-urban phase of 400 s (EUDC).

The CADC has been developed to better simulate typical driving behavior in Europe (122). Experiments with this cycle are performed after a pre-conditioning of the vehicle i.e., with a warm engine. The CADC consists of three phases, representative of urban (920 s), rural (1081 s) and motorway (1067 s) driving. Figure 5.1 depicts the speed profiles of both studied cycles. The tests were conducted at two temperatures, 22°C and -7°C, and 50% relative humidity.

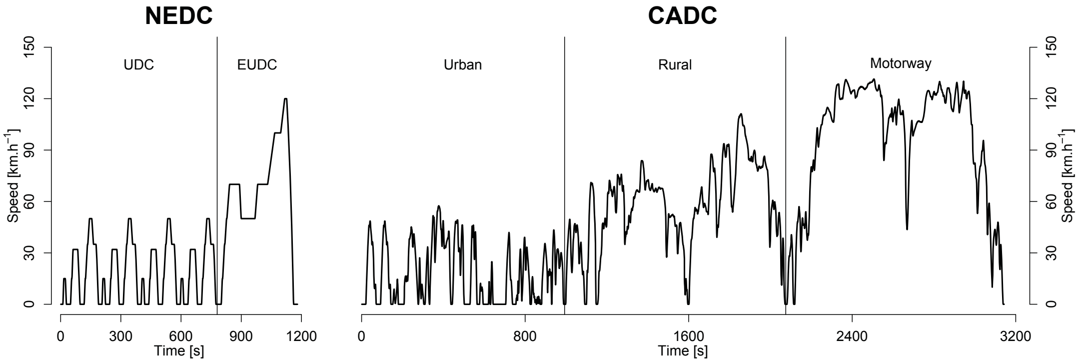

Figure 5.1: Driving cylces studied. - Driving cycles performed in the test cells.

A certified reference fuel E5 (called hereinafter RFG) was used in all the vehicles. Non-flexi vehicles were also fuelled with a 10% ethanol blend with gasoline (E10), whereas flexi-fuel vehicles were also fuelled with E85 and E75 while running at 22°C and -7°C, respectively. A detailed description of the fuel characteristics is available in Table 5.1. Table 5.2 gives an overview of the combination of fuels, cycles, and ambient temperatures studied.

Property	Method	E5	E10	E75	E85
RON	EN ISO 5164	96.9	95.4	102	107.8
MON	EN ISO 5163	86.6	85.7	88	89
Density @15°C [g/l]	EN ISO 12185	737.9	745.0	772.8	785.7
Sulfur [ppm]	EN ISO 20846	<10	<10	<3	3.2
DVPE [Kpa]	EN 13016-1	64.3	60	50.3	35.2
Ethanol [vol. %]	EN 13132	5.01	9.28	73.7	85.7
Carbon [wt %]	ASTM D 3343	84.8	83.3	60.4	57.4
Hydrogen [wt %]	ASTM D 3343	13.4	13.3	13.1	13.1
Oxygen [wt %]	EN 13132	1.8	3.4	26.5	29.5
Trace Lead [g l^{-1}]	EN 237	<10	<10	<5	<5
Calorific Value [MJ kg^{-1}]	ASTM D 3338	42.72	41.94	30.85	29.43

Table 5.1: Gasoline fuel specifications.

Denomination	**Car 1**	**Car 2**	**Car 3**	**Car 4**	**Car 5**
Combustion Type	Gasoline	Gasoline	Gasoline	Flex-Fuel Gasoline-Ethanol	Flex-Fuel Gasoline-Ethanol
Model	2008	2008	2007	2009	2010
EU Emission Standard	Euro 4	Euro 4	Euro 4	Euro 4	Euro 5a
aftertreatment	TWC	TWC	TWC	TWC	TWC
Fuel	E5 and E10	E5 and E10	E5 and E10	E5, E75, and E85	E5, E75, and E85
Engine Supply	PFI	PFI	PFI	PFI	DI
Engine Capacity [ccm^3]	1596	1368	1598	1798	1984
Engine Power [kW]	85	88	128	92	132
Odometer [km]	20815	1261	6248	11772	1441
Vehicle Weight [kg]	1204	1250	1205	1377	1570
Ambient testing temperature	22°C	22°C	22°C	-7°C and 22°C	-7°C and 22°C
Test Cycles	NEDC	NEDC	NEDC	NEDC and CADC	NEDC and CADC

Table 5.2: Technical characteristics of the test fleet and experimental details (PFI: port fuel injection, DI: direct injection).

5.1.2.2 Analytical instrumentation

The regulated emissions from all vehicles were measured in accordance with directive 70/220/EEC and its following amendments (75), with an integrated setup which uses following techniques: non-dispersive infrared (for CO/CO_2), a chemiluminiscence (for NO_x) and a heated (191°C) flame ionization detector (FID for THC) (Horiba, Japan).

A selection of unregulated gaseous emission, including (i) small hydrocarbons like methane (CH_4), ethylene (C_2H_4), and toluene (C_7H_8), (ii) nitrogen species like nitric oxide (NO), nitrogen dioxide (NO_2), nitrous oxide (N_2O), NH_3, and hydrogen cyanide (HCN), and (iii) oxygenated compounds like formaldehyde, acetaldehyde, and ethanol, were monitored at 1 Hz acquisition frequency by a High Resolution Fourier Transform Infrared spectrometer (HR-FTIR - MKS Multigas analyzer 2030, Wilmington, MA, USA). The method is described in detail in the literature (162), therefore, only a brief description is given here. The device is made up of a multipath cell (optical length: 5.11 m), a Michelson interferometer (spectral resolution: 0.5 cm^{-1}, spectral range: 600-3500 cm^{-1}) and a liquid nitrogen cooled mercury cadmium telluride detector (MCT). The raw exhaust was sampled directly from the tailpipe of the vehicles with a heated PTFE (politetrafluoroetilene) line and a pumping system (flow: ca. 10 L min^{-1}, T: 191°C) in order to avoid the absorption of hydrophilic compounds (i.e., NH_3, NO_2, carbonyls, or ethanol) in condensed water. The residence time of the undiluted exhaust gas in the heated line before the HR-FTIR measurement cell was less than 2 s. The pressure during the measurement was 1013 hPa (± 20), and the temperature was set to 191°C. The calibration of the instrument was based on a factory developed multivariate model.

CO, CO_2 and NO_x measurements from the previously described analyzers were used to check the HR-FTIR calibration model, and to synchronize the time-resolved signal.

Recent studies pointed out the lack of selectivity of the heated FID towards oxygenated hydrocarbon compounds emitted in the exhaust from engines fuelled with high ethanol blended mixtures (239, 240). Therefore, we corrected the time-resolved THC volumetric concentration measured with the FID with the concentration of selected aldehydes and alcohols measured with the FTIR as follows:

$$[THC]_{cor,t} = [THC]_{un,t} + [CH_3CH_2OH]_t \times (1 - RF_{CH_3CH_2OH})$$

$$+[CH_3OH]_t \times (1 - RF_{CH_3OH}) + [CH_3CHO]_t \times (1 - RF_{CH_3CHO})$$

$$+ [HCHO]_t \times (1 - RF_{HCHO}), \tag{5.1}$$

where *[THC]*$_{cor,t}$ is the corrected volumetric concentration of THC in ppm at time t. *[THC]*$_{un,t}$ is the raw volumetric concentration of THC in ppm monitored by the heated FID at time t. $[x]_t$ is the volumetric concentration of x in ppm monitored by the FTIR at time t. RF_x is the response factor of the FID for the compound x (0.68, 0.36, 0.6, and 0.2 for ethanol, methanol, acetaldehyde, and formaldehyde respectively as defined in Wallner (2011) (240)).

In order to estimate the ozone formation potential (OFP), volatile hydrocarbons (VOCs) and carbonyls known as ozone precursors were sampled from the dilution tunnel during the entire driving cycles. VOCs were collected in opaque PVF (polyvinyl fluoride) bags and measured within 30 min after sampling. A selection of 22 VOCs (from C_2 to C_9) listed as ozone precursors in the European air quality directive (53) were quantified with dual column gas chromatography with FID (6890, Agilent, Santa Clara, USA) calibrated with a multi-standard gas (National Physical Laboratory, Middlesex-UK) as described elsewhere (131). Carbonyls were collected with 2,4-dinitrophenylhydrazine-silica cartridges and analyzed by high performance liquid chromatography (1100 Series, Agilent, Santa Clara, USA) equipped with a C_{18} column (New Allure AK, Restek corporation, Bellefonte, PA, USA) and ultra-violet detector, as defined in the EPA methods (210, 211). Calibration of the instrument was performed with an analytical standard (Supelco, Bellefonte, PA, USA) including 13 carbonyls (formaldehyde, acetaldehyde, acrolein, acetone, propionaldehyde, crotonaldehyde, methacrolein, butyraldehyde, 2-butanone, benzaldehyde, valeraldehyde, p-tolualdehyde and hexaldehyde) following the accuracy profiles method described elsewhere (130). The OFP of each VOC and carbonyl listed above, as well as of CO, were calculated in accordance to the maximum incremental reactivity concept (MIR) (132). In this method, the ozone produced from a precursor is estimated under optimal atmospheric composition (precursor/NO_x ratios). The OFP was the sum of the ozone produced from each precursors emitted during the entire driving cycle.

5.1.2.3 Data processing (Statistic, CSEE approach)

The first step of the data processing consisted in synchronizing the different VELA sensors (fuel consumption flow meter), as well as the time-resolved regulated and unregulated tailpipe emissions. The starting time delay of the different instruments and sensors was carefully adjusted along the on-board diagnostic (OBD) data available from the Euro5a light-duty vehicle. Then after correction by linear interpolation of the short time losses of emission data recording, the volumetric time-resolved emission (in ppm) was converted into mass emission (expressed in mg s^{-1}) using the real time exhaust flow. The CO_2 tracer method associated with the critical flow Venturi, was used to estimate the real time exhaust flow (i.e. by the ratio of the instantaneous CO_2 concentration at the tailpipe and the CO_2 concentration at the dilution tunnel corrected by the background CO_2 of the diluted air). The integration of the mass emission over the driven distance allowed to expressing emission factors (in mg km^{-1}) for each pollutant. In the particular case of THC, the mass flow (in g s^{-1}) was calculated with the corrected THC volumetric concentration as previously defined and the fuel dependent THC molecular mass (81). The non-methane hydrocarbon (NMHC) emission factor was calculated by subtracting the CH_4 emission factor from the corrected THC.

In addition, the cold start excess emission (CSEE), as described in previous studies (241, 242), was estimated over the UDC phase of the NEDC. The UDC consists of 4 repetitions of the ECE15 module (average speed is 18.7 km h^{-1}, average positive acceleration 0.348 m s^{-2} (120)). It is suited for estimating CSEE since the initial 40 s idle period are to be neglected after Euro3 legislation revisions (243). Figure 5.2 illustrates the applied methodology by means of CH_4 measured by HR-FTIR for Car 5 at -7°C and with E75. The CH_4 emission occurred mostly at the beginning of the cycle (the cold phase), before the light-off of the catalyst at 240 s. Then, the emission of the pollutant stabilized along the second part of the cycle (the warm phase), as described by the asymptotic behavior of the cumulative mass. A linear regression is carried out as soon as the standard deviation of the cumulative emission reaches a maximum value. Then, the offset of this regression model correspond to the CSEE mass (CSEE$_m$), i.e., the mass of pollutant emitted during the cold phase. The CSEE duration (CSEE$_t$), i.e., the duration of the cold phase event, was estimated when the difference between the regression model and the cumulative mass curves reached 3%. Values estimated by this method are cycle dependent, so related to the UDC used for their calculation.

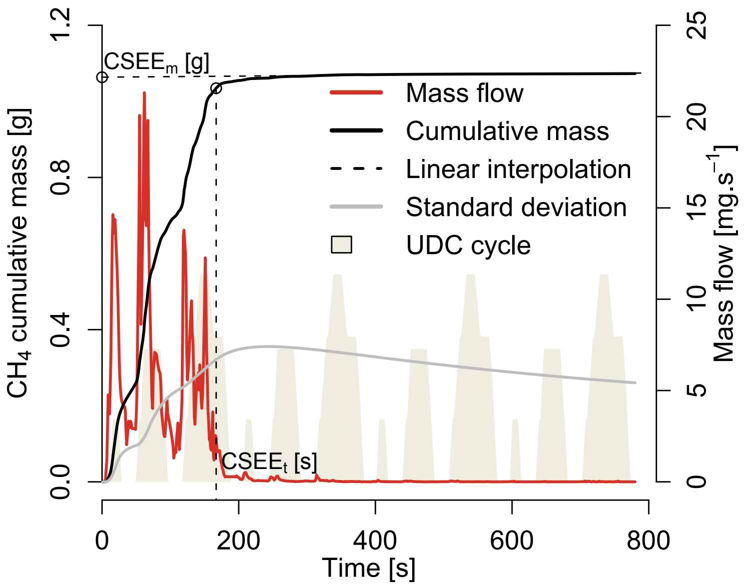

Figure 5.2: Cold start excess emission methodology description. - CH$_4$ Cold Start Excess Emission (CSEE$_m$) estimation for the Euro 5a Car 5, at -7°C and with E75 during the urban part of the NEDC. The cycle is depicted in the background (50 km h^{-1} maximum velocity, see Fig. 5.1), the red line is the CH$_4$ mass flow determined by HR-FTIR.

The emission factors and the OFPs for each fuel were compared with a two-way t-student test. The impact of the temperature and fuel on the CSEE$_m$ was investigated by Principal Component Analysis (PCA). PCA aims to reduce the total number of variables to uncorrelated variables called principal components (PC). This model provided a simpler basis for summarizing the data and highlighting underlying correlation between explanative factors (temperature and fuel), and the original variables (CSEE_m of the different pollutants). Data pre-processing, statistical calculations and CSEE determinations were performed with R software and its “ade4" package (216).

5.1.3 Results and discussion

5.1.3.1 Emission factors of regulated gases

The regulated emission factors for the 5 vehicles over the NEDC at 22°C are presented in Table 5.3. For any ethanol/gasoline ratio (5%, 10%, or 85%), the vehicles complied with the most stringent emission standard, Euro 5a. Statistical differences (P value $<$ 0.05) were associated with the type of fuel. Car 2 emitted significantly less THC (and NMHC) and CO when E10 was used, whereas the flexi-fuel Car 4 and Car 5 emitted significantly less CO and NO_x, respectively, when E85 was used. In addition, the CO_2 emission factors from both flexi-fuel vehicles with high ethanol content fuel were 5% lower than with RFG.

Vehicles	**Car 1 Euro 4**		**Car 2 Euro 4**		**Car 3 Euro 4**		**Car 4 Euro 4**		**Euro 4**
Fuel	E5	E10	E5	E10	E5	E10	E5	E85	**limits**
HC	76 (7)	69 (3)	34 (3)^b	25 (3)^b	28 (2)	30 (4)	73 (22)	67 (14)	**100**
NMHC	66 (7)	60 (3)	31 (3)^b	22 (3)^b	24 (2)	25 (4)	68 (23)	56 (14)	**-**
CO	584 (127)	488 (73)	411 (22)^c	280 (35)^c	387 (57)	395 (32)	755 (99)^c	162 (12)^c	**1000**
NO_x	44 (3)	46 (5)	11 (2)	14 (2)	3.5 (0.3)	3.7 (0.4)	27 (6)	21 (2)	**80**
PM	0.6 (0.3)	0.6 (0.2)	0.44 (0.08)	0.5 (0.3)	0.7 (0.2)	0.75 (0.07)	N/A	N/A	**-**
$CO_2{}^{\triangle}$	160.9 (0.9)	160 (1)	159 (2)	159 (1)	166 (2)	165 (2)	173 (1)^b	165 (3)^b	**-**

Vehicles	**Car 5 Euro 5a**		**Euro 5a**
Fuel	E5	E85	**limits**
HC	47 (8)	57 (8)	**100**
NMHC	43 (8)	41 (7)	**68**
CO	471 (181)	268 (83)	**1000**
NO_x	26 (5)^b	10.9 (0.3)^b	**60**
PM	0.7 (0.3)	0.41 (0.03)	**5.0**
$CO_2{}^{\triangle}$	191 (2)^c	180 (2)^c	**-**

Table 5.3: Regulated emission factors (in mg km^{-1} except $^{\triangle}$ in g km^{-1}) for the vehicles over the NEDC at 22°C with E5, E10 and E85. The standard deviations are in brackets and were calculated from a minimum of 3 test repetitions (N/A: not available). Statistically significant differences between fuels are indicated as follow: (a) P value $<$ 0.05, (b) P value $<$ 0.01, (c) P value $<$ 0.001.

The flexi-fuel vehicles tested at low temperature (-7°C) over the UDC phase of the NEDC complied with the type 6 test emission standards (THC: 1.8 g km^{-1} and CO: 15 g km^{-1} (81)) when RFG was used (Table 5.4). In the case of Car 4, the CO emission factor over the UDC at 22°C was significantly lower when E75 was used (P value $<$ 0.001), whereas the opposite occurred at -7°C (emission factor almost 2 times higher, P value $<$ 0.001). This caused this vehicle to exceed the limit of 15 g km^{-1} in force for standard gasoline. Even if not statistically significant (P value $>$ 0.05), this trend was identical for the Euro 5a Car 5. The emission factors of ethanol over the UDC were a significant fraction of the THC, especially when fuel with high ethanol content was used. At 22°C, the averaged amount of unburned ethanol accounted for 15% (RFG) and 61% (E85) of the THC. These values are consistent with a previous study on a DI spark-ignition engine fuelled with E85 (93). However, at -7°C the amounts of ethanol were even higher with E75, and exceeded the THC for the Euro 4 flexi-fuel vehicle. For this reason, the corrected NMHC emission factors are more relevant to comment on the unburned hydrocarbons. Latter pollutants were consistently more emitted with E75 at -7°C, by an averaged factor of almost 3, which led to exceed the THC standard for gasoline. Note that this measurement methodology was different than the type 6 test method which is based on bag sampling (81). It was nearly equivalent to the non-methane organic gases quantification implemented by the EPA for alcohol fuelled vehicles (129).

5.1.3.2 Emission factors of unregulated gases

Most of the regulated and unregulated gaseous compounds were emitted during the first seconds of the NEDC, i.e., before the catalyst reached the optimal working conditions. For Car 4 and 5, Table 5.4 summarizes the averaged, relative mass contribution of the UDC phase over the entire NEDC (UDC/NEDC ratio) for a selection of gaseous pollutants, for different temperatures and fuels. The UDC contribution to the total NEDC was higher for the CO and THC (e.g., CH_4, C_2H_4) in comparison with the nitrogen species. This tendency was slightly less pronounced for the Euro 5a Car 5, probably due to a more efficient aftertreatment system. Consequently, the emission of these gaseous pollutants over the UDC phase is indicated in Table 5.4. The emission factors for the 3 CADC phases together with the EUDC phase of the NEDC are available in the supplementary material (Tables 5.6, 5.7, 5.8 and 5.9).

Figure 5.3 shows the total emission for a selection of unregulated compounds (formaldehyde, acetaldehyde, ethanol, CH_4, NH_3, and C_7H_8) during the UDC, with both fuels and temperatures. On the one hand, the vehicles fuelled with high ethanol content

Car 4 Euro 4	UDC Emission factor (in mg km^{-1} except $^{\square}$ in g km^{-1})				
Temperature	**22°C**		**-7°C**		**Averaged ratio**
Fuel	E5	E85	E5	E75	**UDC/NEDC**
NO (nitric oxide)	52 (6)^a	36 (4)^a	83.7 (0.3)^b	48 (7)^b	**82%**
NO_2 (nitrogen dioxide)	0.085 (0.008)	0.04 (0.04)	0.10 (0.03)	12 (20)	**61%**
N_2O (nitrous oxide)	1.2 (0.3)	1.2 (0.6)	1.7 (0.4)	0.8 (0.9)	**100%**
NH_3 (ammonia)	11.1 (1.6)^b	3.6 (0.7)^b	141.2 (7.2)^a	66 (21)^a	**88%**
HCN (hydrogen cyanide)	0.05 (0.04)	0.009 (0.005)	1.8 (0.4)	1.3 (0.3)	**90%**
HCHO (formaldehyde)	1.1 (0.2)^a	3.4 (0.5)^a	2.09 (0.05)^a	6 (1)^a	**94%**
CH_3CHO (acetaldehyde)	4 (3)^b	28 (3)^b	17.0 (0.4)^b	178 (30)^b	**94%**
CH_3CH_2OH (ethanol)	14 (15)^a	111 (38)^a	43 (6)	2981 (1745)	**97%**
CH_4 (methane)	20 (5)	20.3 (0.9)	44 (1)^a	201 (66)^a	**99%**
C_2H_4 (ethylene)	15 (5)	14 (3)	48 (3)	158 (50)	**99%**
C_7H_8 (toluene)	39 (18)^a	3.9 (0.7)^a	263 (21)^b	73 (16)^b	**99%**
CO (carbon monoxide)$^{\triangle\square}$	1.8 (0.4)^c	0.34 (0.04)^c	8 (2)^c	15 (1)^c	**90%**
CO_2 (carbon dioxide)$^{\triangle\square}$	241 (2)^a	231 (7)^a	290 (8)	280 (2)	**52%**
NO_x (nitrogen Oxide)$^{\triangle}$	69 (18)	49 (7)	111 (24)	101 (7)	**86%**
THC (total hydrocarbons)$^{\triangle}$	195 (80)	179 (26)	637 (1)^c	891 (1)^c	**98%**
NMHC FID corrected$^{\circ}$	200 (87)	188 (42)	1215 (72)^b	5092 (944)^b	**99%**

Car 5 Euro 5a					
Temperature	**22°C**		**-7°C**		**Averaged ratio**
Fuel	E5	E85	E5	E75	**UDC/NEDC**
NO (nitric oxide)	23 (2)^b	15 (1)^b	35.68 (0.03)^b	20 (3)^b	**54%**
NO_2 (nitrogen dioxide)	1.1 (0.7)	1.5 (0.2)	0.6 (0.7)	0.9 (0.2)	**48%**
N_2O (nitrous oxide)	1.1 (0.2)^a	1.7 (0.5)^a	0.8 (0.7)	0.8 (0.2)	**60%**
NH_3 (ammonia)	15 (3)^a	7 (1)^a	61 (2)^b	33 (3)^b	**78%**
HCN (hydrogen cyanide)	1.2 (0.4)	0.8 (0.4)	5 (5)	2.2 (0.3)	**58%**
HCHO (formaldehyde)	1.7 (0.1)^b	3.0 (0.7)^b	1.5 (0.4)^b	5.2 (0.3)^b	**65%**
CH_3CHO (acetaldehyde)	6 (3)^b	29 (8)^b	19.6 (0.9)^b	199 (21)^b	**70%**
CH_3CH_2OH (ethanol)	30 (4)^c	86 (6)^c	32 (36)^c	1075 (73)^c	**70%**
CH_4 (methane)	12 (3)^b	29 (5)^b	81 (2)^c	285 (21)^c	**96%**
C_2H_4 (ethylene)	10 (2)^a	18 (5)^a	78 (2)^c	166 (6)^c	**93%**
C_7H_8 (toluene)	82 (22)	49 (35)	348 (5)^b	149 (29)^b	**71%**
CO (carbon monoxide)$^{\triangle\square}$	1.2 (0.5)	0.66 (0.07)	10 (2)	10.1 (0.9)	**95%**
CO_2 (carbon dioxide)$^{\triangle\square}$	250 (4)^b	237 (5)^b	272 (5)	269 (6)	**48%**
NO_x (nitrogen Oxide)$^{\triangle}$	32 (3)^c	19 (2)^c	64 (6)^c	32.2 (0.8)^c	**59%**
THC (total hydrocarbons)$^{\triangle}$	120 (23)	141 (27)	959 (3)^b	1471 (166)^b	**95%**
NMHC FID corrected$^{\circ}$	100 (20)	140 (30)	1361 (30)^c	2069 (79)^c	**95%**

Table 5.4: Regulated and unregulated emission factors for Car 4 and Car 5, over the UDC phase of the cold started NEDC, at 22°C with E5 and E85, and at -7°C with E5 and E75. The relative contribution of the mass of the UDC phase to the total NEDC mass (in %) is indicated in the right column. The standard deviations are in brackets and were calculated from 3 test repetitions for each mode (fuel and temperature). $^{\triangle}$ Bag measurements carried out according to Directive 70/220/EEC and its amendments (75). $^{\circ}$ Flame ionization detector response factor corrected (240). Statistically significant differences between fuels are indicated as follow: (a) P value < 0.05, (b) P value < 0.01, (c) P value < 0.001.

emitted significantly more formaldehyde and acetaldehyde whatever the temperature of the test was (Fig. 5.3-A and 5.3-B). Acetaldehyde is classified as probably carcinogenic whereas formaldehyde is classified as human carcinogen by the US Department of Health and Human Services (39). Formaldehyde increased with ethanol content with an average of 139% and 205% at 22°C and -7°C, respectively, whereas the acetaldehyde increased with an average of 521-932% at 22°C and -7°C, respectively. These percentages were lower than those reported in a previous publication (101), this might reflect to a certain extent the developments in aftertreatment technology. The results are in a good agreement with previous studies where a relationship between fuel composition and formaldehyde/acetaldehyde concentrations in air was established (42, 43, 101, 237, 244). Acetaldehyde emissions were enhanced at low temperature in comparison with formaldehyde, suggesting different formation mechanisms. Over the UDC, the acetaldehyde emission increased due to the low temperature by an average of +300%, whereas the averaged increase due the oxygenated fuel was roughly +500% in comparison with RFG. Nevertheless, the combined effect of the temperature and the fuel (from RFG at 22°C toward E75 at -7°C) resulted in an increase of +4000% of acetaldehyde emission, which was 5 times higher than algebraic sum of the individual fuel and temperature effects (+800%).

Figures 5.3-C and 5.3-D display the neat emission of ethanol and CH_4 over the UDC from the 2 flexi-fuel vehicles. The emissions of these two compounds were affected by the amount of ethanol in the fuels, which was more evident at low temperature. In both vehicles, unburned ethanol emission was more pronounced when high ethanol content was used at low temperature. The excess of unburned ethanol with this fuel was, on average, 2 times and 20 times higher at 22°C and -7°C, respectively. This finding at low temperature may be of concern for the European directive in force for THC regulation. The recommended method could underestimate by a factor of ca. 2 the oxygenated fraction (composed mainly by alcohol and carbonyls species) of the THC. The carbon contained in this oxygenated fraction accounted for 30% of the carbon contained in THC, and up to 4% of the total carbon (from THC, CO and CO_2) instantaneously released by the Car 5 during the first seconds of the cycle (i.e., before the catalyst light-off). Moreover, this unburned ethanol could have an environmental impact by forming acetaldehyde through chemical transformation. This contribution might increase even more the atmospheric acetaldehyde concentration in addition to the direct emission

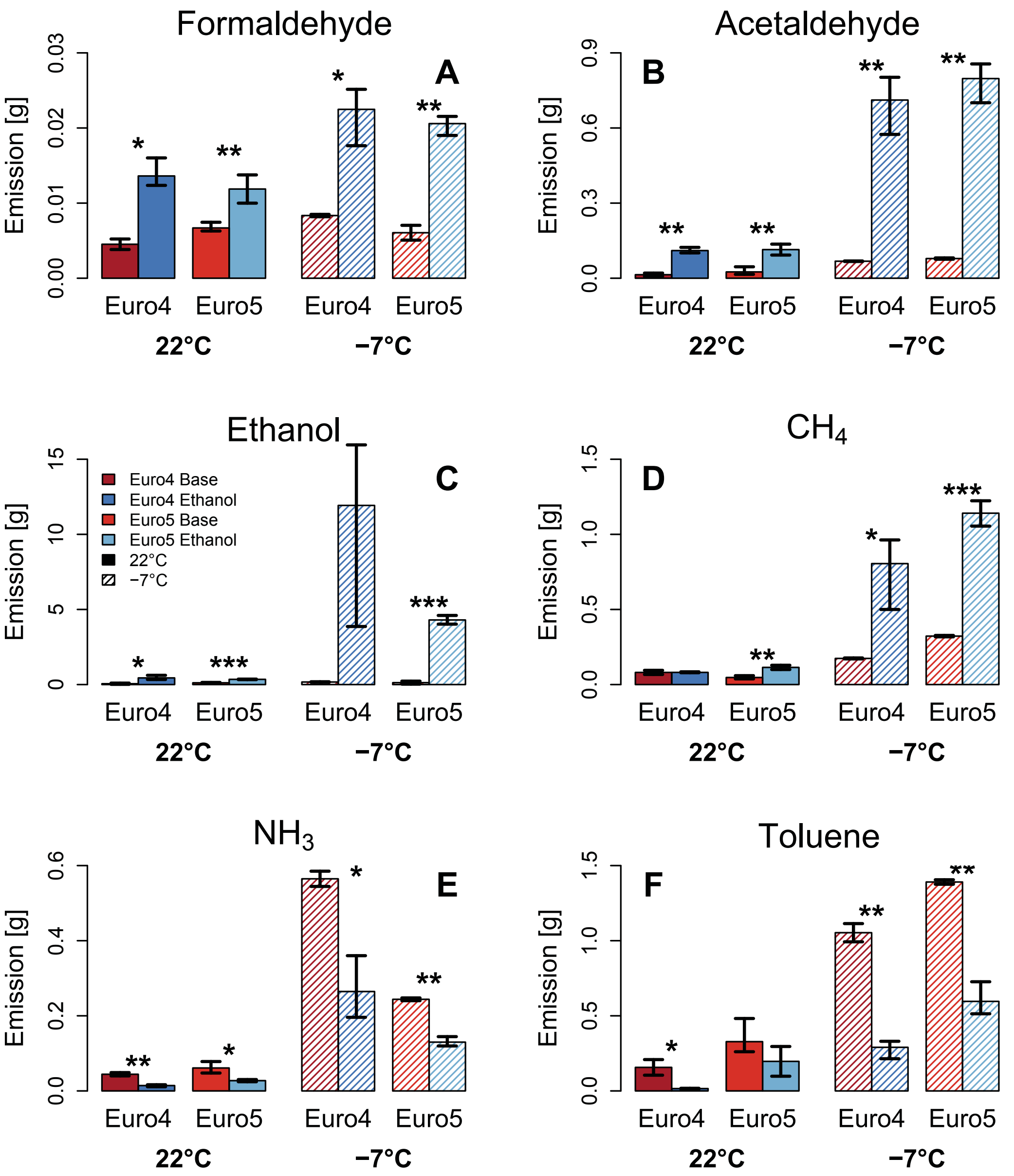

Figure 5.3: Selection of unregulated emissions of Car 4 and Car 5 at 22°C and -7°C over the urban phase (UDC) of the NEDC. - Selection of unregulated emissions of Car 4 and Car 5 at 22°C and -7°C over the urban phase (UDC) of the NEDC. The confidence interval is the maximum and minimum values obtained with a 3 test repetitions. Statistically significant differences are indicated as follow: (*) P value $<$ 0.05, (**) P value $<$ 0.01, (***) P value $<$ 0.001.

discussed before. Furthermore, the CH_4 emissions were approximately 3 times higher at -7°C when E75 was used (Fig. 5.3-D). More CH_4 with E85 at 22°C was observed in a previous study (+63%) on relatively older flexi-fuel vehicles (Tier 0 US standard) (245). Here, considering the global warming potential of CH_4 (25 eq g CO_2 over 100 years), such a larger emission with E75 attenuated, or even cancelled the substantial CO_2 reduction observed over the UDC at -7°C. Nevertheless, since the CO_2 is emitted constantly over the complete cycle, this surplus of CH_4 may hardly compensate the benefit of ethanol fuel on lowering CO_2 emission over the total vehicle lifetime. CH_4 is known to be particularly resistant to catalytic oxidation, and consequently, associated with the cold start of the vehicle (236). Generally, the exhaust from engines operating with high ethanol content fuels contains more water, which can disturb the catalytic reaction by condensing onto the catalyst surface (246). This mechanism is expected to be more pronounced in the case of CH_4, considering its low solubility in water (much more hydrophobic than carbonyls, or short chain fraction of THC).

On the other hand, the vehicles fuelled with high ethanol content had lower emissions of C_7H_8 and NH_3 (both toxic compounds), whatever the temperature of the test (Fig. 5.3-E and 5.3-F). The differences in C_7H_8 emission were most likely due to the lower concentration of C_7H_8, as well as C_7H_8 precursors, in the high ethanol content fuel (93, 247). Concerning the NH_3, on average, the high concentration of ethanol in the fuel led to decreased emission by 62% at 22°C, and 50% at -7°C, in comparison with RFG. The NH_3 emission factors reported here are lower than in other studies (64, 66, 157). This difference might be explained by the less aggressive driving cycle (NEDC) and the recent vehicles in the present study. This assumption was confirmed by lower NH_3 emissions of the Euro 5a Car 5 at -7°C in comparison with the Euro 4 Car 4.

5.1.3.3 NH_3 formation description

Traffic-related NH_3 is mainly produced in the Three-Way-Catalyst (TWC) of gasoline light-duty vehicles. The formation mechanism involves NO and H_2. NO is generated by the oxidation of N_2 during combustion. H_2 is mainly produced in the catalyst during the water gas shift reaction of CO (60, 61). Accordingly, NH_3 formation in the catalyst is enhanced at rich conditions (low air/fuel ratios) where higher CO concentrations can produce more H_2 (62, 63).

Figure 5.4 illustrates the time-resolved concentration of NH_3, together with the established precursor molecules NO and CO, in the exhaust of the Euro5a flexi-fuel vehicle for both fuels and temperatures. The air/fuel ratio (lambda factor) is plotted in the upper graphic, together with the time-resolved concentration of NH_3. At 22°C, the concentrations of CO and NO were lower with E85. This effect, already observed in a test bench study of a direct-injection engine (93), could explain the lower NH_3 yield with the oxygenated fuel. This assumption is consistent with a previous vehicle chassis dynamometer study carried out at 22°C in which NH_3 and CO emissions factors were correlated (66). The two vertical dashed lines indicate the time of the first observable NH_3 increases (t_1) and decreases (t_2) in each of the 4 modalities (categorized by different temperatures and fuels). The NH_3 increase appeared together with the decrease of NO. The type of fuel had almost no effect on t_1, whereas temperature generated a moderate increase of t_1 of 30 s at -7°C. The NH_3 decrease appeared together with the decrease of CO. The type of fuel had a significant effect on t_2, particularly at low temperature. Indeed, at -7°C the CO concentration appeared to drop earlier when oxygenated fuel was used (with a difference of up to 120 s). The plotted lambda factor confirms these assumptions since before the catalyst light-off, the air/fuel mixture was slightly richer (lambda < 1) in order to allow good drivability. This fuel enrichment was maintained longer at -7°C when RFG was used. Consequently, the leaner conditions (higher air/fuel ratio) during the cold start of Car 4 and Car 5 fuelled with ethanol fuel (E75/E85) might explain the difference of NH_3. Since NH_3 is not a regulated pollutant, the lambda control depends on the strategy of each car manufacturer as long as the emissions comply with the NO_x standards (NO-NH_3 trade-off) (59). Nevertheless, in the case of the studied flexi-fuel vehicles both NO_x and NH_3 were lowered when ethanol fuel was used at both temperatures. Moreover, in contrast to CH_4 discussed before, the condensed water particularly present with the oxygenated fuel at the beginning of the cycle might play a role. The layer of water on the catalyst may locally disturb the water gas shift reaction and consequently limit the H_2 required for the NH_3 formation. In addition, the condensed water may absorb the catalytic formed NH_3 (which is highly hygroscopic). Therefore, it could contribute to lowering the NH_3 emission when high ethanol contents fuels were used.

Nevertheless, as described elsewhere (59), NH_3 emission did not completely disappear after the first peak (after catalyst light-off). The emission continued to a lower

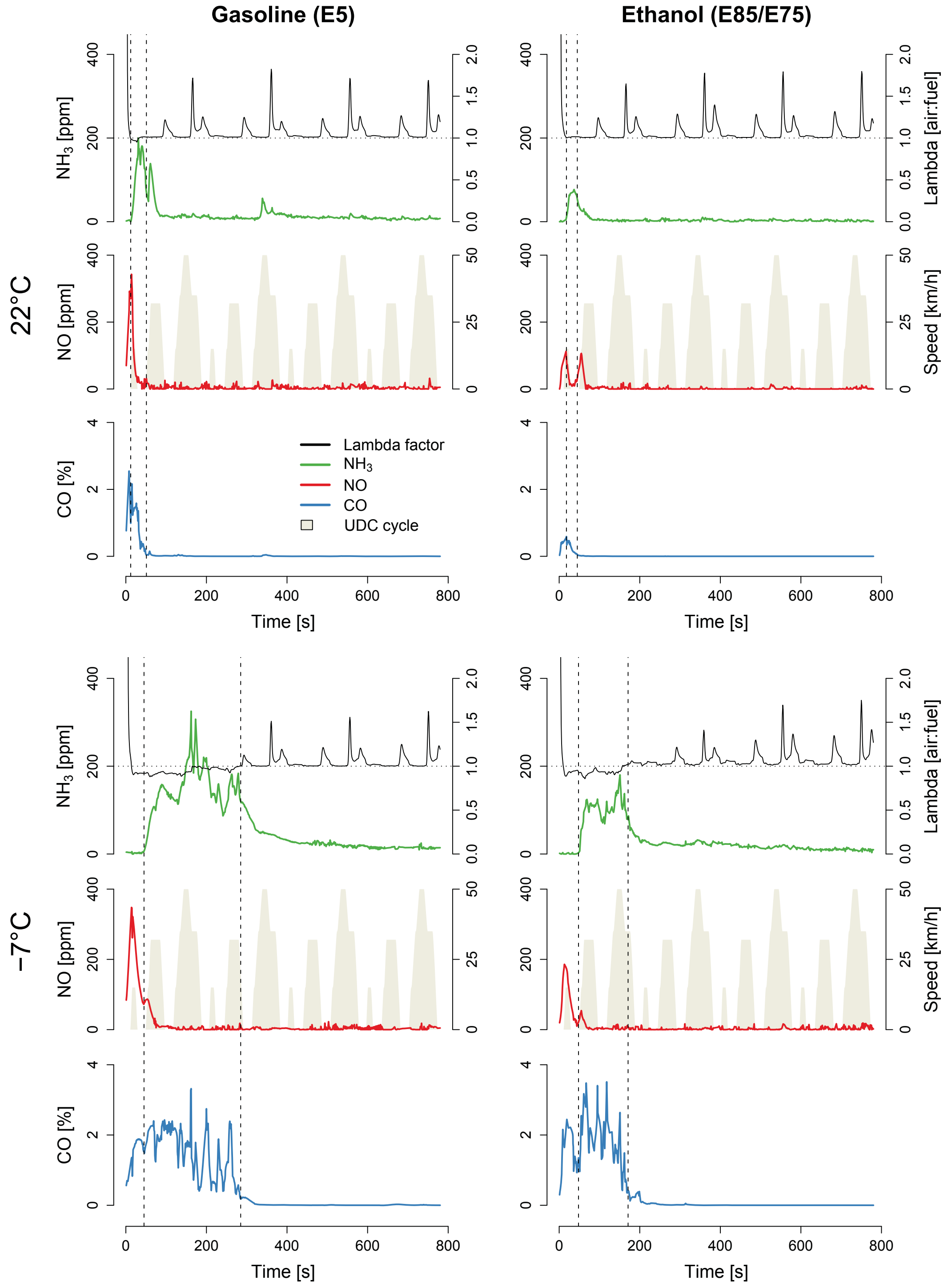

Figure 5.4: Time-resolved concentrations of NH_3, NO and CO in the exhaust of the Car 5 Euro 5a under the UDC phase of the NEDC. - Time-resolved concentrations of NH_3, NO and CO in the exhaust of the Car 5 Euro 5a under the UDC phase of the NEDC with reference fuel E5 (left side), and E85/E75 (right side). Tests carried out at 22°C and -7°C display in the upper and lower part respectively.

degree, producing a smaller contribution than the first emission peak, in particular at low temperature. The average UDC/NEDC ratios of NH_3 for the two flexi-fuel vehicles were 76% and 90% at 22°C and -7°C, respectively.

5.1.3.4 Cold start excess emission determination

The CSEE of most pollutants was quantified for the two flexi-fuel vehicles (Car 4 and Car 5) for both fuels and temperatures. Mass and duration of the CSEE are summarized in Table 5.5. The obtained $CSEE_m$ for each pollutant accounted for, on average, more than 85% of their respective UDC emissions factors (Table 5.4). Consequently, the emission factors integrated over the UDC phase of the NEDC could be a reliable indicator of the $CSEE_m$. Only the NO values were lower ($CSEE_m$/UDC average ratio of 70%). This finding for NO, together with the averaged UDC/NEDC ratios reported in Table 5.4 may indicate that the contribution of NO_x excess emissions is lower than for the other pollutants such as CO or THC. As observed in another study with less modern gasoline vehicles, the ambient temperature had a poor effect on the NO_x $CSEE_m$ (248). The authors also showed that the NO_x $CSEE_m$ decreased with vehicle emission standards evolution, which could be caused by (i) richer stoichiometric conditions at the start of the cycle, or (ii) a more efficient aftertreatment system. In fact, the implementation of the Euro5a regulation implicated a neat reduction of 25% of NO_x, by shifting the emission standard from 80 to 60 mg km^{-1}.

Car 4 Euro 4	**Cold Start Excess Emission mass (in mg) and duration (in s)**							
Temperature	**22°C**				**-7°C**			
Fuel	E5		E85		E5		E75	
	CSEE$_t$ [s]	CSEE$_m$ [mg]	CSEE$_t$ [s]	CSEE$_m$ [mg]	CSEE$_t$ [s]	CSEE$_m$ [mg]	CSEE$_t$ [s]	CSEE$_m$ [mg]
NO	135 (21)	321 (29)	110 (19)	135 (18)	136 (6)	20 (0)	nd	nd
N_2O	5 (1)	126 (1)	5 (3)	78 (2)	7 (2)	142 (2)	3 (4)	198 (53)
HCHO	3.9 (0.7)	262 (20)	11 (2)	147 (4)	7.8 (0.4)	523 (21)	15 (5)	329 (50)
CH_3CHO	11 (8)	83 (18)	106 (5)	34 (4)	67 (2)	131 (2)	720 (124)	139 (1)
CH_3CH_2OH	51 (52)	90 (56)	433 (128)	65 (4)	168 (16)	161 (16)	11939 (7012)	189 (44)
C_2H_4	60 (20)	52 (2)	54 (11)	29 (4)	193 (11)	128 (1)	632 (203)	135 (2)
C_7H_8	159 (75)	52 (2)	16 (3)	40 (9)	1072 (91)	130 (1)	290 (66)	115 (35)
THC	801 (318)	67 (9)	661 (137)	102 (20)	4680 (270)	134 (1)	17958 (2582)	143 (4)
CO	6131 (1629)	184 (16)	864 (94)	61 (4)	29168 (1637)	138 (1)	58737 (5784)	143 (5)
CH_4	73 (16)	162 (47)	73 (5)	140 (3)	168 (2)	145 (0)	834 (294)	146 (2)
NH_3	nd	nd	nd	nd	503 (23)	322 (5)	213 (74)	332 (14)

Car 5 Euro 5a								
Temperature	**22°C**				**-7°C**			
Fuel	E5		E85		E5		E75	
	CSEE$_t$ [s]	CSEE$_m$ [mg]	CSEE$_t$ [s]	CSEE$_m$ [mg]	CSEE$_t$ [s]	CSEE$_m$ [mg]	CSEE$_t$ [s]	CSEE$_m$ [mg]
NO	77 (9)	59 (5)	43 (10)	61 (4)	124 (6)	70 (2)	58 (15)	61 (5)
N_2O	3.2 (0.3)	74 (22)	4.5 (0.5)	61 (3)	2 (2)	194 (1)	nd	nd
HCHO	nd	nd	nd	nd	nd	nd	nd	nd
CH_3CHO	nd	nd	58 (15)	45 (12)	52 (7)	145 (11)	773 (88)	149 (2)
CH_3CH_2OH	nd	nd	215 (21)	64 (3)	nd	nd	3703 (198)	269 (10)
C_2H_4	35 (9)	51 (7)	59 (16)	45 (5)	306 (6)	187 (37)	664 (23)	147 (7)
C_7H_8	nd	nd	nd	nd	1123 (11)	218 (58)	179 (311)	306 (6)
THC	375 (77)	59 (1)	481 (86)	79 (17)	5339 (126)	260 (2)	7707 (256)	172 (5)
CO	3865 (1134)	52 (3)	1927 (282)	56 (6)	39276 (635)	261 (2)	37535 (3503)	157 (3)
CH_4	45 (10)	62 (3)	103 (11)	95 (31)	326 (4)	268 (4)	1150 (85)	167 (3)
NH_3	38 (7)	80 (4)	17 (2)	96 (42)	199 (11)	361 (5)	101 (8)	408 (40)

Table 5.5: Cold Start Excess Emission mass and duration (CSEE$_m$ and CSEE$_t$ respectively) determined for several regulated and unregulated pollutants for Car 4 and Car 5, over the UDC phase of the cold started NEDC, at 22°C with E5 and E85, and at -7°C with E5 and E75. The standard deviations are in brackets and were calculated from 3 test repetitions for each mode (fuel and temperature). ŞndŤ was indicated when no CSEE was determined by the applied methodology.

Figure 5.5 depicts the output from a multivariate analysis approach to the CSEEm. The two first PCs explained 76% of the total variance. The loading plot highlights the contribution of the variables to the PCs. PC1 (53% of explained variance) originated mainly from a group including 6 variables namely acetaldehyde (CH_3CHO), CH_4, ethanol (CH_3CH_2OH), C_2H_4, THC, and CO $CSEE_m$, whereas PC2 (23%) originated from a second group including C_7H_8 and NH_3 $CSEE_m$. The projection of the tests in the sub-space created by the PCA model is displayed in the score plot. Tests carried out at 22°C clustered in the upper left of the graph for both fuels, demonstrating the relatively low $CSEE_m$ differences between these tests at 22°C in comparison with the differences between the tests at -7°C. PC1 separated well the tests with high ethanol content fuel at -7°C from those at 22°C. PC2 was mostly associated with tests carried out with RFG at -7°C. The tests at -7°C had a significant influence on the $CSEE_m$. On the one hand, the use of RFG was clearly distinguished by higher C_7H_8 and NH_3 $CSEE_m$. On the other hand, the use of high ethanol content fuels was associated with higher short hydrocarbons, CO and oxygenated compounds $CSEE_m$.

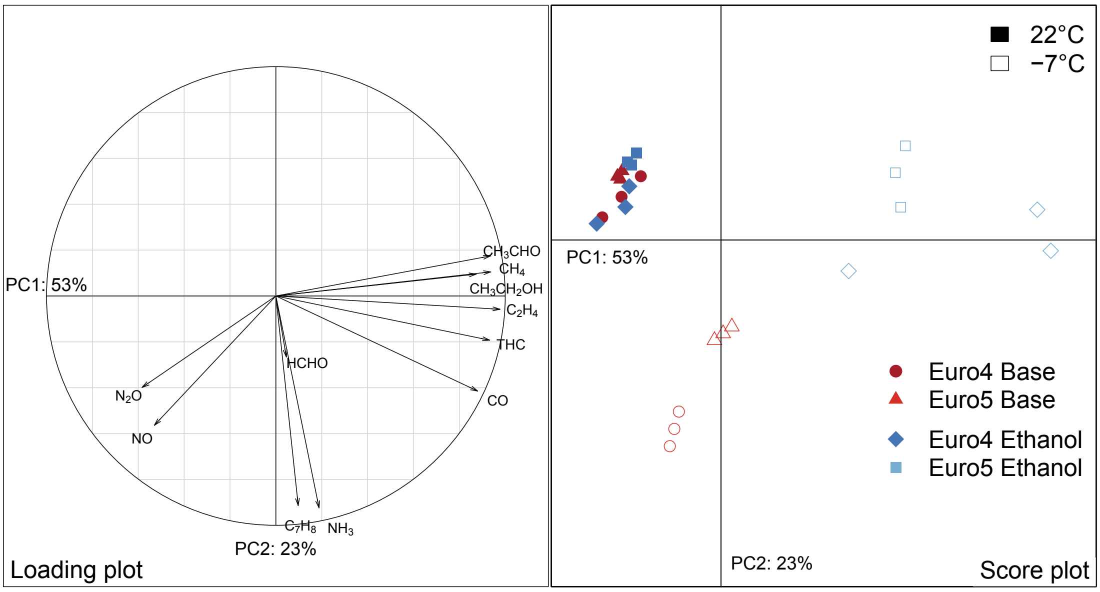

Figure 5.5: PCA of $CSEE_m$ over the UDC phase of the NEDC for Car 4 and Car 5 at 22°C and -7°C. - PCA of $CSEE_m$ over the UDC phase of the NEDC for Car 4 and Car 5 at 22°C and -7°C. The loading plot (left side) displays the contribution of the variables in the PCA model. The samples are projected in the score plot (right side).

Concerning $CSEE_t$, CH_4, ethanol and NH_3 were emitted for the longest time. Some hydrocarbons such as C_2H_4 and C_7H_8 were emitted over a relatively short period. This behavior was particularly noticeable at -7°C and the resistance of the pollutants against catalytic oxidation might be a reason for this. The catalyst light-off temperature might differ for each compounds and previous studies emphasized the resistance of oxygenated compounds and CH_4 to TWC oxidation in comparison with shorter hydrocarbons and aromatic compounds (236, 249). Consequently, this behavior is more significant at low temperature because of the extended rich engine conditions and delayed light-off of the catalyst.

5.1.3.5 Ozone formation potential

The determined OFPs of the 5 vehicles over the NEDC at 22°C are presented in Fig. 5.6-A. The OFPs were not significantly influenced by the fuel type. On average, the test fleet generated 0.15 g O_3 km^{-1}. These results were slightly higher than OFP from other Euro4 gasoline vehicles studied under similar conditions (driving cycle and temperature) (250). The contribution of carbonyls to the total OFP shifted from 6% with RFG to 34% with E85. Although the CADC is a more aggressive driving cycle, the OFP values were found 3 times lower at 22°C in comparison with the NEDC (average of 0.05 g O_3 km^{-1}; Fig. 5.6-B). Reasons for this are the longer duration of the CADC as well as the prior conditioning. Consequently, the early emitted short chain fraction (C_2) of VOCs decreased from 48% over the cold started NEDC to 19% over the CADC. In addition, CO increased from 14% to 50% of the total emitted OFP.

Concerning the effect of the fuel, a discrepancy was found between the two studied flexi-fuel vehicles. Car 4 emitted more O_3 precursors when high blended ethanol fuel was used (P value < 0.05 at -7°C). In contrast, the more recent DI Car 5 exhibited significantly higher O_3 precursor emission with the RFG, for both ambient temperatures (P value < 0.001 and 0.01 at 22°C and -7°C, respectively). In addition, over the CADC, Car 5 behaved almost identically in terms of OFP for both temperatures, which suggests that the pre-conditioning had different influences on the two vehicle engines. Finally, Fig. 5.6-C presents the results of the cold-started NEDC from the flexi-fuel vehicles at both temperatures. In this case, the cold temperature had a significant influence on the O_3 precursors emitted by both vehicles. The averaged factor was 5 with RFG and 10 with high-ethanol blend fuel. Consequently, the OFP from oxygenated fuel was 2 times higher, with an average of 1.5 g O_3 km^{-1} in comparison with 0.67 g O_3 km^{-1} with RFG.

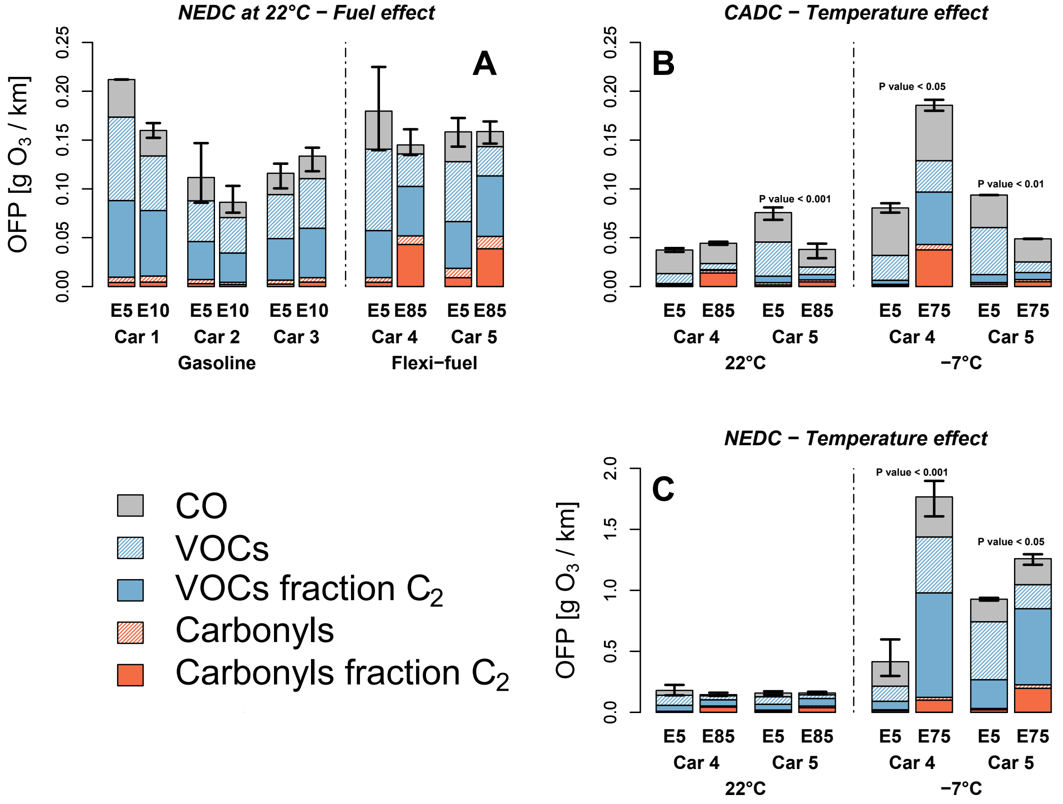

Figure 5.6: Ozone formation potential determined for RFG and oxygenated fuel at 22°C and -7°C. - Ozone formation potential determined for RFG and oxygenated fuel from (A) the 5 vehicles at 22°C under the cold started NEDC, (B) Car 4 and Car 5 at 22°C and -7°C over the CADC, and (C) Car 4 and Car 5 at 22°C and -7°C over the cold started NEDC. The confidence interval is the maximum and minimum values obtained with a 3 test repetitions.

This difference led us to conclude that using high ethanol blended fuel in cold condition might have an impact on human health. Even though the conditions to form ozone at low temperature are not optimal, tropospheric ozone is the second dominating global warming agent (after CO_2) from road transport (25). Finally, as seen in a different study (250), the first minutes of the test are crucial for the determination of OFP especially when low temperature conditions are studied (248). Consequently, the pre-conditioning makes the CADC unsuitable for OFP assessment. In conclusion, the light-off of the catalyst or the engine lambda strategy may reduce or cancel the environmental benefits of alternative fuels such as ethanol. As a consequence, more focus should be placed on the reduction and control of cold start emissions by means of dedicated technology such as engine block heaters or dual-injection strategy (251). This would enhance the positive aspects of ethanol-blended fuels.

5.1.4 Conclusions

Fuels used in on-road transport are constantly evolving, because of industrial, economic, scientific and geopolitical reasons. Promoting alternative fuels should come along with an assessment of their impact on (direct) tailpipe emissions. This chassis dynamometer study aimed to evaluate with online and offline techniques the effects of cold ambient temperature on the primary regulated and unregulated gaseous emission of several conventional and flexi-fuel vehicles. Whereas the investigated vehicles with high ethanol fuel contents emitted significantly less CO_2; the opposite occurred at -7°C with CO and THC. In addition, this study highlighted the future technical challenges in order to determine accurately THC when oxygenated fuels are used, in particular at low temperatures. Concerning the unregulated gaseous pollutant, the combination of ethanol fuel and cold temperature seemed to particularly increase the emission of health-related acetaldehyde and CH_4. The latter, which has a strong global warming potential, could lower the beneficial effects of ethanol fuel on the direct CO_2 emission of the vehicle during the cold start of the vehicle. However, a beneficial effect of ethanol fuel was the decrease of toluene and NH_3 emissions. The cold start excess emissions were found crucial to assess the OFP of the different fuel exhausts. At -7°C, the OFPs of the vehicles fuelled with high ethanol content fuel were found systematically higher when the engine was cold at the beginning of the driving cycle. Implementation and adjustment of newer technical devices such as aftertreatment systems and block-heaters are necessary in order to adapt vehicles to alternative fuel characteristics. These first results show the need to further investigate the emissions from vehicles using alternative fuels.

- **Acknowledgments**

The VELA staff is acknowledged for his skilful technical assistance, in particular R. Colombo, M. Sculati, G. Lanappe, F. Muehlberger, and P. Le Lijour. The authors wish to thank Dr. Mamakos for reading the manuscript and providing constructive comments. Furthermore, we are grateful to Dr. Dardiotis and Dr. Fontaras for their assistance in the data processing, and to A. Marotta for his valuable support and contribution to this project.

5.1.5 Supplementary Materials

Car 4 Euro 4	**EUDC Emission factor (in mg km^{-1} except $^{\square}$ in g km^{-1})**				
Temperature	**22°C**		**-7°C**		**Averaged ratio**
Fuel	E5	E85	E5	E75	**EUDC/NEDC**
NO (nitric oxide)	2.9 (0.1)^a	5.1 (0.6)^a	11 (2)	10 (4)	**8%**
NO_2 (nitrogen dioxide)	0.04 (0.02)	0.010 (0.008)	0.028 (0.006)	7 (12)	**39%**
N_2O (nitrous oxide)	nd	nd	0.0002 (0.0003)	nd	**0%**
NH_3 (ammonia)	1.4 (0.1)^b	0.5 (0.1)^a	2.07 (0.08)	2.3 (0.5)	**12%**
HCN (hydrogen cyanide)	0.005 (0.005)	0.002 (0.001)	0.0006 (0.0007)^a	0.0022 (0.0002)^a	**10%**
HCHO (formaldehyde)	0.05 (0.04)	0.032 (0.006)	0.11 (0.04)	0.3 (0.1)	**6%**
CH_3CHO (acetaldehyde)	0.4 (0.2)	1 (1)	0.14 (0.04)	0.3 (0.4)	**6%**
CH_3CH_2OH (ethanol)	0.6 (0.8)	3 (5)	0.2 (0.3)	nd	**3%**
CH_4 (methane)	0.03 (0.02)^a	0.4 (0.1)^a	0.11 (0.02)	0.09 (0.04)	**1%**
C_2H_4 (ethylene)	0.09 (0.08)	0.19 (0.08)	0.035 (0.002)	0.3 (0.4)	**1%**
C_7H_8 (toluene)	0.137 (0.006)^b	0.080 (0.007)^b	0.12 (0.07)	0.2 (0.4)	**1%**
CO (carbon monoxide)$^{\triangle\square}$	0.134 (0.003)^c	0.059 (0.002)^c	0.18 (0.01)^a	0.14 (0.02)^a	**10%**
CO_2 (carbon dioxide)$^{\triangle\square}$	134 (1)^c	125.8 (0.5)^c	153.1 (0.7)^c	148.4 (0.7)^c	**48%**
NO_x (nitrogen Oxide)$^{\triangle}$	3 (3)	5 (1)	11 (3)	15 (4)	**14%**
THC (total hydrocarbons)$^{\triangle}$	0.9 (0.4)^b	1.9 (0.3)^b	1.9 (0.6)^b	28 (9)^b	**2%**

Car 5 Euro 5a					
Temperature	**22°C**		**-7°C**		**Averaged ratio**
Fuel	E5	E85	E5	E75	**EUDC/NEDC**
NO (nitric oxide)	18 (7)	5 (2)	20 (2)^a	9 (3)^a	**46%**
NO_2 (nitrogen dioxide)	0.9 (0.8)	0.53 (0.07)	0.4 (0.6)	0.74 (0.03)	**52%**
N_2O (nitrous oxide)	0.4 (0.2)	0.3 (0.2)	0.7 (0.7)	0.33 (0.09)	**40%**
NH_3 (ammonia)	3.3 (0.9)	1.7 (0.6)	4 (1)	4.92 (0.05)	**22%**
HCN (hydrogen cyanide)	0.6 (0.3)	0.4 (0.2)	3 (3)	0.6 (0.2)	**42%**
HCHO (formaldehyde)	0.8 (0.2)	0.62 (0.02)	0.6 (0.3)	1.1 (0.3)	**35%**
CH_3CHO (acetaldehyde)	4 (1)^a	8 (3)^a	5 (0.8)	7 (2)	**30%**
CH_3CH_2OH (ethanol)	19 (8)	14 (7)	16 (17)	42 (5)	**30%**
CH_4 (methane)	0.7 (0.3)	1.0 (0.4)	0.6 (0.8)	1.3 (0.2)	**4%**
C_2H_4 (ethylene)	1.2 (0.3)	1.0 (0.2)	1.2 (0.6)	1.3 (0.3)	**7%**
C_7H_8 (toluene)	32 (9)^a	11 (7)^a	43 (12)	39 (3)	**29%**
CO (carbon monoxide)$^{\triangle\square}$	0.04 (0.01)	0.04 (0.01)	0.08 (0.04)	0.05 (0.02)	**5%**
CO_2 (carbon dioxide)$^{\triangle\square}$	157 (1)^c	148.8 (0.5)^c	178.5 (0.5)^c	171 (2)^c	**52%**
NO_x (nitrogen Oxide)$^{\triangle}$	23 (8)	6 (1)	23 (5)^a	10 (3)^a	**41%**
THC (total hydrocarbons)$^{\triangle}$	6 (2)	4.6 (0.3)	11 (1)^b	21 (4)^b	**5%**

Table 5.6: Regulated and unregulated emission factors for Car 4 and Car 5, over the EUDC phase of the cold started NEDC, at 22°C with E5 and E85, and at -7°C with E5 and E75. The relative contribution of the mass of the UDC phase to the total NEDC mass (in %) is indicated in the right column. The standard deviations are in brackets and were calculated from 3 test repetitions for each mode (fuel and temperature). $^{\triangle}$ Bag measurements carried out according to Directive 70/220/EEC and its amendments (75). Statistically significant differences between fuels are indicated as follow: (a) P value $<$ 0.05, (b) P value $<$ 0.01, (c) P value $<$ 0.001. nd : not detectable.

Car 4 Euro 4	**CADC Urban phase emission factor (in mg km^{-1} except $^{\square}$ in g km^{-1})**				
Temperature	**22°C**		**-7°C**		**Averaged ratio**
Fuel	E5	E85	E5	E75	**phase/CADC**
NO (nitric oxide)	N/A	48 (1)	N/A	100 (2)	**30%**
NO_2 (nitrogen dioxide)	N/A	0.14 (0.2)	N/A	0.23 (0.2)	**52%**
N_2O (nitrous oxide)	N/A	0.20 (0.07)	N/A	0.3 (0.1)	**82%**
NH_3 (ammonia)	N/A	10 (3)	N/A	73 (3)	**64%**
HCN (hydrogen cyanide)	N/A	0.016 (0.008)	N/A	1.1 (0.2)	**92%**
HCHO (formaldehyde)	N/A	1.2 (0.4)	N/A	4.3 (0.4)	**85%**
CH_3CHO (acetaldehyde)	N/A	3 (4)	N/A	66 (11)	**73%**
CH_3CH_2OH (ethanol)	N/A	3 (2)	N/A	1923 (200)	**100%**
CH_4 (methane)	N/A	9.0 (0.6)	N/A	88 (2)	**94%**
C_2H_4 (ethylene)	N/A	0.7 (0.2)	N/A	27 (3)	**90%**
C_7H_8 (toluene)	N/A	0.005 (0.005)	N/A	5.6 (0.5)	**88%**
CO (carbon monoxide)$^{\triangle\square}$	0.48 (0.07)	0.34 (0.04)	2.5 (0.4)^{a}	5.9 (0.8)^{a}	**26%**
CO_2 (carbon dioxide)$^{\triangle\square}$	285.2 (0.7)	273 (10)	320 (3)	326.8 (0.3)	**17%**
NO_x (nitrogen Oxide)$^{\triangle}$	133 (26)	81.3 (0.2)	279 (65)	217 (18)	**48%**
THC (total hydrocarbons)$^{\triangle}$	7.7 (0.8)	32 (13)	92.0 (0.2)^{c}	967 (2)^{c}	**62%**

Car 5 Euro 5a					
Temperature	**22°C**		**-7°C**		**Averaged ratio**
Fuel	E5	E85	E5	E75	**phase/CADC**
NO (nitric oxide)	11 (2)	10 (8)	36 (3)	23 (10)	**8%**
NO_2 (nitrogen dioxide)	2 (2)	1.0 (0.1)	2 (2)	1.38 (0.08)	**13%**
N_2O (nitrous oxide)	0.5 (0.4)	0.4 (0.3)	0.87 (0.04)	0.9 (0.3)	**10%**
NH_3 (ammonia)	7 (2)	7 (2)	1 (2)	5 (2)	**7%**
HCN (hydrogen cyanide)	1.0 (0.4)	1.0 (0.4)	2.78 (0.06)^{a}	1.5 (0.3)^{a}	**11%**
HCHO (formaldehyde)	1.3 (0.6)	1.2 (0.3)	1.2 (0.6)	1.6 (0.2)	**12%**
CH_3CHO (acetaldehyde)	10 (7)	5.5 (0.7)	12 (5)	9 (3)	**10%**
CH_3CH_2OH (ethanol)	44 (11)	33 (15)	35 (13)	62 (12)	**14%**
CH_4 (methane)	1.4 (0.7)^{a}	4 (2)^{a}	1.6 (0.8)	6 (3)	**9%**
C_2H_4 (ethylene)	2.3 (0.2)	2.0 (0.4)	2.2 (0.7)	2.0 (0.2)	**10%**
C_7H_8 (toluene)	75 (24)	49 (43)	221 (107)	77 (7)	**16%**
CO (carbon monoxide)$^{\triangle\square}$	0.22 (0.04)^{b}	0.11 (0.02)^{b}	0.2 (0.2)	0.119 (0.005)	**4%**
CO_2 (carbon dioxide)$^{\triangle\square}$	288 (2)^{a}	268 (7)^{a}	287 (18)	291 (14)	**14%**
NO_x (nitrogen Oxide)$^{\triangle}$	13 (4)	13 (8)	43 (10)	30 (12)	**6%**
THC (total hydrocarbons)$^{\triangle}$	10 (4)	9 (3)	11.7 (0.6)^{a}	17 (2)^{a}	**6%**

Table 5.7: Regulated and unregulated emission factors for Car 4 and Car 5, over the Urban phase of the CADC, at 22°C with E5 and E85, and at -7°C with E5 and E75. The relative contribution of the mass of the Urban phase to the total CADC mass (in %) is indicated in the right column. The standard deviations are in brackets and were calculated from 3 test repetitions for each mode (fuel and temperature). $^{\triangle}$ Bag measurements carried out according to Directive 70/220/EEC and its amendments (75). Statistically significant differences between fuels are indicated as follow: (a) P value < 0.05, (b) P value < 0.01, (c) P value < 0.001. N/A : not available.

Car 4 Euro 4	**CADC Rural phase emission factor (in mg km^{-1} except $^{\square}$ in g km^{-1})**				
Temperature	**22°C**		**-7°C**		**Averaged ratio**
Fuel	E5	E85	E5	E75	**phase/CADC**
NO (nitric oxide)	N/A	22 (6)	N/A	23 (9)	**31%**
NO_2 (nitrogen dioxide)	N/A	0.020 (0.008)	N/A	0.023 (0.009)	**22%**
N_2O (nitrous oxide)	N/A	0.03 (0.02)	N/A	0.0007 (0.0009)	**16%**
NH_3 (ammonia)	N/A	1.3 (0.2)	N/A	1.5 (0.3)	**8%**
HCN (hydrogen cyanide)	N/A	0.007 (0.003)	N/A	0.0010 (0.0007)	**2%**
HCHO (formaldehyde)	N/A	0.014 (0.006)	N/A	0.08 (0.04)	**5%**
CH_3CHO (acetaldehyde)	N/A	2 (2)	N/A	0.97 (0.04)	**9%**
CH_3CH_2OH (ethanol)	N/A	nd	N/A	nd	**0%**
CH_4 (methane)	N/A	0.41 (0.03)	N/A	0.11 (0.03)	**2%**
C_2H_4 (ethylene)	N/A	0.2 (0.1)	N/A	0.031 (0.002)	**3%**
C_7H_8 (toluene)	N/A	0.06 (0.03)	N/A	0.064 (0.009)	**7%**
CO (carbon monoxide)$^{\triangle\square}$	0.366 (0.005)^c	0.151 (0.005)^c	0.375 (0.001)^a	0.25 (0.04)^a	**17%**
CO_2 (carbon dioxide)$^{\triangle\square}$	158 (1)^c	128.4 (0.6)^c	150 (2)^a	145.1 (0.7)^a	**28%**
NO_x (nitrogen Oxide)$^{\triangle}$	9.4 (0.6)	32 (9)	28 (18)	37 (16)	**24%**
THC (total hydrocarbons)$^{\triangle}$	1.1 (0.4)	2.4 (0.5)	1.2 (0.3)^a	17 (3)^a	**9%**

Car 5 Euro 5a					
Temperature	**22°C**		**-7°C**		**Averaged ratio**
Fuel	E5	E85	E5	E75	**phase/CADC**
NO (nitric oxide)	12 (2)^b	5 (2)^b	12 (3)	7 (1)	**13%**
NO_2 (nitrogen dioxide)	1 (2)	0.4 (0.2)	1 (1)	0.7 (0.2)	**25%**
N_2O (nitrous oxide)	0.5 (0.2)	0.24 (0.05)	0.2 (0.2)	0.43 (0.06)	**19%**
NH_3 (ammonia)	7 (3)	10 (2)	2.3 (0.9)^a	9 (2)^a	**36%**
HCN (hydrogen cyanide)	0.9 (0.2)^b	0.3 (0.1)^b	1.5 (0.7)	0.9 (0.2)	**24%**
HCHO (formaldehyde)	1.0 (0.1)^b	0.5 (0.2)^b	0.53 (0.05)^b	0.96 (0.03)^b	**24%**
CH_3CHO (acetaldehyde)	6 (3)	8 (4)	6 (5)	5.3 (0.1)	**24%**
CH_3CH_2OH (ethanol)	21 (10)	21 (12)	10 (2)	30 (10)	**24%**
CH_4 (methane)	1.3 (0.3)	1.7 (0.5)	0.7 (0.4)^a	1.9 (0.1)^a	**14%**
C_2H_4 (ethylene)	1.6 (0.4)^a	0.9 (0.2)^a	1.4 (0.6)	1.51 (0.06)	**23%**
C_7H_8 (toluene)	46 (5)^b	20 (10)^b	105 (78)	35 (7)	**27%**
CO (carbon monoxide)$^{\triangle\square}$	0.49 (0.09)^a	0.32 (0.08)^a	0.6 (0.1)	0.358 (0.007)	**33%**
CO_2 (carbon dioxide)$^{\triangle\square}$	157 (3)^b	145 (3)^b	165.5 (0.7)^b	158.8 (0.2)^b	**27%**
NO_x (nitrogen Oxide)$^{\triangle}$	14 (2)^c	7 (2)^c	14 (5)	10 (3)	**12%**
THC (total hydrocarbons)$^{\triangle}$	9 (1)^a	7 (1)^a	12 (2)	10 (2)	**18%**

Table 5.8: Regulated and unregulated emission factors for Car 4 and Car 5, over the Rural phase of the CADC, at 22°C with E5 and E85, and at -7°C with E5 and E75. The relative contribution of the mass of the Rural phase to the total CADC mass (in %) is indicated in the right column. The standard deviations are in brackets and were calculated from 3 test repetitions for each mode (fuel and temperature). $^{\triangle}$ Bag measurements carried out according to Directive 70/220/EEC and its amendments (75). Statistically significant differences between fuels are indicated as follow: (a) P value < 0.05, (b) P value < 0.01, (c) P value < 0.001. nd : not detectable, N/A : not available.

Car 4 Euro 4	**CADC Motorway phase emission factor (in mg km^{-1} except $^{\square}$ in g km^{-1})**				
Temperature	**22°C**		**-7°C**		**Averaged ratio**
Fuel	E5	E85	E5	E75	**phase/CADC**
NO (nitric oxide)	N/A	16 (6)	N/A	17.1 (0.4)	**39%**
NO_2 (nitrogen dioxide)	N/A	0.012 (0.006)	N/A	0.02 (0.02)	**26%**
N_2O (nitrous oxide)	N/A	0.002 (0.002)	N/A	nd	**2%**
NH_3 (ammonia)	N/A	3.5 (0.8)	N/A	2.6 (0.6)	**28%**
HCN (hydrogen cyanide)	N/A	0.0093 (0.0007)	N/A	0.0024 (0.0009)	**5%**
HCHO (formaldehyde)	N/A	0.017 (0.007)	N/A	0.09 (0.03)	**10%**
CH_3CHO (acetaldehyde)	N/A	2 (2)	N/A	1.06 (0.05)	**17%**
CH_3CH_2OH (ethanol)	N/A	nd	N/A	nd	**0%**
CH_4 (methane)	N/A	0.5 (0.2)	N/A	0.3 (0.3)	**4%**
C_2H_4 (ethylene)	N/A	0.3 (0.1)	N/A	0.06 (0.03)	**7%**
C_7H_8 (toluene)	N/A	0.04 (0.04)	N/A	0.01 (0.02)	**5%**
CO (carbon monoxide)$^{\triangle\square}$	0.45 (0.03)	0.50 (0.04)	0.85 (0.06)^{a}	0.61 (0.02)^{a}	**57%**
CO_2 (carbon dioxide)$^{\triangle\square}$	166.8 (0.5)^{a}	156 (3)^{a}	181 (4)	176.29 (0.07)	**55%**
NO_x (nitrogen Oxide)$^{\triangle}$	10.8 (0.8)	23 (9)	11 (4)^{a}	24.3 (0.5)^{a}	**28%**
THC (total hydrocarbons)$^{\triangle}$	3.6 (0.6)	3.0 (0.3)	3.4 (0.7)^{a}	9 (2)^{a}	**30%**

Car 5 Euro 5a					
Temperature	**22°C**		**-7°C**		**Averaged ratio**
Fuel	E5	E85	E5	E75	**phase/CADC**
NO (nitric oxide)	34 (5)^{b}	18 (2)^{b}	53 (13)	27 (8)	**79%**
NO_2 (nitrogen dioxide)	2 (2)	1.1 (0.3)	2 (2)	0.38 (0.07)	**62%**
N_2O (nitrous oxide)	0.8 (0.6)	1.0 (0.2)	0.9 (0.5)	0.5 (0.2)	**71%**
NH_3 (ammonia)	5 (3)	9 (2)	2 (2)^{a}	10.3 (0.2)^{a}	**56%**
HCN (hydrogen cyanide)	1.4 (0.4)^{a}	0.72 (0.08)^{a}	3.0 (0.5)^{a}	0.76 (0.05)^{a}	**65%**
HCHO (formaldehyde)	1.2 (0.6)	1.5 (0.6)	1.3 (0.8)	0.75 (0.05)	**64%**
CH_3CHO (acetaldehyde)	5 (4)^{b}	22 (6)^{b}	10.3 (0.3)^{b}	3.6 (0.3)^{b}	**66%**
CH_3CH_2OH (ethanol)	29 (16)	48 (26)	22 (18)	28 (7)	**61%**
CH_4 (methane)	2.9 (0.6)^{c}	7.4 (0.4)^{c}	1.9 (0.4)^{b}	6.67 (0.07)^{b}	**77%**
C_2H_4 (ethylene)	2.5 (0.5)	2.2 (0.6)	2.9 (0.2)^{a}	2.1 (0.2)^{a}	**67%**
C_7H_8 (toluene)	50 (34)	40 (24)	149 (89)	26 (3)	**58%**
CO (carbon monoxide)$^{\triangle\square}$	0.6 (0.2)^{a}	0.35 (0.09)^{a}	0.6 (0.2)	0.500 (0.004)	**63%**
CO_2 (carbon dioxide)$^{\triangle\square}$	209 (2)^{c}	197 (2)^{c}	231.0 (0.6)^{a}	219 (2)^{a}	**60%**
NO_x (nitrogen Oxide)$^{\triangle}$	51 (7)^{c}	24 (6)^{c}	79 (18)	47 (10)	**81%**
THC (total hydrocarbons)$^{\triangle}$	23 (4)	20 (2)	28 (4)	26 (2)	**76%**

Table 5.9: Regulated and unregulated emission factors for Car 4 and Car 5, over the Motorway phase of the CADC, at 22°C with E5 and E85, and at -7°C with E5 and E75. The relative contribution of the mass of the Motorway phase to the total CADC mass (in %) is indicated in the right column. The standard deviations are in brackets and were calculated from 3 test repetitions for each mode (fuel and temperature). $^{\triangle}$ Bag measurements carried out according to Directive 70/220/EEC and its amendments (75). Statistically significant differences between fuels are indicated as follow: (a) P value < 0.05, (b) P value < 0.01, (c) P value < 0.001. nd : not detectable, N/A : not available.

5. ALTERNATIVE FUELS AND POWERTRAIN TECHNOLOGIES EFFECTS ON EXHAUST EMISSIONS

5.2 Part B - Liquefied petroleum gas fuel

Chemical analysis and ozone formation potential of exhaust from dual-fuel (liquefied petroleum gas/gasoline) light-duty vehicles

T.W. Adam[a], C. Astorga[a], M. Clairotte[a], M. Duane[a], M. Elsasser[b,c], A. Krasenbrink[a], B.R. Larsen[a], U. Manfredi[a], G. Martini[a], L. Montero[a], M. Sklorz[c], R. Zimmermann[b,c], A. Perujo[a]

Atmospheric Environment, 45 - 2011, volume: 45, pages: 2842-2848

[a] European Commission Joint Research Centre Ispra, Institute for Energy, Sustainable Transport Unit, 21027 Ispra, Italy

[b] Cooperation Group Complex Molecular Systems/Joint Mass Spectrometry Centre, Helmholtz Zentrum München, 85764 Neuherberg, Germany

[c] Chair of Analytical Chemistry/Joint Mass Spectrometry Centre, Institute of Chemistry, University of Rostock, 18051 Rostock, Germany

Abstract

Measures must be undertaken to lower the transport sectorŠs contribution to anthropogenic emissions. Vehicles powered by liquefied petroleum gas (LPG) are an option due to their reduced emissions of air pollutants compared to engines with conventional fuels. In the present study, ten different dual-fuel LPG/gasoline light-duty vehicles were tested, which all complied with European emission level legislation Euro 4. Tests with LPG and gasoline were performed on a chassis dynamometer by applying the New European Driving Cycle (NEDC) and emission factors and ozone formation potentials of both kinds of fuels were compared. The components investigated comprised regulated compounds, CO_2, volatile hydrocarbons and carbonyls. On-line analysis of aromatic species was carried out by resonanceenhanced multiphoton ionizationetime-of-flight mass spectrometry (REMPI-ToF-MS).

We demonstrate that utilization of LPG can entail some environmental benefits by reducing emissions. However, for dual-fuel LPG/gasoline vehicles running on LPG the benefits are less than expected. The main reason is that dual-fuel vehicles usually start the engine up on gasoline even when LPG is selected as fuel. This cold-start phase is crucial for the quality of the emissions. Moreover, we demonstrate an influence on the chemical composition of emissions of vehicle performance, fuel and the evaporative emission system of the vehicles.

Keywords: liquefied petroleum gas; exhaust emission; dual-fuel vehicle; ozone formation potential.

5.2.1 Introduction

Climate change and air pollution are two of the greatest environmental challenges mankind faces in the next decades and the transport sector plays a key role for both of these (6, 25). Transport is not only one of the most significant sources of air pollution in urban areas but also on a global scale (6, 25). Recent estimates show that transportŠs contribution to global anthropogenic emissions amount to 21% for carbon dioxide (CO_2), 37% for nitrogen oxides (NO_x), 19% for volatile organic compounds, 18% for carbon monoxide (CO) and 14% for black carbon (6, 25).

Significant abatement of road transport emissions may be achieved in the future by replacing gasoline and diesel fueled combustion engines with alternative powertrains such as electric or hydrogen-powered vehicles. However, there is an evident need for instant measures and the use of alternative fuels with lower emissions has increased in many countries such as liquefied petroleum gas (LPG), compressed natural gas (CNG), alcohol-gasoline blends, and biodiesel (252).

The number of LPG-powered vehicles exceeded 13 million in 2009 resulting in a consumption of ca. 20 million tons LPG per year (253). The major components of LPG (autogas) are propane and butane. In contrast to CNG, which mainly consists of methane, LPG can be stored as a liquid under relatively low pressure (254). The chemical composition of LPG is simple compared to gasoline. It combusts almost entirely and has been proposed as a cleaner fuel (255, 256). In fact, previous studies have shown that as an alternative to conventional fueled vehicles, LPG-powered vehicles can considerably reduce the emissions of greenhouse gases (256, 257), particulate matter (PM) (257), metal elements (258), ozone precursors (255), and polycyclic aromatic hydrocarbons (PAH) (141). The main disadvantage of LPG compared to traditional fuels in Europe today is the limited number of LPG re-fueling stations and the highly varying availability in different regions and countries. These facts strongly influence sales figures of LPG cars even though several countries apply reduced fuel taxes (259). As a consequence, car manufacturers offer dual-fuel vehicles, which can run on either LPG or gasoline and allows the driver to choose between fuels.

Recently Yang et al. (252) have reported reductions of various exhaust constituents of cars, which were converted from gasoline-powered to LPG/gasoline dual-fuel retrofits. It may be envisaged that vehicles designed ab initio to run on dual fuels provide even higher emission reductions than retrofits. On that background we have set up the present study, in which a representative selection of LPG/gasoline dual-fuel vehicles on the European market is investigated. The vehicles were tested with both fuel types using a standard test cycle relevant for European driving conditions (New European Driving Cycle) and a comprehensive analysis of the chemical composition of gaseous emissions was carried out. The exhaust constituents investigated were the following: Total hydrocarbons (THC), NO_x, CO, and CO_2 as well as individual volatile hydrocarbons (HC_s) and carbonyls relevant for the environment as ozone precursors (255) or for human health as carcinogens. The results obtained with the two fuels (gasoline and LPG) were compared with focus on their impact on the environment. In order to address the emissions during the cold-start phase, high frequency (1 Hz) time-resolved analysis of aromatic HCs was also conducted. This is particularly important for dual-fuel vehicles, which usually start up on gasoline even when LPG is selected as fuel.

5.2.2 Experimental part

All experimental work was carried out at the Vehicle Emissions Laboratory (VELA) of the Institute for Environment and Sustainability (IES) at the European Commission Joint Research Centre (EC-JRC) Ispra, Italy.

5.2.2.1 Test fleet and fuels

The test fleet consisted of 10 dual-fuel cars of different manufacturers. The vehicles are designed to be powered by LPG or gasoline. Car 2 and car 10 were of the same model. Test vehicles with varying engine size and mileage were carefully selected to represent a wide fleet of the European market. All complied with European emission level legislation Euro 4.

Tests of the vehicles 1-9 were carried out by using certified reference fuels of gasoline (R) and LPG grade A (A). Car 9 was additionally tested with LPG grade B (B), which has a C_3-content of 85% compared to 30% for LPG A. For car 10 commercial fuels (C) of gasoline and LPG were applied. More information on the vehicles and the used fuels can be found in Table 5.10 and the Supplementary Materials (Tables 5.13 and 5.14) respectively.

Vehicle	Car 1	Car 2	Car 3	Car 4	Car 5	Car 6	Car 7	Car 8	Car 9	Car 10
Power [kW]	70	44	44	51	46	75	55	103	75	44
Displacement [cm^3]	1300	1242	1242	1242	1000	1595	1199	1796	1595	1242
Odometer [km]	711	3612	7989	1142	5447	44,765	21,076	255	2697	9533
Gasoline Type	R	R	R	R	R	R	R	R	R	C
LPG Type	A	A	A	A	A	A	A	A	A, B	C

Table 5.10: Characteristics of the ten investigated dual fuel (LPG/gasoline) light-duty vehicles and indications of the fuels used for testing (R: reference gasoline fuel, A: reference LPG fuel grade A, B: reference LPG fuel grade B, C: commercial fuels gasoline and LPG).

5.2.2.2 Dynamometer and driving cycle

Testing was carried out on a 48” chassis dynamometer (Maha GmbH, Germany) equipped with a conventional constant volume sampling (CVS) system with a critical flow venturi (Horiba, Germany).

The driving cycle conducted was the New European Driving Cycle (NEDC). NEDC is applied for emission certification of light-duty vehicles in Europe and all tests were performed in accordance with the related legislative regulation and following amendments (171). The cycle consists of four repeated urban driving cycles and an extra-urban driving cycle (EUDC) and lasts for 1180 s. Legislation requires a pre-conditioning of the vehicle including fuel (soaking) of at least 6 h prior to the test with sampling starting at the engine start.

5.2.2.3 Evaporative emissions control system

The influence of the automotive evaporative emissions control system on the exhaust was investigated. The purpose of this system is to reduce or eliminate the release of fuel vapors from the tank into the atmosphere. Thereby, when the engine is switched off, evaporative emissions from the fuel tank are trapped in a charcoal canister until they are reintroduced into the intake air stream of the engine when the engine is running. A purge valve allows for drawing a part of the combustion air used by the engine through the canister, thus purging the activated charcoal. In total, three measurements were carried out for car 5 (one test) and car 10 (two tests) with the carbon canister disconnected thereby preventing the release of additional fuel vapors into the combustion chamber.

5.2.2.4 Chemical analysis

The regulated exhaust constituents THC, NO_x, and CO were measured according to the legislative procedures for vehicle emissions and following amendments (75).

Carbonyl samples from the CVS-diluted exhaust were collected and analyzed by high performance liquid chromatography with ultra violet (UV) detection according to the methods described elsewhere (210, 211). The focus was on the main constituents formaldehyde, acetaldehyde, propionaldehyde, acetone, and acrolein since amounts of the others were close to or below detection limits. In addition, total carbonyl content was estimated by adding up all individual carbonyl emission factors.

Regarding HC_S focus was on the C_2-C_9 hydrocarbons being listed as ozone precursors for ambient air in the EU directive 2002/3/EC (53). Sampling was done with Tedlar® bags at the dilution tunnel and chemical analysis was performed by dual-column gas chromatography with flame ionization detection as described in detail in ref. Latella et al. (131). In so doing, 22 HC_S could be clearly quantified (see Table 5.11). All HC_S emission factors were summed up to give an estimate of total HC_S.

The concept of maximum incremental reactivity (MIR) of ozone formation was applied to evaluate the ozone formation potential (OFP) of the emissions. In general, the MIR method is based on a scenario in which optimum conditions of precursor/NO_x ratios yield in maximumozone formation. For all sorts of ozone precursors, MIR factors have been derived, whose product with the compoundŠs emission factor results in the potential amount of ozone formed (132). The OFP of a mixture is determined by adding up the individual contributions of all emission constituents. By following this procedure OFP of HC_S, carbonyls and CO was calculated.

Furthermore, for car 10 time-resolved analysis of the exhaust emissions was carried out by resonance-enhanced multiphoton ionizationetime-of-flight mass spectrometry (REMPI-ToF-MS). This technique is known to be a sensitive on-line method for the detection of gaseous aromatic compounds. The REMPI-ToF-MS was connected to the tailpipe of the vehicle by using a heated pump and sampling line (200°C, 4 L min^{-1}) to which, in turn, the heated transfer line of the REMPI-ToF-MS was orthogonally attached. The latter consisted of a deactivated silica capillary (length 1.5 m; i.d. 0.32 mm; $T = 250°C$) by which a constant volume of exhaust was continuously drawn into the instrument (8 mL min^{-1}; residence time < 1 s). This enabled to analyze undiluted,

Car 10	Gasoline	LPG		LPG w/o canister	
	1 Test	Mean	Stdev	Mean	Stdev
Main Components [g km^{-1}]					
THC	0.032	0.078	0.017	0.050	0.000
CO	0.237	0.310	0.014	0.235	0.054
CO_2	135.506	122.771	1.440	123.702	2.032
NO_x	0.069	0.143	0.032	0.119	0.023
HC_S [mg km^{-1}]					
ethane	0.675	1.340	0.079	0.984	0.063
ethene	3.960	4.777	1.277	2.855	0.285
propane	0.088	4.411	0.068	3.416	0.467
propene	0.960	2.221	0.613	1.458	0.385
acetylene	3.162	3.693	0.015	2.831	0.259
isobutane	0.084	3.508	0.426	2.463	0.168
n-butane	0.230	5.702	0.851	3.876	0.142
trans-2-butene	0.101	0.455	0.058	0.231	0.006
1-butene	0.160	0.386	0.119	0.193	0.036
cis-2-butene	0.098	0.257	0.055	0.135	0.011
i-pentane	0.714	1.267	0.607	0.639	0.077
1,3-butadiene	0.183	0.284	0.139	0.142	0.021
n-pentane	0.340	0.358	0.136	0.204	0.046
trans-2-pentene	0.082	0.105	0.028	0.051	0.023
2-methylpentane	0.345	0.622	0.313	0.312	0.046
isoprene	0.123	0.221	0.099	0.126	0.006
n-hexane	0.080	0.088	0.039	0.053	0.011
n-heptane	0.060	0.215	0.022	0.124	0.017
benzene	0.636	0.927	0.056	0.723	0.062
toluene	0.431	0.501	0.154	0.423	0.182
ethylbenzene	0.157	0.309	0.141	0.175	0.010
m/p-xylene	0.162	0.336	0.158	0.200	0.007
Total HC_S	12.83	31.98	4.978	21.61	2.204
Carbonyls [mg km^{-1}]					
Formaldehyde	0.368	0.417	-	0.436	-
Acetaldehyde	0.280	0.333	-	0.558	-
Acetone	n.d.	n.d.	-	0.117	-
Acroleine	0.126	0.219	-	0.297	-
Propionaldehyde	n.d.	0.146	-	0.170	-
Total Carbonyls	0.774	1.115	-	1.578	-

Table 5.11: Emission factors of THC, NO_x, CO, CO_2, HC_s and carbonyls for car 10. Values represent mean values and standard deviations of two measurements (one measurement for carbonyls; n.d.: not detectable).

unfiltered and non-aged exhaust. The principle of REMPI-ToF-MS is described in detail in the literature e.g. (260, 261, 262), therefore, only a brief description is given here. A fundamental Nd:YAG laser (1064 nm) is used for non-linear generation of UV light pulses (266 nm, 2.2 mJ, 1.48 x 10^7cm^{-2}). The UV pulses are directed into the ionization chamber straight underneath the inlet needle of the transfer line, inducing soft photoionization of the aromatics in the analyzed exhaust by a sequential two-photon absorption process via an electronic transition state. The generated molecular ions are extracted into the flight tube of the reflectron ToF-MS (Kaesdorf Instruments, Germany) and mass spectra are recorded via an ultrafast analog to digital converter PC card. Data processing is done by a LabView (National Instruments, USA) based custom-made software. Calibration is carried out by applying external gas standards. In principle, 20 complete mass spectra per second can be recorded since a 20 Hz laser was used. In the framework of this paper, on-line data averaged to a time-resolution of 1 Hz is presented. Detection limits depend on various parameters such as spectroscopic properties of the compounds, laser characteristics (e.g. wavelength, pulse energy) and time-resolution (averaging). For the presented set-up detection limits were determined to be 670 ppb for benzene, and 8.4 ppb for naphthalene (263).

5.2.3 Discussion of results

Emission factors and OFP values of car 10 for all compounds investigated, both fuel types, with the evaporative emission control system connected and disconnected are illustrated as example in Table 5.11 and Table 5.12. Values represent the mean of two measurements including standard deviation if not indicated otherwise.

5.2.3.1 Emission factors

All regulated compounds were below legislative levels of Euro 4 positive ignition cars except NO_x of car 10 for LPG (0.143 ± 0.032 g km^{-1}), which exceeded the threshold (0.08 g km^{-1}) significantly. Car 10 was powered by commercial LPG and resulted in much higher NO_x yields than car 2 (0.015 ± 0.001 gkm^{-1}),which was of the same model but powered by reference LPG A. Variation of NO_x between both vehicles also occurred when run on gasoline (reference and commercial) but to a smaller extent. In addition, car 9 was tested on both LPG reference fuels (A and B) with B leading to an increase of NO_x of more than 100% (A: 0.018 ± 0.008 g km^{-1}; B: 0.038 ± 0.009

Car 10	Gasoline	LPG		LPG w/o canister	
	1 Test	Mean	Stdev	Mean	Stdev
CO [mg O_3 km^{-1}]	13.53	17.67	0.82	13.4	3.11
HC_S [mg O_3 km^{-1}]					
ethane	0.21	0.42	0.02	0.31	0.02
ethene	35.90	43.33	11.58	25.90	2.58
propane	0.05	2.47	0.04	1.91	0.26
propene	11.10	25.70	7.09	16.87	4.45
acetylene	3.92	4.58	0.02	3.51	0.32
isobutane	0.11	4.70	0.57	3.30	0.22
n-butane	0.30	7.53	1.12	5.12	0.19
trans-2-butene	1.40	6.33	0.81	3.21	0.08
1-butene	1.64	3.94	1.22	1.97	0.37
cis-2-butene	1.29	3.40	0.73	1.78	0.14
i-pentane	1.19	2.12	1.01	1.07	0.13
1,3-butadiene	2.47	3.82	1.88	1.91	0.28
n-pentane	0.52	0.55	0.21	0.31	0.07
trans-2-pentene	0.84	1.07	0.29	0.52	0.23
2-methylpentane	0.61	1.11	0.56	0.55	0.08
isoprene	n.d.	n.d.	-	n.d.	-
n-hexane	0.11	0.13	0.06	0.08	0.02
n-heptane	0.08	0.27	0.03	0.16	0.02
benzene	0.52	0.75	0.05	0.59	0.05
toluene	1.71	1.99	0.61	1.68	0.72
ethylbenzene	0.44	0.86	0.39	0.49	0.03
m/p-xylene	1.72	3.57	1.68	2.13	0.08
Total OFP HC_S	66.2	118.6	28.6	73.3	10.3
Carbonyls [mg O_3 km^{-1}]					
Formaldehyde	3.30	3.74	-	3.90	-
Acetaldehyde	1.91	2.27	-	3.81	-
Acetone	n.d.	n.d.	-	0.88	-
Acroleine	0.05	0.09	-	0.13	-
Propionaldehyde	n.d.	1.15	-	1.34	-
Total OFP Carbonyls	5.26	7.26	-	10.06	-
Total OFP [mg O_3 km^{-1}]	84.9	143.6		96.8	

Table 5.12: Ozone formation potentials of CO, HC_s and carbonyls for car 10. Values represent mean values and standard deviations of two measurements if not indicated elsewise (n.d.: not detectable).

g km^{-1}). However, more tests on different LPG types would be necessary to clearly estimate the influence of LPG quality on the emission. In this regard, it has to be borne in mind that depending on region and season the variation in the composition of LPG might vary tremendously e.g. in North America from 50% to near 100% propane (264). For THC, CO, HC$_S$, and carbonyls no clear trend could be determined with the fuel type. However, emission factors between cars varied within several hundred percent e.g. THC of car 1 (gasoline: 0.062 g km^{-1}, LPG: 0.081 g km^{-1}) and car 2 (gasoline: 0.027 g km^{-1}, LPG: 0.036 g km^{-1}) as well as CO of car 3 (gasoline: 0.70 g km^{-1}, LPG: 0.49 g km^{-1}) and car 4 (gasoline: 0.22 g km^{-1}, LPG: 0.12 g km^{-1}) although engine sizes were about the same (see Table 5.10). Consequently, the engine performance seemed to be very different within the studied test fleet.

An increase in NO$_x$ to a varying degree could be observed for several cars when powered by LPG. This effect is usually explained by the higher LPG combustion temperature (900-1000°C) compared with gasoline (500-800°C) leading to increased thermal NO$_x$ (252). An influence of fuel control to near stoichiometry and itŠs potential impact on the three-way catalystŠs activity might play a role as well. Short duration lean excursions can have a significant impact on tailpipe NO$_x$ emissions. With respect to CO$_2$, emissions spanned a range from 114 g km^{-1} (car 5, LPG) to 202 g km^{-1} (car 8, gasoline). Nine vehicles featured a reduction in CO$_2$ of up to 14% (car 3) when LPG-powered, which is illustrated in Fig. 5.7. Only for car 1 no difference could be determined. In this regard, no influence of fuel grade could be observed. The main reason for the reduction of CO$_2$ is the higher hydrogen-to-carbon ratio of LPG compared to gasoline (265).

5.2.3.2 On-line analysis of emission

Many compounds e.g. HC$_S$ did not feature a clear difference between fuel types although their quantities in LPG should be low compared to gasoline. Therefore, on-line analysis was applied in order to study their time-resolved behavior throughout the test runs. While the THC sensor only gives an estimate of the sum value for a large number of compounds, here the focus is on selected individual substances that are relevant for environment and human health. Monitoring of aromatic species was carried out for vehicle 10 by REMPI-ToF-MS. Figure 5.8A shows the time-resolved concentration of benzene over the whole driving cycle with the fuel continuously set to LPG. Benzene

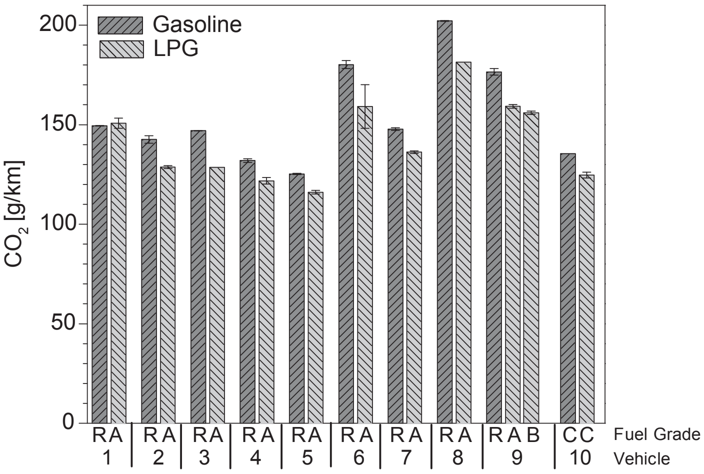

Figure 5.7: Mean of emission factor and standard deviation of CO_2 for all ten tested dual-fuel LPG/gasoline light-duty vehicles powered by gasoline and LPG. - (R: reference gasoline, A: reference LPG grade A, B: reference LPG grade B, C: commercial fuel).

is known to be a human carcinogen (class 1) (39). The close-up illustrates the same test for the first 120 s. In comparison, the starting phase of a test on gasoline is plotted. It can be seen that the signal of benzene sharply increased (test start: 11 s) during the first acceleration phase and reached its maximum shortly after. After deceleration a strong reduction of benzene occurred and during the second acceleration phase a less intense signal for benzene reappeared. For the rest of the whole test hardly any benzene could be detected. Consequently, only the first two acceleration events of NEDC contributed to the emission factor of benzene. The same trend could be observed for the higher homologues of benzene e.g. toluene. Moreover, no clear difference was detected between gasoline and LPG when considering all tests. This behavior can be explained by the fact that dual-fuel LPG/gasoline cars usually start up the engine on gasoline even though LPG is selected as fuel. LPG has a higher ignition temperature (ca. 500°C) than gasoline (ca. 250°C), which can result in ignition difficulties for LPG when the engine is cold (252). Subsequently, dual-fuel cars are ignited by gasoline but switch to LPG mode after a certain time or when a certain engine temperature has been reached (252). This parameter varies depending on vehicle/manufacturer as well as on the outside temperature but can last between seconds and several minutes. Because the test cell was kept to a constant temperature of 22°C car 10 ran on gasoline for less than

1 min (ca. 55 s). It is known that gasoline vehicles emit high amounts of numerous hydrocarbons during the first seconds of the starting phase because unburned fuel is traveling through the engine and the cold catalytic converter system (266). For benzene and many other gasoline constituents, this part is the greatest contributor to the final exhaust emission, also when switched to LPG. It should be noted, that during real life on-road driving in cold environments the impact of this start-up phenomenon on emissions from dual-fuel vehicles may be higher than estimated in the present study at 22°C.

A similar behavior is featured by CO, which mainly contributed to its emission factor during the first three acceleration phases (ca. 150 s) with the highest yield during the first 30 s. This means a clear drawback for most dual-fuel LPG/gasoline cars with respect to air quality, especially when the engine heats up slowly in winter times and during heavy traffic. In contrast, several PAH like naphthalene and its homologues as well as phenanthrene could also be detected in the final extra-urban part of the driving cycle. Figure 5.8B depicts this behavior for naphthalene as an example. Naphthalene is reasonably to be expected a human carcinogen (class 2B) (39). Like for benzene, the highest concentrations appeared during the cold engine start but lasted for a longer period of up to ca. 200 s. A reason for the longer occurrence could be the cold engine and catalytic converter but also a memory-effect in the cold exhaust pipe. Significant memory-effects in the REMPI-ToF-MS can be excluded due to the heated and deactivated sampling line. In addition, signals of naphthalene also appeared during the final stage of NEDC. This effect was observed when the vehicle was powered by LPG as well as by gasoline. It has to be born in mind that the vehicle solely runs on LPG at this stage of the test when LPG is selected as fuel. Moreover, in order to exclude possible effects of the evaporative emission control system, measurements were additionally carried out with the canister disconnected and the outcome was the same. The close-up of Fig. 5.8B illustrates the EUDC part of NEDC with the engine gasoline-powered as well as LPG-powered and with the evaporative emission control canister separated. Subsequently, gasoline can be excluded as a source. The most plausible reason for the occurrence of PAH at higher speeds is the lubricant oil, which has been also reported in (252).

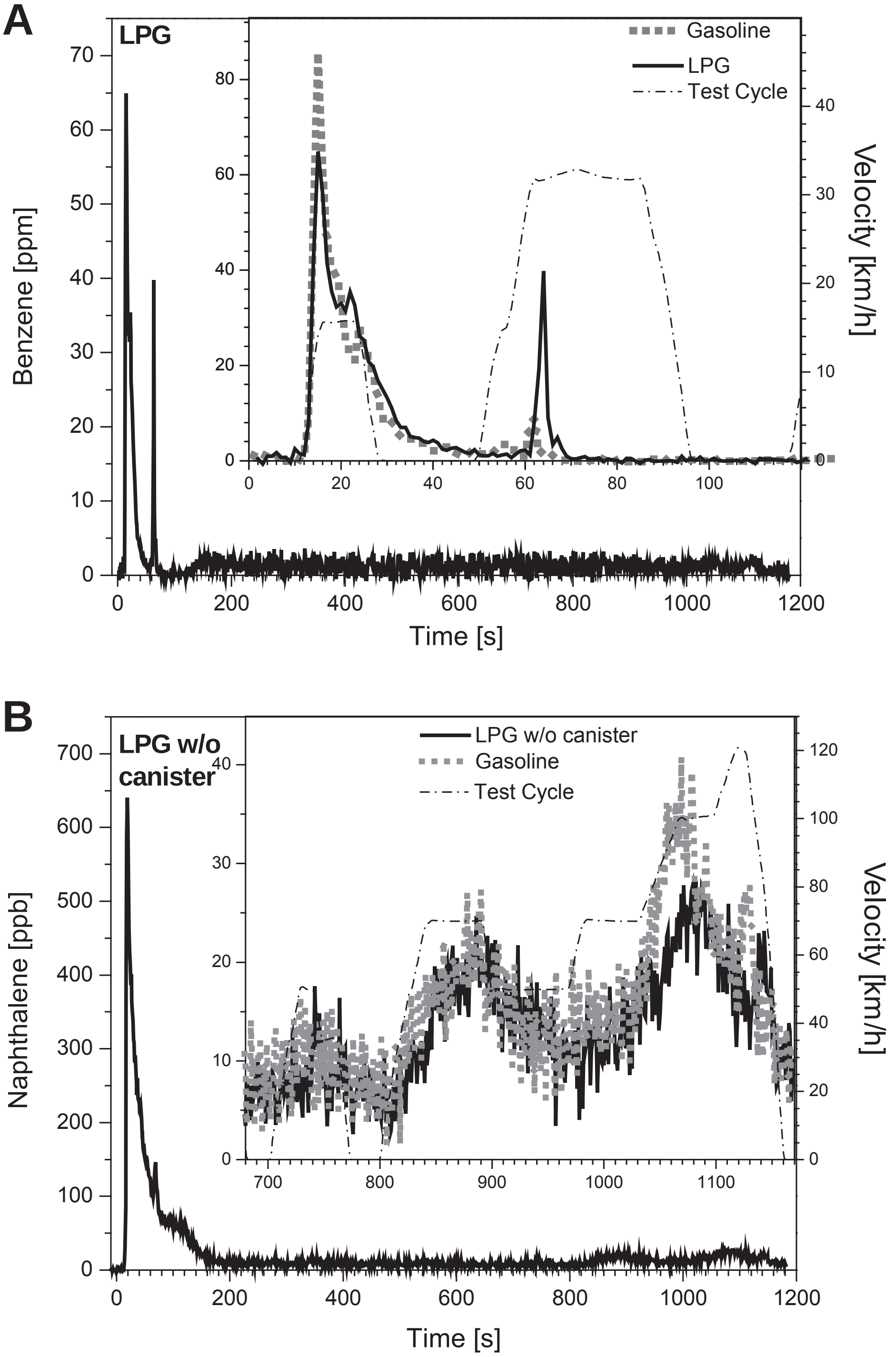

Figure 5.8: - A: Time-resolved concentration of benzene for the dual-fuel LPG/gasoline light-duty vehicle 10 when powered by LPG (large image) as well as LPG/gasoline (close-up image) by applying the New European Driving Cycle. B: Time-resolved concentration of naphthalene for the dual-fuel LPG/gasoline light-duty vehicle 10 when powered by LPG w/o carbon canister (large image) as well as LPG (w/o canister)/gasoline (close-up image) by applying the New European Driving Cycle.

5.2.3.3 Influence of evaporative emission control system

Emission factors of benzene for the three measurements on LPG with the carbon canister disconnected and, for comparison, the corresponding runs on LPG with the canister connected are illustrated in Fig. 5.9. These results show that emission factors of benzene were decreased between 20 and 33% when the carbon canister was disconnected. An influence could also be observed for other HC_S, like hexane, heptane, toluene, and C_2-benzenes with reductions of similar measures. However, the number of tests was not sufficient to demonstrate a statistically significant reduction. Therefore, these reductions should be taken only as an indication. In general, the purging strategy of the canister depends on various factors, which are not known in detail since manufacturers do not release such information. In fact, the purging strategy is a compromise between different needs such as the control of the exhaust emissions during the cold-start, a good drivability and the need to achieve a sufficient degree of purging of the activated carbon in order to pass the evaporative emission test (before running an evaporative emission test, the vehicle is pre-conditioned by driving a NEDC cycle plus an additional urban part of the cycle). In addition, the amount of hydrocarbon stored in the canister depends on many factors like previous usage of the vehicle, the type of the fuel used, temperature to which the vehicle has been exposed etc. This means that the amount of hydrocarbons coming from the canister during an emission test is very difficult to estimate.

5.2.3.4 Ozone formation potential

The OFP for all test cars powered by both fuel types were determined and are illustrated in Fig. 5.10. The columns represent total OFP and are additionally divided into their proportions deriving from CO (OFP-CO), carbonyls (OFP-carbonyls), and HC_S (OFP-HCS). For car 3, 4, and 10 as well as car 5 run on LPG carbonyls were not determined; therefore, these OFP values are missing. The OFP ranged from 0.045 g O_3 km^{-1} (car 9, LPG) to 0.136 g O_3 km^{-1} (car 10, LPG). For all cars and both fuel types the highest contribution to OFP was caused by HCS with proportions from 51% (car 1, gasoline) to 87% (car 10, LPG, no carbonyls analyzed), followed by CO from 13% (car 10, LPG, no carbonyls analyzed) to 42% (car 1, gasoline). However, no clear difference between gasoline and LPG was obtained.

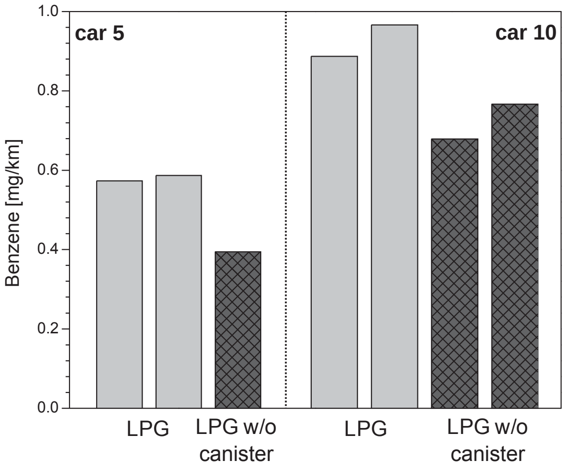

Figure 5.9: - Emission factor of benzene for the dual-fuel LPG/gasoline light-duty vehicles 5 and 10 powered by LPG with the carbon canister connected and disconnected.

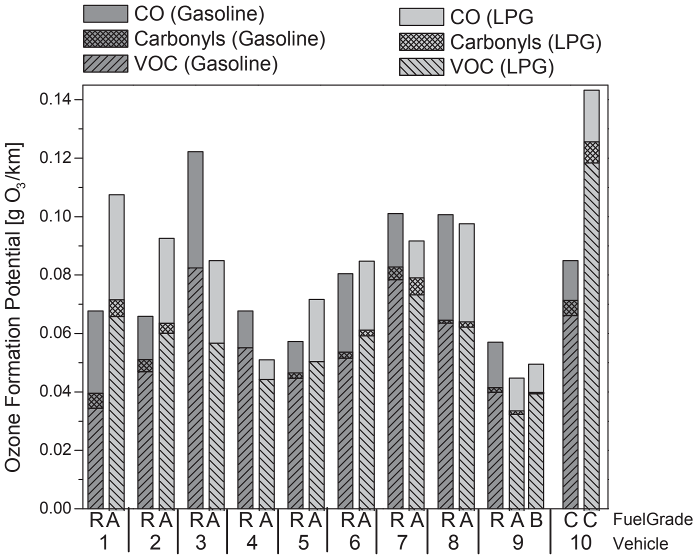

Figure 5.10: Mean of ozone formation potential for all ten tested dual-fuel LPG/gasoline light-duty vehicles powered by gasoline and LPG - (R: reference gasoline, A: reference LPG grade A, B: reference LPG grade B, C: commercial fuel).

The percentage contribution of all individual HC$_S$ to OFP-HC$_S$ is shown in Fig. 5.11. In brief, the greatest contributors to OFP-HC$_S$ for all fuels were ethene (28-54%) followed by propene (17-23%). Only for LPG B, propane (28%) contributed more than propene (14%). Further significant OFP-contributors were xylene, toluene, 1,3-butadiene, and propane with varying importance. Butane only played a role for LPG producing between 6% (LPG B) and 10% (LPG A) of the OFP-HC$_S$.

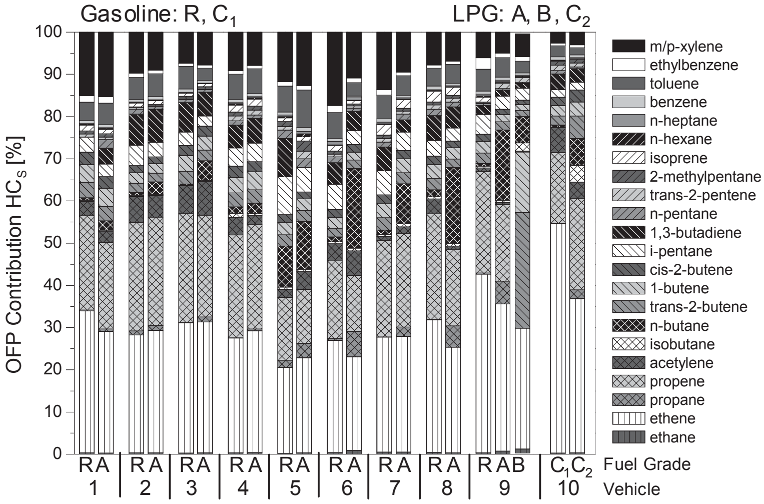

Figure 5.11: Percentage contribution of HCs to OFP for all ten tested dual-fuel LPG/gasoline light-duty vehicles powered by gasoline and LPG - (R: reference gasoline, A: reference LPG grade A, B: reference LPG grade B, C: commercial fuel).

With the exception of the OFP caused by unburned propane/butane bulk components of the LPG fuel, only little difference between gasoline-powered and LPG-powered tests was discerned. The main reason for this is the start up on gasoline as already demonstrated with the high frequency on-line analysis of the exhaust. Chang et al. (2001) (255) reported a decrease of 47% of OFP in exhaust emissions when gasoline is replaced by LPG in single-fuel LPG vehicles. This was not the case for dual-fuel vehicles in the present study, where no clear benefits were evident of running the engines on LPG. In addition to the start-up problematic, the reduced positive effects of using LPG for dual-fuel engines can be attributed to the technical implementation of the evaporative emission control system and the technical performance of the individual vehicles as well as to the quality of LPG. In real driving conditions, long-distance driving with dual-fuel vehicles is expected to increase the positive effects of LPG as fuel. In contrast, driving conditions like short distances, frequent cold-starts, slow warm-up of the engine due to heavy traffic etc. minimize these benefits.

5.2.4 Conclusion

The emission and OFP results demonstrate that several aspects influence the exhaust emissions from dual-fuel vehicles, namely fuel, vehicle performance, cold-start, and the evaporative emission control system. All this should be kept in mind when comparing the present results with those of other studies. Yang et al. (2007) (252) ran 1370 s pre-conditioning of the engines with LPG before each test in order to ensure that only LPG was combusted during the test. Consequently, a significant decrease of most exhaust constituents was reported by these authors. It is known that engine cold-starts contribute considerably to overall exhaust emissions e.g. (248). Thus, in the present study we have aimed at test conditions that are closer to the European real-world utilization and driving conditions, which implies that even when the dual-fuel engine is set to LPG a significant amount of fuel is gasoline during the cold engine start phase. As a consequence, the environmental benefits were less than expected.

- **Acknowledgments**

The VELA staff is acknowledged for their skillful technical assistance, in particular R. Colombo, M. Sculati, G. Lanappe, F. Muehlberger, and P. Le Lijour.

5.3 Supplementary Materials

Property	Units	Limits		Test Method
		Max.	Min.	
Research octane number		95.0	-	EN 25164
Motor octane number		85.0	-	EN 25163
Density 15 °C	kg m^3	740	754	ISO 3675
Vapour pressure	kPa	56.0	60.0	prEN ISO 13016-1 (DVPE)
Distillation:				EN-ISO 3405
Evporated at 70°C	% v/v	24.0	40.0	
Evporated at 100°C	% v/v	50.0	58.0	
Evporated at 150°C	% v/v	83.0	89.0	
FBP	°C	190	210	
Residue	% v/v	-	2	
Hydrocarbon analysis:				
Olefins	% v/v	-	10	ASTM D 1319
Aromatics	% v/v	29.0	35.0	ASTM D 1319
Benzene	% v/v	-	1.0	pr. EN 12177
Saturates	% v/v	report	report	ASTM D 1319
Carbon/Hydrogen ratio Induction period	minutes	480	-	EN-ISO 7536
Oxygen content	% m/m	-	1.0	EN 1601
Existent gum	mg mL^{-1}	-	0.04	EN-ISO 6246
Sulphur content	mg kg^{-1}	-	10	pr. EN-ISO/DIS 14596
Copper corrosion at 50°C		-	Class 1	EN-ISO 2160
Lead content	mg mL^{-1}	-	5	EN 237
Phosphorous content	mg mL^{-1}	-	1.3	ASTM D3231

Table 5.13: Certificate of the Gasoline Reference Fuel Type I (Directive 2002/80/EC).

Property	Units	Fuel A	Fuel B	Test Method
Composition	% v/v			ISO 7941
C_3 content		30 ± 2	85 ± 2	
C_4 content		balance	balance	
$< C_3$, $> C_4$		2 (max)	2 (max)	
Olefin content		12 (max)	15 (max)	
Evaporation residue	mg kg^{-1}	50 (max)	50 (max)	ISO 13575
Water at 0°C		free	free	Visual inspection
Total sulphur content	mg kg^{-1}	50 (max)	50 (max)	EN 24260
Hydrogen sulphide	-	none	none	ISO 8819
Copper strip corrosion	rating	class 1	class 1	ISO 6251
Odour		characteristic		
Motor octane number		89 (min)	89 (min)	EN 589 Annex B

Table 5.14: Certificate of the LPG Reference Fuel Type I (Directive 2002/80/EC).

Chapter 6

Heavy-duty vehicles emissions

The share of freight transport by road in Europe amounts to 90%, mainly through the tractor-trailers (267). In spite of the importance that could have trucks and buses emissions on the atmosphere, relatively few studies are available on this issue. These are focussed on the effect of modern aftertreatment devices on regulated emissions (NO_x, PM, CO, HC). In the "Air Resources Board Heavy-Duty Emissions Testing Laboratory" (HDETL - Los Angeles), Biswas et al. (2008 and 2009) studied the emissions from 4 trucks equipped with different aftertreatment devices. In this case, the study reports the physical properties of the semi-volatile and non-volatile PM fractions of particles emmitted. Three driving cycles were used : steady state, urban and idle. The aftertreatment devices were based on continuously technology, with passive or active filters, with catalyst or uncatalyzed (CRT, see section 1.4.2). The results showed the overall efficiency of the aftertreatment devices tested for reducing up to 90% of PM mass. However, only few systems were also efficient in reducing PM number (268, 269). In another study, Herner et al. (2009) investigated the impact of SCR and DPF aftertreatment systems on the truck exhaust emissions. Abatements of 95% and 75% were found for PM mass and NO_x respectively (270). In addition, from this study, Hu et al. (2009) underscored the relationship between metals emitted(catalyst used in the aftertreatment systems), and the driving cycle. The study concluded that metals are more likely to be released during cruise operation and under high temperature conditions (271).

The effect of alternative fuels on NO_x and PM emissions from trucks was approached by Wang et al. (1997) with a transportable chassis dynamometer testinfg facility. A fleet of more than 300 buses and trucks were tested. The lower NO_x and PM emissions were obtained with vehicles running with compressed natural gas (CNG), methanol and ethanol fuels (272). However, during a subsequent study carried out in the HDETL by Kado et al. (2005) on CNG and diesel fueled buses, the highest mutagen emission rates were associated with the CNG-fueled vehicle. This vehicle had no aftertreatment, and its specific mutagenic activity was related to the highest emissions of 1,3-butadiene, benzene and carbonyls (273). In the study of Lev-On et al. (2002) carried out on several trucks and buses, the CNG fueled vehicles exhibited higher gaseous pollutant emissions in comparison with diesel vehicles equipped with DPF. In addition, CNG-fueled vehicles did not emitted less PM than diesel vehicles equipped with DPF (151). This fact could be explain by the absence of aftertreatment system for the CNG-fueled vehicles tested in the previous studies. The implementation of DOC on the same bus as the one tested by Kado et al. (2005) has caused a reduction of mutagenic compounds to a level similar to that obtained with the diesel fueled bus equipped with a DOC (274).

Finally, within the framework of the collaboration between COST action 346 (the European cooperation in the field of scientific and technical research) and group 400 of ARTEMIS project (Assessment and Reliability of Transport Emission Models and Inventory Systems), a methodology was developed to assess pollutant emissions from trucks circulating in Europe (275, 276). Supported by 17 contries, this project aimed at designing the vehicle test conditions prior to enlarging the knowledge base on emissions caused by trucks. The last stage consisted in developing models to predict these emissions. However, this project was carried out between 1999 and 2005 and emission factors from Euro IV and Euro V trucks were not covered.

The main technical constraints to face when studying truck emissions are caused by the size of the vehicle and the power required to simulate the forces to apply to the vehicle. For these reasons, relatively few studies are available on this topic. Consequently, many scientific studies on truck emissions are based on engine test bench experiements where constraints are directly applied to the engine. To address the specific issue of the impact of emissions from transport on climate and the environment, the European Commission has established one of the most advanced laboratory dedicated to trucks and buses emissions : the VELA 7. This laboratory enable to host the whole truck or bus in order to monitor the exhaust gas thanks to analytical instruments dedicated to the measurement of regulated and unregulated pollutants. Particulate and gaseous phases compositions are measured online, which allows following closely their fluctuations, and interpreting them in regards of the speed profile of the vehicle, the temperature of the engine, or the fuel consumption for instance. This new facility allows operating tests with cell temperature ranging between -30 to +50°C. Inaugurated in March 2009 (277), the VELA 7 has already assessed emissions from more than 20 vehicles, including road tractors, waste removal trucks and buses. Table 6.1 details the fleet of vehicles studied in VELA 7 since it was commissioned in 2009.

Index	Vehicles	Emission Standards	Type	Aftertreatment Systems	Driving Cycles
1	IVECO Bus 480 Turbocity	Pre-Euro 1	Bus	none	ETC
2	IVECO Bus 491 CityClass	Euro II	Bus	none	ETC
3	MAN Bus	Euro IV	Bus	DPF et DOC	Start/Stop
4	Peugeot Boxer	Euro 3	Van	DOC	ETC
5	Peugeot Boxer	Euro 3	Van	DOC	NEDC
6	IVECO Eurotech	Euro II	Waste removal truck	DPF	ETC, AMSA, SS
7	Mercedes Economic 2613	Euro V	Waste removal truck	Urea-SCR	ETC
8	IVECO Eurotech	Euro II	Waste removal truck	DPF	ETC, AMSA, SS
9	Iveco EuroTech Cursor 7790cc 200kw	Euro II	Waste removal truck	DPF	AMSA
10	IVECO Stralis500	Euro V	Road tractor	Urea-SCR	ETC
11	IVECO Eurocargo	Euro III	Road tractor	none	NEDC, SS
12	IVECO Stralis 360HP	Euro V	Road tractor	Urea-SCR	ETC, SS
13	IVECO Cargo	Euro III	Road tractor	DPF	ETC
14	MAN TGX 4*2	Euro V	Road tractor	Urea-SCR	ETC
15	IVECO E560	Euro V	Road tractor	Urea-SCR	ETC, SS
16	Renault 460	Euro V	Road tractor	Urea-SCR	ETC, SS
17	Volvo (prototype)	Euro VI	Road tractor	-	-
18	DAF XF105.460	Euro V	Road tractor	Urea-SCR	ETC
19	DAF XF105.460	Euro V	Road tractor	Urea-SCR	ETC
20	Renault	Euro V	Road tractor	Urea-SCR	ETC
21	DAF XF105.460	Euro V	Road tractor	Urea-SCR	ETC
22	Scania	Euro V	Road tractor	Urea-SCR	ETC

Table 6.1: List of trucks studied between 2009 and 2011 in the VELA 7. 4 categories of trucks were tested : bus, van, waste removal truck and road tractor.

During these 3 years, the VELA 7 hosted a large number of trucks, including many modern trucks complying with the latest European emission standard legislation Euro V. The tests carried out on this fleet allowed providing valuable inputs to update existing databases of emission factors. Numerous data are collected for every single test, such as time-resolved emission profiles for a great number of gaseous and solid pollutants, together with the dynamic data of the vehicle. The data processing is still ongoing, consequently, only few preliminary results are presented in this section. In chapter 3, among all the vehicles studied, the truck was the highest emitter of NO_x and black carbon (see Fig. 6.1).

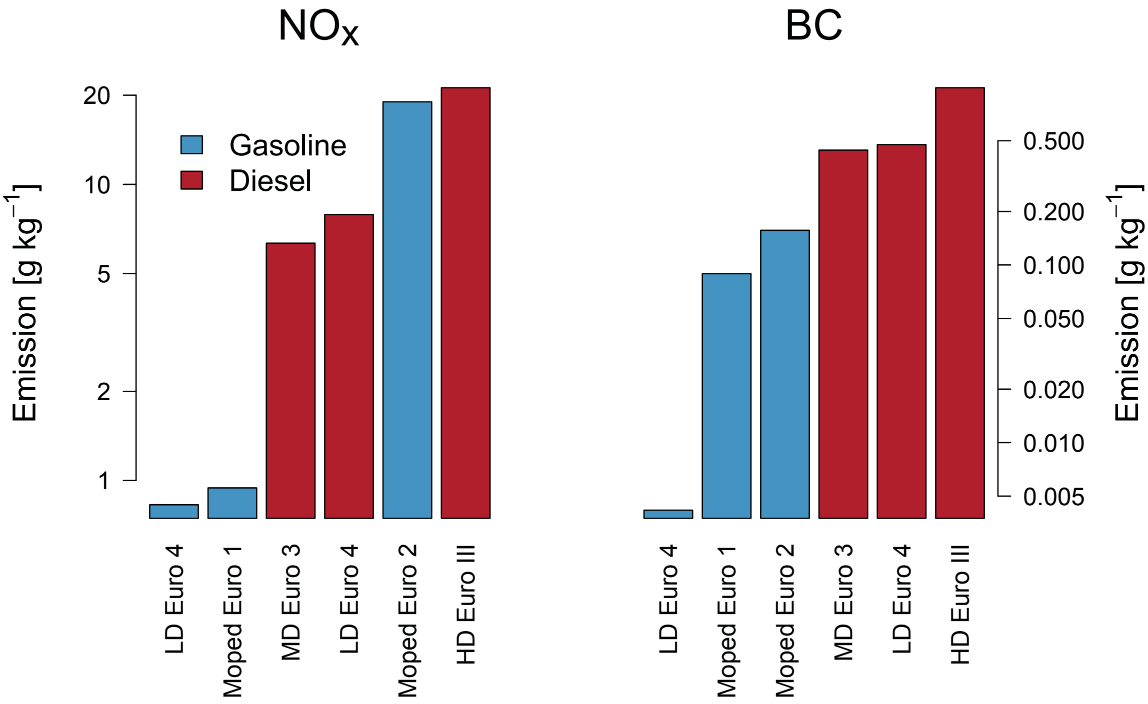

Figure 6.1: NO_x and black carbon emissions from different categories of vehicles. - Data are expressed in mass of pollutant per mass of fuel consumed, and are shown in a log scale. HD and LD stand for heavy-duty and light-duty vehicles respectively. A full description of the vehicles is available in chapter 3.

Three examples are presented in this chapter. The first one is dedicated to the Urea-SCR aftertreatment system, which is one of the most commonly implemented in the Euro V trucks. This system aims at reducing NO_x emissions, however, it could be the source of undesired NH_3. The second example focusses on the use of natural oxygenates as additives in the fuel in order to reduce PM emissions from buses. Finally, the last example presents the potential of VELA 7 to investigate regulated and unregulated emissions from trucks. An extensive description of gaseous and particulate exhaust emissions from a Euro III truck (number 11 in Table 6.1) was carried out. Investigation of the time-resolved emission profiles provided insightful informations on the formation mechanisms of several pollutants in the exhaust gas. Whereas somes time-resolved emission profiles were correlated with the fuel consumption, other pollutants had their time-resolved emission profiles correlated with exhaust gas temperature. This study stresses once again the key role played by the cold start of the vehicle on the quality of the emissions.

- NO_x emissions from Euro V road tractors - “NH_3 slip”.

Currently, the most widespread aftertreatment system which equips trucks complying with the Euro V emission standard runs with urea (Urea-SCR). As indicated in Table 6.1, more than 10 vehicles equipped with this system were investigated in the VELA 7. The aim was to check the effectiveness of such system against various operative conditions (like the driving cycle followed, or the ambient temperatures for instance). In addition, a specific focus was given to the potential emissions of NH_3 which migh arise during a wrong setting of the aftertreatment system. The results showed that NO_x emissions from trucks following the regulatory cycle (ETC) were below the Euro V standard. However, in some cases, NH_3 emissions were detected as shown in Fig. 6.2 obtained with the truck 10 during the ETC. In this case, NO_x emissions started to decrease at the beginning of the third phase of the cycle ETC (“ motorway ” part) around 1200 s, when the temperature of the exhaust gas reached 200°C. This reduction of NO_x concentration came with the outbreak of NH_3. Several orders of magnitude lower than NO_x concentrations observed early in the cycle, NH_3 concentration reached in this case 15 ppm, value which would be beyond the 10 ppm proposed for the upcoming regulation Euro VI (219). The aftertreatment system seemed to be effective when the catalyst reached a sufficent temperature. However, this condition was not met for all the vehicles investigated, as for example, for the waste removal truck 7 following a custom driving cycle simulating its typical journey of collection. Indeed, with low speed, and several start and stop events, the aftertreatment system was never warm enough to release urea, and consequently, to reduce NO_x emissions. Despite the fact that vehicle 7 complied with the Euro V emission standards with the ETC, the Urea-SCR system was poorly adapted with the useage of the vehicle. This example provides a good illustration of the difficulty to shape the regulation related to trucks, which are vehicles covering a broad range of use.

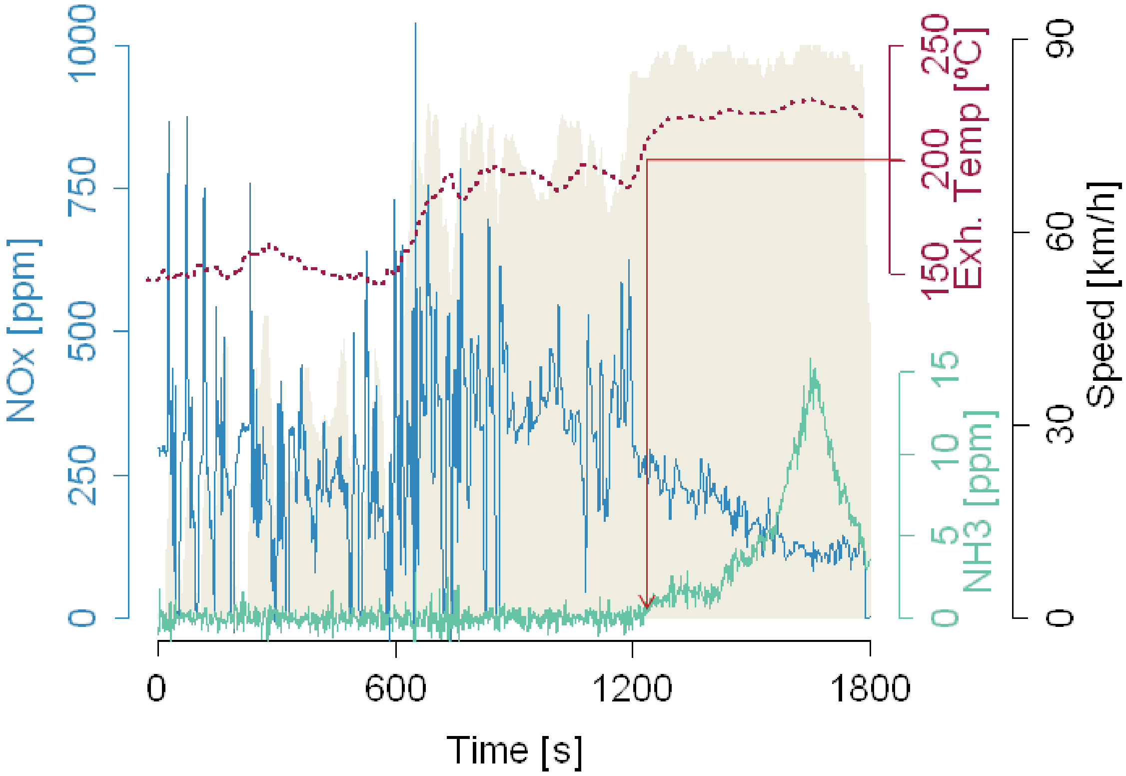

Figure 6.2: NO_x and NH_3 emissions from truck 10 during the regulatory ETC. - NO_x concentration decrease together with NH_3 apparition (at around 1200 s). Exhaust gas temperature is displayed in the upper part of the graph.

- Effect of natural oxygenates on particulate emissions from pre-Euro I and Euro II buses.

In this second example, a retrofit solution was investigated on the bus emissions. The term “ retrofit ” refers to the implementation of a modern technology in order to decrease the emissions from an old vehicle. This kind of technique is particularly suitable for vehicles with long lifetime like trucks and buses. An oxygenate produced from natural wastes (citrus peels) was used as an additive in the diesel for 2 buses in order to reduce their regulated emissions (PM et NO_x). The 2 buses studied were a pre-Euro 1 and a Euro 2 vehicles, and were still in circulation in the Venice area. The approximative mileages were 400 000 and 200 000 km for the pre-Euro I and the Euro II buses respectively. Two different formulations of oxygenates were investigated (with high and low boiling points, A and B respectively). The oxygenates were mixed with the diesel with range from 5 to 16%. Oxygenates used as additive in the fuel enhance the combustion, and the increase of oxygen in the fuel is generally associated with the reduction of particulate emissions (278). However, the main drawback is the potential emission of oxygenated pollutants like aldehydes (formaldehyde or acetaldehyde) (279). In this study, the 2 buses were tested with the urban part of the ETC (see Fig. 2.3 in section 2). Fig. 6.3 presents the effect of oxygenates on PM emission factors from the Euro II bus. The use of oxygenates allowed reducing by a factor of 2 PM emissions, and the sufficient proportion of oxygenates in fuel to reach this value was 8%. In Fig. 6.3, results are displayed ordered chronologically from left to right, so no memory effect was noticed in this experiment.

NO_x emission factors are reported in Fig. 6.4 for the pre-Euro I bus with oxygenate B (low boiling point). NO_x emissions were cut by almost 6% thanks to the addition of 8% of oxygenate in the fuel. Fig. 6.5 illustrates the impact of the addition of oxygenate B on aldehyde emissions for the Euro II bus. Aldehyde emissions remained constant whatever the concentration of oxygenate in the fuel.

This study allows highlighting an efficient technic of retrofitting. The implementation of such technic could help cities which want to reduce the impact of the emissions from public transport, without modifying the fleet of buses availables.

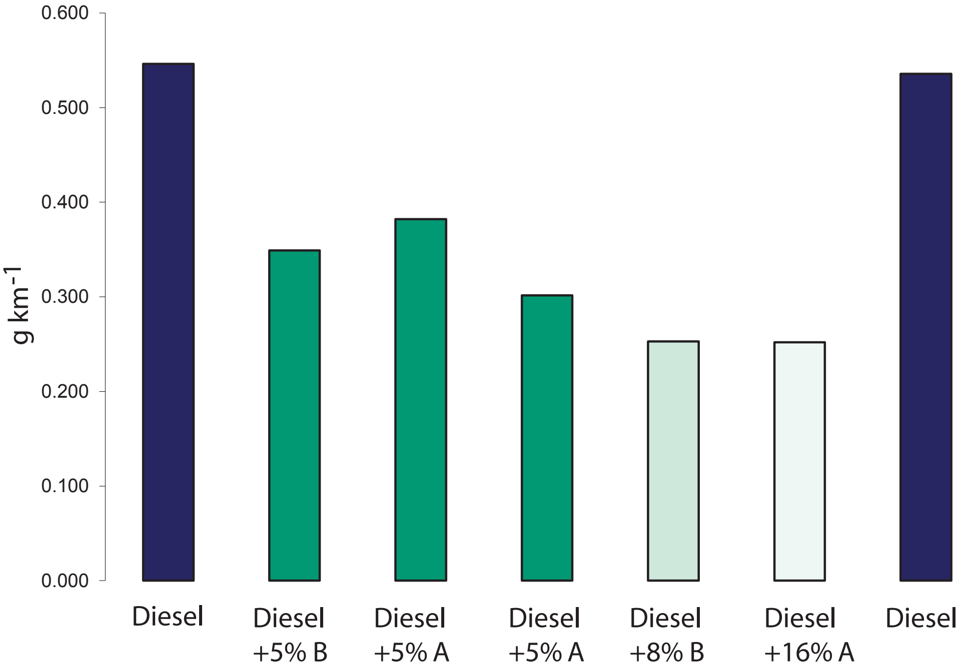

Figure 6.3: Effect of oxygenated fuel additives A and B on PM emissions from the Euro II bus. - Exhaust gas was sampled during the urban part of the ETC which is more characteristic of buses driving behaviour.

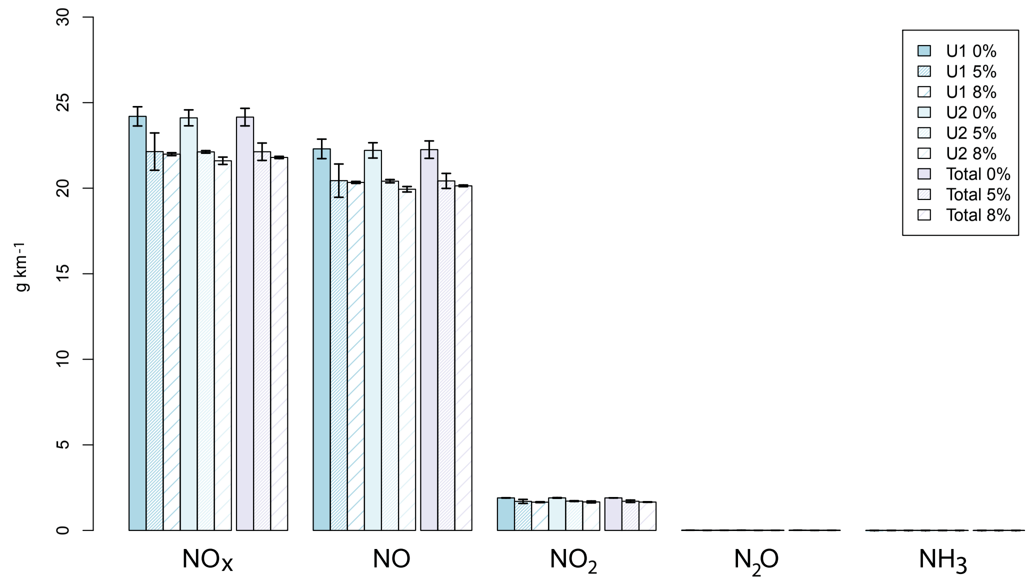

Figure 6.4: Effect of oxygenated fuel additive B on N-species emissions from the Pre-Euro I bus. - Exhaust gas was sampled during two consecutive urban parts of the ETC. Emission factors are displayed for the first urban part (U1), the second urban part (U2) and the total of the two parts (Total).

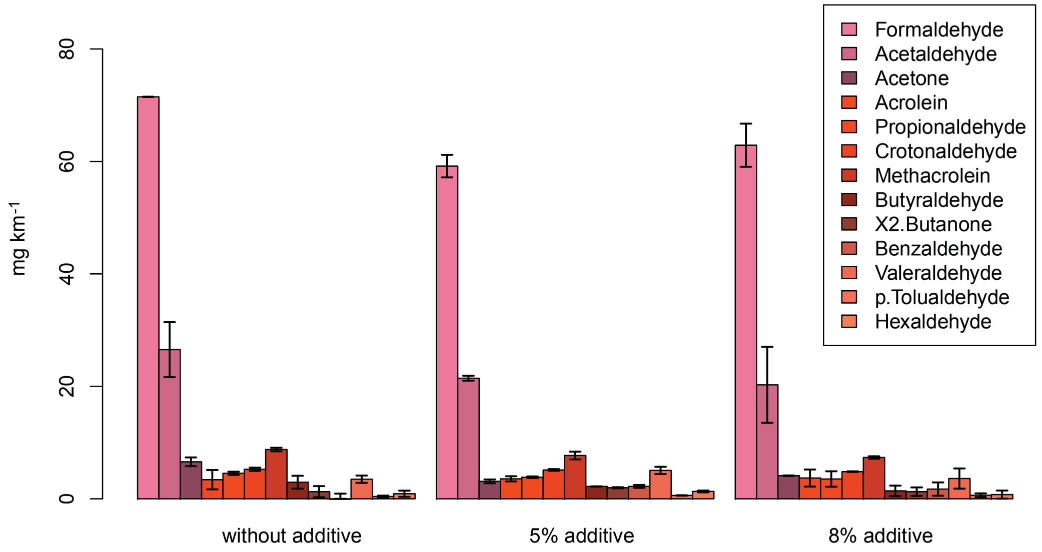

Figure 6.5: Effect of oxygenated fuel additive B on carbonyl emissions from the Euro II bus. - Carbonyls were sampled during the urban part of the ETC. Emissions factors displayed are the average of 2 tests, and error bars reflect the maximum and minimum values recorded with each fuel.

- Comprehensive study of gaseous and particulate exhaust emissions from the Euro III truck (vehicle 11 in the table 6.1).

Results from this last example are presented in the following scientific peer-reviewed paper.

Application of modern online instrumentation for chemical analysis of gas and particulate phases of Exhaust at the European Commission heavy-duty vehicle emission laboratory

T. W. Adam[a], R. Chirico[b,c], M. Clairotte[a], M. Elsasser[d,e], U. Manfredi[a], G. Martini[a], M. Sklorz[e], T. Streibel[e], M. F. Heringa[b],P. F. DeCarlo[f], U. Baltensperger[b], G. De Santi[a], A. Krasenbrink[a], R. Zimmermann[d,e], A. S. H. Prevot[b], and C. Astorga[a,*]

Analytical Chemistry - 2011, Volume: 83, Numero: 1, Pages: 67-76

[a] European Commission Joint Research Centre Ispra, Institute for Energy, Sustainable Transport Unit, 21027 Ispra, Italy

[b] Paul Scherrer Institut, Laboratory of Atmospheric Chemistry, CH-5232 Villigen, Switzerland

[c] Italian National Agency for New Technologies, Energy and Sustainable Economic Development (ENEA), UTAPRAD-DIM, Via E. Fermi 45, 00044 Frascati, Italy

[d] Institute of Ecological Chemistry, Cooperation Group Complex Molecular Systems/Joint Mass Spectrometry Centre, Helmholtz Zentrum München, 85764 Neuherberg, Germany

[e] Chair of Analytical Chemistry/Joint Mass Spectrometry Centre, Institute of Chemistry, University of Rostock, 18051 Rostock, Germany

[f] Drexel University, Department of Civil, Architectural and Environmental Engineering, Philadelphia, PA 19104, United States

Abstract

The European Commission recently established a novel test facility for heavy-duty vehicles to enhance more sustainable transport. The facility enables the study of energy efficiency of various fuels/scenarios as well as the chemical composition of evolved exhaust emissions. Sophisticated instrumentation for real-time analysis of the gas and particulate phases of exhaust has been implemented. Thereby, gas-phase characterization was carried out by a Fourier transform infrared spectrometer (FT-IR; carbonyls, nitrogen-containing species, small hydrocarbons) and a resonance-enhanced multiphoton ionization time-of-flight mass spectrometer (REMPI-ToF-MS; monocyclic and polycyclic aromatic hydrocarbons). For analysis of the particulate phase, a high-resolution time-of-flight aerosol mass spectrometer (HR-ToF-AMS; organic matter, chloride, nitrate), a condensation particle counter (CPC; particle number), and a multiangle absorption photometer (MAAP; black carbon) were applied. In this paper, the first application of the new facility in combination with the described instruments is presented, whereby a medium-size truck was investigated by applying different driving cycles. The goal was simultaneous chemical characterization of a great variety of gaseous compounds and particulate matter in exhaust on a real-time basis. The time-resolved data allowed new approaches to view the results; for example, emission factors were normalized to time-resolved consumption of fuel and were related to emission factors evolved during high speeds. Compounds could be identified that followed the fuel consumption, others showed very different behavior. In particular, engine cold start, engine ignition (unburned fuel), and high-speed events resulted in unique emission patterns.

Keywords: polycyclic aromatic-hydrocarbons; ionization mass-spectrometry; diesel-engine; black carbon; time; fuel.

6.1 Introduction

In recent years, it has been recognized that climate change and air pollution are linked in several ways, with transportation playing a key role (6, 280). It is the main source of anthropogenic nitrogen oxides (NO_x) and a major contributor of carbon dioxide (CO_2), volatile organic hydrocarbons (VOC), carbon monoxide (CO), and black carbon (BC) (25). CO_2 and BC are indicated as the largest contributors to global warming (6, 281). NO_x and VOC produce ozone by photochemical processes. Ground-level ozone is one of the air pollutants of most concern in Europe (238).

Freight transport contributes a large factor. The total freight volume increased in the European Union (EU) by 35% between 1996 and 2006 (excluding Cyprus and Malta), with road and air freight volumes rising faster than other sectors (282). Although, at the same time, total transport emissions of particulate matter (PM), acidifying substances, and ozone precursors decreased due to the continued tightening of emission standards and improvements of fuel quality, values remain high in many urban areas, which is still a major concern with respect to human health (49, 282).

To develop more sustainable transport, the European Commission recently established, at the Joint Research Centre (EC-JRC) Ispra, the currently most advanced vehicle emission laboratory (VELA) for heavy-duty (HD) in Europe. Research at this facility began in March 2009 (277). The fundamental idea was to provide an independent testing facility where it is possible to evaluate the impact of full-size trucks and buses on the environment under simulated road driving conditions by investigating a wide range of regulated and nonregulated combustion emissions. Additionally, the facility enables a more in-depth study of energy efficiency from present as well as future vehicles and fuels under various scenarios. In doing so, the facility is equipped to measure a great variety of fuels.

Substantial information can be found in the literature on the characterization of HD exhaust, mainly with focus on PM and regulated compounds. In summary, vehicle exhaust is a complex and dynamic mixture containing a large number of species. It consists of gaseous and particulate material, and many constituents partition between these two phases (see, for example, ref (283) and references therein). Attached laboratories at the HD test facility are capable of carrying out a great variety of chemical and physical analyses of the exhaust (see Fig. 6.6). Besides conventional online sensors for the main constituents, offline techniques are available for detection of many trace constituents. However, the exhaust composition changes continuously and can be influenced by many factors such as time, sampling, or chemical analysis, which might lead to aging and artifact formation. Subsequently, the ideal way to comprehensively investigate vehicle emissions and the combustion behavior would be to simultaneously analyze as many relevant components as possible, in both phases, in real time. As part of a joint project, several sophisticated online instruments were deployed together at the new testing facility. To measure gas-phase composition, a Fourier-transform infrared spectrometer (FT-IR) was implemented for coincident real-time analysis of up to 25 exhaust constituents. A resonance-enhanced multiphoton ionization time-of-flight mass spectrometer (REMPI-ToF-MS) was applied in order to evaluate gaseous monocyclic and polycylic aromatic hydrocarbons (PAH). Particulate-phase species were monitored with a high-resolution time-of-flight aerosol mass spectrometer (HR-ToF-AMS) used to identify the nonrefractory chemical composition of the particles. A multiangle absorption photometer (MAAP) was installed to measure the BC concentration. The particle number was measured with a condensation particle counter (CPC).

In this paper, we present the first application of the novel HD test facility in combination with the modern online techniques described above. The goal of this project was the simultaneous chemical characterization of a great variety of gaseous compounds and PM in HD exhaust on a real-time basis. Conventional offline methods were not considered in this work. The vehicle studied was a common in-use medium truck without any exhaust aftertreatment (Euro III). This enabled the investigation of raw exhaust emissions without being influenced by, for example, catalytic converters. For data processing and interpretation, we suggest some new approaches, and some selected results are shown. Besides presentation of concentrations of exhaust components, emission data were related to fuel consumption as well as concentrations during high speeds. In addition, chemometric data treatment methods were applied (shown in Supporting Information 6.5).

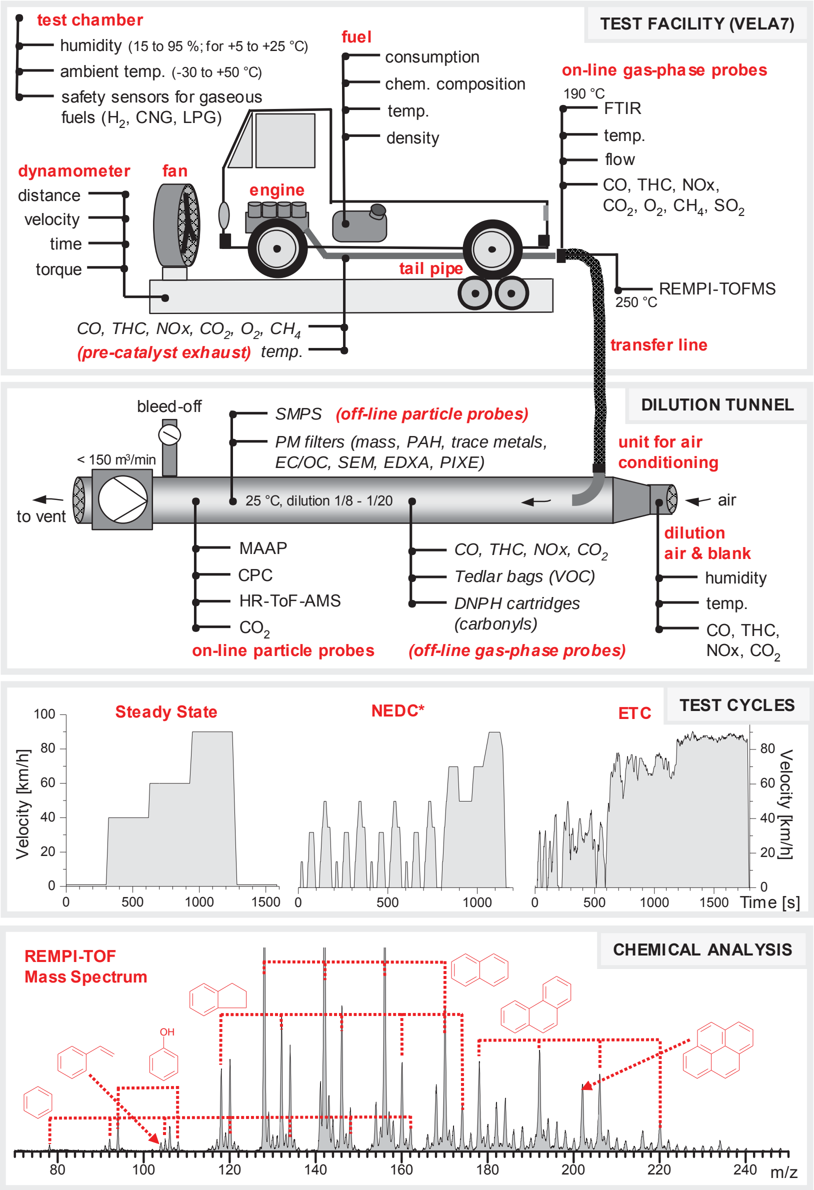

Figure 6.6: Sketch of the novel HD test facility and dilution tunnel including all measurement probes and sensors. - Probes shown in brackets and sensors/instrumentation shown in italic type were not considered in the framework of this study. In addition, the applied driving cycles ETC, NEDC, and steady state and a REMPI-ToF mass spectrum are shown. Therein, several aromatic species and their higher homologues are assigned to the corresponding signal peaks. (NEDC*: driving cycle was modified to a top speed of 90 km h^{-1} instead of 120 km h^{-1} for light-duty vehicles).

6.2 Experimental Section

All experimental work was carried out at the Vehicle Emissions Laboratory (VELA) of the Institute for Environment and Sustainability (IES) at the EC-JRC Ispra, Italy.

Truck and Fuel. The HD vehicle investigated was an in-use medium-size truck (empty weight 8 tons; odometer 140 000 km) of common type in Europe. It was not equipped with an aftertreatment device and complied with European emission standard legislation Euro III. Medium-size trucks are of particular interest because their numbers have grown faster than the numbers of large HD trucks in Europe (284). More information on the truck can be found in Table 6.2.

model	2002
engine	turbo diesel
emission level	Euro III
aftertreatment	none
power	176 kW at 3500 rpm
displacement	5880 cm^3
cylinders	4
weight empty	8 tons
injection system	common rail (1600 bar)
odometer	140 000 km

Table 6.2: Characteristics of the Investigated Heavy-Duty Truck.

For all tests, a certified reference diesel fuel was used. It had less than 10 ppm sulfur content and fulfilled EN 590 diesel standard. More detailed information on the diesel can be found in Table 6.4 in the Supporting Information.

Test Facility. Figure 6.6 is a scheme illustrating the most important features of the chassis dynamometer, test cell, and dilution tunnel. The chassis dynamometer (Zoellner GmbH, Germany) can host trucks and buses of up to 40 tons in weight, 12 m in length, and 5 m in height; maximal test speed is 150 km h^{-1}. The test cell can be conditioned between -30 and +50°C with relative humidity between 15% and 95% (in the temperature range of +5 to +25°C). It is equipped with safety sensors for gaseous fuels and an air circulation system that provides sufficient air exchange to run tests on hydrogen (H_2), liquefied H_2, liquefied petroleum gas (LPG), liquefied natural gas (LNG), and compressed natural gas (CNG) besides diesel and gasoline.

The constant-volume sampler (CVS) for full exhaust dilution (AVL, Graz, Austria) is equipped with 4 Venturis of 10, 20, 40, and 80 m^3 min^{-1} in order to achieve a maximum air flow of 150 m^3 min^{-1}. Dilution air is taken from the test cell, conditioned to 22°C, and filtered through high-efficiency particulate air (HEPA) and activated charcoal filters.

Driving Cycles. Three different driving cycles were conducted: the European transient cycle (ETC), the new European driving cycle (NEDC), and a steady-state speed test. All three cycles are illustrated in Fig. 6.6.

The ETC test cycle (also referred to as FIGE transient cycle) is applied for emission certification of HD diesel engines in Europe and is based on real road cycle measurements (123). The three different driving conditions simulated by the test are representative of urban, rural, and motorway driving. Duration of the entire cycle is 1800 s.

The NEDC test cycle is applied for emission certification of light-duty (LD) vehicles in Europe (171). This cycle consists of four repeated urban driving cycles and one extra-urban driving cycle and lasts for 1180 s. For this HD study, the NEDC cycle was modified so the maximum speed was 90 km h^{-1} for the extra urban part (instead of 120 km h^{-1} for LD vehicles). Although NEDC is not an official test cycle for HD vehicles, NEDC tests were carried out in order to observe the vehicleŠs behavior during a stop-and-go scenario and to verify the results from the ETC tests.

For ETC and NEDC, legislation requires a preconditioning of the vehicle including fuel of at least 6 h prior to the test with sampling starting at the engine start (cold test/engine) (123, 171). It should be noted that, in cold condition, the truck required some idling of ca. 20 s to reach the required operational air pressure before the test could be started. In addition, tests were performed that immediately followed a previous test (hot test/engine) in order to enable comparisons between both modes.

Finally, steady-state tests were performed, in which each state/velocity was kept for 300 s before continuing to the next speed. The applied states were idle; 40, 60, and 90 km h^{-1}; and again idle. This cycle is simple and comprises less acceleration events and varying velocities than ETC and NEDC. Although it does not reflect real-world driving conditions, it is suitable to study the complex formation and decomposition mechanisms of exhaust constituents. Steady-state tests were performed with the engine hot, that is, following a previous test. In total, five ETC, five NEDC, and six steady-state cycles were carried out.

Analytical Instrumentation. The test cell is equipped with various analyzers, sensors, and sampling ports for chemical and physical analysis of the exhaust (see Fig. 6.6). An FT-IR (model SESAM, AVL, Graz, Austria) enables the online measurement of gaseous constituents in undiluted raw exhaust with a time resolution of 1 Hz and a wavenumber resolution of 0.5 cm^{-1}. Quantification is carried out automatically by means of factory calibration, after a daily prerecorded background spectrum. The FT-IR was connected to the tail pipe via a heated transfer line including pump and PM filter (temperature 190°C; flow 4.6 L min^{-1}, length ca. 3 m). Temperature in the FT-IR system was held constant at 185°C. Results of the conventional sensors for NO_x (chemiluminescence) and CO/CO_2 (nondispersive infrared) analysis were continuously cross-checked with the concentrations of the FT-IR and turned out to be in very good agreement.

In addition, the following analytical devices were temporarily installed.

Resonance-Enhanced Multiphoton Ionization Time-of-Flight Mass Spectrometer. Time-resolved analysis of monocyclic aromatics and PAH was carried out by REMPI-ToF-MS. This technique is known to be a sensitive online method for the detection of gaseous aromatic species. A home-built, mobile photoionization mass spectrometer (Mass Spectrometry Centre, University of Rostock) was applied. The heated transfer line of the REMPI-ToF-MS was attached orthogonally to the heated sampling line of the FT-IR described above. The former consisted of a deactivated silica capillary (length 1.5 m, i.d. 0.32 mm, T 220°C) by which a constant volume of exhaust was continuously drawn into the instrument (flow 8 mL min^{-1}; residence time <1 s). This enabled the analysis of undiluted and nonaged exhaust. The principle of REMPI-TOFMS is described in detail in the literature (see, for example, refs (260, 261, 262) and references therein), and therefore only a brief description is given here. Fundamental Nd:YAG laser pulses (1064 nm) are used for nonlinear generation of UV light (266 nm). The UV pulses are directed into the ionization chamber straight underneath the inlet needle of the transfer line. Soft photoionization (without fragmentation) of the aromatic species in the exhaust is induced by a sequential two-photon absorption process via an electronic transition state. The generated molecular ions are extracted into the flight tube of the reflectron ToF-MS. Mass spectra are recorded via an ultrafast analog-to-digital converter PC card (Acqiris, Switzerland). Data processing is done by a LabView (National Instruments) based custom-made software. Calibration is performed by applying external gas standards and was done for a variety of monocyclic aromatics, for example, benzene, toluene, and C2-benzene (Cx = C_xH_{2x} side chains).

Compounds where no calibration gases are available were semiquantified by multiplying the measured signal by the ratio of the photoionization cross-section of the target compound and one of the calibrated species. The photoionization cross-section is a property that accounts for the compoundŠs probability of being ionized under certain conditions and is constant for a fixed UV wavelength and photon density (170). As a consequence, the ratio of two photoionization cross sections is also constant. These ratios were determined beforehand under lab conditions at the Mass Spectrometry Centre of the University of Rostock. Detection limits depend on various parameters such as spectroscopic properties of the compounds, laser characteristics (e.g., wavelength, pulse energy) as well as time resolution (averaging) and can be in the parts per trillion (ppt) region for specific compounds (285). For the present setup, detection limits were determined to be 670 ppb for benzene and 8.4 ppb for naphthalene, with a linear range of 10^4 (263). A verification with conventional offline techniques can be found in, for example, ref (286). In principle, 20 complete mass spectra per second can be recorded since a 20 Hz laser was used. In the framework of this paper, online data were averaged to a time resolution of 1 Hz. A REMPI mass spectrum of the truckŠs exhaust emission at 90 km h^{-1} is illustrated in Fig. 6.6. Signal peaks are assigned to the exhaust components benzene, phenol, styrene, indane, naphthalene, phenanthrene, pyrene, and higher homologues.

High-Resolution Time-of-Flight Aerosol Mass Spectrometer. The HR-ToF-AMS (Aerodyne) enables real-time measurements of the submicrometer nonrefractory aerosol components such as organic matter (OM), sulfate, nitrate, and chloride. The term Şnonrefractory" is assigned to the species that evaporate rapidly at the AMS heater temperature (165). A detailed description of the principle and the instrument can be found elsewhere (for example, refs (287) and (163)). In brief, particles enter the system through an aerodynamic lens, forming a narrow beam, which in turn is transmitted into the ionization volume where nonrefractory species are flash-vaporized upon impact on a hot surface (≈600°C) under high vacuum and ionized by electron ionization (EI) at 70 eV. After ionization, mass spectra are recorded by a high-resolution ToF-MS. The inlet system has 100% transmission efficiency of particles in the vacuum aerodynamic diameter range 70-500 nm and substantial transmission of particles in the 30-70 nm and 500 nm-1.5 μm ranges. The instrument is calibrated with ammonium nitrate. A relative ionization efficiency of 1.4 is used for organic molecules. The detection limit of the HR-ToF-AMS is ca. 0.04 μg m^3 for a time resolution of 1 min. Data analysis was done in Igor Pro 6.03A (Wavemetrics, Lake Oswego, OR) by use of the AMS Analysis Toolkit Squirrel v.1.44.

Gas-phase corrections were made by HEPA-filtered air sampled at the end of each test with the engine running at idle mode. Temporal fluctuations of the diluted CO_2 concentration were measured during each test by means of an IR gas analyzer (model LI-7000, LI-COR Biosciences). The varying gas-phase CO_2 concentrations were taken into account to estimate the temporal contribution of the organic aerosol at m/z 44.

Condensation Particle Counter. The particle number was investigated by a condensation particle counter (CPC, model 3022A, TSI). It had a flow of 0.3 L min^{-1} through the measuring cell with a detection limit of 0.2 particle cm^3 on average.

Multiangle Absorption Photometer. Concentrations of BC were determined with a MAAP (model 5012, Thermo). The MAAP quantifies the BC content of the aerosols by measuring the optical absorption of light at 630 nm by particles collected on a glass fiber filter. The conversion to BC is done by assuming a standard absorption efficiency of 6.6 m^2 g^{-1}. The detection limit is better than 0.1 μg m^3 for 2 min averages (167).

HR-ToF-AMS, MAAP, and IR gas analyzer sampled from the CVS by use of an in-house built Dekati dilutor system consisting of a stainless steel tube (length 3 m, i.d. 10 mm, residence time 1 s, not heated).

Data Analysis. Data from the instrumentation sampling at the tail pipe and the CVS were gathered and corrected for dilution, temperature, pressure, and delay times. A summary of all quantified exhaust components by the described techniques can be found in Table 6.3.

gas phase			**particulate phase**		
FT-IR		**REMPI-ToF-MS**	**HR-ToF-AMS**	**MAAP**	**CPC**
CO_2	formaldehyde	benzene	organic mass	black carbon	number
CO	acetaldehyde	C1-C6 benzenes°	sulfate		
H_2O	formic acid	naphthalene	nitrate		
NO	ethane	C1-C6 naphthalenes°	chloride		
NO_2	propane	phenanthrene	ammonium		
N_2O	ethene	C1-C3 phenanthrenes°			
SO_2	acetylene	pyrene			
		C1-C2 pyrenes°			

Table 6.3: These were quantitatively investigated by the various analytical online techniques. ° Cx = C_xH_{2x} side chains.

Interpretation of the comprehensive data set was carried out by different approaches. First, data are presented as the componentsŠ emission in terms of mass per time (time resolution for gas-phase components was 1 s; time resolution for particulate phase components was 5 s). This gives the truckŠs time-resolved contribution of exhaust emission to the atmosphere. Results of this approach are referred to as "emissions". Second, in order to study the relationship between exhaust components and fuel consumption, emissions were divided by the amount of consumed fuel. Results are described as "emission factor_consumption" (ef_c) and given in mass of compound per volume of fuel. Additionally, emission of each species was normalized to its corresponding value at high speed with the engine hot. This is a new approach to assess the influence of, for example, cold engine starts, intensive accelerations, etc., in comparison to constant speeds and warmed-up engines. Therefore, emissions of the constant top speed of 90 km h^{-1} were averaged over 200 s. This mean value (abbreviated as 90_hot) was subtracted from all the time-resolved emission values for all tests; then results were divided by 90_hot. Results are named as "emission factor_normalization"(ef_n) and, expressed in percent, account for the percent increase or decrease of the emitted compound in relation to 90_hot (i.e., 0% means no change compared to 90_hot, and +100% signifies a doubling of the emission). Moreover, the data set was incorporated in chemometric data analysis methods (principal component analysis, PCA) to visualize possible changes in the overall chemical pattern of the emissions. Selected results are presented in Fig. 6.10 in the Supporting Information.

6.3 Results and discussion

Online Data (Emission). Figure 6.7 shows some selected examples of exhaust components as well as engine and emission properties of a steady-state test, whereby the various gradients demonstrate the complexity of exhaust composition and generation. Data was processed as described for emissions.

Exhaust temperature, exhaust volume, and air/fuel ratio (Fig. 6.7A) are crucial factors for the emission. The exhaust temperature strongly influences formation and decomposition reactions; the volume determines the absolute yields. The temperature, measured at the tailpipe, featured moderate increases during the three constant speeds but significant changes between the different states (on average, 40 km h^{-1}, ca. 110°C;

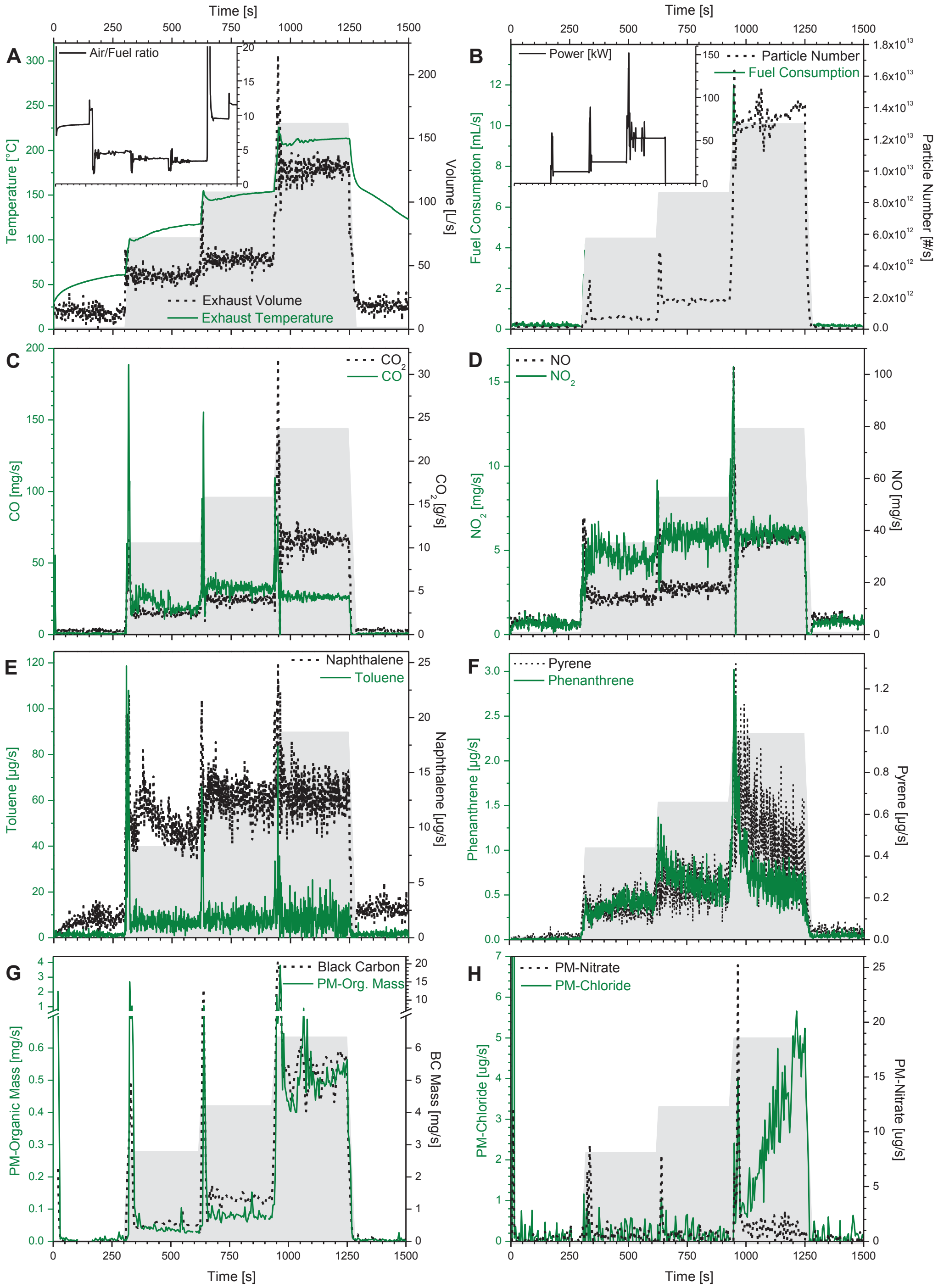

Figure 6.7: Results (emissions) of the following selected exhaust/engine properties and constituents of the HD truck by applying the steady-state test. - (A) exhaust volume, exhaust temperature, and air/fuel ratio (inset); (B) particle number, fuel consumption, and power (inset); (C) CO and CO_2; (D) NO and NO_2; (E) naphthalene and toluene; (F) pyrene and phenanthrene; (G) black carbon and PM organic mass; and (H) PM nitrate and PM chloride. The driving cycle is indicated in gray (idle, 40-60-90 km h^{-1}, idle).

60 km h^{-1}, ca. 150°C; 90 km h^{-1}, ca. 210°C). Temperature variations during both idling phases were more strongly pronounced than for the three velocities.

The acceleration phases were reflected in the exhaust volume by sharp peaks. Differences of the flows for the constant speeds of 40 and 60 km h^{-1} were small (both ca. 50 L s^{-1}) compared to the volume for 90 km h^{-1} (ca. 125 L s^{-1}).

The air/fuel ratio is often defined in terms of the excess air factor, or λ factor. A λ factor of unity ($\lambda = 1$) corresponds to an air/fuel ratio of 14.7:1. This is the stoichiometric ratio of air and fuel that is required for complete combustion. A greater portion of fuel ($\lambda < 1$) is termed a rich mixture, whereas a greater portion of air ($\lambda > 1$) gives a lean mixture. The air/fuel ratio for the three velocities was low and showed only small variations; however, during both idling phases the proportion of air rose and reached a λ factor close to unity. At the deceleration, the air/fuel ratio increased tremendously because hardly any fuel was provided.

A further important factor for emission is the fuel consumption, which is directly related to the exhaust volume and the engine power (Fig. 6.7B); consumption was up to ca. 4 mL s^{-1} during 90 km h^{-1} with approximately a 3-fold increase for the preceding acceleration. The compounds measured behaved in different ways with respect to fuel consumption. Some compounds showed a strong dependence on fuel consumption, others a weak dependence, and some species showed little to no dependence.

Compounds like CO_2 (Fig. 6.7C), NO (Fig. 6.7D), H_2O, SO_2, N_2O, and to a certain extent acetylene, pyrenes (Fig. 6.7F), and some higher homologues of benzene (starting from C3-benzene) featured a very similar trend as the fuel consumption.

The PM parameters particle number (Fig. 6.7B), organic mass (Fig. 6.7G), and BC (Fig. 6.7G) featured a similar behavior but yields for the top speed of 90 km h^{-1} were even higher; for example, particle number increased by 7-fold from 60 to 90 km h^{-1}.

Nonrefractory particulate chloride (Fig. 6.7H) showed a unique profile. Apart from the common peaks for the acceleration events, emissions were continuously increasing to ca. 5 μg s^{-1} during the 90 km h^{-1} state. The reason for this might be an increasing influence of lubricant oil during long periods of high speed. None of the other investigated compounds followed this behavior. Similar observations were made for the driving cycles NEDC and ETC, with PM chloride appearing only during the final high-speed step. During the extra-urban phase of NEDC, values rose to ca. 3 μg s^{-1}, whereas for the motorway phase of ETC, an increase and subsequent saturation at ca. 10 μg s^{-1}

could be observed. This indicates that HD emission might be a perceptible source of non-sea salt particulate chloride.

Numerous constituents had elevated but similar emissions for the three different velocities, with short-time peaks occurring during the accelerations. Compounds belonging to this class were, for example, CO (Fig. 6.7C), NO2 (Fig. 6.7D), benzene, toluene (Fig. 6.7E), C2-benzene, naphthalenes (Fig. 6.7E), formaldehyde, formic acid, ethane, and to a certain extent phenanthrenes (Fig. 6.7F). The different behaviors of NO_2 and NO were interesting since both compounds are usually analyzed as a sum (NO + NO_2 = NO_x), whereby the overall trend is dominated by the higher amounts of NO.

Species like CO or formaldehyde are preferably formed under less complete combustion conditions than the previous group of oxygen-containing compounds (CO_2, H_2O, etc.). Consequently, the more extreme conditions during higher speeds with higher fuel consumption and higher engine temperatures did not lead to a further increase of their emissions. Reaction mechanisms during combustion are complex and depend on various parameters. In terms of aromatic species in diesel exhaust, two main mechanisms are known: (1) compounds present in the fuel survive the combustion process (survival pathway) and (2) formation by partially fragmented species (pyrosynthesis pathway) (see refs (46, 288, 289) and references therein). An additional source is provided by unburned or modified lubricating oil. Rhead and Hardy (46) studied the fate of various radiolabeled PAH species added to the fuel and concluded that both survival and pyrosynthesis contributed to PAH levels in exhaust emissions. Survival played a greater role for benzo[a]pyrene, for example, whereas naphthalene mainly originated from pyrosynthesis. The vast majority of the naphthalene recovered had been formed from sources other than original naphthalene in the fuel. However, a dependency on engine conditions such as speed and load was reported as well. Different preferred conditions for PAH were confirmed in our study, which is demonstrated by means of the examples naphthalene (Fig. 6.7E), phenanthrene (Fig. 6.7F), and pyrene (Fig. 6.7F). In this study, the profile of naphthalene showed a similar profile as CO; that is, hardly any differences for the three velocities. In contrast, the occurrence of pyrene was pronounced for the high-speed event.

In the case of some monoaromatics like toluene (Fig. 6.7E) and benzene, strong signals for the three acceleration phases were determined but the emissions during the constant velocities were comparably low. This indicates a potential influence on these species from excessive fuel. Intense signal peaks during accelerations were also observed for particulate nitrate (Fig. 6.7H).

The ratio of emissions between PM organic mass and BC varied for the three velocities (Fig. 6.7G). While for 90 km h^{-1} the ratio of PM organic mass to BC (OM/BC) was roughly 10%, this value was less for the lower velocities. A possible role could have been that concentrations of volatile organic compounds might be higher in the CVS due to reduced dilution factors (30, 25, and 10 for 40, 60, and 90 km h^{-1}, respectively), which influences the gas to particle partitioning of intermediate/semivolatile compounds (37). Similar levels (with oxidation catalyst) have been reported by others (290, 291). For some tests, extraordinarily high peaks of PM organic mass (up to 1.5 g m^3) were detected during the first seconds of the test. However, this was not the case for all runs. This effect was probably caused by unburned fuel passing through while the engine was started.

Fuel Consumption (Emission factor_consumption). Another way in which to view the data is by means of the "emission factor_consumption", abbreviated as ef_c. Figure 6.8 depicts this method for a steady-state test by four selected examples: CO (Fig. 6.8A), NO (Fig. 6.8B), naphthalene (Fig. 6.8C), and phenanthrene (Fig. 6.8D). CO had the highest ef_c during the start and the first and second acceleration phase. At 40 km h^{-1}, ef_c fluctuated until a rather constant value of 18 mg mL^{-1} was reached. This ef_c was similar for 60 km h^{-1} (after the acceleration event). During the 90 km h^{-1} phase, a lower ef_c of ca. 7 mg mL^{-1} fuel was observed. This value is similar to the first idle phase and only slightly higher than the second idling. Subsequently, the vehicle featured the lowest CO ef_c for the top speed and both idle phases. For the moderate velocities of 40 and 60 km.h^{-1}, ef_c increased by more than a factor of 2.

In general, compounds with similar trends for emissions exhibited similar behaviors for ef_c; however, for some species a closer look revealed variations. Ef_c of phenanthrene (Fig. 6.8D) increased in the second idling phase (ca. 0.25 μg mL^{-1}) compared to the first idling phase, although consumption was about the same. This indicates that, under idling conditions, phenanthrene is preferably formed when the engine is very hot (directly after a high-speed event). Memory effects in the exhaust pipe might play a role as well. Most of the investigated PAH in this study showed this behavior, especially phenanthrenes and pyrenes. The effect was also notable for naphthalenes and higher homologues of benzene (from C3-benzene) but to a lesser extent.

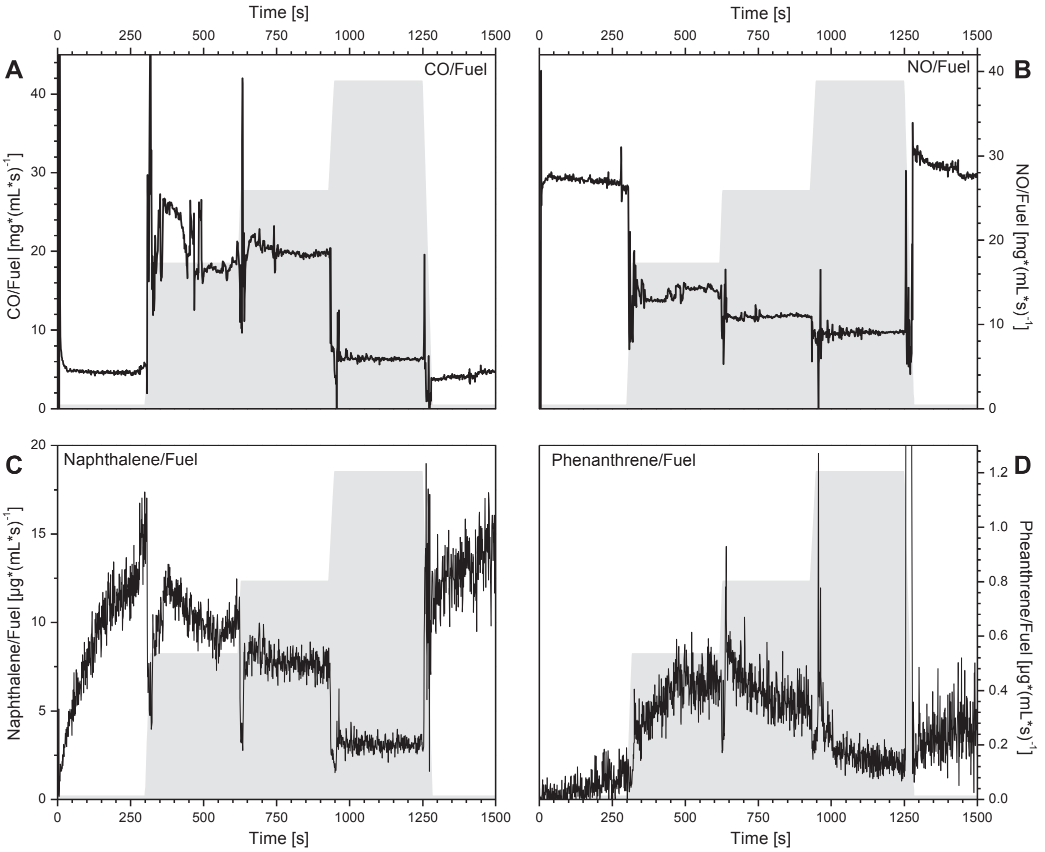

Figure 6.8: Emission factors_consumption (ef_c, normalized to fuel consumption) of the following selected exhaust constituents of the HD truck by applying the steady-state test: (A) CO, (B) NO, (C) naphthalene, and (D) phenanthrene. - The driving cycle is indicated in gray (idle, 40-60-90 km h^{-1}, idle).

NO (Fig. 6.8B) showed a different trend, which followed the profile of the air/fuel ratio (Fig. 6.7A). Here, both idling phases reached the highest ef_c of ca. 28 mg mL^{-1}, whereby hardly any differences could be observed for the two states. Ef_c values for the constant speeds were lower and decreased with increasing velocity. The same behavior was observed for H_2O, SO_2, and to a certain extent monoaromatics and two-ring PAH like naphthalene (Fig. 6.8C). However, ef_c of naphthalene (and higher homologues) slowly increased during the first idling phase. The reason could be a memory effect in the exhaust pipe or the growing importance of pyrosynthetic formation. In contrast to most other components, naphthalene showed a sharp decrease in every acceleration phase. This indicates a lack of dependence on excessive fuel for its presence in exhaust, confirming the findings by Rhead and Hardy (46).

Data Normalized to High-Speed Emission (Emission factor_normalization). Ignition of the engine (unburned fuel) and cold-start phase are crucial events for the emission of air pollutants. Figure 6.9 illustrates ef_n of four selected examples measured with the engine cold and hot. Figure 6.9 panels A and B show organic PM and CO for the ETC driving cycle. Figure 6.9 panels C and D illustrate the first 600 s of naphthalene and toluene under the NEDC cycle. The gray dashed line at 0% signifies no change in comparison to 90_hot. For organic PM (Fig. 6.9A), the largest factor increase compared to 90_hot occurs during the engine start. Ef_n increased shortly by more than 1 order of magnitude. However, no clear difference between cold and hot engine could be observed for the test start. This indicates once more that the unburned fuel traveling through the engine during ignition was mainly responsible for the elevated levels of organic PM. The engine temperature seemed to play a minor role. Later, the transitions from the urban to the rural phase and from the rural to the motorway phase resulted in ef_n of sometimes similar measures. During the urban and rural phases, variations in the range of ±100% could be observed with the cold tests leading to higher and mainly positive ef_n at velocity changes compared to the hot tests. During the final motorway phase, the engine has warmed up and ef_n values were close to 0% (i.e., emissions were about the same as at 90_hot). This visualizes that engine start and dramatic velocity changes can contribute significant amounts of particulate organic matter to the atmosphere. These short-time concentrations are much higher than during high constant speeds.

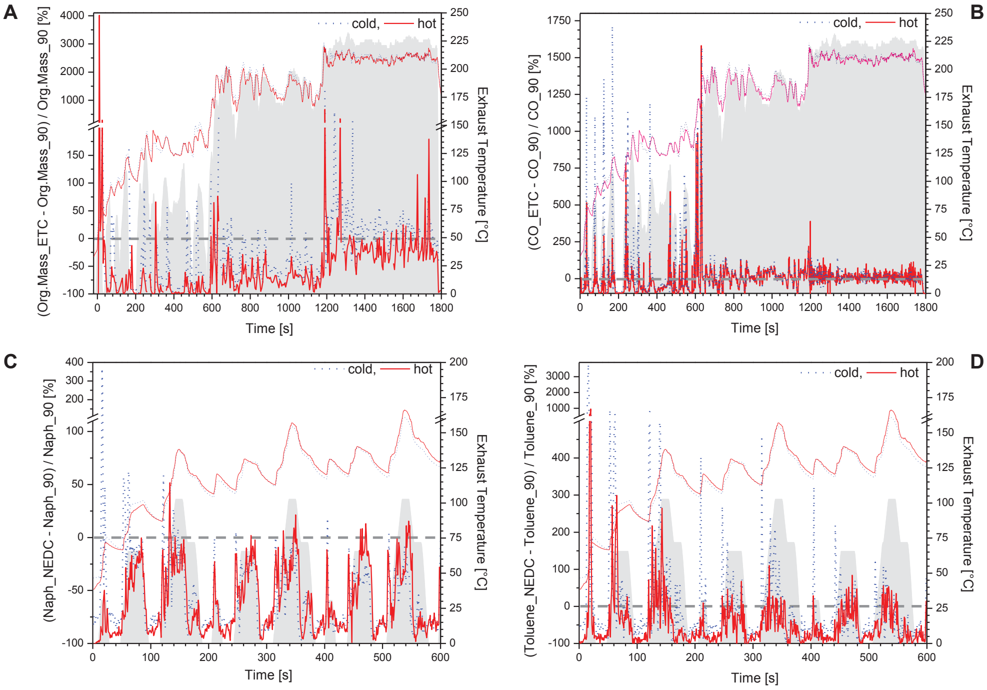

Figure 6.9: Emission factors_normalization (ef_n, normalized to 90 km h^{-1} of a steady-state test) of the following selected exhaust constituents and corresponding exhaust temperatures of the HD truck with the engine hot (solid red lines) and cold (dotted blue lines) at test start by applying the driving cycles ETC (panels A and B) and NEDC (panels C and D): (A) PM organic mass, (B) CO, (C) naphthalene, and (D) toluene. - The driving cycle is indicated in gray (for NEDC, only half the cycle is shown); for units of velocity see Fig. 6.6.

CO showed a different behavior (Fig. 6.9B). Ef_n featured a strong difference between the engine hot and cold, with the latter resulting in an up to 10-fold increase for almost all accelerations of the urban phase. The last strong signals occurred for both modes during the transition from the urban to the rural phase. A short rise could be detected during the transition from the rural to the motorway phase. For the rest of the test ef_n fluctuated around 0%. Subsequently, once the exhaust temperature increased to ca. 180°C and the velocity reached ca. 70 km h^{-1}, CO emissions remained constant at concentrations similar to 90_hot. Consequently, the greatest contribution of CO is caused by velocity changes with a cold engine. These short-time contributions can be more than an order of magnitude higher than at high constant speeds.

For some species the status of a warmed-up engine is reached earlier than for others. The individual warm-up phase can be visualized by the gradual approximation of the compoundsŠ emission when a hot test and a cold test are illustrated together. Ef_n values of naphthalene (Fig. 6.9C) and toluene (Fig. 6.9D) are shown as examples. For naphthalene, the first accelerations under hot engine conditions led to similar emissions as at 90_hot (ef_n close to 0%). In contrast, the first acceleration with the cold engine produced higher emissions (ef_n of several hundred percent) but the signals converged to the values of the hot engine within three acceleration events (ca. 150 s, exhaust temperature >100°C). After that, no clear difference between the two modes could be observed anymore. For toluene, the cold and hot engines lead to positive ef_n with the first acceleration being more than an order of magnitude higher than at 90_hot. Approximation of ef_n to 90_hot took longer (hot test ca. 200 s, cold test ca. 450 s) than for naphthalene. For the rest of the cycle, no difference between cold and hot modes was observed (data not shown). An explanation might be varying proportions of survival and pyrosynthesis for toluene and naphthalene during hot tests and cold starts. This demonstrates that aromatic compounds in vehicle emission cannot be treated across-the-board but have different individual behaviors based on many variables.

Finally, cold start signals of various components are not aligned with hot mode signals throughout NEDC runs. This was usually not observed for the ETC tests. This suggests that NEDC did not lead to a complete warm-up of the tested truck engine for some exhaust components.

6.4 Conclusion

The new testing facility in combination with modern online instrumentation has given new insights into the formation and decomposition conditions of exhaust components by applying new methodologies of data interpretation. It has been demonstrated that the sole interpretation of offline data and focus on regulated compounds is not sufficient to unravel the complex behavior of vehicle emission. However, to have deep knowledge on this is a prerequisite in order to eliminate hazardous species from exhaust.

The results obtained in this work will be used for comparisons with upcoming tests. Similar measurements are planned with different fuel types (biodiesel, ethanol, CNG, LPG) and fuel additives to suppress PM formation, as well as modern aftertreatment and engine technologies (selective catalytic reduction, diesel particulate filter, oxidation catalyst). Emission factors determined from these studies will be used for source apportionment studies. Moreover, data can be converted to enable comparisons with results from the EC-JRC test bench for HD engines.

In this regard, the new HD test facility will play a key role in support to EU Member States and the European Commission for the development and implementation of EU policy on emissions and air quality.

- **Acknowledgments**

The VELA staff is acknowledged for their skillful technical assistance, in particular R. Colombo, M. Sculati, G. Lanappe, F. Muhlberger, and P. Le Lijour. This work was supported by the NEADS project (Next Generation Exhaust aftertreatment for Diesel Propulsion Systems) of the Competence Center Energy and Mobility (CCEM).

6.5 Supplementary Materials

Property	Units	Limits		Test Method
		Min.	Max.	
Cetane number		52.0	54.0	EN-ISO 5165
Density at 15°C	kg m^3	833	837	EN-ISO 3675
Distillation				EN-ISO 3405
50% v/v point	°C	245	-	
95% v/v point	°C	345	350	
FBP	°C		370	
Flash point	°C	55	55	EN 22719
CFPP	°C	-	-	EN 116
Viscosity at 40°C	mm^2 s^{-1}	2.5	3.5	EN-ISO 3104
PAH	% m/m	3.0	6.0	IP 391
S content	mg kg^{-1}	-	300	pr. EN-ISO/DIS 14596
Cu corrosion		-	Class 1	EN-ISO 2160
Conradson C residue on 10% dist. residue	% m/m	-	0.2	EN-ISO 10370
Ash content	% m/m	-	0.01	EN-ISO 6245
H_2O content	% m/m	-	0.02	EN-ISO 12937
Neutralisation (strong acid) number	mg KOH g^{-1}	-	0.02	ASTM D974
Oxidation stability	mg mL^{-1}	-	0.025	EN-ISO 12205

Table 6.4: Characteristics of the used reference diesel fuel, Directive 2002/80/EC - Type I Emissions Certification Test (Euro 3 Limits).

Description Fig. 6.10 . Due to the high number of analyzed aromatic compounds, only the non-methylated structures as well as toluene were used. Scattering of the scores of the accelerations was greater than for the steady states, which indicates a rapid change of the chemical pattern during acceleration. A clear discrimination between all accelerations was observed with the final deceleration being unique. Acceleration to 90 km h^{-1} (60 - 90) was separated on PC1, which are mainly species following the fuel consumption. In contrast, acceleration to 40 km h^{-1} (0 - 40) was stronger influenced by CO and compounds with a similar behavior on PC2. The second acceleration event (40 - 60) was found between the two others. With PCA no clear difference of the overall chemical patterns between the first and the second idling phase could be determined (therefore 'idle' represents idle 1 and idle 2). For the three constant velocities, two main clusters were formed. The moderate velocities of 40 km h^{-1} and 60 km h^{-1} featured rather similar chemical patterns but for 90 km h^{-1} a separation occurred on both PC. Besides the same components as for the clustering of the acceleration events, particle properties played a bigger role for the separation of the high speed. The preceding acceleration (60 - 90) was slightly more influenced by components

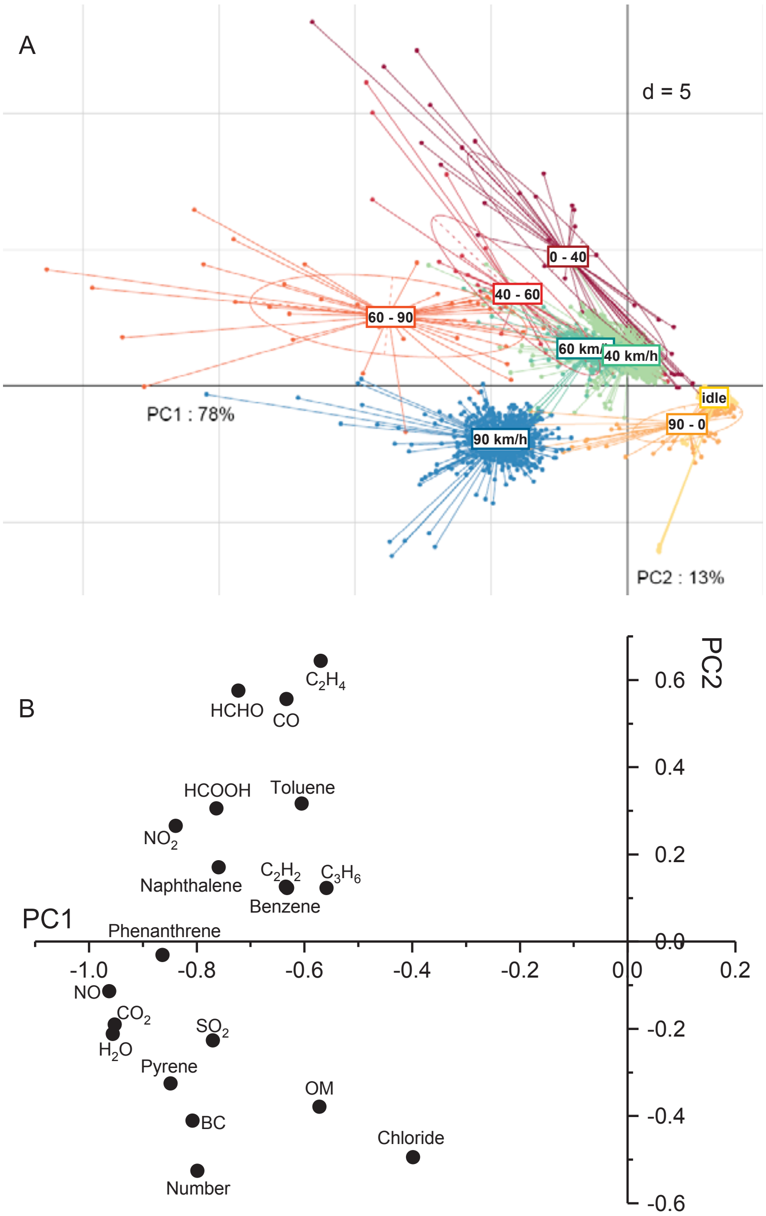

Figure 6.10: Score-plot (A) and loading-plot (B) of steady states (idle 1, 40 km h^{-1}, 60 km h^{-1}, 90 km h^{-1}, idle 2) and acceleration events (0-40 km h^{-1}, 40-60 km h^{-1}, 60-90 km h^{-1}, 90-0 km h^{-1}). - Prior to PCA autoscaling of the data set was carried out.

indicating unburned fuel and incomplete combustion e.g. carbonyls, small aromatics, small hydrocarbons, CO. As a result, it can be concluded that PC1 is strongly related to the fuel consumption, PC2 characterizes the behavior during the high speed step (90 km h^{-1}); the more negative the loadings of PC2 the greater is the contribution during 90 km h^{-1}. Most likely, PC2 is influenced by warm-up and temperature effects of e.g. engine and exhaust pipe.

Chapter 7

Conclusions and perspectives

This project aimed at contributing to the knowledge on vehicular emissions, in terms of regulated and unregulated pollutants. Several objectives were fixed in order to promote a better understanding of pollutant formation mechanisms, and emission factors from a wide range of on-road vehicles. A particular interest was paid to the radiatively active species on climate, and to the harmful pollutants for human health.

Our first objective was to assess and compare the emissions from a fleet of vehicles including mopeds, light, medium and heavy-duty vehicles (cf. chapter 3). In addition, the effect of alternative fuels such as ethanol and biodiesel on the environment and human health was addressed in this project, together with the impact of custom driving cycles. This first study carried out at the beginning of the PhD program had the ambition to provide an inventory of the situation in terms of aerosol and unregulated gaseous emissions on which the subsequent studies could be based. In addition, an original set of analytical instrument dedicated to the characterization of these pollutants was gathered and tested together for the first time in the VELA facilities during chassis dynamometer experiments. For the gaseous phase, the chemical analysis of the nitrogen species, the small hydrocarbons, and some small oxygenated hydrocarbons was achieved by a HR-FTIR; the PAHs by a REMPI-ToF-MS; the non-oxygenated VOCs by a GC-FID; and the carbonyls by a HPLC-UV. For the solid phase, the chemical analysis of the aerosols was realized by a HR-Tof-AMS and a MAAP, whereas the physical analysis was realized by a FMPS and a CPC. The results of the first campaign indicated that among the vehicles investigated, the mopeds were the highest emitters of organic aerosol, with several orders of magnitude of differences with respect to the other vehicles. Concerning the chemical speciation of the PM emitted from both diesel and gasoline engines of the fleet, moped excluded, the composition consisted mostly of BC. The highest emission factor of BC (in g km^{-1} and in g kg^{-1} of fuel) came from the diesel heavy-duty vehicle. Concerning the gaseous pollutants, the mopeds were once again the top emitter of HC and PAHs, followed by the gasoline light-duty vehicles and the diesel vehicles. The fuel quality of the mopeds (mixture of gasoline and lubricant oil), together with the low combustion efficiency of their two-stroke engines explained this result. Finally, the NO_x emissions was particularly high for the heavy duty vehicles, both in terms of g km^{-1} and g kg^{-1} of fuel. As for the biofuel topic, the objective to investigate their impact was only partially reached. Whereas experiments conducted with blends of rapeseed methyl ester biodiesel displayed lower emission of OA, BC and HC, experiments conducted with ethanol were inconclusive because of vehicle malfunction. Overall, the objectives of this project were mainly achieved, and the data collected gave a brief snapshot of the current emissions due to on-road transport in EU. The emission factors obtained in this study could be useful to update emission inventories used in chemical transport models, and therefore, could contribute to assess the impact of the transport sector on the environment and human health. Nevertheless, only a limited number of vehicles were tested during these 3 years and further research is needed on more modern vehicles to complete and consolidate this inventory.

Effect of exhaust aftertreatment strategies on moped emissions

The chapter 4 of this project aimed to investigate in more details the emissions from the mopeds. This category of vehicles has the same emission standard in force since 2002, which is rather old. However, mopeds can be a very popular means of transport in some area where the traffic situation becomes complex. The inventory provided previously presents moped as the higher emitter of PM and VOCs. These findings associated to the mopeds pushed us to give particular emphasis to the aerosol emission patterns. This investigation was all the more interesting because PM belongs to the unregulated pollutants for the mopeds according to the regulation Euro 2 in force at the date of these experiments. Among the set of instruments implemented during the campaign described previously, most of them had the capability to provide time-resolved data series of emission. This project aimed to describe in detail the emission patterns of 2 mopeds belonging to 2 emission standards (Euro 1 and 2). A special interest was applied on the role played by the engine technologies and aftertreatment devices (carburetor with oxidant catalyst on one side and direct injection with an oxidant catalyst and a secondary air system on the other) on the regulated emission abatement, and the unregulated solid emissions.

The emissions patterns were compared using a multivariate analysis which aimed to highlight the potential underlying correlation that could be present between emissions profiles, or between emissions and physical parameters of the engine. Through principal components analysis of the time-resolved data, the importance of the temperature on the aerosols emissions was demonstrated. The strategy selected for the more modern moped equipped with the secondary air system consisted in providing additional air in the catalyst in order to achieve a more complete combustion. However, this air injection had the side-effect to cause lower temperature in the catalyst, which could be the cause of the condensation of the less volatile fraction of the gaseous HC. In this way, the HC abatement was even better, but at the expense of higher primary organic aerosol emissions. Consequently, after atmospheric dilution and evaporation of the particulate emissions, the environmental impact in terms of HC of the modern Euro 2 moped could be at the same level as the older Euro 1.

For the motorbike, the catalyst size and the exhaust temperature are generally lower than in light-duty application, which result in lower catalyst performance. This study highlighted the temperature constraints encountered when SAS is used. The pre-heating of the air injected by the SAS could represent a part of the technical solution to both reduce primary aerosol and HC emissions. These results illustrate the impact that a new emissions standard could have on the unregulated emissions (here the aerosols). Exploratory research in the field of the unregulated emissions is crucial to update the list of pollutants to include in the next standard and to guide the technical choice for the manufacturer to comply with.

Impact of alternative fuels on modern light-duty vehicle emissions

As the initial targets addressed by the chapter 3 were not fully reached, in particular concerning the impact of ethanol fuel on the direct emission of vehicles, this point was approached in detail during two additional experimental campaigns dedicated to the impact of alternative fuels on the unregulated emissions (cf. chapter 5). Two different engine technologies dedicated to light-duty vehicles were investigated during this project. Emissions from modern engines tuned to be fed by ethanol fuel in high concentration (E85) and LPG were monitored. In addition, the effect of the cold ambient temperature (-7°C) was explored when ethanol fuel was used. Whereas emissions associated to E85 were found to be lower in terms of toluene and NH_3, the same fuel displayed larger emissions of acetaldehyde and methane, especially at low ambient temperature (-7° C). Consequently, the OFPs associated to the use of oxygenated fuel were considerably higher at low temperature in comparison with standard fuel. Indeed, the main precursors of ozone were two-carbon chain hydrocarbons mostly present when high ethanol content fuel was used. Concerning the LPG, in spite of the reduction of CO_2 emission, most of the other exhaust constituents were found emitted at equivalent level in comparison with standard fuel. For the modern vehicles, the fact that most of the emissions occur during the cold start event explained this result. Indeed, the LPG dual-fuel vehicles used to start their engine with gasoline, even if LPG mode was selected. Since LPG has a higher ignition temperature than standard gasoline, the engine was fed with gasoline during the first minutes of the driving cycles, especially when the catalyst was not enabled, before shifting to LPG.

These two studies on the alternative fuel powertrain highlighted the key role played by the cold start event for modern gasoline vehicles. While the current standards for type approval of new vehicles are based on emission factors, expressed in g km^{-1}, it was demonstrated that it could be expressed only in g for some pollutants since their cumulative emission curves flatten after the cold start event. Consequently, emissions are much more dependent on the cold start duration, and the fuel consumption during this cold start event (i.e. number and intensity of the acceleration, velocity) than on the total distance driven during the cycle. Except for the CO_2 emission, the emission factors of the vehicle tested decrease with the increase of the driving distance. It explains for instance the difference of OFP observed between the driving cycles. Whereas the CADC is a longer cycle (51 km for 3143 s) than the NEDC (11 km for 1180 s), the OFP associated to the former cycle were found to be three times lower in average than those of the latter cycle (see figure 5.6). In addition, the CADC is performed after a warm-up of the vehicle, which emphasizes the importance of the cold start emissions. Consequently, together with the engine performance, the cold start influenced considerably the global emissions associated with the vehicles, and when the ambient temperatures are low, this influence become more important and could cancel the benefit expected from an alternative fuel.

Future legislation should take into consideration the cold start emissions. Such regulation could assess the real impact of alternative powertrain and fuels since it could encompass short journey driving behaviors, where the catalyst light-off is hardly reached. For car manufacturers, it could provide an incentive in terms of appropriate engine or technology development to tackle these cold start excess emissions. As initiated with the regulation 725/2011 related to “eco-innovation" for reducing CO_2 emissions, a regulation dedicated not only to the CO_2, but also to other cold-start related harmful pollutants (acetaldehyde, NH_3Ě) could be beneficial to improve air quality. The assessment of the appropriate technology would be guaranteed thanks to a specific driving cycle, particularly short, to be carried out at different (cold) ambient temperature. One example of technology dedicated to reduce the cold start emissions is the block heater already implemented in Northern Europe. With a low initial investment, this system allows to schedule the warm up of the engine thanks to an electrical resistance located in the motor compartment. This technology is not systematically implemented by car manufacturers, despite the fact that it allows to reduce the cold start emission (by shortening the period before the light-off of the catalyst), together with substantial fuel economy. Another promising example is the implementation of modern LPG-DI engine, with optimization of fuel injection, spark timing and mixture preparation during the cold start in order to reduce most of the pollutants emitted (292). Consequently, a dedicated regulation could promote the development of such technologies, and therefore, could lead to an improvement of urban air quality.

Retrofit systems for PM and NO_x reduction from truck emissions

The last objective was to assess heavy-duty emissions, especially in terms of PM and NO_x (cf. chapter 6). Through the example of oxygenated additive, we saw that efficient retrofit technologies are available to reduce the PM emissions from in-use heavy-duty vehicles. The NO_x reduction with the use of dedicated Urea-SCR system was approached with chassis dynamometer tests of more than 10 trucks. This aftertreatment showed effective results for all the vehicles tested over the regulated ETC, however, in the case of specific start and stop driving cycles, the NO_x reduction was mitigated by the two low temperature reached by the exhaust gas. In addition, NH_3 emission was observed from several Euro V heavy-duty vehicles equipped with the first generation of catalyst. The heavy-duty configuration is generally adjusted to fit closely with the specific customer requirements and the mission profile of the vehicle. Consequently, heavy-duty vehicle market is difficult to characterize since the original equipment manufacturers are not responsible of the final configuration of the vehicle. Therefore, an effective emission regulation is hard to set up. These first preliminary results obtained from the new facility demonstrate that the VELA 7 is a promising platform for assessing the impact of new technologies on the environment. Among the vehicles tested, several were running with retrofit systems like DPF, dual-fuel system (LPG-Diesel and CNG/Diesel), and differential oil volume management. These technologies have brought significant advantages in terms of regulated and GHG emissions. Consequently, the exploitation of these research results represents the next step of this project. New technologies developed to tackle the GHG emissions from heavy-duty vehicle were tested, especially technologies targeting powertrain efficiency improvement which are thought to have the potential for the largest CO_2 emissions reduction (293). It should be borne in mind that a fuel consumption reduction, even low, can have a substantial impact on the overall CO_2 emission considering the distance driven by these vehicles and their average fuel consumption. CO_2 emissions from heavy-duty vehicles are estimated to account for 26% of the total CO_2 emissions associated to road transport by 2030 in EU, thus, the dissemination of these results can provide valuable input for assessing the future trend of GHGs emissions from the transport sector.

Perspectives - impact of primary emissions on the secondary organic aerosol formation

Airborne particles have both impact on Earth's climate and air quality. As evidenced in the research on mopeds reported in chapter 4, impact of exhaust aftertreatment strategy employed to comply with the latest emission standards raised the issue of the environmental fate of direct emissions. A comprehensive assessment of the real impact of vehicular emission should not be limited only to the frame of direct emissions, but also to the evolution of these emissions in the atmosphere. Indeed, in the same way as the O_3 formation control through the limitation of the O_3 precursors emissions, the aerosol formation potential should be controlled through the aerosols precursors emissions. The diesel combustion is responsible of a considerable fraction of the PM emissions in the atmosphere. In addition, low-volatility gas phase materials are also directly associated to diesel combustion, by either direct emission or evaporation of the semi-volatile part of the primary organic aerosol emitted. The photo-oxidation of the semi-volatile organic compounds can react with OH radicals, ozone, and NO_3 radicals to form ultrafine particles (147, 193). These oxidation reactions result rapidly in secondary organic aerosols (SOA) formation in the atmosphere (36). The simulation of these photochemical reactions is possible during smog chamber investigations, where the atmospheric chemical composition, exhaust gas dilution and light condition can be simulated in a reaction cell. The smog chamber experiment is particularly useful for studying SOA, and the secondary aerosol production potential (SAPP) (294). A study from Chirico et al. (2010) with diesel vehicles equipped with various aftertreatment devices demonstrated that the SAPP varied according to several factor such as the engine temperature, the engine load, and the aftertreatment device (164). However, a recent study from Bahreini et al. (2012) pointed out that whereas diesel vehicles were the main emitters of direct PM emissions, gasoline vehicles could contribute more to the SOA formation (295). Consequently, the estimation of the SAPP from vehicle used in realistic condition is of the utmost importance. These investigations should combine chassis dynamometer studies with smog chamber aging experiments in order to encompass the full potential of vehicle exhaust to contribute to the SOA. Such experimental setup enables comprehensive assessment of the overall impact that fuel quality (alternative fuels), aftertreatment devices, or engine condition (cold start emissions) can have on the human health and the environment.

References

[1] Almut Arneth, Nadine Unger, Markku Kulmala, and Meinrat O. Andreae. **Clean the Air, Heat the Planet?** *Science*, **326**(5953):672–673, 2009. 1

[2] Ministry of Health. **Mortality and morbidity during the London fog of December 1952**. *Reports on Public Health and Medical Subjects - HMSO*, **95**, 1954. 1

[3] International Agency for Research on Cancer World Health Organization. **IARC: DIESEL ENGINE EXHAUST CARCINOGENIC**. *PRESS RELEASE*, **213**:1–4, 2012. URL: `http://press.iarc.fr/pr213_E.pdf`. 1

[4] B. Sportisse. **Fundamentals in Air Pollution: From Processes to Modelling**. *Springer*, page 299, 2010. 2, 5, 7, 13

[5] J.T. Houghton, Y. Ding, D.J. Griggs, M. Noguer, P.J. van der Linden, X. Dai, K. Maskell, and C.A. Johnson. **Climate Change 2001: The Scientific Basis. Contribution of Working Group I to the Third Assessment Report of the Intergovernmental Panel on Climate Change**. *Cambridge University Press, Cambridge, United Kingdom and New York, NY, USA*, page 881p, 2001. 2, 4, 5, 6, 10, 13

[6] P. Forster, V. Ramaswamy, P. Artaxo, T. Berntsen, R. Betts, D.W. Fahey, J. Haywood, J. Lean, D.C. Lowe, G. Myhre, J. Nganga, R. Prinn, G. Raga, M. Schulz, and R. Van Dorland. **2007: Changes in Atmospheric Constituents and in Radiative Forcing. In: Climate Change 2007: The Physical Science Basis**. *Climate Change 2007: The Physical Science Basis, Cambridge University Press, Cambridge, United Kingdom and New York, NY, USA*, pages 129–234, 2007. 2, 3, 4, 5, 6, 8, 171, 201

[7] E.A. Davidson and I.L. Ackerman. **Changes in soil carbon inventories following cultivation of previously untilled soils**. *Biogeochemistry*, **20**(3):161–193, 1993. 4

[8] G. Brasseur, J. Orlando, and G. Tyndall. **Atmospheric Chemistry and Global Change**. *Oxford University Press*, page 688, 1999. 4

[9] C. Frankenberg, J. F. Meirink, M. vanWeele, U. Platt, and T. Wagner. **Assessing Methane Emissions from Global Space-Borne Observations**. *Science*, **308**(5724):1010–1014, 2005. 4

[10] T.E. Lipman and M.A. Delucchi. **Emissions of nitrous oxide and methane from conventional and alternative fuel motor vehicles**. *Climatic Change*, **53**(4):477–516, 2002. 4, 32

[11] K.H. Becker, J.C. Lorzer, R. Kurtenbach, P. Wiesen, T.E. Jensen, and T.J. Wallington. **Nitrous oxide (N_2O) emissions from vehicles**. *Environmental Science and Technology*, **33**(22):4134–4139, 1999. 4

[12] J. Farman, B.G. Gardinier, and J. Shanklin. **Large losses of total ozone in Antarctica reveal seasonal ClO_x/NO_x interactions**. *Nature*, **315**(6016):207–210, 1985. 5

[13] L.T. Molina and M.J. Molina. **Production of Cl_2O_2 from the Self-Reaction of the ClO Radical**. *Journal of Physical Chemistry*, **91**(2):433–436, 1987. 5

[14] J.H. Seinfeld and S.N. Pandis. **ATMOSPHERIC CHEMISTRY AND PHYSICS From Air Pollution to Climate Change - Second Edition**. *John Wilez and Sons, Inc.*, page 1326, 1998. 5, 12

[15] B.J. Finlayson-Pitts and J.N. Pitts. **Tropospheric air pollution: Ozone, airborne toxics, polycyclic aromatic hydrocarbons, and particles**. *Science*, **276**(5315):1045–1052, 1997. 5, 64

[16] Roger Atkinson. **Atmospheric chemistry of VOCs and NOx**. *Atmospheric Environment*, **34**(12Ũ14):2063 – 2101, 2000. 5, 6, 12

[17] M.C. Dodge. **Combined use of modeling techniques and smog chamber data to derive ozoneŮprecursor relationships, Environmental Protection Agency, Environmental Sciences Research Laboratory, Research Triangle Park, N.C.** *International Conference on Photochemical Oxidant Pollution and its Control: Proceedings*, **2**:881–889, 1977. 7

[18] Nadine Unger, Tami C. Bond, James S. Wang, Dorothy M. Koch, Surabi Menon, Drew T. Shindell, and Susanne Bauer. **Attribution of climate forcing to economic sectors**. *Proceedings of the National Academy of Sciences*, **107**(8):3382–3387, 2010. 6, 9, 113, 142

[19] V. Ramanathan and Y. Feng. **Air pollution, greenhouse gases and climate change: Global and regional perspectives**. *Atmospheric Environment*, **43**(1):37–50, 2009. 6, 8

[20] World Health Organization. **Health risks of particulate matter from long-range transboundary air pollution**. 2006. URL: `http://www.euro.who.int/__data/assets/pdf_file/0006/78657/E88189.pdf`. 6

[21] S.A. Twomey. **Aerosols, clouds and radiation**. *Atmospheric Environment PartA - Generals Topics*, **25**(11):2435–2442, 1991. 8

[22] B.A. Albrecht. **Aerosols, cloud microphysics, and fractional cloudiness**. *Science*, **245**(4923):1227–1230, 1989. 8

[23] J Hansen, M Sato, and R Ruedy. **Radiative forcing and climate response**. *JOURNAL OF GEOPHYSICAL RESEARCH-ATMOSPHERES*, **102**(D6):6831–6864, MAR 27 1997. 8

[24] European Environment Agency. **Annual European Union greenhouse gas inventory 1990 - 2009 and inventory report 2011**. *Communication*, **Technical Report**(2/2011), 2011. 8, 19, 22

[25] J. Fuglestvedt, T. Berntsen, G. Myhre, K. Rypdal, and R. B. Skeie. **Climate forcing from the transport sectors**. *Proceedings of the National Academy of Sciences of the United States of America*, **105**(2):454–458, 2008. 9, 20, 162, 171, 201

[26] T.J. Grahame and R.B. Schlesinger. **Health effects of airborne particulate matter: Do we know enough to consider regulating specific particle types or sources?** *Inhalation Toxicology*, **19**(6-7):457–481, 2007. 9

[27] C.A. Pope and D.W. Dockery. **Health effects of fine particulate air pollution: Lines that connect**. *Journal of the Air and Waste Management Association*, **56**(6):709–742, 2006. 9, 13, 15, 64

[28] M.J. Utell and M.W. Frampton. **Acute Health Effects of Ambient Air Pollution: The Ultrafine Particle Hypothesis**. *Journal of Aerosol Medicine*, **13**:355–359, 2000. 9, 13, 15

[29] Aphekom team. **Summary report of the Aphekom project 2008-2011**. pages 1–12, 2011. URL: `http://www.endseurope.com/docs/110302b.pdf`. 9, 11, 15

[30] Environmental Protection Agency. **EPA Proposes New Regulations for the National Renewable Fuel Standard Program for 2010 and Beyond**. *Regulatory Announcement*, **EPA-420-F-09-023**, 2009. 10, 142

[31] S. Reis, R.W. Pinder, M. Zhang, G. Lijie, and M. A. Sutton. **Reactive nitrogen in atmospheric emission inventories**. *Atmospheric Chemistry and Physics*, **9**:7657–7677, 2009. 10, 13, 14

[32] Jos G.J. Olivier, Jan Pieter J. Bloos, Jan J.M. Berdowski, Antoon J.H. Visschedijk, and Alex F. Bouwman. **A 1990 global emission inventory of anthropogenic sources of carbon monoxide on 1o Œ 1o developed in the framework of EDGAR/GEIA**. *Chemosphere - Global Change Science*, **1**(1-3):1–17, 1999. 10

[33] The Council of the European Communities. **Council Directive 93/12/EEC of 23 March 1993 relating to the sulphur content of certain liquid fuels**. *Official J. Eur. Communities*, **L074**:81–83, 1993. 11

[34] European Commission. **Directive 98/70/EC of the European Parliament and of the Council of 13 October 1998 relating to the quality of petrol and diesel fuels and amending Council Directive 93/12/EEC**. *Official J. Eur. Communities*, **L350**:58–68, 1998. URL: `http://eur-lex.europa.eu/LexUriServ/LexUriServ.do?uri=OJ:L:1998:350:0058:0067:EN:PDF`. 11, 67

[35] European Commission. **Directive 2009/30/EC of the European Parliament and of the Council of 23 April 2009 amending Directive 98/70/EC as regards the specification of petrol, diesel and gas-oil and introducing a mechanism to monitor and reduce greenhouse gas emissions and amending council Directive 1999/32/EC as regards the specification of fuel used by inland waterway vessels and repealing Directive 93/12/EEC**. *Official J. Eur. Communities*, **L140/88**, 2009. 11, 16, 142

[36] Allen L. Robinson, Neil M. Donahue, Manish K. Shrivastava, Emily A. Weitkamp, Amy M. Sage, Andrew P. Grieshop, Timothy E. Lane, Jeffrey R. Pierce, and Spyros N. Pandis. **Rethinking Organic Aerosols: Semivolatile Emissions and Photochemical Aging**. *Science*, **315**(5816):1259–1262, 2007. 11, 12, 64, 229

[37] Manish K. Shrivastava, Eric M. Lipsky, Charles O. Stanier, and Allen L. Robinson. **Modeling Semivolatile Organic Aerosol Mass Emissions from Combustion Systems**. *Environmental Science & Technology*, **40**(8):2671–2677, 2006. 11, 12, 213

[38] R. Atkinson and J. Arey. **Atmospheric degradation of volatile organic compounds**. *Chemical Review*, **2003**(103):4605–4638, 2003. 11, 64

[39] US Departement of Health and Human Services. **Report on Carcinogens, twelfth Edition; U.S. Department of Health and Human Services, Public Health Service, National Toxicology Program**. 2011. URL: `http://ntp.niehs.nih.gov/ntp/roc/twelfth/roc12.pdf`. 11, 123, 152, 179, 180

[40] Georgios Fontaras, Georgios Karavalakis, Marina Kousoulidou, Leonidas Ntziachristos, Evangelos Bakeas, Stamoulis Stournas, and Zissis Samaras. **Effects of low concentration biodiesel blends application on modern passenger cars. Part 2: Impact on carbonyl compound emissions**. *Environmental Pollution*, **158**(7):2496 – 2503, 2010. 11

[41] M. Colón, J. D. Pleil, T. A. Hartlage, M. Lucia Guardani, and M. Helena Martins. **Survey of volatile organic compounds associated with automotive emissions in the urban airshed of São Paulo, Brazil**. *Atmospheric Environment*, **35**(23):4017–4031, 2001. 11, 19, 142

[42] J. B. De Andrade, M. V. Andrade, and H. L. C. Pinheiro. **Atmospheric levels of formaldehyde and acetaldehyde and their relationship with the vehicular fleet composition in Salvador, Bahia, Brazil**. *Journal of the Brazilian Chemical Society*, **9**(3):219–223, 1998. 11, 19, 142, 152

[43] D. Grosjean, E. Grosjean, and L. F. R. Moreira. **Speciated ambient carbonyls in Rio de Janeiro, Brazil**. *Environmental Science and Technology*, **36**(7):1389–1395, 2002. 11, 19, 142, 152

[44] California Environmental Protection Agency Air Resources Board. **Analysis of the Ambient VOC Data Collected in the Southern California Air Quality Study**. *Final Report*, 1992. URL: `http://o3.arb.ca.gov/research/apr/past/a832-130a.pdf`. 11

[45] Environmental Protection Agency. **Health Assessment Document for Diesel Engine Exhaust (Final 2002)**. *Report*, **EPA/600/8-90/057F**, 2002. 11, 15, 64

[46] M.M. Rhead and S.A. Hardy. **The sources of polycyclic aromatic compounds in diesel engine emissions**. *Fuel*, **82**(4):385–393, 2003. 11, 212, 215

[47] Environmental Protection Agency. **Provisional Guidance for Quantitative Risk Assessment of Polycyclic Aromatic Hydrocarbons**. *EPA method*, **EPA/600/R-93/089**, 1989. 11

[48] The Royal Society. **Ground-level ozone in the 21st century: future trends, impacts and policy implications**. *Science Policy Report*, **15/08**:148, 2008. URL: `http://royalsociety.org/uploadedFiles/Royal_Society_Content/policy/publications/2008/7925.pdf`. 12

[49] European Environment Agency. **Europe's environment Ů The fourth assessment**. *Communication*, **EEA Report**(1/2007):452, 2007. 12, 201

[50] M. R. Ashmore. **Assessing the future global impacts of ozone on vegetation**. *Plant, Cell & Environment*, **28**(8):949–964, 2005. 12

[51] European Commission. **Directive 2008/50/EC of the European Parliament and the Council of 21 May 2008 on ambient air quality and cleaner air for Europe**. *Official J. Eur. Communities*, **L152**, 2008. URL: `http://eur-lex.europa.eu/LexUriServ/LexUriServ.do?uri=OJ:L:2008:152:0001:0044:EN:PDF`. 12

[52] European Environment Agency. **Air pollution by ozone across Europe during summer 2010 Overview of exceedances of EC ozone threshold values for AprilŰSeptember 2010**. *Communication*, **EEA Technical Report**(6/2011), 2011. 12

[53] European Commission. **Directive 2002/3/EC of the European Parliament and of the Council of 12 February 2002 relating to ozone in ambient air**. *Official J. Eur. Communities*, **L67**:14–30, 2002. 12, 55, 56, 118, 146, 174

[54] A.F. Bouwman, D.S. Lee, W.A.H. Asman, F.J. Dentener, K.W. VanderHoek, and J.G.J. Olivier. **A global high-resolution emission inventory for ammonia**. *GLOBAL BIOGEOCHEMICAL CYCLES*, **11**(4):561–587, DEC 1997. 13

[55] S. V. Krupa. **Effects of atmospheric ammonia (NH3) on terrestrial vegetation: a review**. *Environmental Pollution*, **124**(2):179–221, 2003. 13, 143

[56] J.G. Irwin and M.L. Williams. **Acid rain - Chemistry and transport**. *Environmental Pollution*, **50**(1-2):29–59, 1988. 13

[57] Peter J. Groblicki, George T. Wolff, and Richard J. Countess. **Visibility-reducing species in the denver "brown cloud"–I. Relationships between extinction and chemical composition**. *Atmospheric Environment*, **15**(12):2473–2484, 1981. 13, 143

[58] William Battye, Viney P. Aneja, and Paul A. Roelle. **Evaluation and improvement of ammonia emissions inventories**. *Atmospheric Environment*, **37**(27):3873–3883, 2003. 13, 143

[59] Norbert V. Heeb, Christian J. Saxer, Anna-Maria Forss, and Stefan Brühlmann. **Correlation of hydrogen, ammonia and nitrogen monoxide (nitric oxide) emissions of gasoline-fueled Euro-3 passenger cars at transient driving**. *Atmospheric Environment*, **40**(20):3750–3763, 2006. 13, 155

[60] R.L. Bradow and F.D. Stump. **Unregulated Emissions from Three-Way Catalyst Cars**. *SAE Technical Paper*, **770369**, 1977. 13, 26, 32, 89, 154

[61] J. Barbier Jr and D. Duprez. **Steam effects in three-way catalysis**. *Applied Catalysis B, Environmental*, **4**(2-3):105–140, 1994. 13, 32, 89, 154

[62] B. I. Whittington, C. J. Jiang, and D. L. Trimm. **Vehicle exhaust catalysis: I. The relative importance of catalytic oxidation, steam reforming and water-gas shift reactions**. *Catalysis Today*, **26**(1):41–45, 1995. 13, 89, 154

[63] J. Czerwinski, N. Heeb, Y. Zimmerli, A. M. Forss, T. Hilfiker, and C. Bach. **Unregulated Emissions with TWC, Gasoline & CNG**. *SAE Technical Paper*, **2010-01-1286**, 2010. 13, 89, 154

[64] T. D. Durbin, R. D. Wilson, J. M. Norbeck, J. W. Miller, T. Huai, and S. H. Rhee. **Estimates of the emission rates of ammonia from light-duty vehicles using standard chassis dynamometer test cycles**. *Atmospheric Environment*, **36**(9):1475–1482, 2002. 13, 154

[65] U. Sutton, M. A. adn Dragosits, Y. S. Tang, and D. Fowler. **Ammonia emissions from non-agricultural sources in the UK**. *Atmospheric Environment*, **34**(6):855–869, 2000. 13, 143

[66] Cody Livingston, Paul Rieger, and Arthur Winer. **Ammonia emissions from a representative in-use fleet of light and medium-duty vehicles in the California South Coast Air Basin**. *Atmospheric Environment*, **43**(21):3326–3333, 2009. 13, 123, 154, 155

[67] Health Effects Institute. **Traffic-related air pollution: A critical review of the literature on emissions, exposure, and health effects**. *Special Report*, **17**, 2010. URL: `http://pubs.healtheffects.org/getfile.php?u=553`. 13, 15, 64, 65, 89

[68] C. Mohr, P.F. DeCarlo, M.F. Heringa, R. Chirico, J.G. Slowik, R. Richter, C. Reche, A. Alastuey, X. Querol, R. Seco, J. Penuelas, J.L. Jimenez, M. Crippa, R. Zimmermann, U. Baltensperger, and A.S.H. Prevot. **Identification and quantification of organic aerosol from cooking and other sources in Barcelona using aerosol mass spectrometer data**. *Atmospheric Chemistry and Physics*, **12**(4):1649Ű1665, 2011. 13

[69] D.B. Kittelson. **Engines and nanoparticles: a review**. *Journal of Aerosol Science*, **29**(5-6):575–588, 1998. 13, 15, 83

[70] B.J. Finlayson-Pitts and J.N. Pitts. **Chemistry of the upper and lower atmosphere**. *Academic Press*, **ISBN: 978-0-12-257060-5**:969, 2000. 15

[71] T.F. Mar, G.A. Norris, J.Q. Koenig, and T.V. Larson. **Associations between air pollution and mortality in Phoenix, 1995-1997**. *Environmental Health Perspectives*, **108**(4):347–353, 2000. 15, 64

[72] Bert Brunefreef and Stephen T. Holgate. **Air pollution and Health**. *The Lancet*, pages 1233–1242, 2002. 15

[73] Magdi K. Khair and W. Addy Majewski. **Diesel Emissions and Their Control**. *SAE International*, **ISBN: 978-0-7680-0674-2**:584, 2006. 15, 29, 30

[74] J.P. Shi and R.M. Harrison. **Investigation of Ultrafine Particle Formation during Diesel Exhaust Dilution**. *Environmental Science and Technology*, **33**(21):3730Ű3736, 1999. 16

[75] The Council of the European Communities. **Council Directive 70/220/EEC of 20 March 1970 on the approximation of the laws of the Member States relating to measures to be taken against air pollution by gases from positive-ignition engines of motor vehicles**. *Official J. Eur. Communities*, **L076**:1–22, 1970. 16, 39, 42, 145, 151, 164, 165, 166, 167, 174

[76] European Commission. **Commission regulation (EU) No 582/2011 of 25 May 2011 implementing and amending Regulation (EC) No 595/2009 of the European Parliament and of the Council with respect to emissions from heavy duty vehicles (Euro VI) and amending Annexes I and III to Directive 2007/46/EC of the European Parliament and of the Council**. *Official J. Eur. Communities*, **L167/1**, 2011. 17, 21

[77] European Commission. **Directive 2009/28/EC of the European Parliament and of the Council of 23 April 2009 on the promotion of the use of energy from renewable sources and amending and subsequently repealing Directives 2001/77/EC and 2003/30/EC**. *Official J. Eur. Communities*, **L140/16**, 2009. 16, 142

[78] European Commission. **Regulation (EC) No 443/2009 of the European Parliament and of the Council of 23 April 2009 setting emission performance standards for new passenger cars as part of the CommunityŠs integrated approach to reduce CO2 emissions from light-duty vehicles**. *Official J. Eur. Communities*, **L140**, 2009. 18

[79] The International Council on Clean Tranportation. **EU 2020 CO2 emission standards for cars and vans**. *Policy Update*, **12 July 2012**, 2011. URL: `http://www.theicct.org/sites/default/files/publications/ICCT%20Policy%20Update%20EU%20PV%20CO2%20July2012final_0.pdf`. 18

[80] European Commission. **Commission implementing Regulation (EU) No 725/2011 of 25 July 2011 establishing a procedure for the approval and certification of innovative technologies for reducing CO 2 emissions from passenger cars pursuant to Regulation (EC) No 443/2009 of the European Parliament and of the Council**. **L194/19**, 2011. 18

[81] European Commission. **Commission Regulation (EC) No 692/2008 of 18 July 2008 implementing and amending Regulation (EC) No 715/2007 of the European Parliament and of the Council on type-approval of motor vehicles with respect to emissions from light passenger and commercial vehicles (Euro 5 and Euro 6) and on access to vehicle repair and maintenance information**. *Official J. Eur. Communities*, **L199**, 2008. 21, 42, 64, 84, 142, 143, 147, 149, 150

[82] David J.C. MacKay. **Sustainable Energy Ů without the hot air**. *UIT Cambridge*, pages 1–383, 2008. URL: `http://www.inference.phy.cam.ac.uk/sustainable/book/tex/sewtha.pdf`. 21

[83] Adolfo Perujo, Christian Thiel, and Francoise Nemry. **Electric Vehicles in an Urban Context: Environmental Benefits and Techno-Economic Barriers, Electric Vehicles – The Benefits and Barriers**. *Seref Soylu (Ed.)*, **ISBN: 978-953-307-287-6**:19–34, 2011. URL: `http://www.intechopen.com/books/electric-vehicles-the-benefits-and-barriers`. 21

[84] James Murray and David King. **Climate policy: Oil's tipping point has passed**. *Nature*, **481**(7382):433–435, 2012. 22

[85] Christian Thiel, Adolfo Perujo, and Arnaud Mercier. **Cost and CO2 aspects of future vehicle options in Europe under new energy policy scenarios**. *Energy Policy*, **38**(11):7142 – 7151, 2010. <ce:title>Energy Efficiency Policies and Strategies with regular papers.</ce:title>. 22

[86] Adolfo Perujo and Biagio Ciuffo. **The introduction of electric vehicles in the private fleet: Potential impact on the electric supply system and on the environment. A case study for the Province of Milan, Italy**. *Energy Policy*, **38**(8):4549 – 4561, 2010. 22

[87] Poonam Singh Nigam and Anoop Singh. **Production of liquid biofuels from renewable resources**. *Progress in Energy and Combustion Science*, **37**(1):52 – 68, 2011. 22, 23, 24

[88] P.J. Crutzen, A.R. Mosier, K.A. Smith, and W. Winiwarter. **N_2O release from agro-biofuel production negates global warming reduction by replacing fossil fuels**. *Atmospheric Chemistry and Physics Discussions*, **7**(4):11191–11205, 2007. 23

[89] Avinash Kumar Agarwal. **Biofuels (alcohols and biodiesel) applications as fuels for internal combustion engines**. *Progress in Energy and Combustion Science*, **33**(3):233 – 271, 2007. 23

[90] Robert Edwards, Declan Mulligan, and Luisa Marelli. **Indirect Land Use Change from increased biofuels demand**. *JRC Scientific and Technical Report*, **EUR 24485 EN - 2010**, 2010. URL: `http://ec.europa.eu/energy/renewables/consultations/doc/public_consultation_iluc/study_4_iluc_modelling_comparison.pdf`. 23

[91] Timothy D. Searchinger, Steven P. Hamburg, Jerry Melillo, William Chameides, Petr Havlik, Daniel M. Kammen, Gene E. Likens, Ruben N. Lubowski, Michael Obersteiner, Michael Oppenheimer, G. Philip Robertson, William H. Schlesinger, and G. David Tilman. **Fixing a Critical Climate Accounting Error**. *Science*, **326**(5952):527–528, 2009. 23

[92] Robert K. Niven. **Ethanol in gasoline: environmental impacts and sustainability review article**. *Renewable and Sustainable Energy Reviews*, **9**(6):535 – 555, 2005. 23, 142

[93] T. Wallner and R. Frazee. **Study of Regulated and Non-Regulated Emissions from Combustion of Gasoline, Alcohol Fuels and their Blends in a DI-SI Engine**. *SAE Technical Paper*, (2010-01-1571), 2010. 23, 150, 154, 155

[94] M. Lapuerta, O. Armas, and J. Rodriguez-Fernandez. **Effect of biodiesel fuels on diesel engine emissions**. *Progress in Energy and Combustion Science*, **34**(2):198Ũ223, 2008. 24, 65, 84, 87

[95] Noboru Miyamoto, Hideyuki Ogawa, Nabi Md. Nurun, Kouichi Obata, and Teruyoshi Arima. **Smokeless, low NOx, high thermal efficiency, and low noise diesel combustion with oxygenated agents as main fuel**. *SAE Technical Paper*, (980506), 1998. 24

[96] Erica Trapel, Christian Mayer, Christof Schulz, and Paul Roth. **Effects of Bio Diesel Injection in a DI Diesel Engine on Gaseous and Particulate Emission**. *SAE Technical Paper*, (2005-01-2204), 2005. 24

[97] George Karavalakis, Stamoulis Stournas, George Fontaras, Zissis Samaras, George Dedes, and Evangelos Bakeas. **The Effect of Biodiesel on PAHs, Nitro-PAHs and Oxy-PAHs Emissions from a Light Vehicle Operated over the European and the Artemis Driving Cycles**. *SAE Technical Paper*, **2009-01-1895**, 2009. 24, 65

[98] S. M. Corrêa and G. Arbilla. **Aromatic hydrocarbons emissions in diesel and biodiesel exhaust**. *Atmospheric Environment*, **40**(35):6821–6826, 2006. 24, 92

[99] F. Black, S. Tejada, and M. Gurevich. **Alternative fuel motor vehicle tailpipe and evaporative emissions composition and ozone potential**. *Journal of the Air and Waste Management Association*, **48**(7):578–591, 1998. 24, 142

[100] J. J. Winebrake. **Hazardous air pollution from mobile sources: A comparison of alternative fuel and reformulated gasoline vehicles**. *Journal of the Air and Waste Management Association*, **49**(5):576–581, 1999. 24, 142

[101] Mark Z. Jacobson. **Effects of Ethanol (E85) versus Gasoline Vehicles on Cancer and Mortality in the United States**. *Environmental Science & Technology*, **41**(11):4150–4157, 2007. 24, 152

[102] M. Clairotte, T.W. Adam, A.A. Zardini, U. Manfredi, G. Martini, A. Krasenbrink, A. Vicet, T. Tournie, and C. Astorga. **Effects of low temperature on the cold start gaseous emission from light duty vehicles fuelled by ethanol-blended gasoline**. *Applied Energy*, **Accepted**, 2012. 24, 89

[103] World Commission on Environment and Development. **The World Commission on Environment and Development Our Common Future**. *Oxford, UK: Oxford University Press*, page 416, 1987. 24

[104] The Council of the European Communities. **Council Directive 85/210/EEC of 20 March 1985 on the approximation of the laws of the Member States concerning the lead content of petrol**. *Official J. Eur. Communities*, **L96**:25–29, 1985. 25

[105] Cherian A. Idicheria and Lyle M. Pickett. **Soot Formation in Diesel Combustion under High-EGR Conditions**. *SAE Technical Paper*, **2005-01-3834**, 2005. 25

[106] T. Johnson. **Diesel Engine Emissions and Their Control - An overview**. *Platinium Metal Review*, **52**(1):23–37, 2008. 26, 27, 31, 32

[107] Ronald M. Heck and Robert J. Farrauto. **Automobile exhaust catalysts**. *Applied Catalysis A: General*, **221**(1Ũ2):443 – 457, 2001. <ce:title>Hoelderich Special Issue</ce:title>. 28, 29, 31

[108] ShinŠichi Matsumoto. **Recent advances in automobile exhaust catalysts**. *Catalysis Today*, **90**(3Ũ4):183 – 190, 2004. <ce:title>Environmental Catalysis and Eco-materials</ce:title>. 29

[109] Paul Zelenka, Wolfgang Cartellieri, and Peter Herzog. **Worldwide diesel emission standards, current experiences and future needs**. *Applied Catalysis B: Environmental*, **10**(1Ũ3):3 – 28, 1996. 29

[110] A.P. Walker. **Controlling particulate emissions from diesel vehicles**. *Topics in Catalysis*, **28**(1-4):165–170, 2004. 29, 65

[111] Norbert V. Heeb, Peter Schmid, Martin Kohler, Erika Gujer, Markus Zennegg, Daniela Wenger, Adrian Wichser, Andrea Ulrich, Urs Gfeller, Peter Honegger, Kerstin Zeyer, Lukas Emmenegger, Jean-Luc Petermann, Jan Czerwinski, Thomas Mosimann, Markus Kasper, and Andreas Mayer. **Secondary Effects of Catalytic Diesel Particulate Filters: Conversion of PAHs versus Formation of Nitro-PAHs**. *Environmental Science & Technology*, **42**(10):3773–3779, 2008. PMID: 18546721. 30, 31, 32

[112] B. Cooper and J. Thoss. **Role of NO in Diesel Particulate Emission Control**. *SAE Technical Paper*, **890404**, 1989. 30

[113] D. Fino. **Diesel emission control: Catalytic filters for particulate removal**. *Science and Technology of Advanced Materials*, **8**(1-2):93–100, 2007. 31, 65

[114] S.R. Katare, J.E. Patterson, and P.M. Laing. **Diesel aftertreatment modeling: A systems approach to NOx control**. *Industrial and Engineering Chemistry Research*, **46**(8):2445–2454, 2007. 31, 82, 88

[115] PÃĎr L.T. Gabrielsson. **Urea-SCR in Automotive Applications**. *Topics in Catalysis*, **28**:177–184, 2004. 10.1023/B:TOCA.0000024348.34477.4c. 31

[116] M Koebel, M Elsener, and M Kleemann. **Urea-SCR: a promising technique to reduce NOx emissions from automotive diesel engines**. *Catalysis Today*, **59**(3Ű4):335 – 345, 2000. 32

[117] C. Scott Sluder, John M. E. Storey, Samuel A. Lewis, and Linda A. Lewis. **Low Temperature Urea Decomposition and SCR Performance**. *SAE Technical Paper*, (2005-01-1858), 2005. 32

[118] Ikuhisa Hamada, Yasuyoshi Kato, Naomi Imada, Masatoshi Fujisawa, Akihiro Yamada, and Toshihumi Mukai. **A Preliminary Evaluation of Unregulated Emissions During Low Temperature Operation of a Small Diesel Engine with a Multi-Function SCR Catalyst**. *SAE Technical Paper*, **2006-01-0641**, 2006. 32

[119] Association des Constructeurs Européens de Motocycles. **ACEM Motorcycle Unregulated emissions report**. 2002. URL: `http://www.acem.eu/media/d_ACEM_yb_08_75492.pdf`. 32, 113

[120] T.J. Barlow, S. Latham, I.S. McCrae, and P.G. Boulter. **A reference book of driving cycles for use in the measurement of road vehicle emissions**. *TRL Limited*, **Published project report PPR354**:1–284, 2009. URL: `http://assets.dft.gov.uk/publications/road-vehicle-emission-factors-2009/ppr-354.pdf`. 39, 73, 147

[121] European Commission. **Directive 97/24/EC of the European Parliament and of the Council of 17 June 1997 on certain components and characteristics of two or three-wheel motor vehicles**. *Official J. Eur. Communities*, **L226**:1–454, 1997. 39, 65, 67, 113, 115

[122] Michel André. **The ARTEMIS European driving cycles for measuring car pollutant emissions**. *Science of The Total Environment*, **334-335**(0):73–84, 2004. 39, 144

[123] European Commission. **Directive 1999/96/EC of the European Parliament and of the Council of 13 December 1999 on the approximation of the laws of the Member States relating to measures to be taken against the emission of gaseous and particulate pollutants from compression ignition engines for use in vehicles, and the emission of gaseous pollutants from positive ignition engines fuelled with natural gas or liquefied petroleum gas for use in vehicles and amending Council Directive 88/77/EEC**. *Official J. Eur. Communities*, **L44**:1–155, 1999. 39, 205

[124] European Commission. **Directive 97/68/EC of the European Parliament and of the Council of 17 June 1997 on the approximation of the laws of the Member States relating to measures against the emission of gaseous and particulate pollutants from internal combustion engines to be installed in non-road mobile machinery**. *Official J. Eur. Communities*, **L59**, 1997. 42, 119, 127

[125] Beate Heller, Horst Klingenberg, Gerhard Lach, and Jürgen Winckler. **Performance of a New System for Emission Sampling and Measurement (SESAM)**. *SAE Technical Paper*, **900275**, 1990. 44

[126] Inc. MKS Instruments. **MGRefsMaster Reference Calibrations Version 2006**. 2006. URL: `http://www.meca.org/galleries/default-file/motorcycle.pdf`. 47

[127] California Environmental Protection Agency Air Resources Board. **California exhaust emission standards and test procedures for 1988-2000 model passenger cars, light-duty trucks, and medium-duty vehicles**. 1999. URL: `http://www.arb.ca.gov/regact/levii/to_oal/ldvtp88.pdf`. 51

[128] California Environmental Protection Agency Air Resources Board. **California assembly-line test procedures for 2001 and subsequent model-year passenger cars, light-duty trucks and medium-duty vehicles**. 1999. URL: `http://www.arb.ca.gov/msprog/levprog/cleandoc/altps01.pdf`. 51

[129] California Environmental Protection Agency Air Resources Board. **California Non-Methane Organic Gas Test Procedure**. 2002. URL: `http://www.arb.ca.gov/msprog/levprog/cleandoc/clean_nmogtps_final.pdf`. 51, 150

[130] M. Feinberg. **Validation of analytical methods based on accuracy profiles**. *Journal of Chromatography A*, **1158**(1-2):174–183, 2007. 52, 54, 147

[131] A. Latella, G. Stani, L. Cobelli, M. Duane, H. Junninen, C. Astorga, and B.R. Larsen. **Semicontinuous GC analysis and receptor modelling for source apportionment of ozone precursor hydrocarbons in Bresso, Milan, 2003**. *Journal of Chromatography A*, **1071**(1-2):29–39, 2005. 55, 56, 118, 123, 146, 174

[132] W.P.L. Carter. **Development of ozone reactivity scales for volatile organic compounds**. *Journal of the Air and Waste Management Association*, **44**(7):881–899, 1994. 56, 57, 118, 147, 174

[133] P. Picini, P. Spezzano, D. Cataldi, F. Messale, C. Manni, D. Santino, and E. Donato. **Particulate polycyclic aromatic hydrocarbons and particulate matter emissions from two-wheel motor vehicles**. *SAE Technical Paper*, (2005-24-020), 2005. 64

[134] T.W. Adam, A. Farfaletti, L. Montero, G. Martini, U. Manfredi, B.R. Larsen, G. De Santi, A. Krasenbrink, and C. Astorga. **Chemical Characterization of Emissions from Modern Two-Stroke Mopeds Complying with Legislative Regulation in Europe (EURO-2)**. *Environmental Science & Technology*, **44**(1):505–512, 2010. 64, 65, 87, 113, 114, 116, 125, 127

[135] S. Solomon, Q. Qin, M. Manning, Z. Chen, M. Marquis, K.B. Averyt, M. Tignor, and H.L. Miller. **Contribution of Working Group I to the Fourth Assessment Report of the Intergovernmental Panel on Climate Change**. *Climate Change 2007:*

The Physical Science Basis, Cambridge University Press, Cambridge, United Kingdom and New York, NY, USA, 2007. 64, 122

[136] Wolfgang F. Rogge, Lynn M. Hildemann, Monica A. Mazurek, Glen R. Cass, and Simoneit Bernd R. T. **Sources of fine organic aerosol. 2. Noncatalyst and catalyst-equipped automobiles and heavy-duty diesel trucks**. *Environmental Science and Technology*, **27**(4):636Ũ651, 1993. 64

[137] JJ Schauer, MJ Kleeman, GR Cass, and BRT Simoneit. **Measurement of emissions from air pollution sources. 2. C-1 through C-30 organic compounds from medium duty diesel trucks**. *Environmental Science and Technology*, **33**(10):1578–1587, 1999. 64

[138] K.B. Metzger, P.E. Tolbert, M. Klein, J.L. Peel, W.D. Flanders, K. Todd, J.A. Mulholland, P.B. Ryan, and H. Frumkin. **Ambient air pollution and cardiovascular emergency department visits**. *Epidemiology*, **15**(1):46–56, 2004. 64

[139] Glen R. Cass. **Organic molecular tracers for particulate air pollution sources**. *TrAC Trends in Analytical Chemistry*, **17**(6):356Ũ366, 1998. 64

[140] A.L.C. Lima, J.W. Farrington, and C.M. Reddy. **Combustion-derived polycyclic aromatic hydrocarbons in the environment - A review**. *Environmental Forensics*, **6**(2):109–131, 2005. 64, 92

[141] M.C.H. Lim, G.A. Ayoko, L. Morawska, Z.D. Ristovski, and E.R. Jayaratne. **Influence of fuel composition on polycyclic aromatic hydrocarbon emissions from a fleet of in-service passenger cars**. *Atmospheric Environment*, **41**(1):150–160, 2007. 64, 171

[142] Neville Thompson, Richard Stradling, Peter J. Zemroch, Roger de Craecker, Theodor Sams, and Alexandra Neunteufel. **Fuel Effects on Regulated Emissions From Advanced Diesel Engines and Vehicles**. *SAE Technical Paper*, (2004-01-1880), 2004. 65

[143] A. Mayer, J. Czerwinski, M. Wyser, P. Mattrel, and A. Heitzer. **Impact of RME/Diesel Blends on Particle Formation, Particle Filtration and PAH Emissions**. *SAE Technical Paper*, (2005-01-1728), 2005. 65, 82

[144] Y.G. Di, C.S. Cheung, and Z.H. Huang. **Comparison of the Effect of Biodiesel-Diesel and Ethanol-Diesel on the Particulate Emissions of a Direct Injection Diesel Engine**. *Aerosol Science and Technology*, **43**(5):455–465, 2009. 65

[145] L. Ntziachristos, P. Pistikopoulos, and Z. Samaras. **Particle characterization from two-stroke powered two-wheelers**. *International Journal of Engine Research*, **6**(3):263–275, 2005. 65, 79, 113

[146] Maria Vittoria Prati and Maria Antonietta Costagliola. **Emissions of Fine Particles and Organic Compounds from Mopeds**. *Environmental Engineering Science*, **26**(1):111–121, 2009. 65, 113

[147] L. Morawska, Z. Ristovski, E.R. Jayaratne, D.U. Keogh, and X. Ling. **Ambient nano and ultrafine particles from motor vehicle emissions: Characteristics, ambient processing and implications on human exposure**. *Atmospheric Environment*, **42**(35):8113 – 8138, 2008. 65, 229

[148] J. Yanowitz, M.S. Graboski, L.B.A. Ryan, T.L. Alleman, and R.L. McCormick. **Chassis dynamometer study of emissions from 21 in-use heavy duty diesel vehicles**. *Environmental Science and Technology*, **33**(2):209–216, 1999. 65

[149] S.D. Shah, D.R. Cocker, J.W. Miller, and J.M. Norbeck. **Emission rates of particulate matter and elemental and organic carbon from in-use diesel engines**. *Environmental Science and Technology*, **38**(9):2544–2550, 2004. 65

[150] Neville Thompson, Leonidas Ntziachristos, Zissis Samaras, Paivi Aakko, Urban Wass, Stephan Hausberger, and Theodor Sams. **Overview of the European "Particulates" project on the characterization of exhaust particulate emissions from road vehicles: Results for heavy-duty engines**. *SAE Technical Paper*, (2004-01-1986), 2004. 65

[151] Miriam Lev-On, Chuck LeTavec, Jim Uihlein, Ken Kimura, Teresa L. Alleman, Douglas R. Lawson, Keith Vertin, Mridul Gautam, Gregory J. Thompson, W. Scott Wayne, Nigel Clark, Robert Okamoto, Paul Rieger, Gary Yee, Barbara Zielinska, John Sagebiel, Sougato Chatterjee, and Kevin Hallstrom. **Speciation of organic compounds from the exhaust of trucks and buses: Effect of fuel and after-treatment on vehicle emission profiles**. *SAE Technical Paper*, **2002-01-2873**, 2002. 65, 188

[152] Leonidas Ntziachristos, Athanasios Mamakos, Zissis Samaras, Urs Mathis, Martin Mohr, Neville Thompson, Richard Stradling, Laurent Forti, and Claes de Serves. **Overview of the European "Particulates" project on the characterization of exhaust particulate emissions from road vehicles: Results for light-duty vehicles**. *SAE Technical Paper*, (2004-01-1985), 2004. 65, 82

[153] D. Bosteels, J. May, H. Karlsson, and C. de Serves. **"Regulated" and "Non-Regulated" Emissions From Modern European Passenger Cars**. *SAE Technical Paper*, **2006-01-1516**, 2006. 65

[154] I. Caplain, F. Cazier, H. Nouali, A. Mercier, J.C. Dechaux, V. Nollet, R. Journard, J-M. Andre, and R. Vidon. **Emissions of unregulated pollutants from European gasoline and diesel passenger cars**. *Atmospheric Environment*, **40**(31):5954–5966, 2006. 65, 92

[155] H.L. Karlsson. **Ammonia, nitrous oxide and hydrogen cyanide emissions from five passenger vehicles**. *Science of the Total Environment*, **334**:125–132, 2004. 65

[156] O. Devos, E. Combet, P. Tassel, and L. Paturel. **Exhaust emissions of PAHs of passenger cars**. *Polycyclic Aromatic Compounds*, **26**(1):69–78, 2006. 65

[157] Norbert V. Heeb, Christian J. Saxer, Anna-Maria Forss, and Stefan Brühlmann. **Trends of NO-, NO2-, and NH3-emissions from gasoline-fueled Euro-3- to Euro-4-passenger cars**. *Atmospheric Environment*, **42**(10):2543–2554, 2008. 65, 89, 131, 154

[158] Leonidas Ntziachristos, Barouch Giechaskiel, Panayiotis Pistikopoulos, Evaggelos Fysikas, and Zissis Samaras. **Particle emissions characteristics of different on-road vehicles**. *SAE Technical Paper*, (2003-01-1888), 2003. 65

[159] Manjula R. Canagaratna, John T. Jayne, David A. Ghertner, Scott Herndon, Quan Shi, Jose L. Jimenez, Philip J. Silva, Paul Williams, Thomas Lanni, Frank Drewnick, Kenneth L. Demerjian, Charles E. Kolb, and Douglas R. Worsnop. **Chase Studies of Particulate Emissions from in-use New York City Vehicles**. *Aerosol Science and Technology*, **38**(6):555–573, 2004. 66

[160] Barouch Giechaskiel, Rafael Munoz-Bueno, Lauretta Rubino, Urbano Manfredi, Panagiota Dilara, Giovanni De Santi, and Jon Andersson. **Particle Measurement Program (PMP): Particle Size and Number Emissions Before, During and After Regeneration Events of a Euro 4 DPF Equipped Light-Duty Diesel Vehicle**. *SAE Technical Paper*, **2007-01-1944**, 2007. 69, 83, 84

[161] T.W. Adam, R. Chirico, M. Clairotte, M. Elsasser, U. Manfredi, G. Martini, M. Sklorz, T. Streibel, M. F. Heringa, P. F. DeCarlo, U. Baltensperger, G. De Santi, A. Krasenbrink, R. Zimmermann, A.S.H. Prevot, and C. Astorga. **Application of Modern Online Instrumentation for Chemical Analysis of Gas and Particulate Phases of Exhaust at the European Commission Heavy-Duty Vehicle Emission Laboratory**. *Analytical Chemistry*, **83**(1):67–76, 2011. 69, 128

[162] M. Clairotte, T. W. Adam, R. Chirico, B. Giechaskiel, U. Manfredi, M. Elsasser, M. Sklorz, P. F. DeCarlo, M. F. Heringa, R. Zimmermann, G. Martini, A. Krasenbrink, A. Vicet, E. Tournié, A. S. H. Prévôt, and C. Astorga. **Online characterization of regulated and unregulated gaseous and particulate exhaust emissions from two-stroke mopeds: A chemometric approach**. *Analytica Chimica Acta*, **717**:28–38, 2012. 69, 79, 145

[163] Peter F. DeCarlo, Joel R. Kimmel, Achim Trimborn, Megan J. Northway, John T. Jayne, Allison C. Aiken, Marc Gonin, Katrin Fuhrer, Thomas Horvath, Kenneth S. Docherty, Doug R. Worsnop, and Jose L. Jimenez. **Field-Deployable, High-Resolution, Time-of-Flight Aerosol Mass Spectrometer**. *Analytical Chemistry*, **78**(24):8281–8289, 2006. 70, 118, 207

[164] R. Chirico, P. F. DeCarlo, M. F. Heringa, T. Tritscher, R. Richter, A. S. H. Prevot, J. Dommen, E. Weingartner, G. Wehrle, M. Gysel, M. Laborde, and U. Baltensperger. **Impact of aftertreatment devices on primary emissions and secondary organic aerosol formation potential from in-use diesel vehicles: results from smog chamber experiments**. *Atmospheric Chemistry and Physics Discussions*, **10**(6):16055–16109, 2010. 70, 229

[165] J.D. Allan, A.E. Delia, H. Coe, K.N. Bower, M.R. Alfarra, J.L. Jimenez, A.M. Middlebrook, F. Drewnick, T.B. Onasch, M.R. Canagaratna, J.T. Jayne, and D.R. Worsnop. **A generalised method for the extraction of chemically resolved mass spectra from aerodyne aerosol mass spectrometer data**. *Journal of Aerosol Science*, **35**(7):909–922, 2004. 70, 207

[166] A.C. Aiken, P.F. Decarlo, J.H. Kroll, D.R. Worsnop, J.A. Huffman, K.S. Docherty, I.M. Ulbrich, C. Mohr, J.R. Kimmel, D. Sueper, Y. Sun, Q. Zhang, A. Trimborn, M. Northway, P.J. Ziemann, M.R. Canagaratna, T.B. Onasch, M.R. Alfarra, A.S.H. Prevot, J. Dommen, J. Duplissy, A. Metzger, U. Baltensperger, and J.L. Jimenez. **O/C and OM/OC ratios of primary, secondary, and ambient organic aerosols with high-resolution time-of-flight aerosol mass spectrometry**. *Environmental Science and Technology*, **42**(12):4478–4485, 2008. 70

[167] Andreas Petzold and Markus Schönlinner. **Multi-angle absorption photometry–a new method for the measurement of aerosol light absorption and atmospheric black carbon**. *Journal of Aerosol Science*, **35**(4):421–441, 2004. 71, 118, 208

[168] F. Muhlberger, R. Zimmermann, and A. Kettrup. **A Mobile Mass Spectrometer for Comprehensive On-Line Analysis of Trace and Bulk Components of Complex Gas Mixtures: Parallel Application of the Laser-Based Ionization Methods VUV Single- Photon Ionization, Resonant Multiphoton Ioniza- tion, and Laser-Induced Electron Impact Ionization**. *Analytical Chemistry*, **73**(15):3590–3604, 2001. 72, 117

[169] T. Adam, M. Clairotte, T. Streibel, M. Elsasser, A. Pommeres, U. Manfredi, M. Carriero, G. Martini, M. Sklorz, A. Krasenbrink, C. Astorga, and R. Zimmermann. **Real-time analysis of aromatics in combustion engine exhaust by resonance-enhanced multiphoton ionisation time-of-flight mass spectrometry (REMPI-TOF-MS): a robust tool for chassis dynamometer testing**. *Analytical and Bioanalytical Chemistry*, **404**:273–276, 2012. 10.1007/s00216-012-6112-6. 72

[170] C.W. Wilkerson, S.M. Colby, and J.P. Reilly. **Determination of polycyclic aromatic hydrocarbons using gas chromatography/laser ionization mass spectrometry with picosecond and nanosecond light pulses**. *Analytical Chemistry*, **61**(23):2669–2673, 1989. 72, 207

[171] European Commission. **Directive 98/77/EC of 2 October 1998 adapting to technical progress council directive 70/220/EEC on the approximation of the laws of the member states relating to measures to be taken against air pollution by emissions from motor vehicles**. *Official J. Eur. Communities*, **L286**:34–52, 1998. 73, 173, 205

[172] M. Sharma, A.K. Agarwal, and K.V.L. Bharathi. **Characterization of exhaust particulates from diesel engine**. *Atmospheric Environment*, **39**(17):3023–3028, 2005. 79

[173] E.M. Lipsky and A.L. Robinson. **Effects of dilution on fine particle mass and partitioning of semivolatile organics in diesel exhaust and wood smoke**. *Environmental Science and Technology*, **40**(1):155–162, 2006. 79, 80

[174] A.P. Leskinen, J.K. Jokinlemi, and K.E.J. Lehtinen. **Transformation of diesel engine exhaust in an environmental chamber**. *Atmospheric Environment*, **41**(39):8865–8873, 2007. 79

[175] S. Tang, B.P. Frank, T. Lanni, G. Rideout, N. Meyer, and C. Beregszaszy. **Unregulated emissions from a heavy-duty diesel engine with various fuels and emission control systems**. *Environmental Science and Technology*, **41**(14):5037–5043, 2007. 79

[176] J. Andersson, D. Lance, and C. Jemma. **DfT Motorcycle emissions measurement programmes: Unregulated emission results**. *SAE Technical Paper*, **2003-01-1898**, 2003. 79, 84

[177] M. M. Maricq, R.E. Chase, and R. Podsiadlik, D. H.and Vogt. **Vehicle exhaust particle size distributions: A comparison of tailpipe and dilution tunnel measurements**. *SAE Technical Paper*, (1999-01-1461), 1999. 80

[178] G. Andrews, A. Clarke, N. Rojas, T. Sale, and D Gregory. **The transient storage and blow-out of diesel particulate in practical exhaust systems**. *SAE Technical Paper*, **2001-01-0204**, 2001. 80

[179] I. Khalek, D. Kittelson, and F. Brear. **The influence of dilution conditions on diesel exhaust particle size distribution measurements**. *SAE Technical Paper*, **1999-01-1142**, 1999. 81

[180] B. Giechaskiel, L. Ntziachristos, and Z. Samaras. **Effect of ejector dilutors on measurements of automotive exhaust gas aerosol size distributions**. *Measurement Science and Technology*, **20**(4):045703, 2009. 81

[181] M.D. Geller, L. Ntziachristos, A. Mamakos, Z. Samaras, D.A. Schmitz, J.R. Froines, and C. Sioutas. **Physicochemical and redox characteristics of particulate matter (PM) emitted from gasoline and diesel passenger cars**. *Atmospheric Environment*, **40**(36):6988–7004, 2006. 82

[182] Thomas W. Kirchstetter, Robert A. Harley, Nathan M. Kreisberg, Mark R. Stolzenburg, and Susanne V. Hering. **On-road measurement of fine particle and nitrogen oxide emissions from light- and heavy-duty motor vehicles**. *Atmospheric Environment*, **33**(18):2955 – 2968, 1999. 82

[183] A.P. Grieshop, E.M. Lipsky, N.J. Pekney, S. Takahama, and A.L. Robinson. **Fine particle emission factors from vehicles in a highway tunnel: Effects of fleet composition and season**. *Atmospheric Environment*, **40**(S2):S287–S298, 2006. 82

[184] A. Kristensson, C. Johansson, R. Westerholm, E. Swietlicki, L. Gidhagen, U. Wideqvist, and V. Vesely. **Real-world traffic emission factors of gases and particles measured in a road tunnel in Stockholm, Sweden**. *Atmospheric Environment*, **38**(5):657–673, 2004. 83

[185] D. Imhof, E. Weingartner, C. Ordonez, R. Gehrigt, N. Hill, B. Buchmann, and U. Baltensperger. **Real-world emission factors of fine and ultrafine aerosol particles for different traffic situations in Switzerland**. *Environmental Science and Technology*, **39**(21):8341–8350, 2005. 83

[186] B. Giechaskiel, R. Chirico, P.F. DeCarlo, M. Clairotte, T. Adam, G. Martini, M.F. Heringa, R. Richter, A.S.H. Prevot, U. Baltensperger, and C. Astorga. **Evaluation of the particle measurement programme (PMP) protocol to remove the vehicles' exhaust aerosol volatile phase**. *Science of The Total Environment*, **408**(21):5106–5116, 2010. 83, 84, 129

[187] H. Burtscher. **Physical characterization of particulate emissions from diesel engines: a review**. *Journal of Aerosol Science*, **36**(7):896 – 932, 2005. 84

[188] M. Kozak and M. Jerzy. **The mechanics of fuel sulphur influence on exhaust emissions from diesel engines**. *TEKA Kom. Mot. Energ. Roln.*, **5**:96–106, 2005. 84

[189] Volker Scheer, Ulf Kirchner, Roberto Casati, Rainer Vogt, Birgit Wehner, Sabine Philippin, Alfred Wiedensohler, Nele Hock, Johannes Schneider, Silke Weimer, and Stephan Borrmann. **Composition of Semi-Volatile Particles From Diesel Exhaust**. *SAE Technical Paper*, (2005-01-0197), 2005. 84

[190] J. Schneider, N. Hock, S. Weimer, and S. Borrmann. **Nucleation particles in diesel exhaust: Composition inferred from in situ mass spectrometric analysis**. *Environmental Science and Technology*, **39**(16):6153–6161, 2005. 84

[191] J. Schneider, S. Weimer, F. Drewnick, S. Borrmann, G. Helas, P. Gwaze, O. Schmid, M.O. Andreae, and U. Kirchner. **Mass spectrometric analysis and aerodynamic properties of various types of combustion-related aerosol particles**. *International Journal of Mass Spectrometry*, **258**(1-3):37–49, 2006. 84

[192] R. Alvarez, M. Weilenmann, and J.Y. Favez. **Evidence of increased mass fraction of NO2 within real-world NOx emissions of modern light vehicles - derived from a reliable online measuring method**. *Atmospheric Environment*, **42**(19):4699–4707, 2008. 88, 89

[193] Barbara Zielinska. **Atmospheric transformation of diesel emissions**. *Experimental and Toxicologic Pathology*, **57, Supplement 1**(0):31 – 42, 2005. 89, 229

[194] S. Grice, J. Stedman, A. Kent, M. Hobson, J. Norris, J. Abbott, and S. Cooke. **Recent trends and projections of primary NO2 emissions in Europe**. *Atmospheric Environment*, **43**(13):2164–2167, 2009. 89

[195] I.O.Y. Liu, N.W. Cant, M. Kogel, and T. Turek. **The formation of HCN during the reduction of NO by isobutane over Fe-MFI made by solid-state ion exchange**. *Catalysis Letters*, **63**(3-4):241–244, 1999. 89

REFERENCES

[196] M.M. Baum, J.A. Moss, S.H. Pastel, and G.A. Poskrebyshev. **Hydrogen cyanide exhaust emissions from in-use motor vehicles**. *Environmental Science and Technology*, **41**(3):857–862, 2007. 89

[197] G.A. Ban-Weiss, J.P. Mclaughlin, R.A. Harley, A.J. Kean, E. Grosjean, and D. Grosjean. **Carbonyl and nitrogen dioxide emissions from gasoline- and diesel-powered motor vehicles**. *Environmental Science and Technology*, **42**(11):3944–3950, 2008. 89

[198] A. Gelencser, K. Siszler, and J. Hlavay. **Toluene-benzene concentration ratio as a tool for characterizing the distance from vehicular emission sources**. *Environmental Science and Technology*, **31**(10):2869–2872, 1997. 92

[199] C. Jordan, E. Fitz, T. Hagan, B. Sive, E. Frinak, K. Haase, L. Cottrell, S. Buckley, and R. Talbot. **Long-term study of VOCs measured with PTR-MS at a rural site in New Hampshire with urban influences**. *Atmospheric Chemistry and Physics*, **9**(14):4677–4697, 2009. 92

[200] European Commission. **Energy 2020 A strategy for competitive, sustainable and secure energy, Communication from the commission to the European Parliament, the Council, the European Economic and Social Committee and the Committee of the Regions, Brussels, 10.11.2010.** *Communication*, **COM2010**(639), 2010. 113

[201] Hsi-Hsien Yang, Lien-Te Hsieh, Hsu-Chung Liu, and Hsiao-Hsuan Mi. **Polycyclic aromatic hydrocarbon emissions from motorcycles**. *Atmospheric Environment*, **39**(1):17–25, 2005. 113, 125

[202] Joseph McDonald, John Menter, Jane Armstrong, and Jitendra Shah. **Evaluation of emissions from Asian 2-stroke motorcycles**. *SAE Technical Paper*, (2005-32-0114), 2005. 113

[203] Pasquale Spezzano, Paolo Picini, Dario Cataldi, Fabrizio Messale, and Claudio Manni. **Particle- and gas-phase emissions of polycyclic aromatic hydrocarbons from two-stroke, 50-cm3 mopeds**. *Atmospheric Environment*, **42**(18):4332–4344, 2008. 113, 114, 125

[204] European Commission. **Regulation (EU) of the European Parliament and of the Council on the approval and market surveillance of two- or three-wheel vehicles and quadricycles**. *Communication*, **COM2010**(542), 2010. 113

[205] Loretta Müller, Pierre Comte, Jan Czerwinski, Markus Kasper, Andreas C. R. Mayer, Peter Gehr, Heinz Burtscher, Jean-Paul Morin, Athanasios Konstandopoulos, and Barbara Rothen-Rutishauser. **New Exposure System To Evaluate the Toxicity of (Scooter) Exhaust Emissions in Lung Cells in Vitro**. *Environmental Science & Technology*, **44**(7):2632–2638, 2010. 113

[206] Leonidas Ntziachristos, Athanasios Mamakos, Zissis Samaras, Anastasios Xanthopoulos, and Eleftherios Iakovou. **Emission control options for power two wheelers in Europe**. *Atmospheric Environment*, **40**(24):4547–4561, 2006. 113

[207] J. Czerwinski, B. Larsen, G. Martini, and A. Mayer. **Research on Particle Emissions of Modern 2-Stroke Scooters**. *SAE Technical Paper*, **2006-01-1078**, 2006. 113

[208] P. Bonnel, G. Martini, and A. Krasenbrink. **Euro 3 Stage for motorcycles: Derivation of equivalent limits for the WMTC driving cycle**. *JRC Technical Report*, **I.03.94**, 2003. 113

[209] John Hoard, Rachel Snow, Lifeng Xu, Christine Gierczak, Robert Hammerle, Cliff Montreuil, and S. Iskander Farooq. **NOx Measurement Errors in Ammonia-Containing Exhaust**. *SAE Technical Paper*, **2007-01-0330**, 2007. 116

[210] Environmental Protection Agency. **Compendium of Methods for the Determination of Toxic Organic Compounds in Ambient Air**. *EPA method*, **EPA/625/R-96/010b**, 1999. 118, 146, 174

[211] Environmental Protection Agency. **Determination of Formaldehyde in Ambient Air Using Adsorbent Cartridge Followed by High Performance Liquid Chromatography (HPLC)**. *EPA method*, **EPA TO-11A**, 1999. 118, 146, 174

[212] G. J. Sem. **Design and performance characteristics of three continuous-flow condensation particle counters: A summary**. *Atmospheric Research*, **62**(3-4):267–294, 2002. 118

[213] Cheol-Heon Jeong and Greg J. Evans. **Inter-Comparison of a Fast Mobility Particle Sizer and a Scanning Mobility Particle Sizer Incorporating an Ultrafine Water-Based Condensation Particle Counter**. *Aerosol Science and Technology*, **43**(4):364–373, 2009. 118

[214] S. Weimer, C. Mohr, R. Richter, J. Keller, M. Mohr, A. S. H. Prevot, and U. Baltensperger. **Mobile measurements of aerosol number and volume size distributions in an Alpine valley: Influence of traffic versus wood burning**. *Atmospheric Environment*, **43**(3):624–630, 2009. 118

[215] Christof Asbach, Heinz Kaminski, Heinz Fissan, Christian Monz, Dirk Dahmann, Sonja Mülhopt, Hanns Paur, Heinz Kiesling, Friedhelm Herrmann, Matthias Voetz, and Thomas Kuhlbusch. **Comparison of four mobility particle sizers with different time resolution for stationary exposure measurements**. *Journal of Nanoparticle Research*, **11**(7):1593–1609, 2009. 118

[216] S. Dray and A.B. Dufour. **The ade4 package: implementing the duality diagram for ecologists**. *Journal of Statistical Software*, **22**(4):1–20, 2007. 120, 149

[217] Manufacturers of Emission Controls Association. **Emission Control of Two-and Three-Wheel Vehicles**. 1999. URL: `http://www.meca.org/galleries/default-file/motorcycle.pdf`. 122

[218] European Commission. **Progress report on implementation of the Community's integrated approach to reduce CO2 emissions from light-duty vehicles - Report from the commission to the European Parliament, the Council, and the European Economic and Social Committee**. *Communication*, **COM2010**(656), 2010. 122

[219] European Commission. **Regulation (EC) No 595/2009 of the European Parliament and of the Council of 18 June 2009 on type-approval of motor vehicles and engines with respect to emissions from heavy duty vehicles (Euro VI) and on access to vehicle repair and maintenance information and amending Regulation (EC) No 715/2007 and Directive 2007/46/EC and repealing Directives 80/1269/EEC, 2005/55/EC and 2005/78/EC**. *Official J. Eur. Communities*, **L188**, 2009. 123, 192

[220] R. Chirico, M. Clairotte, T.W. Adam, B. Giechaskiel, M.F. Heringa, P.F. DeCarlo, M. Elsasser, G. Martini, U. Manfredi, T. Streibel, M. Sklorz, R. Zimmermann, C. Astorga, U. Baltensperger, and A.S.H. Prévôt. **Chassis dynamometer measurements of organic mass, black carbon, particle number, and regulated and unregulated gas emissions from mopeds, light and heavy duty vehicles with different fuels**. *Atmospheric Chemistry and Physics*, 2012. 123

[221] Pasquale Spezzano, Paolo Picini, and Dario Cataldi. **Gas- and particle-phase distribution of polycyclic aromatic hydrocarbons in two-stroke, 50-cm3 moped emissions**. *Atmospheric Environment*, **43**(3):539–545, 2009. 125

[222] P. Spezzano, P. Picini, and D. Cataldi. **Contribution of unburned lubricating oil and gasoline-derived n-alkanes to particulate emission from non-catalyst and catalyst-equipped two-stroke mopeds operated with synthetic lubricating oil**. *Journal of Environmental Monitoring*, **10**(10):1202–1210, 2008. 127

[223] Rudolf Rijkeboer, Dion Bremmers, Zissis Samaras, and Leonidas Ntziachristos. **Particulate matter regulation for two-stroke two wheelers: Necessity or haphazard legislation?** *Atmospheric Environment*, **39**(13):2483–2490, 2005. 129

[224] D. Etissa, M. Mohr, D. Schreiber, and P.A. Buffat. **Investigation of particles emitted from modern 2-stroke scooters**. *Atmospheric Environment*, **42**(1):183–195, 2008. 129

[225] Roger Magnusson, Calle Nilsson, and Barbro Andersson. **Emissions of Aldehydes and Ketones from a Two-Stroke Engine Using Ethanol and Ethanol-Blended Gasoline as Fuel**. *Environmental Science & Technology*, **36**(8):1656–1664, 2002. 131, 132

[226] H. Richter and J. B. Howard. **Formation of polycyclic aromatic hydrocarbons and their growth to soot–a review of chemical reaction pathways**. *Progress in Energy and Combustion Science*, **26**(4-6):565–608, 2000. 131

[227] European Commission. **Communication from the Commission - An EU Strategy for Biofuels: Brussels**. *Communication*, **COM2006**, 2006. 142

[228] European Environment Agency. **Laying the foundations for greener transport - TERM 2011: transport indicators tracking progress towards environmental targets in Europe**. *Communication*, **EEA Report**(7/2011), 2011. 142

[229] Pasquale Spezzano, Paolo Picini, and Dario Cataldi. **Gas- and particle-phase distribution of polycyclic aromatic hydrocarbons in two-stroke, 50-cm3 moped emissions**. *Atmospheric Environment*, **44**(37):4772–4816, 2010. 142

[230] European Commission. **Directive 2003/30/EC of the European Parliament and the Council - 8 May 2003 on the promotion of the use of biofuels or other renewable fuels for transport**. *Official J. Eur. Communities*, **L?**, 2003. 142

[231] Ayhan Demirbas. **Political, economic and environmental impacts of biofuels: A review**. *Applied Energy*, **86, Supplement 1**(0):S108 – S117, 2009. <ce:title>Bio-fuels in Asia</ce:title>. 142

[232] Takayuki Takeshita. **Assessing the co-benefits of CO2 mitigation on air pollutants emissions from road vehicles**. *Applied Energy*, **97**(0):225 – 237, 2012. <ce:title>Energy Solutions for a Sustainable World - Proceedings of the Third International Conference on Applied Energy, May 16-18, 2011 - Perugia, Italy</ce:title>. 142

[233] Arnaldo Walter, Paulo Dolzan, Oscar Quilodrán, Janaína G. de Oliveira, Cinthia da Silva, Fabrício Piacente, and Anna Segerstedt. **Sustainability assessment of bio-ethanol production in Brazil considering land use change, GHG emissions and socio-economic aspects**. *Energy Policy*, **39**(10):5703–5716, 2011. 142

[234] European Commission. **Commission implementing decision 2011/441/EU of 19 July 2011 on the recognition of the ŠGreenergy Brazilian Bioethanol verification programmeŠ scheme for demonstrating compliance with the sustainability criteria under Directives 2009/28/EC and 2009/30/EC of the European Parliament and of the Council**. *Official J. Eur. Communities*, **L190/85**, 2011. 142

[235] F. D. Stump, K. T. Knapp, and W. D. Ray. **Influence of ethanol-blended fuels on the emissions from three pre-1985 light-duty passenger vehicles**. *Journal of the Air and Waste Management Association*, **46**(12):1149–1161, 1996. 142

[236] S. G. Poulopoulos, D. P. Samaras, and C. J. Philippopoulos. **Regulated and unregulated emissions from an internal combustion engine operating on ethanol-containing fuels**. *Atmospheric Environment*, **35**(26):4399–4406, 2001. 142, 154, 160

[237] S. M. Corrêa, G. Arbilla, E. M. Martins, S. L. Quitério, C. de Souza Guimarães, and L. V. Gatti. **Five years of formaldehyde and acetaldehyde monitoring in the Rio de Janeiro downtown area - Brazil**. *Atmospheric Environment*, **44**(19):2302–2308, 2010. 142, 152

[238] European Environment Agency. **EMEP/EEA emission inventory guidebook 2009, updated June 2010**. *Communication*, **EEA Report**(9/2009), 2009. 142, 201

[239] Charlotte Sandstroem-Dahl, Lennart Erlandsson, Jan Gasste, and Magnus Lindgren. **Measurement Methodologies for Hydrocarbons, Ethanol and Aldehyde Emissions from Ethanol Fuelled Vehicles**. *SAE Technical Paper*, (2010-01-1557), 2010. 142, 146

[240] T. Wallner. **Correlation between speciated hydrocarbon emissions and flame ionization detector response for gasoline/alcohol blends**. *Journal of Engineering for Gas Turbines and Power*, **133**(8), 2011. 146, 151

[241] J-M. André and R. Joumard. **Modelling of Cold Start Excess Emission for Passenger Cars**. *INRETS Report*, **LTE0509**:1–239, 2005. URL: `http://www.inrets.fr/ur/lte/publications/publications-pdf/Joumard/A323_report_LTE0509_JMA_4.pdf`. 147

[242] Jean-Yves Favez, Martin Weilenmann, and Jan Stilli. **Cold start extra emissions as a function of engine stop time: Evolution over the last 10 years**. *Atmospheric Environment*, **43**(5):996–1007, 2009. 147

[243] Martin Weilenmann, Patrik Soltic, Christian Saxer, Anna-Maria Forss, and Norbert Heeb. **Regulated and nonregulated diesel and gasoline cold start emissions at different temperatures**. *Atmospheric Environment*, **39**(13):2433–2441, 2005. 147

[244] J. J. Winebrake, M. Q. Wang, and D. He. **Toxic emissions from mobile sources: A total fuel-cycle analysis for conventional and alternative fuel vehicles**. *Journal of the Air and Waste Management Association*, **51**(7):1073–1086, 2001. 152

[245] Kenneth J. Kelly, Brent K. Bailey, Timothy Coburn, Wendy Clark, and Peter Lissiuk. **Federal Test Procedure Emissions Test Results from Ethanol Variable-Fuel Vehicle Chevrolet Luminas**. *SAE Technical Paper*, **961092**, 1996. 154

[246] Manish Sharma, Carolyn Hubbard, and John Roth. **Catalyst Performance Evaluation on E0 and E85 Fuels**. *SAE Technical Paper*, (2011-01-0904), 2011. 154

[247] J. Wu, K. H. Song, T. Litzinger, S. Y. Lee, R. Santoro, M. Linevsky, M. Colket, and D. Liscinsky. **Reduction of PAH and soot in premixed ethylene-air flames by addition of ethanol**. *Combustion and Flame*, **144**(4):675–687, 2006. 154

[248] Martin Weilenmann, Jean-Yves Favez, and Robert Alvarez. **Cold-start emissions of modern passenger cars at different low ambient temperatures and their evolution over vehicle legislation categories**. *Atmospheric Environment*, **43**(15):2419–2429, 2009. 157, 162, 185

[249] Norbert V. Heeb, Anna-Maria Forss, Christian J. Saxer, and Patrick Wilhelm. **Methane, benzene and alkyl benzene cold start emission data of gasoline-driven passenger cars representing the vehicle technology of the last two decades**. *Atmospheric Environment*, **37**(37):5185–5195, 2003. 160

[250] T.W. Adam, C. Astorga, M. Clairotte, M. Duane, M. Elsasser, A. Krasenbrink, B.R. Larsen, U. Manfredi, G. Martini, L. Montero, M. Sklorz, R. Zimmermann, and A. Perujo. **Chemical analysis and ozone formation potential of exhaust from dual-fuel (liquefied petroleum gas/gasoline) light duty vehicles**. *Atmospheric Environment*, **45**(17):2842–2848, 2011. 160, 162

[251] Xuesong Wu, Ritchie Daniel, Guohong Tian, Hongming Xu, Zuohua Huang, and Dave Richardson. **Dual-injection: The flexible, bi-fuel concept for spark-ignition engines fuelled with various gasoline and biofuel blends**. *Applied Energy*, **88**(7):2305 – 2314, 2011. 162

[252] H. H. Yang, S. M. Chien, M. T. Cheng, and C. Y. Peng. **Comparative study of regulated and unregulated air pollutant emissions before and after conversion of automobiles from gasoline power to liquefied petroleum gas/gasoline dual-fuel retrofits**. *Environmental Science and Technology*, **41**(24):8471–8476, 2007. 171, 178, 179, 180, 185

[253] World LP Gas Association. **LP Gas Exceptional Energy**. 2009. URL: `http://www.worldlpgas.com`. 171

[254] H. Engerer and M. Horn. **Natural gas vehicles: An option for Europe**. *Energy Policy*, **38**(10):1017–1029, 2010. 171

[255] C.C. Chang, J.G. Lo, and J.L. Wang. **Assessment of reducing ozone formation potential for vehicles using liquefied petroleum gas as an alternative fuel.** *Atmospheric Environment*, **35**(35):6201–6211, 2001. 171, 172, 184

[256] E.D. Gamas, L. Diaz, R. Rodriguez, E. Lopez-Salinas, I. Schifter, and L. Ontiveros. **Exhaust emission from gasoline and LPG-powered vehicles operating at the altitude of Mexico City**. *Journal of the Air and Waste Management Association*, **49**(10):1179–1189, 1999. 171

[257] Z.D. Ristovski, E.R. Jayaratne, L. Morawska, G.A. Ayoko, and M. Lim. **Particle and carbon dioxide emissions from passenger vehicles operating on unleaded petrol and LPG fuel**. *Science of the Total Environment*, **345**(1-3):93–98, 2005. 171

[258] M.C.H. Lim, G.A. Ayoko, L. Morawska, Z.D. Ristovski, E.R. Jayaratne, and S. Kokot. **A comparative study of the elemental composition of the exhaust emission of cars powered by liquefied petroleum gas and unleaded petrol**. *Atmospheric Environment*, **40**(17):3111–3122, 2006. 171

[259] M. Achtnicht, G. Buehler, and C. Hermeling. **Impact of Service Station Networks on Purchase Decisions of Alternative-fuel Vehicles**. *ZEW Discussion Paper*, **08**(088), 2008. URL: `ftp://ftp.zew.de/pub/zew-docs/dp/dp08088.pdf`. 171

[260] U. Boesl, H.J. Neusser, and E.W. Schlag. **Two-photon ionization of polyatomic molecules in a mass spectrometer**. *Zeitschrift für Naturforschung*, **33**(12):1546–1548, 1978. 176, 206

[261] U. Boesl, R. Weishaeupl, P. Püffel, and W. Thiel. **Laser mass spectrometry of compounds in exhaust emissions from otto and diesel engines adapted for use at motor test facilities**. *VDI-Berichte*, **1863**:239–247, 2004. 176, 206

[262] Ralf Zimmermann. **Laser ionisation mass spectrometry for on-line analysis of complex gas mixtures and combustion effluents**. *Analytical and Bioanalytical Chemistry*, **381**:57–60, 2005. 10.1007/s00216-004-2886-5. 176, 206

[263] S. Mitschke, T. Adam, T. Streibel, R.R. Baker, and R. Zimmermann. **Application of time-of-flight mass spectrometry with laser-based photo-ionization methods for time-resolved on-line analysis of mainstream cigarette smoke**. *Analytical Chemistry*, **77**(8):2288–2296, 2005. 176, 207

[264] West Virginia University. **National Alternative Fuels Training Consortium**. *Morgantown, U.S.*, 2010. URL: `http://assets.slate.wvu.edu/resources/527/1287596146.pdf`. 178

[265] L. Diaz, I. Schifter, E. Lopez-Salinas, E. Gamas, R. Rodriguez, and J. Avalos. **Optimizing automotive LPG blend for Mexico City**. *Fuel*, **79**(1):79–88, 2000. 178

[266] T.W. Adam and R. Zimmermann. **Determination of single photon ionization cross sections for quantitative analysis of complex organic mixtures**. *Analytical and Bioanalytical Chemistry*, **389**:1941–1951, 2007. 180

[267] Environmental Protection Agency. **Panorama of Transport**. *Eurostat Statistical books*, **ISSN 1831-3280**, 2009. 187

[268] Subhasis Biswas, Shaohua Hu, Vishal Verma, Jorn D. Herner, William H. Robertson, Alberto Ayala, and Constantinos Sioutas. **Physical properties of particulate matter (PM) from late model heavy-duty diesel vehicles operating with advanced PM and NOx emission control technologies**. *Atmospheric Environment*, **42**(22):5622 – 5634, 2008. 187

[269] Subhasis Biswas, Vishal Verma, James J. Schauer, and Constantinos Sioutas. **Chemical speciation of PM emissions from heavy-duty diesel vehicles equipped with diesel particulate filter (DPF) and selective catalytic reduction (SCR) retrofits**. *Atmospheric Environment*, **43**(11):1917 – 1925, 2009. 187

[270] Jorn Dinh Herner, Shaohua Hu, William H. Robertson, Tao Huai, John F. Collins, Harry Dwyer, and Alberto Ayala. **Effect of Advanced Aftertreatment for PM and NOx Control on Heavy-Duty Diesel Truck Emissions**. *Environmental Science & Technology*, **43**(15):5928–5933, 2009. 187

[271] Shaohua Hu, Jorn D. Herner, Martin Shafer, William Robertson, James J. Schauer, Harry Dwyer, John Collins, Tao Huai, and Alberto Ayala. **Metals emitted from heavy-duty diesel vehicles equipped with advanced PM and NOX emission controls**. *Atmospheric Environment*, **43**(18):2950 – 2959, 2009. 187

[272] Wen G. Wang, N. N. Clark, D. W. Lyons, R. M. Yang, M. Gautam, R. M. Bata, and J. L. Loth. **Emissions Comparisons from Alternative Fuel Buses and Diesel Buses with a Chassis Dynamometer Testing Facility**. *Environmental Science & Technology*, **31**(11):3132–3137, 1997. 188

[273] Norman Y. Kado, Robert A. Okamoto, Paul A. Kuzmicky, Reiko Kobayashi, Alberto Ayala, Michael E. Gebel, Paul L. Rieger, Christine Maddox, and Leo Zafonte. **Emissions of Toxic Pollutants from Compressed Natural Gas and Low Sulfur Diesel-Fueled Heavy-Duty Transit Buses Tested over Multiple Driving Cycles**. *Environmental Science & Technology*, **39**(19):7638–7649, 2005. 188

[274] Robert A. Okamoto, Norman Y. Kado, Paul A. Kuzmicky, Alberto Ayala, and Reiko Kobayashi. **Unregulated Emissions from Compressed Natural Gas (CNG) Transit Buses Configured with and without Oxidation Catalyst**. *Environmental Science & Technology*, **40**(1):332–341, 2006. 188

[275] the European COoperation in the field of Scientific and Technical Research. **Energy and fuel consumption drom heavy duty vehicles**. *COST 346 Ũ Final Report including Final Report of Working Group A*, 2005. URL: `http://www.transport-research.info/Upload/Documents/200906/20090619_171415_76456_I_COST346_FinalReport.pdf`. 188

[276] Assessment, Reliability of Transport Emission Models, and Inventory Systems ARTEMIS WP400. **Heavy duty vehicle emissions**. *Final Report*, pages 1–176, 2005. URL: `http://inrets.fr/ur/lte/publi-autresactions/fichesresultats/ficheartemis/road3/modelling33/Artemis_del4_HDV.pdf`. 188

[277] European Commission Joint Research Centre. **JRC Newsletter. March 2009**, 2009. URL: `http://ec.europa.eu/dgs/jrc/downloads/jrc_newsletter_2009_03.pdf`. 189, 201

[278] Robert L. McCormick, Jeffrey D. Ross, and Michael S. Graboski. **Effect of Several Oxygenates on Regulated Emissions from Heavy-Duty Diesel Engines**. *Environmental Science & Technology*, **31**(4):1144–1150, 1997. 194

[279] Kent E. Nord and Dan Haupt. **Reducing the Emission of Particles from a Diesel Engine by Adding an Oxygenate to the Fuel**. *Environmental Science & Technology*, **39**(16):6260–6265, 2005. 194

[280] P.S. Monks, C. Granier, S. Fuzzi, A. Stohl, M.L. Williams, H. Akimoto, M. Amann, A. Baklanov, U. Baltensperger, I. Bey, N. Blake, R.S. Blake, K. Carslaw, O.R. Cooper, F. Dentener, D. Fowler, E. Fragkou, G.J. Frost, S. Generoso, P. Ginoux, V. Grewe, A. Guenther, H.C. Hansson, S. Henne, J. Hjorth, A. Hofzumahaus, H. Huntrieser, I.S.A. Isaksen, M.E. Jenkin, J. Kaiser, M. Kanakidou, Z. Klimont, M. Kulmala, P. Laj, M.G. Lawrence, J.D. Lee, C. Liousse, M. Maione, G. McFiggans, A. Metzger, A. Mieville, N. Moussiopoulos, J.J. Orlando, C.D. O'Dowd, P.I. Palmer, D.D. Parrish, A. Petzold, U. Platt, U. Pöschl, A.S.H. Prévôt, C.E. Reeves, S. Reimann, Y. Rudich, K. Sellegri, R. Steinbrecher, D. Simpson, H. ten Brink,

J. Theloke, G.R. van der Werf, R. Vautard, V. Vestreng, Ch. Vlachokostas, and R. von Glasow. **Atmospheric composition change Ũ global and regional air quality**. *Atmospheric Environment*, **43**(33):5268 – 5350, 2009. <ce:title>ACCENT Synthesis</ce:title>. 201

[281] V. Ramanathan and G. Carmichael. **Global and regional climate changes due to black carbon**. *NATURE GEOSCIENCE*, **1**(4):221–227, APR 2008. 201

[282] European Environment Agency. **Transport at a crossroads. TERM 2008: indicators tracking transport and environment in the European Union**. *Communication*, **EEA Report**(3/2009):1–56, 2009. 201

[283] World Health Organization. **DIESEL FUEL AND EXHAUST EMISSIONS**. *INTERNATIONAL PROGRAMME ON CHEMICAL SAFETY*, **ENVIRONMENTAL HEALTH CRITERIA 171**, 1996. URL: `http://http://www.inchem.org/documents/ehc/ehc/ehc171`. 201

[284] European Environment Agency. **Climate for a transport change. TERM 2007: indicators tracking transport and environment in the European Union**. *Communication*, **EEA Report**(1/2008), 2008. 204

[285] H.J. Heger, R. Zimmermann, R. Dorfner, M. Beckmann, H. Griebel, A. Kettrup, and U. Boesl. **On-line emission analysis of polycyclic aromatic hydrocarbons down to pptv concentration levels in the flue gas of an incineration pilot plant with a mobile resonance enhanced multiphoton ionization time-of-flight mass spectrometer**. *Analytical Chemistry*, **71**(1):46–57, 1999. 207

[286] L. Oudejans, A. Touati, and B.K. Gullett. **Real-time, on-line characterization of diesel generator air toxic emissions by resonance-enhanced multiphoton ionization time-of-flight mass spectrometry**. *Analytical Chemistry*, **76**(9):2517–2524, 2004. 207

[287] M.R. Canagaratna, J.T. Jayne, J.L. Jimenez, J.D. Allan, M.R. Alfarra, Q. Zhang, T.B. Onasch, F. Drewnick, H. Coe, A. Middlebrook, A. Delia, L.R. Williams, A.M. Trimborn, M.J. Northway, P.F. DeCarlo, C.E. Kolb, P. Davidovits, and D.R. Worsnop. **Chemical and microphysical characterization of ambient aerosols with the aerodyne aerosol mass spectrometer**. *Mass Spectrometry Reviews*, **26**(2):185–222, 2007. 207

[288] P.T. Williams, M.K. Abbass, G.E. Andrews, and K.D. Bartle. **Diesel Particulate-Emissions - The Role of Unburned Fuel**. *Combustion and Flame*, **75**(1):1–24, JAN 1989. 212

[289] R. Barbella, C. Bertoli, A. Ciajolo, and A. Danna. **Behavior of a Fuel-Oil During the Combustion Cycle of a Direct Injection Diesel-Engine**. *Combustion and Flame*, **82**(2):191–198, NOV 1990. 212

[290] Martin Mohr, Urs Lehmann, and Giovanni Margaria. **ACEA program on the emissions of fine particulates from passenger cars (2) - Part 2: Effect of sampling conditions and fuel sulfur content on the particle emission**. *SAE Technical Paper*, (2003-01-1890), 2003. 213

[291] Jon D. Andersson, Barbara G. A. Wedekind, Diane Hall, Richard Stradling, and Geoff Wilson. **DETR/SMMT/CONCAWE Particulate Research Program: Light-duty results**. *SAE Technical Paper*, **2001-01-3577**, 2001. 213

[292] Cha-Lee Myung, Kwanhee Choi, Juwon Kim, Yunsung Lim, Jongtae Lee, and Simsoo Park. **Comparative study of regulated and unregulated toxic emissions characteristics from a spark ignition direct injection light-duty vehicle fueled with gasoline and liquid phase LPG (liquefied petroleum gas)**. *Energy*, **44**(1):189 – 196, 2012. Integration and Energy System Engineering, European Symposium on Computer-Aided Process Engineering 2011. 227

[293] AEA. **Reduction and Testing of Greenhouse Gas (GHG) Emissions from Heavy Duty Vehicles Ũ Lot 1: Strategy**. pages 1–309, 2011. URL: `http://ec.europa.eu/clima/policies/transport/vehicles/docs/ec_hdv_ghg_strategy_en.pdf`. 228

[294] M. Hallquist, J. C. Wenger, U. Baltensperger, Y. Rudich, D. Simpson, M. Claeys, J. Dommen, N. M. Donahue, C. George, A. H. Goldstein, J. F. Hamilton, H. Herrmann, T. Hoffmann, Y. Iinuma, M. Jang, M. E. Jenkin, J. L. Jimenez, A. Kiendler-Scharr, W. Maenhaut, G. McFiggans, Th. F. Mentel, A. Monod, A. S. H. Prévôt, J. H. Seinfeld, J. D. Surratt, R. Szmigielski, and J. Wildt. **The formation, properties and impact of secondary organic aerosol: current and emerging issues**. *Atmospheric Chemistry and Physics*, **9**(14):5155–5236, 2009. 229

[295] R. Bahreini, A. M. Middlebrook, J. A. de Gouw, C. Warneke, M. Trainer, C. A. Brock, H. Stark, S. S. Brown, W. P. Dube, J. B. Gilman, K. Hall, J. S. Holloway, W. C. Kuster, A. E. Perring, A. S. H. Prevot, J. P. Schwarz, J. R. Spackman, S. Szidat, N. L. Wagner, R. J. Weber, P. Zotter, and D. D. Parrish. **Gasoline emissions dominate over diesel in formation of secondary organic aerosol mass**. *GEOPHYSICAL RESEARCH LETTERS*, **39**, MAR 20 2012. 229

European Commission
EUR 25583 EN – Joint Research Centre – Institute for Energy and Transport

Title: Impact of fuels and exhaust aftertreatment systems on the unregulated emissions from mopeds, light and heavy-duty vehicles

Author: Michaël Clairotte
Supervisor: Covadonga Astorga-Llorens

Luxembourg: Publications Office of the European Union

2014 – 244 pp. – 21.0 x 29.7 cm

EUR – Scientific and Technical Research series – ISSN 1018-5593
ISBN 978-92-79-27305-6

doi: 10.2790/67104

Abstract

Transport sector plays a key role in climate change and air pollution. Among the anthropogenic sectors, on-road transport is recognized as the first contributor to global warming, mainly due to its emission of carbon dioxide, ozone precursors and carbonaceous aerosols. In addition, on-road transport contributes to the deterioration of air quality by releasing nitrogen oxides, hydrocarbons, carbonyls, ammonia, and aerosols. However, the current
European legislation of vehicles emissions focusses on a limited number of pollutants, namely hydrocarbons, carbon monoxide, nitrogen oxides, and particulate matter.

The aim of this work was to improve the knowledge about the emission factors of gas phase and particle-associated emissions from vehicle exhaust. The impacts of aftertreatment devices and fuel quality on regulated and unregulated species were studied. Several sampling campaigns with different types of vehicles were conducted in the vehicle emission laboratory (VELA) at the European Commission Joint Research Centre (EC-JRC) Ispra, Italy. The vehicles chosen were representative of some categories circulating in Europe (heavy duty vehicles, light duty vehicles, two-stroke mopeds), and either standard fuel or some alternative fuels (ethanol and liquefied petroleum gas) were used. The gas phase was monitored by a Fourier transform infrared spectrometer (carbonyls, nitrogen-containing species, small hydrocarbons), and a resonance-enhanced multiphoton ionization time-of-flight mass spectrometer (mono and polycyclic aromatic hydrocarbons). The particulate phase was analyzed by a high-resolution time-of-flight aerosol mass spectrometer (organic aerosol, chloride, nitrate), and a multiangle absorption photometer (black carbon).

The mopeds were found to have the higher emission factors of primary organic aerosol and polycyclic aromatic hydrocarbons. While efficient to reduce the regulated emissions, the aftertreatment used to comply with the moped Euro 2 emission standard might be responsible of large emission of unregulated organic aerosols. Most of the emission linked to the gasoline light duty vehicles were released before the light-off of the catalyst. Whereas alternative fuels studied helped to reduce ozone precursor emissions, the pollutants associated to the cold start of the vehicle reduced this beneficial effect. Finally, the heavy duty diesel vehicles featured the highest
nitrogen oxides and black carbon emissions. Despite efficient retrofit and aftertreatment systems (for particles and nitrogen oxides), these vehicles could release significant amount of ammonia. These results provided valuable insights for the drafting of legislation related to the achievement of sustainable transport in Europe.

LD-NA-25583-EN-C

As the Commission's in-house science service, the Joint Research Centre's mission is to provide EU policies with independent, evidence-based scientific and technical support throughout the whole policy cycle.

Working in close cooperation with policy Directorates-General, the JRC addresses key societal challenges while stimulating innovation through developing new standards, methods and tools, and sharing and transferring its know-how to the Member States and international community.

Key policy areas include: environment and climate change; energy and transport; agriculture and food security; health and consumer protection; information society and digital agenda; safety and security including nuclear; all supported through a cross-cutting and multi-disciplinary approach.

ISBN 978-92-79-27305-6

Publications Office